Genómica y transcriptómica comparativa de *Trypanosoma cruzi*

Lissa Briceida Cruz Saavedra

Documento de tesis presentado como requisito para optar al título de Doctora en Ciencias Biomédicas y Biológicas

DOCTORADO EN CIENCIAS BIOMÉDICAS Y BIOLÓGICAS
UNIVERSIDAD DEL ROSARIO
BOGOTÁ, D.C.
2021

Genómica y transcriptómica comparativa de *Trypanosoma cruzi*

Estudiante:
Lissa Briceida Cruz Saavedra

Director:
Juan David Ramírez González Ph.D.
Profesor Asociado
Facultad de Ciencias Naturales
Universidad del Rosario

Documento de tesis presentado como requisito para optar al título de Doctora en Ciencias Biomédicas y Biológicas

DOCTORADO EN CIENCIAS BIOMÉDICAS Y BIOLÓGICAS
UNIVERSIDAD DEL ROSARIO
BOGOTÁ, D.C.
2021

AGRADECIMIENTOS

Siempre he pensado que la vida nos da la oportunidad de seguir un camino, donde las decisiones que tomamos al largo de esta nos definen, por eso sin lugar a duda, le agradezco infinitamente a ***la vida*** *por haberme permitido escoger a la ciencia como mi camino, para mi este proceso ha sido la respuesta para seguir mi pasión, como resultado cada parte de mi tesis han sido los años más felices y satisfactorios a nivel personal y profesional a pesar del trabajo duro que comprendieron,*

Primero que todo quiere agradecer a la persona por la cual soy lo el ser humano que escribió esta tesis, a ***mi mamá*** *Martha Saavedra, no solamente por haberme dado la vida, ser una excelente madre y enseñarme todos los valores que tengo, sino por haberme permitido seguir mis sueños a pesar de que no siempre comprendieran el mejor escenario, por siempre impulsarme a seguir mi pasión con responsabilidad a pesar de las adversidades en el camino, por no dejarme desfallecer nunca y enseñarme a ver que mañana siempre sería un día nuevo, y por sopórtame durante tantos, sé que no ha sido una tarea fácil. Pero aún más importante por enseñarme por medio del ejemplo a ser una mujer guerrera, luchadora, que de que cada problema sale con su cabeza en alto y logra su mejor versión, esa ha sido la mayor fuente de inspiración para mi vida.*

Quiero agradecer a ***mi novio*** *Juan Hernández****,*** *porque no solamente es la parte que me hace feliz y es un maravilloso ser humano, sino porque además me enseña a ser una mejor profesional y persona, a siempre actuar sin afectar a las personas que lo rodean desde la lógica y no desde los impulsos del momento, a dar todo lo que se tiene para poder ayudar al que no tiene nada, a cuestionar las infinitas cosas que nos rodean de la mejor forma y siempre intentar ser la mejor versión que de uno mismo. Gracias por ser mi compañero, por entenderme, apoyarme, soportarme y levantarme de mis momentos de debilidad, y por mostrarme lo bonito del amor.*

A ***mis amigas*** *que han estado conmigo, algunas durante media vida, siempre mostrándome la cara linda de las personas con las que no se necesita tener la misma sangre para que sean nuestra familia. A* ***Marce,*** *por mostrarme desde mis 15 años que en este largo camino de la vida a pesar de que se escojan diferentes vías siempre se puede ser la mejor versión de cada elección, una persona luchadora, una excelente madre, esposa, y el orgullo más grande de un padre maravilloso como lo era don* ***Manuel,*** *que no tendría más sino felicidad de ver la maravillosa persona que te has convertido, gracias por esos maravillosos recuerdos que has dejado en mi vida durante tanto tiempo. A mis amigas del pregrado, en especial a* ***Panche,*** *gracias por mostrarme toda la bondad y nobleza en un solo ser humano, por ser esa luz en los momentos más oscuros de mi vida, y esa alegría que transformaba una lagrima en una gran carcajada, y ese apoyo incondicional que demuestra lo que es la amistad. Y finalmente a* ***Andre,*** *eres una de las más bonitas coincidencias que me ha dejado la ciencia, de esas conexiones locas con las que se puede echar chisme por horas, preparar "juguitos" de dudosa reputación,*

y reír y llorar relatando el día a día.

Sin lugar a duda a una de las personas más importantes en mi vida durante casi una década, a mi ***padre en la ciencia*** *Juan David Ramírez, siempre he dicho que le agradezco infinitamente por haber visto potencial en mi hace tantos años, pero le agradezco aún más por la persona que ha formado durante los años siguientes, le agradezco por enseñarme disciplina, responsabilidad, carácter, bondad, y a ser un excelente ser humano. Por continuar con este proceso a pesar de las fallas y de los múltiples errores cometidos en el camino (solo me "echo" dos veces así que me doy por bien servida jajaja). En retrospectiva han habido tantos momentos de aprendizaje, logros y felicidad que he podido conseguir gracias al apoyo y ejemplo que he tenido siempre de* ***Juan*** *que las palabras de agradecimiento no serían suficientes en una hoja de papel y no se restringirían solo a una tesis de doctorado. Le agradezco haberme enseñado a seguir mis pasiones, por nunca derribar mis ideas, y recibir con humildad, a pesar de su gran conocimiento, todo lo que se pasaba por mi mente. Para mi ha sido mi gran maestro, mi ejemplo a seguir, mi gran apoyo, y mi* ***padre.*** *Siempre le desearé que cada cosa bonita que le ha regalado a las personas que lo rodean le sea mil veces recompensada en su vida, aunque dudo que pueda ser posible ya que han sido infinitas.*

A mi maravilloso centro de investigación ***CIMBIUR,*** *más que mis compañeros de trabajo con mi familia, el apoyo y la gente bonita con la que cualquier persona quiere encontrase en la vida. A* ***Mary,*** *si se puede describir a una persona, mujer maravillosa, que represente todos lo somos y hemos luchado las mujeres en la historia esa es Mary, gracias por tanto durante estos últimos años, gracias por tanto conocimiento, gracias por tantas alegrías, gracias por tanto amor, gracias por tanto ejemplo, gracias por tantos cocteles, pero lo más importante, gracias por brindarme tu amistad, tu apoyo y tus maravillosos consejos siempre, han sido fundamentales para mí. A mi* ***Natha*** *hermosa, no he conocido una persona tan bondadosa, llena de amor y desinterés como tú, lo más lindo que me has dejado y por lo que siempre te agradeceré es por mostrarme la parte linda, inocente, amorosa y buena de las personas, donde los sentimientos de maldad no están presentes, para mi eres como una hermanita. A* ***Luz****, gracias por haber confiando en mi en los momentos en los que yo ni yo misma lo hacía, por haberme mostrado la parte sensible detrás de esa mujer tan fuerte, y por enseñarme tantas cosas de una mujer absolutamente valiosa y por ser la mejor compañera de viaje que cualquiera puede tener. A* ***Caro,*** *ver todo tu proceso y ejemplo es de las cosas más lindas que he podido tener en mi vida, te agradezco por permitirme ver el ave Fénix salir con éxito y renacida de cada batalla, gracias por llenarme de fuerza siempre. A* ***Gio,*** *después de tantos años aún disfruto molestarlo y ustearlo (jajaja), gracias por el apoyo siempre, ha sido un placer crecer juntos aprendiendo de la fuerza, sagacidad y capacidad para resolver problemas, siempre con la frente en alto pero con bondad en el corazón, gracias por enseñarme el Gio que está dentro del caparazón, el Gio sumamente sensible y de gran corazón que no dudaría en apoyar a las personas que quiere. A* ***David,*** *que lindo es encontrarse con alguien que genere tanta felicidad y miles de carcajadas solo con verlo, gracias por sacarme una sonrisa en los*

momentos más duros, y gracias por enseñarme ese hombre absolutamente guerrero, que pelea con sus propios demonios con un toque de alegría y buen baile. A ***Adri H,*** *gracias por mostrarme esa mujer multifuncional que puede ser madre, científica, y buen ser humano a pesar de todas las adversidades y responsabilidades del día a día, pero muchas más gracias por mostrarme lo que una madre puede llegar a hacer por dar lo mejor a sus hijas. A* ***Adri C,*** *gracias por mostrar esa linda persona que está detrás de la mujer de carácter fuerte, esa persona absolutamente responsable, de buen corazón, correcta en sus acciones, que franqueza siempre dice lo que siente, siempre es bonito encontrarse con personas así. A* ***Vivi,*** *gracias por regalarme tantos momentos de carcajadas infinitas, siempre será contigo bailar el "Super Bowl" de Shakira, gracias por intentar hacer de mi una persona "Fit" aunque la pandemia se interpuso en tu objetivo (jajaja), pero aún gracias por compartir conmigo todas tus luchas y tu fortaleza para hacerle frente. A* ***Jesus, Laura, Sergio y Natha V,*** *gracias por enseñarme todo ese talento que se puede tener como científico y siempre brindarme su apoyo cuando más lo he necesitado, Nombrar lo que cada uno de los integrantes de* ***CIMBIUR*** *ha hecho por mí me tomaría más de las páginas imaginadas, pero quiero agradecerle a cada uno por los miles de miles de momentos y enseñanzas que le han regalado a mi vida.*

A ***Martin Llewellyn,*** *por brindarme la oportunidad de realizar mi pasantía doctoral en una de las mejores universidades en el estudio de Trypanosoma cruzi, y por ser la maravillosa persona que es a pesar de todos sus conocimientos y múltiples ocupaciones. A* ***Philipp Schwabl,*** *por brindarme su amistad, todos sus maravillosos conocimientos, su tiempo y tener esa gran paciencia para enseñarme bioinformática y el "exorcismo de mis demonios" (alias Trypanosoma cruzi) durante el transcurso de mi pasantía y mi tesis en general.*

A ***mis jurados****, por dedicar su tiempo en la lectura y evaluación de mi tesis de investigación a pesar sus apretadas agendas, es para mi todo un honor que personas expertas en las áreas desarrolladas en esta tesis puedan leer mis resultados y darme su opinión sobre los análisis aquí desarrollados.*

A la ***Dirección de Investigación e Innovación*** *de la universidad del Rosario, por la asistencia graduada con la cual pude realizar mi programa de doctorado y aumentar mis conocimientos como docente. Y el* ***Comité de becas de la Dirección Académica*** *de la universidad del Rosario, por la beca que permitió la realización de mi pasantía en la universidad de Glasgow, Escocia.*

Finalmente, a el Departamento Administrativo de Ciencia, Tecnología e Innovación COLCIENCIAS por la financiación de este proyecto (120465843375), bajo el contrato 063-2015.

TABLA DE CONTENIDO

1. LISTA DE PUBLICACIONES

Todos los artículos se encuentran anexos a este documento, la información suplementaria y/o tablas serán anexadas en archivos comprimidos siguiendo el número de artículos que se mencionan a continuación:

- **Artículo 1:** Cruz-Saavedra L., Schwabl P., Munoz M., Patino L., Vallejo GA, Llewellyn M., Ramírez, J. D. Evidence of genomic plasticity in *Trypanosoma cruzi* I driven by aneuploidy and loss of heterozygosity. (**SOMETIDO)**

- **Artículo 2:** Cruz-Saavedra L, Muñoz M, León C, Patarroyo MA, Arevalo G, Pavia P, Vallejo G, Carranza JC, Ramírez JD. Purification of *Trypanosoma cruzi* metacyclic trypomastigotes by ion exchange chromatography in sepharose-DEAE, a novel methodology for host-pathogen interaction studies. J Microbiol Methods. 2017 Nov;142:27-32. doi: 10.1016/j.mimet.2017.08.021. Epub 2017 Sep 1. PMID: 28865682.

- **Artículo 3:** Cruz-Saavedra L, Muñoz M, Patiño LH, Vallejo GA, Guhl F, Ramírez JD. Slight temperature changes cause rapid transcriptomic responses in *Trypanosoma cruzi* metacyclic trypomastigotes. Parasit Vectors. 2020 May 14;13(1):255. doi: 10.1186/s13071-020-04125-y. PMID: 32410662; PMCID: PMC7226949

- **Artículo 4:** Cruz-Saavedra L, Vallejo GA, Guhl F, Messenger LA, Ramírez JD. Transcriptional remodeling during metacyclogenesis in *Trypanosoma cruzi* I. Virulence. 2020 Dec;11(1):969-980. doi: 10.1080/21505594.2020.1797274. PMID: 32715914; PMCID: PMC7549971.

- **Artículo 5:** Cruz-Saavedra L, Vallejo GA, Guhl F, Ramírez JD. Transcriptomic changes across the life cycle of *Trypanosoma cruzi* II. PeerJ. 2020 May 14;8:e8947. doi: 10.7717/peerj.8947. PMID: 32461822; PMCID: PMC7231504.

2. LISTA DE ANEXOS

2.1**Anexos de artículos**

Artículo 1
Artículo 3
Artículo 4
Artículo 5

2.2 Anexos de productos de la tesis

10.2 Capítulos de libro
10.3 Presentación en eventos
10.4 Cursos
10.5 Pasantía
10.6 Reconocimientos

3. LISTA DE FIGURAS

4. LISTA DE ABREVIATURAS

OMS: Organización Mundial de la Salud
DTU: Discrete Typing Units
TcI: *Trypanosoma cruzi* I
TcII: *Trypanosoma cruzi* II
TcBat: *Trypanosoma cruzi* - Bat
TcI_{dom}: genotipo asociado a ciclo domestico de *Trypanosoma cruzi* I
LOH: Loss of heterozygocity – Perdida de heterocigosidad
SA: Segmental aneuploidy – Aneuploidia segmental
RHS: Retrotransposon Hot Spot – Puntos calientes de retrotransposon
LIT: Liver Infusion Tryptose medium
DEAE: Diethylaminoethyl
ADN: Ácido desoxirribonucleico
SL-IR: región intergénica del gen miniexon
MLST: Multilocus Sequence Typing
MASP: Mucin-associated surface proteins
DGF-1: Dispersed gene family 1
GC: Guanina-Citosina
IL: Interleuquina

5. RESUMEN

El parásito *Trypanosoma cruzi* es conocido como el agente etiológico de la enfermedad de Chagas, según reportes de la Organización Mundial de la Salud (OMS) se encuentra dentro de las 17 enfermedades tropicales desatendidas y es la tercera infección parasitaria más común en todo el mundo después de la malaria y la esquistosomiasis. *T. cruzi* muestra una marcada diversidad genética que ha permitido clasificarlo al menos en seis unidades discretas de tipificación (DTUs). Así mismo, una alta variabilidad genética intra-DTU ha sido observada en TcI, la DTU más prevalente en Colombia y altamente distribuida a nivel mundial. Esta variabilidad ha llevado a algunos autores a clasificarla en genotipos, que en algunos casos son asociados a los ciclos eco-epidemiológicos de la transmisión de este parásito. De igual manera, una alta plasticidad genómica ha sido reportada en *T. cruzi*, reflejada en aneuploidías cromosómicas y re-arreglos estructurales entre los genes codificantes para las familias multigénicas. Sin embargo, y a pesar de los avances en los últimos años en el estudio del genoma de *T. cruzi* muy pocos estudios han evaluado la arquitectura genómica de este parásito.

Por otro lado, este parásito posee un complejo ciclo de vida que transcurre entre humanos, mamíferos-reservorios e insectos triatominos de la subfamilia Reduviidae; presenta varios estadios morfológicos con características antigénicas distintas. Uno de los procesos más importantes durante su ciclo de vida es la metaciclogénesis, cuyo objetivo final es la transformación de epimastigotes replicativos a tripomastigotes metacíclicos infectivos. Durante este proceso se generan cambios morfológicos, metabólicos, transcriptómicos y proteómicos que permiten su progreso y confieren características infectivas al mismo; además de características virulentas de invasión de células y tropismo hacia diferentes tejidos. A pesar de los estudios realizados sobre la metaciclogénesis, el conjunto de cambios que ocurren en el transcriptoma durante este proceso biológico no se ha evaluado a profundidad en *T. cruzi*. Por otro lado, el ciclo de vida en el mamífero, donde se incluyen los estadios amastigotes y tripomastigotes derivados de células, cobra gran importancia ya que durante el desarrollo de este se pueden llegar a generar las manifestaciones clínicas relacionadas con la enfermedad de Chagas, producida por este parásito, principalmente por la invasión celular, replicación y lisis celular, que adicionalmente desencadena una fuerte respuesta inmune por parte del hospedero que no es efectiva en la eliminación de este, pero si afecta y daña los tejidos en el hospedero, lo que hace aún más interesante el estudio en la expresión génica de *T. cruzi* en estos estadios.

Por los motivos anteriormente expuestos, el objetivo general de este trabajo fue "Evaluar la arquitectura genómica y los perfiles de expresión génica durante el ciclo de vida de *Trypanosoma cruzi*", del cual se desencadenan tres objetivos específicos: 1. Describir la arquitectura genómica y diversidad genética de clones de *Trypanosoma cruzi* I (TcI). 2. Evaluar los perfiles de expresión génica de *Trypanosoma cruzi* I durante el proceso de metaciclogénesis *in vitro*. 3. Determinar la remodelación en la expresión génica durante el ciclo de vida de

Trypanosoma cruzi II. Siendo cada uno de los anteriores objetivos asociados a un capítulo dentro de este trabajo de tesis.

En relación con el primer capítulo de este estudio, se exploró la diversidad genómica entre 18 clones colombianos de *T. cruzi* I y 15 clones de *T. cruzi* I de otros países de América. Los resultados obtenidos confirman la alta variabilidad genética descrita con anterioridad a un nivel filogenético, la presencia de una alta heterocigosidad entre los genomas, y la existencia de un clado compatible con el genotipo TcI_{dom}, descrito previamente para cepas asiladas a partir de humanos en Colombia y Venezuela. Adicionalmente, se reportan diferentes procesos compatibles con una alta plasticidad en el genoma de TcI. Eventos de aneuploidía total y segmentaria (SA) presentes a lo largo de los cromosomas con características diferenciales entre cepas e incluso entre clones de la misma cepa fueron encontrados y corroborados por medio de cálculos de la profundidad y la frecuencia alélica. Así mismo, se encontró pérdida de heterocigosidad (LOH) en diferentes cromosomas, la ubicación de los fragmentos que presentaban LOH, al igual que la extensión a lo largo de cada cromosoma, no estuvo relacionada entre los distintos clones aislados de cada cepa. Por último, los genes presentes en los segmentos con SA y LOH fueron evaluados. Los genes relacionados con puntos calientes de retrotransposón (RHS) se encontraron flanqueando el inicio de las secuencias que presentaban SA. Los resultados observados sugieren que la compleja regulación del genoma involucrado en este parásito implica más procesos que otros eucariotas y podría estar involucrada en la respuesta para evitar diferentes tipos de estrés durante el complejo ciclo de vida de este parásito.

Para responder el segundo y tercer capítulo de esta tesis, se determinó el momento exacto de obtención de los tripomastigotes metacíclicos realizando curvas de metaciclogénesis en medio LIT y se seleccionó el día donde se presentó una diferencia estadísticamente significativa en el aumento de la producción de estas formas respecto al día cero. Como resultados en general, se logró establecer el día de inicio de la metaciclogénesis para las DTUs TcI y TcII y se estandarizó un protocolo para la producción y purificación de tripomastigotes metacíclicos en cultivo LIT por medio del uso de una cromatografía en resina de sefarosa-DEAE, de igual manera, se comprobó que esta técnica no afecta la capacidad infectiva del parásito de manera *in vivo* e *in vitro.*

Los resultados obtenidos para el segundo capítulo, relacionados con los perfiles de expresión de *T. cruzi* I, permitieron determinar que existía una diferencia entre la expresión génica de epimastigotes y tripomastigotes metacíclicos para la DTU TcI. Además, que una de las principales vías reguladas diferencialmente estaba relacionada con los ribosomas, de los cuales se infiere juegan un papel fundamental durante la regulación génica y mantenimiento del proteoma celular en el proceso de metaciclogénesis; otra vía diferencialmente expresada fue la autofagia, que se sabe participa durante todo el ciclo de vida de *T. cruzi* y es un estímulo fundamental en la metaciclogénesis, los perfiles energéticos relacionados con la glucosa, el metabolismo de los aminoácidos, y por último, los procesos celulares y de DNA. Para el

capítulo 3, se logró determinar que existían diferencias estadísticamente significativas entre todos los estadios presentes en el ciclo de vida de *T. cruzi* II, siendo importante destacar una clara diferenciación en la expresión génica entre los tripomastigotes derivados de células y los tripomastigotes metacíclicos. Al igual que como se reportó para el capítulo 2, una gran cantidad de genes relacionados con los procesos energéticos de la glucosa, la autofagia y los perfiles de genes codificantes para proteínas ribosomales fue diferencialmente expresado a lo largo del ciclo de vida de TcII demostrando su importancia en el ciclo de vida de este parásito. Sin embargo, de manera interesante este estudio fue capaz de captar la expresión de genes específicos relacionados con meiosis y recombinación homologa SPO11 y RAD51. Los resultados obtenidos abren una ventana de conocimiento para el análisis de diferentes procesos fundamentales en el ciclo de vida de *Trypanosoma cruzi*¸ e incluso algunos que no habían sido previamente descritos, que podrían aportar al entendimiento de la historia natural y biología de este parásito.

5. MARCO TEORICO

5.1 Taxonomía de *T. cruzi*

T. cruzi pertenece al dominio Eukarya, filo Euglenozoa, clase Kinetoplastidea, esta última, se caracteriza por la presencia de un organelo formado por un alto contenido de ADN extra-nuclear denominado kinetoplasto. Así mismo, este parásito se encuentra dentro de la familia Trypanosomatidae, formada únicamente por parásitos que presentan un solo flagelo, y donde se encuentran otros protozoos como *Leishmania spp* y *Trypanosoma brucei* (1).

5.2 Epidemiología

El protozoo flagelado *T. cruzi* es el agente causal de la enfermedad de Chagas, enfermedad que afecta a 8 millones de personas en el mundo, se estima que genera 12,500 muertes al año y aproximadamente 25’000.000 de personas están en riesgo de adquirirla (2). En nuestro país, se estima que alrededor de 437,960 personas se encuentran infectadas con el parásito, lo que corresponde a cerca del 5% de la población (3). Además, este parásito se encuentra asociado a diferentes manifestaciones clínicas y escenarios eco-epidemiológicos zoonóticos y enzooticos, hallándose desde el sur de Estados Unidos hasta Argentina y Chile (4, 5).

5.3 Variabilidad genética

T. cruzi presenta una alta variabilidad genética, exhibida en al menos seis unidades discretas de tipificación (DTUs) y TcBat, un genotipo asociado a la infección en murciélagos (TcI-TcVI y TcBat), siendo TcBat asociado a diferentes manifestaciones clínicas y escenarios eco-epidemiológicos zoonóticos y enzooticos. Las DTUs son definidas como "conjunto de poblaciones genéticamente más relacionadas entre sí que con cualquier otra población, y que son identificables por marcadores genéticos, moleculares o inmunológicos comunes" (Figura 1) (4, 5, 6, 7).

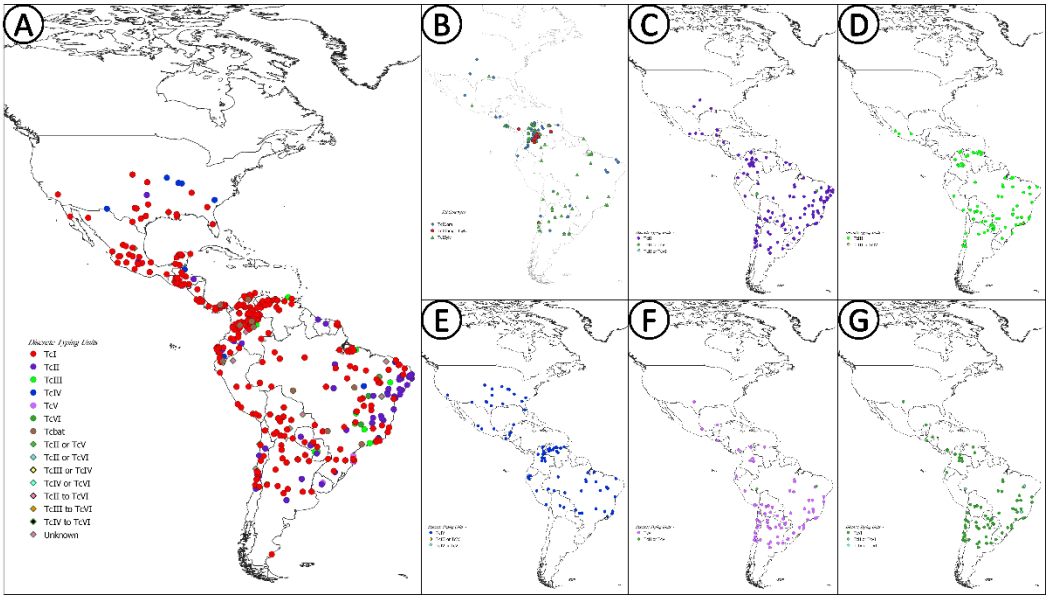

Figura 1. Distribución geográfica de: (A) DTUs de *Trypanosoma cruzi.* (B) Genotipos de TcI, (C) TcII, (D) TcIII, (E) TcIV, (F) TcV, (G) TcVi
Tomado de de: (8).

5.3.1 Diversidad genética de TcI

La DTU TcI está ampliamente distribuida a lo largo del continente americano, hallándose desde el sur de Estados Unidos hasta Argentina y Chile (5), además, posee una alta variabilidad genética, reflejada en genotipos asociados a los ciclos de transmisión doméstico y selvático (9-12).

En el año 2007, se reportó la presencia de variabilidad genética intra-específica en TcI, permitiendo así, la clasificación de esta DTU en cuatro haplotipos diferentes (a, b, c, d), siendo estos asociados a los ciclos de transmisión de la enfermedad en Colombia (10). Seguido a esto, y basándose en el estudio de polimorfismos de la secuencia de la región intergénica del gen mini-exón (SL-IR), estos haplotipos fueron denominados genotipos como: TcIa, asociado al ciclo doméstico de transmisión de la enfermedad y a la infección en humanos, TcIb, asociado a los ciclos doméstico y peridoméstico, TcIc, sin una asociación claramente definida, y TcId, asociado al ciclo selvático; estudios adicionales demostraron la existencia del genotipo TcIe, asociado al ciclo doméstico en Argentina y al ciclo selvático en Chile (9, 11). Posteriormente, por medio del uso de marcadores microsatélites en cepas obtenidas de todo el continente americano, se identificó un genotipo emergente aislado del ciclo de transmisión doméstico a quien denominaron Ven_{dom} (previamente TcIa), y que se encontraba asociado a la infección en humanos en Venezuela (13). Así mismo, en el año 2010, Ramírez *et al* evaluaron los genotipos de TcI circulantes en pacientes con cardiomiopatía Chagásica crónica, encontrando que aquellos pacientes infectados con TcId (cepas selváticas) presentaban más alteraciones cardíacas que aquellos infectados con TcIa (TcI_{dom}) (14). En el año 2013, Ramírez *et al* realizaron un análisis filogenético de 24 repeticiones cortas en tándem (STR), en 269 clones de TcI, y 10 marcadores mitocondriales, en 100 clones Colombianos; los resultados allí obtenidos

indicaron la existencia de un genotipo emergente asociado a la infección humana y que denominado TcI_{dom}, dicho genotipo correspondía a la clasificación previa de TcIa (15). En este mismo año, este genotipo fue confirmado a nivel continental por Zumaya-Estrada *et al*., reafirmando la importancia de TcI_{dom} en América (16). Por último, análisis filogenéticos adicionales donde se emplearon marcadores nucleares sobre clones Colombianos, confirmaron la presencia de TcI_{dom}, además de la presencia de un clado asociado a los ciclos selvático y peri-domestico de esta DTU (Figura 2), demostrando así la heterogeneidad presente en esta DTU (12).

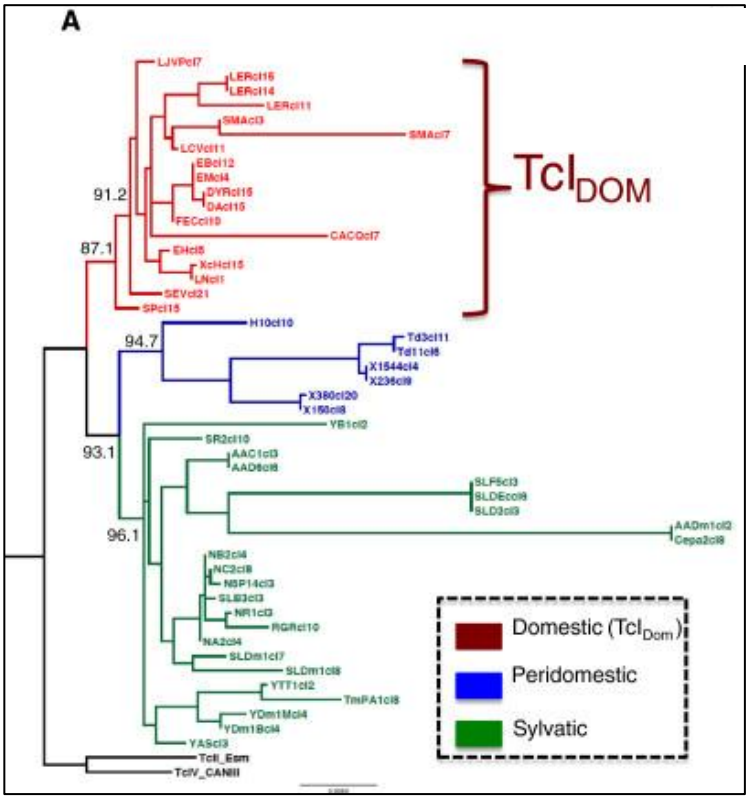

Figura 2. **Reconstrucción filogenética de *Trypanosoma cruzi* I a partir de marcadores nucleares en clones obtenidos de los ciclos de transmisión doméstico, peri-doméstico y selvático.**
Tomada de: (15).

El análisis de la distribución geográfica, sobre 996 reportes de TcI, realizado por Ramírez & Hernández en el año 2018, reitera la presencia de esta DTU a lo largo del continente americano (Figura 3). Mostrando una variación entre los reportes de TcI_{dom} y TcI selvático entre países, con frecuencias de 43.5% y 55.2% respectivamente, y la presencia de infecciones mixtas en el 1.3% de los reportes evaluados (17).

5.3.2 Comportamiento biológico de TcI

En el año 2015, se evaluó el comportamiento biológico de dos cepas caracterizadas con el genotipo TcI_{dom}, dos TcI selvático y una mezcla natural (tres clones domésticos y dos clones selváticos) en ratones ICR -CD1. Los resultados allí obtenidos demostraron que las cepas

domésticas presentaban altas parasitemas en comparación con las cepas selváticas. Además, cuando se evalúo la invasión de tejidos, los ratones infectados con cepas domesticas solo mostraban invasión en el tejido cardiaco y en el músculo esquelético, en contraste, las cepas del genotipo TcI selvático exhibían una alta invasión de tejidos, siendo capaz de infectar todos los tejidos empleados en el estudio, entre los que se encontraban; el tejido cardiaco, el musculo esquelético, tejido adiposo, colon y tejido nervioso. Otro hallazgo relevante, estuvo relacionado con las características encontradas en la infección mixta, que compartía propiedades de ambos genotipos, estando estas relacionadas con las altas parasitemias y la alta invasión de tejido (18). Un estudio de caracterización molecular realizado por Ramírez *et al*., 2013, sobre 50 clones de *T. cruzi*, generados a partir de 10 cepas aisladas de humanos y triatominos en 6 brotes de transmisión oral, demostró que 49 de los clones eran TcI, así mismo, al realizar la secuenciación de la región intergénica del gen miniexon (SL-IR), el 22 % de las cepas pertenecían al genotipo TcIa (TcI_{dom}), el 11% al TcIb (TcI_{dom}), y un 64 % al genotipo TcId (TcI selvático), mostrando así una relación de estos brotes con el ciclo selvático de la enfermedad (15). La presencia del genotipo TcI_{dom} en un explante de corazón en un paciente con enfermedad de Chagas Crónica y la posterior reactivación de la enfermedad luego de la inmunosupresión dada el transplante de corazón al que fue sometido también ha sido reportada (19). Adicionalmente, se ha corroborado que el genotipo TcI_{dom} está mucho más relacionado con altas parasitemias en pacientes agudos y a pacientes en la fase crónica de la enfermedad (17).

5.4 Ciclo de vida

T. cruzi posee un complejo ciclo de vida; se han descrito cuatro etapas morfológicas y funcionales bien diferenciadas: tripomastigotes procíclicos, tripomastigotes metacíclicos, amastigotes y epimastigotes. Tanto los tripomastigotes procíclicos como metacíclicos presentan una alta movilidad y no tienen capacidad de replicarse; por el contrario, las formas amastigotes y epimastigotes muestran una replicación constante y este último estadio es móvil. El ciclo de vida transcurre entre hospederos mamíferos, humanos y reservorios selváticos, donde se pueden encontrar las formas amastigotes y tripomastigotes, y entre vectores de la familia Reduviidae, quienes transmiten el parásito, con formas epimastigotes y tripomastigotes metacíclicos infectivos (Figura 3) (20, 21).

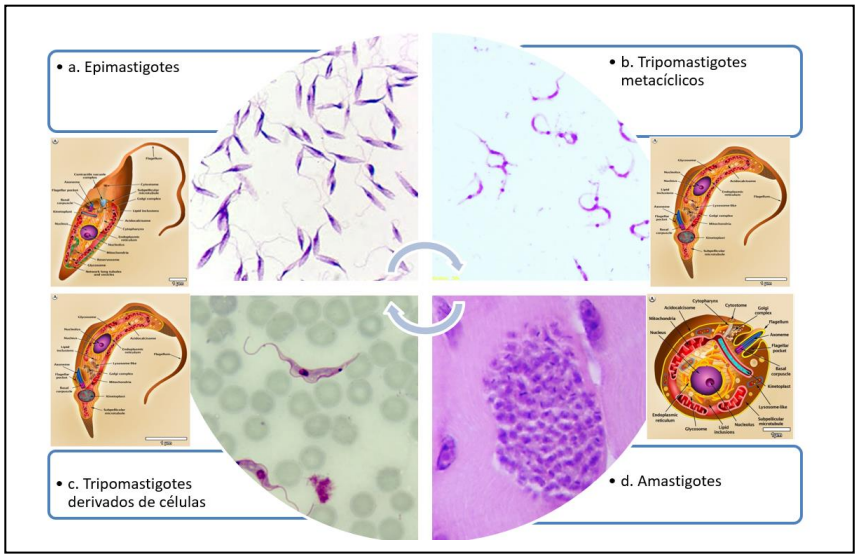

Figura 3. Estadios morfológicos durante el ciclo de vida de *Trypanosoma cruzi*.
(A)Epimastigotes: estadio replicativo móvil, presente en el ciclo de *T. cruzi* en el vector. (B)Tripomastigotes metacíclicos: estadio infectivo de parásito, móvil no replicativo, presente en el ciclo de *T. cruzi* en el vector. (C) tripomastigotes derivados de células: estadio no replicativo móvil, presente en el ciclo de vida del mamífero. (D)Amastigotes: estadio replicativo no móvil, presente en el ciclo de vida del mamífero.
Modificado de: (21)

Durante el ciclo de vida del parasito en el hospedero mamífero, se generan dos fases importantes, la primera corresponde a la infección de las células mononucleares de sangre periférica por parte de los tripomastigotes metacíclicos provenientes del vector, y la segunda, corresponde a la infección de células específicas (cardiacas, enterocitos, adipocitos, tejido nervioso), por tripomastigotes procíclicos liberados a partir de las células mononucleares (22). Durante ambas fases se presenta una serie de pasos necesarios para su progresión, entre estos están: el reconocimiento e infección, la internalización y la diferenciación, la replicación, y finalmente, la transformación y liberación del parásito. Los pasos en ambas fases son iguales, sin embargo, las proteínas expresadas presentan un carácter diferencial dirigido a funciones distintas, como lo es una infección inicial eficaz y la evasión del sistema inmune respectivamente (23).

El ciclo de vida del parásito en mamíferos comienza cuando tripomastigotes metacíclicos provenientes del vector, ingresan a sangre periférica y alcanzan células mononucleares como los monocitos, con las que generan un proceso de reconocimiento con diferentes proteínas de la membrana de la células huésped logrando el ingreso a estas, en el interior, se genera la formación de una vacuola parasitófora que envuelve al tripomastigote, el cual se transforma en amastigote gracias al estrés al que está sometido el parásito; este proceso lleva como nombre amastigogenesis. Los amastigotes, formas no móviles replicativas, realizan múltiples rondas de replicación, hasta transformarse en tripomastigotes procíclicos, que no son replicativos y presentan una alta movilidad. Finalmente, y gracias al alto movimiento mecánico que estos ejercen sobre la célula infectada, la membrana de la célula infectada se rompe liberando una gran cantidad de parásitos a sangre periférica. Los parásitos liberados continúan su viaje en búsqueda de nuevas células por infectar (Figura 4) (21).

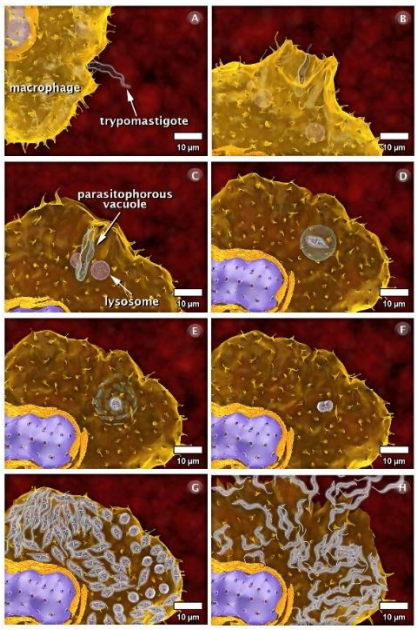

Figura 4. Ciclo biológico de *Trypanosoma cruzi* en células mononucleares.

(A) Reconocimiento de la célula blanco por parte del tripomastigotes metacíclico. (B) Ingreso del tripomastigote metacíclico a la célula y formación de la vacuola parasitófora. (C) Transformación a amastigote. (D) Replicación del amastigote. (E) Transformación a tripomastigotes procíclicos. (F) Liberación de los tripomastigotes procíclicos.

Tomado de: (21)

La segunda fase del ciclo en el mamífero comprende la infección de células especificas (miocitos cardiacos, enterocitos, adipocitos o células de sistemas nervioso central) por parte de los tripomastigotes procíclicos liberados a partir de las células mononucleares de sangre periférica. Este proceso presenta los mismos pasos descritos en la primera fase; sin embargo, se sabe que existe una fuerte modificación en las proteínas de la membrana asociadas a la evasión del sistema inmune, necesaria para la progresión del ciclo (Figura 5).

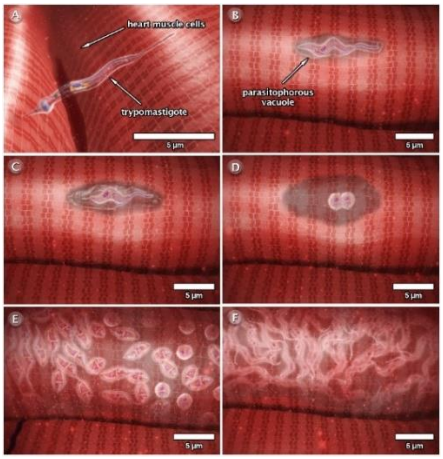

Figura 5. Ciclo biológico de *Trypanosoma cruzi* en células cardiacas.

(A) Reconocimiento de celulas cardiacas por parte de un tripomastigote procíclico. (B) Ingreso del tripomastigote prociclico y formación de la vacuola parasitófora, (C) Transformación en amastigote. (D) Replicación del amaatigote. (E) Transformación en tripomastigote procíclico. (F) Liberación de los tripomastigotes procíclicos.

Tomado de: (21)

El ciclo en el insecto comienza cuando este se alimenta de sangre periférica de mamíferos infectados con tripomastigotes, estos se desplazan hacia el intestino del vector, y gracias a la acción de sustancias como la hemina y la α-globina, los tripomastigotes procíclicos se transforman en epimastigotes replicativos. Los epimastigotes continúan migrando hacia la parte posterior del intestino del insecto, realizando múltiples rondas de replicación durante su paso hasta alcanzar el recto, ya en este, los epimastigotes se adhieren a la película perimicroviliar de las células epiteliales allí presentes, gracias a la acción de diferentes proteínas y al desequilibrio redox al que son sometidos, finalmente se transforman en tripomastigotes metacíclicos. El proceso por el cual epimastigotes replicativos se transforman en tripomastigotes metacíclicos infectivos tiene por nombre metaciclogénesis y comprende un paso fundamental en el ciclo de vida del *T. cruzi* (Figura 5) (24, 25).

Figura 6. Ciclo de vida de *Trypanosoma cruzi* en el insecto.

(A) Ingesta de sangre con tripomastigotes procíclicos. (B) Transformación a epimastigotes y esferomastigotes en el intestino del vector. (C) Replicación de los epimastigotes. (D) Adhesión de los epimastigotes a la película perimicrobiliar de las células del intestino del vector. (E) Transformación a tripomastigotes metacíclicos. (F) Triatomino infectado.

Tomado de: (21)

5.4.1 Metaciclogénesis

La metaciclogénesis cumple uno de los pasos más importantes y esenciales en el ciclo de vida de *T. cruzi*, donde un conjunto de cambios morfológicos, transcriptómicos, proteicos y metabólicos permiten al parásito prepararse para lograr una infección exitosa (26). Entre los cambios morfológicos más relevantes se encuentran la modificación de la posición y forma del núcleo y el kinetoplasto, asociado con un aumento en la heterocromatina, así mismo, un alargamiento del flagelo, y finalmente, una elongación del citoplasma (27). La evaluación del proteoma y fosfoproteoma durante este proceso ha mostrado una regulación de proteínas relacionadas con la transcripción, trans-sialidasas, mucin-associated surface proteins

(MASP), y dispersed gene family 1 (DGF-1), y además, del fosto-proteomaa transcurridas 12 a 24 después de la adhesión (28). El aumento de la expresión de proteínas de familias multigénicas también ha sido reportado para proteínas como la gp82, la colpain y la cruzipain, lo que estaría relacionado con el carácter infectivo que presentan los tripomastigotes metacíclicos (29, 30). Sobre los cambios metabólicos, se ha observado un aumento en la proteólisis, un aumento en el metabolismo asociado a la respuesta al estrés redox, que es coherente con la fuerte influencia de este proceso en la metaciclogénesis, y más recientemente se ha reportado la influencia de la regulación de la autofagia durante este proceso (31-33).

5.5 Las ómicas en el estudio de *T. cruzi*

La necesidad de nuevo conocimiento relacionado principalmente a la comprensión de procesos biológicos desencadenó un aumento en el avance de la tecnología y el desarrollo de diferentes herramientas bioinformáticas. Esto ha permitido dilucidar preguntas e hipótesis a distintos niveles dentro del dogma central de la biología molecular. Algunas de las principales disciplinas ómicas que han sido de ayuda en los procesos de investigación son: la genómica, la transcriptómica, la proteómica y finalmente la metabolómica siendo ampliamente estudiaba en humanos (34). El avance de la biología molecular se dio con el descubrimiento de la estructura del ADN por Watson y Crick en 1953, que se consolido con la implementación del proyecto genoma humano en 1986 y su posterior publicación en el año 2003 (35). La información allí obtenida demostró la necesidad de nuevas tecnologías de secuenciación, generó una gran cantidad de conocimientos y abrió la puerta a nuevos interrogantes y a nuevas disciplinas como la transcriptómica y la proteómica (36). Más recientemente han sido aplicadas todas estas herramientas al estudio de microorganismos como *T. cruzi*.

5.5.1 Genómica de *T. cruzi*

El primer estudio de genoma completo de *T. cruzi* fue reportado en el año 2005 por El-Sayed *et al*., y fue realizado sobre la cepa CL-Brener, cepa clasificada actualmente como TcVI. Entre los hallazgos más importantes, para este protozoo, se predijeron 22570 proteínas codificadas por genes, de los cuales 12570 representan pares alélicos; además se encontró que al menos un 50% del genoma del parásito estaba compuesto por secuencias repetitivas, que codificaban para retrotransposones y moléculas de superficie como las transialidasas (37). Además, el análisis comparativo del genoma de CL-Brener con otros tripanosomátidos como *Trypanosoma brucei* y *Leishmania major* demostró la presencia de al menos 6200 genes policistronicos sinténicos conservados entre las diferentes especies (38). En el año 2011, Franzén *et al*., realizaron un análisis comparativo intra-especie entre la cepa CL-Brener (TcVI), previamente secuenciada, y la cepa Sylvio X10/1 (TcI), secuenciada a partir de la tecnología Roche 454. Los resultados mostraron una disminución en el número de copias de genes multicopia en la cepa TcI respecto a la TcVI; además se evidenciaron eventos de

deleción y cambios no sinónimos en los nucleótidos que afectaron la codificación de los aminoácidos, lo que incidió fuertemente en el tamaño del genoma de Sylvio X10/1. A pesar de esto, no se encontró una gran variación entre la cantidad de ADN presente en las regiones no codificantes (39). En un segundo estudio, se realizó la comparación entre la cepa Sylvio X10/1 (TcI) con otro tripanosomátido, *Trypanosoma cruzi marinkellei*; demostrando una disminución en el tamaño del genoma de este último; esta disminución se debe a una variación en el número de copias de algunos genes codificantes y no codificantes (40). En el año 2014, se realizó la secuenciación del clon Dm28c, clasificado como TcI al igual que la cepa Sylvio X10/1; ambas relacionadas con el ciclo selvático de transmisión del parásito, para dicho fin, fue empleada la tecnología de secuenciación de Roche 454. La anotación de este genoma mostró la presencia de 4144 proteínas homologas en otros organismos. Respecto a la comparación con las cepas Sylvio X10/1 y CL-Brener, se observó una identidad de 98.71% y 90.20% respectivamente, lo que era de esperarse teniendo en cuenta la DTU a la que cada una pertenece; resultados similares fueron obtenidos para el análisis bidireccional de proteínas entre cepas (41).

T. cruzi presenta un complejo genoma constituido por una gran cantidad de regiones repetitivas, lo que dificulta su análisis, esto requiere la secuenciación del genoma por una tecnología más robusta como PacBio Single Molecular Real-Time (SMRT), esta herramienta permite la secuenciación de segmentos más largos y por tal un ensamblaje mucho más confiable. Recientemente, Berná *et al.,* (2018) utilizaron esta metodología para realizar la secuenciación de dos clones, Dm28c (TcI) y TCC (TcVI). Los resultados obtenidos confirmaron la presencia de un amplio grupo de genes multicopia, genes conservados, transposones y repeticiones en tándem a lo largo del genoma de este parásito. Adicionalmente, los autores mostraron que el genoma de *T. cruzi* se encuentra dividido en dos compartimientos que presentan diferencias en el porcentaje de Guanina-Citosina (GC); uno compuesto por genes conservados e hipotéticos llamado “compartimiento central”, y otro por genes de copia múltiple llamado “compartimento disruptivo” (Figura 7). Adicionalmente, el ensamblaje de cromosomas homólogos de forma individual permitió determinar la presencia de recombinaciones homologas entre estos (42).

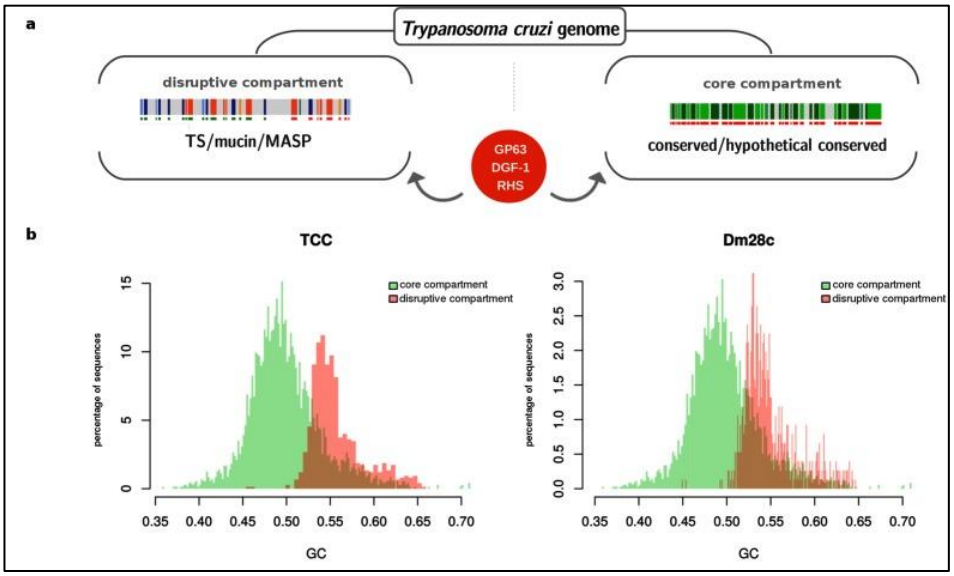

Figura 7. Compartimentación del genoma de *Trypanosoma cruzi.*
*(*A) Estructura del genoma propuesta.
(B) Porcentaje de GC por cada compartimiento para las cepas TCC y DM28c.
Tomado de: (42)

Se realizó la secuenciación por medio de la plataforma PacBio de dos DTUs, TcII (cepa Y) y TcV (Bug2148); este análisis se realizó teniendo en cuenta la diferencia que ha sido descrita entre las DTUs respecto al tamaño del genoma y número de copias para algunos genes. Los resultados obtenidos demostraron que las familias de genes multicopia, donde se encuentran una gran cantidad genes que codifican para proteínas transmembranales importantes en la virulencia del parásito, se ubicaban cerca de las regiones teloméricas, expuestas a una mayor presión evolutiva. Los autores sugieren la presencia de un genoma "core" que comparte una alta homología entre toda la especie, y una expansión en los genes que codifican para estas proteínas entre las distintas DTUs, lo que podría explicar las características biológicas y virulentas diferenciales entre estas (43).

Análisis del genoma de 34 aislamientos de TcI, provenientes de diferentes regiones de América, mostraron una agrupación asociada con su distribución geográfica, lo que podría estar relacionado con una adaptación a los vectores y hospederos presentes en cada región. Por medio de la plataforma PacBio, se logró la secuenciación del genoma de la cepa TcI Sylvio X10/1, demostrando su alta complejidad, la presencia de una gran cantidad de retrotransposones y una alta variabilidad en los grupos de genes multicopia relacionados con los antígenos de membrana presentes en *T. cruzi*; este hallazgo es importante para el análisis y asociación de la virulencia de este parásito (Talavera-Lopez *et al*., 2021). El análisis de 45 genomas de TcI provenientes de Ecuador, permitió establecer una alta variabilidad intra-DTU, donde se encontraron poblaciones coherentes con una estructura poblacional sexual y otras con la clonal. Algunas poblaciones presentaban una alta heterocigosidad, secuencias mitocondriales comunes y niveles de aneuploidía incompatibles con el sexo mendeliano; mientras otras, mostraban menor aneuploidía y una mayor relación con una replicación

parasexual (Figura 8) (Schwabl *et al*., 2019).

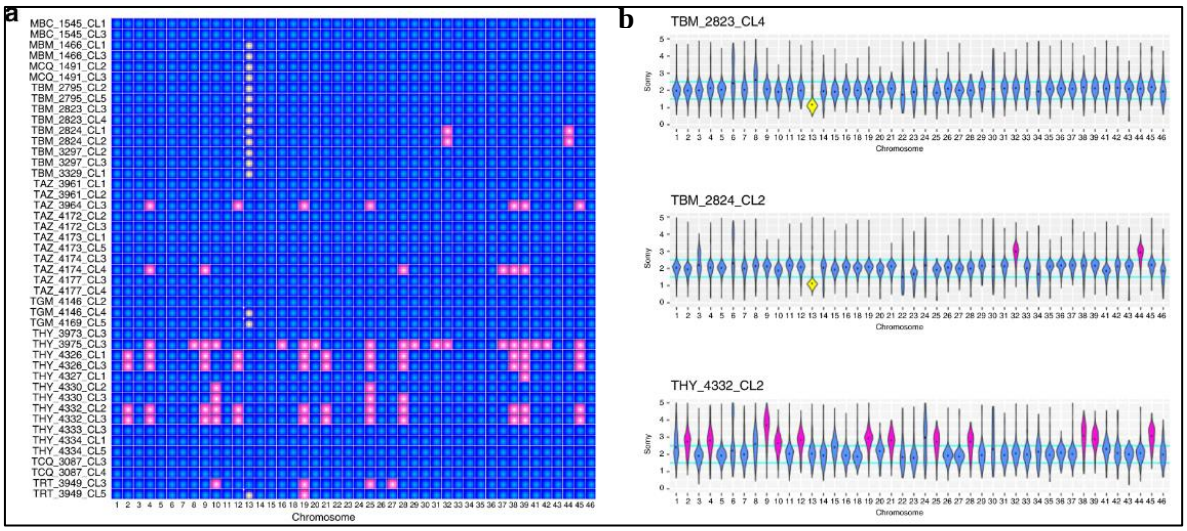

Figura 8. Niveles de aneuploidía entre clones de *Trypanosoma cruzi* I.

(A) El heatmap muestra el numeronúmero de copias por cada cromosoma (eje x) por cada clona evaluado en el estudio (eje y), cromosomas haploides: color blanco, diploides: color azul, y triploides o más: rosado. (B) Gráficas de violines para tres clones con características diferenciales de aneuploidía, cromosomas haploides: color amarillo, cromosomas diploides: azul, triploides o más: rosado.

Tomado de: (43)

Recientemente se reportó el análisis de los genomas de las cepas Brazil-B4 (TcI) y la cepa Y (TcII) a partir de estrategias hibridas de secuenciación de fragmentos cortos y largos y mapeos específicos para lograr genoma de alta calidad. Los análisis corroboraron las características de aneuploidía cromosomal dentro del genomas de *T. cruzi*, siendo el cromosoma 24 uno de los más afectados, y adicionalmente, la presencia de variaciones alélicas en segmentos de cromosomas diploides (Figura 9). Así mismo, reporta procesos de amplificación y dispersión de genes importantes relacionados en su mayoría con las secuencias repetitivas, entre estos: MASP, mucinas, transialidasas y los puntos calientes de retro-transposones (RHS). Así mismo, estos genes podían seguir los procesos mencionados involucrando segmentos que incluían más de un gen y que no necesariamente se encontraran relacionados o en el mismo sentido de la hebra, indicando una influencia de procesos recombinación y mutaciones en la diversificación de los genomas de *T. cruzi*. Adicionalmente, se logró determinar la presencia de una gran cantidad de ARN antisentido indicando la influencia de estos en la regulación postranscripcional del parásito (Wang *et al*., 2021).

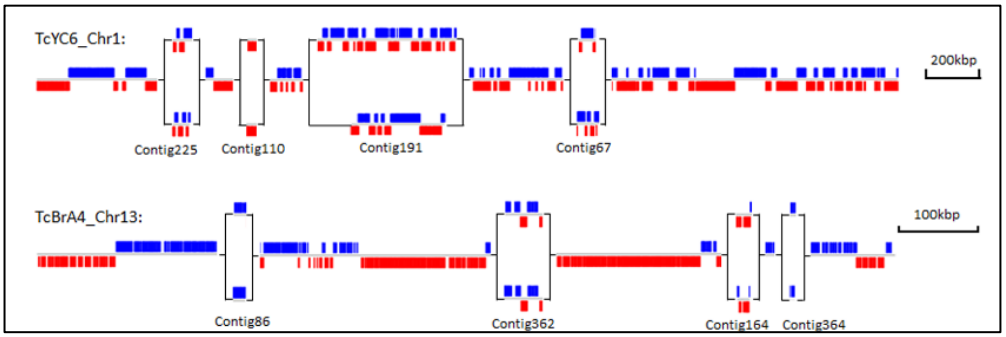

Figura 9. Variación alélica segmental en cromosomas diploides de *Trypanosoma cruzi*. Cromosomas diploides 1 de las cepa Y (TcII) y 13 de la cepa Brazil B4 (TcI), de color rojo y azul cada uno de los alelos, los recuadros muestran áreas con variación alélica donde más de dos alelos son observados.
Tomado de: (45)

5.5.2 Transcriptómica de *T. cruzi*

Una de las características que posee *T. cruzi* es la presencia de una regulación post-transcripcional altamente compleja, donde interactúan ARNs policistrónicos, que a diferencia de los operones de las bacterias no siempre presentan genes relacionados entre sí. Esto ha llevado a hacer de la transcriptómica una herramienta fundamental para comprender y relacionar los hallazgos genómicos y biológicos descritos para este parásito. Una doble captura de ARN entre *T. cruzi* y miocitos primarios humanos, fue realizada por Udoko *et al* en el año 2015. Los resultados obtenidos mostraron un incremento en la expresión de genes fibróticos como EGR1, SNAI1 e IL 6, además de la modulación y activación de otras proteínas como SMAD2/3 y el factor de transcripción JunB; a pesar de que los resultados presentados fueron obtenidos a partir de micro-arreglos, este fue un primer acercamiento a la utilidad de la transcriptómica (46).

En el año 2016 se realizó un estudio cuyo objetivo fue evaluar la remodelación del transcriptoma durante la infección en diferentes periodos de tiempo implementando la tecnología de ARN-seq; los resultados obtenidos mostraron diferencias en el transcriptoma durante la infección temprana comparada con la infección tardía, la cual cuenta con la presencia de amastigotes maduros y entre los tripomastigotes liberados. Además, es importante resaltar que dicha diferencia se mantiene en la expresión génica de la célula infectada, lo que sugiere una modulación de esta por parte del parásito (47).

Previamente se ha mencionado la comparación entre genomas de distintas DTUs, demostrando una clara diferencia entre estos. En el año 2016, se realizó un análisis comparativo entre los transcriptomas de las cepas Sylvio (TcI) y Y (TcII) obtenidos a partir de la infección de fibroblastos humanos con el fin de entender las diferencias biológicas observadas tanto a nivel *in vitro* como *in vivo*. A pesar de que no se encontraron diferencias claras entre la expresión de genes, si se observó un aumento en la expresión de IL-8 en células infectadas con Sylvio X10, esto fue correlacionado con la expresión de proteínas codificadas por genes de múltiple copia, que se encuentran presentes con gran abundancia en el genoma

de *T. cruzi* y que en su mayoría codifican para factores de virulencia del parásito, pero que no fueron capturados por la técnica de secuenciación empleada en este análisis (48).

Teniendo en cuenta la heterogeneidad que presenta este parásito, y en aras de comprender las diferencias en la virulencia entre cepas, se realizó un análisis transcriptómico de dos clones, CL Brener (virulento) y CL-14 (no virulento); aquí, los autores seleccionaron dos puntos durante la infección en células, 60 y 96 horas, tiempos dónde solo se encuentran formas amastigotes intracelulares de parásito y una fase de tripomastigotes libres, respectivamente. Los resultados mostraron una clara diferencia entre la expresión de proteínas en el clon no virulento durante el primer punto de infección (60 horas) y los tripomastigotes libres, respecto al segundo punto de infección (96 horas); en contraste, en el clon virulento, todos los puntos seleccionados mantuvieron niveles similares en la expresión. Estos cambios en la expresión se encuentran relacionados con la presencia de proteínas de superficie implicadas en el proceso de infección del parásito, el retraso en la expresión de estas proteínas podría explicar la disminución de la virulencia en dicho clon (49).

Entre las características más importantes que presenta *T. cruzi* se encuentra su complejo ciclo de vida, en los estudios previamente mencionados se han analizados los amastigotes y tripomastigotes derivados de células, presentes durante el ciclo biológico en el mamífero, mostrando una clara diferencia en la expresión de genes entre estos. Sin embargo, no se había realizado la comparación con estadios presentes en el vector como lo son las formas epimastigotes, dicho estudio fue realizado por Berná *et al.*, en el año 2017. En este, *T. cruzi* mostró una alta plasticidad, relacionada principalmente con la capacidad de adaptación a distintos ambientes de estrés durante su ciclo de vida, donde las formas epimastigotes presentaron una alta expresión de proteínas asociadas al metabolismo energético, los tripomastigotes derivados de células exhibieron una expresión relacionada con la evasión del sistema inmune del hospedero, y finalmente, los amastigotes mostraron la expresión de genes relacionados con la progresión del ciclo de vida. Lo anterior comprueba la importancia de cada una de las formas de vida de *T. cruzi* en la progresión de su ciclo de vida (Figura 10) (50).

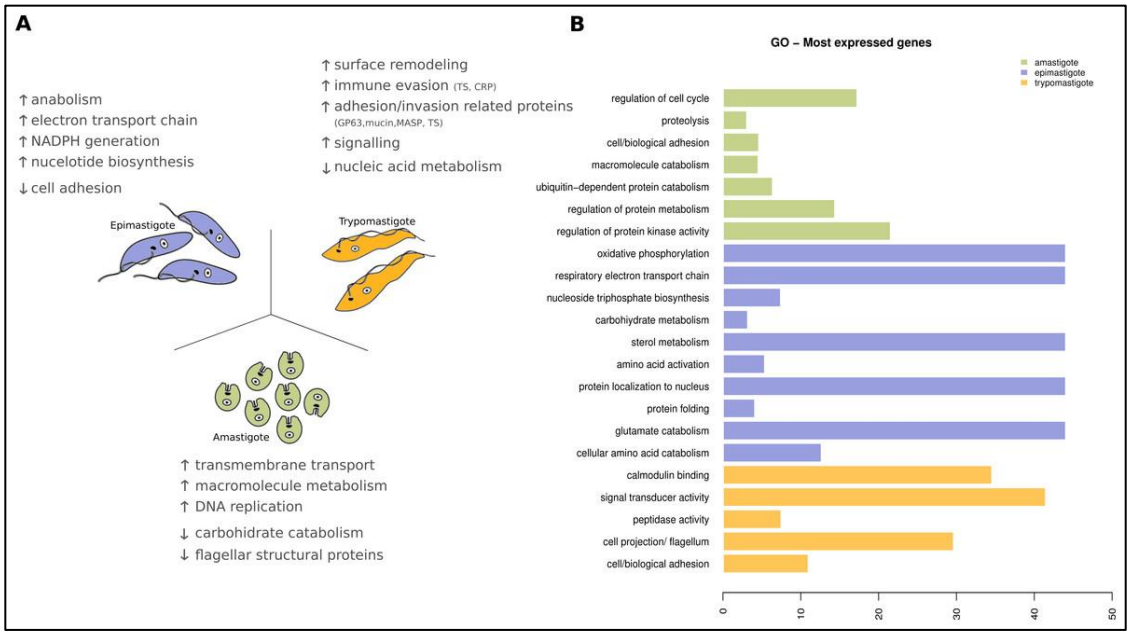

Figura 10. Genes expresados de manera diferencial entre las formas epimastigotes, amastigotes y tripomastigotes de *Trypanosoma cruzi.* (A) Vías más representativas por estadio. (B) Ontología de genes.
Tomada de: (50)

6. OBJETIVOS

OBJETIVO GENERAL

Evaluar la arquitectura genómica y los perfiles de expresión génica durante el ciclo de vida de *Trypanosoma cruzi*.

OBJETIVOS ESPECÍFICOS

1. Describir la arquitectura genómica y diversidad genética de clones de *Trypanosoma cruzi* I (TcI).

2. Evaluar los perfiles de expresión génica de *Trypanosoma cruzi* I durante el proceso de metaciclogénesis *in vitro*.

3. Determinar la remodelación en la expresión génica durante el ciclo de vida de *Trypanosoma cruzi* II.

7. INTRODUCCIÓN A LOS CAPÍTULOS

La alta variabilidad genética de *T. cruzi* ha permitido la clasificación de este parásito en seis DTUs, sin embargo, los análisis a nivel genético de genes únicos y estrategias como Multilocus Sequence Typing (MLST), donde se han incluido genes nucleares, mitocondriales y secuencias microsatélites, han demostrado que la variabilidad genética puede inclusive encontrarse presente a un nivel intra-DTU. Tal es el caso de la DTU TcI, la DTU más ampliamente distribuida, donde se han llegado incluso a describir genotipos con características genómicas y propiedades biológicas diferenciales, pero que, sin embargo, la diversidad presente en esta DTU no ha sido totalmente explorada a un nivel genómico, siendo en parte consecuencia de la ausencia de un genoma de referencia de alta calidad, el cual fue reportado hace aproximadamente cuatro años. El genoma de *T. cruzi* es uno de los grandes desafíos en el estudio de este parásito dada la presencia de secuencias repetitivas a lo largo de este, las cuales adicionalmente codifican para un gran parte de factores de virulencia que se expresaran a lo largo de ciclo de vida en procesos fundamentales de este parásito. Así mismo, y gracias al avance de estrategias de secuenciación de cuarta generación en los últimos años, se ha podido corroborar la alta plasticidad genómica que presenta este parásito incluyendo la capacidad de tolerar aneuploidías en varios cromosomas o la presencia de variación alélica en algunos cromosomas. A pesar del rápido crecimiento de la ciencia en las estrategias de secuenciación de genomas con características complejas como el de *T. cruzi*, no han sido realizados análisis donde se evalúen las características relacionadas con la arquitectura genómica de las cepas colombianas de *T. cruzi* y si existe una relación o diferenciación con las cepas TcI circulantes a lo largo del continente americano siendo Colombia uno de los países donde se ha reportado una gran diversidad genética en esta DTU.

Por otro lado, los procesos de regulación génica son otros de los grandes desafíos en *T. cruzi*, aún más si se tiene en cuenta la alta plasticidad fenotípica de este parásito que incluye la capacidad de diferenciarse a 4 estadios morfológicos durante su ciclo de vida, donde algunos de estos tienen características replicativas o infectivas, siendo para este último el proceso de metaciclogénesis fundamental en la generación de tripomastigotes metacíclicos, forma infectiva del parásito. Este proceso representa un panorama complejo en cuanto a la regulación de procesos biológicos, permitiendo al parásito adaptarse a las condiciones de estrés a las que es sometido y confiriéndole características infectivas y mecanismos de evasión de la respuesta inmune en los huéspedes, lo que, a su vez, le permitirá continuar con el desarrollo de su ciclo de vida de una manera exitosa. La descripción de nuevas enzimas o diferentes cambios morfológicos sobre este proceso, aumenta con el avance en el estudio de este parásito, sin embargo, hasta el momento no se ha logrado obtener una correlación precisa y coherente entre todos estos hallazgos; por lo tanto, una evaluación a mayor escala sobre la expresión génica que presenta *T. cruzi* durante la metaciclogénesis es requerida. Por otro lado, el ciclo de vida que este parásito sigue realiza en mamíferos ha sido un poco más conocido a nivel transcripcional, varios estudios se han enfocado en la de remodelación génica durante la infección celular, los posibles cambios en el transcriptoma entre cepas infectivas y no infectivas, e inclusive han llegado a evaluar los estadios

presentes en el mamífero (amastigotes y tripomastigotes derivados de células) con los epimastigotes, sin embargo, no han sido integrados los tripomastigotes metacíclicos dentro de estos análisis, siendo su expresión génica relacionada o reportada de igual manera que los tripomastigotes derivados de células, y aún más teniendo en cuenta las características infectivas de este estadio. En las últimas décadas el desarrollo de estrategias de secuenciación como ARN-seq, ha permitido la solución a preguntas científicas sobre la biología e interacciones con el hospedero de diferentes tripanosomatidos (51). El enfoque de esta tecnología permite capturar todo el transcriptóma de una célula en un momento determinado e identificar los genes involucrados en la regulación de un proceso específico. Con respecto a *T. cruzi*, ha sido de utilidad en el análisis de la expresión de genes en la infección en células de mamífero, que ha permitido comprobar la diferencia entre los perfiles de expresión de TcI y TcII en fibroblastos, y en la evaluación de la expresión génica en tres de los 4 estadios de este parásito (46-48); No obstante, no ha sido empleada en el análisis del proceso de metaciclogénesis. Un análisis de ARN-seq además de proveer una mayor claridad sobre los genes que se expresan durante la metaciclogénesis, la remodelación y regulación génicas en el ciclo de vida, permitirá correlacionar la expresión de estos genes y las diferentes cepas.

Teniendo en cuenta las características complejas del genoma de *T. cruzi*, y la importancia de la metaciclogénesis, y así mismo del complejo ciclo de vida *T. cruzi*, esta tesis busca responder el objetivo general en tres capítulos:

CAPÍTULO 1: Arquitectura genómica y diversidad genética de clones de *Trypanosoma cruzi* I (TcI).

CAPÍTULO 2: Perfiles de expresión génica de *Trypanosoma cruzi* I durante el proceso de metaciclogénesis *in vitro.*

CAPÍTULO 3: Remodelación en la expresión génica durante el ciclo de vida de *Trypanosoma cruzi* II.

CAPÍTULO 1

Con el fin cumplir con el objetivo específico 1, el capítulo 1 se enfocó en la evaluación de la arquitectura genómica de 18 clones colombianos generados a partir de 5 cepas, de las cuales se extrajo en ADN y posteriormente se secuenciaron mediante la plataforma de Illumina. Adicionalmente, y con el fin de incluir genomas de distintas partes de las Américas, los datos de secuenciación de 15 clones TcI aislados de 5 países diferentes fueron incluidos. Se realizó el análisis filogenético, la determinación de la somia cromosomal, y de eventos de aneuploidía segmental y perdida de heterocigocidad, al igual que la exploración de los genes asociados a estos eventos de plasticidad genómica. Los resultados a mayor detalle pueden ser encontrados en el siguiente artículo:

- **Artículo 1:** Cruz-Saavedra L., Schwabl P., Munoz M., Patino L., Vallejo GA,

Llewellyn M., Ramirez, J. D. Evidence of genomic plasticity in *Trypanosoma cruzi* I driven by aneuploidy and loss of heterozygosity. (SOMETIDO a mBio).

CAPÍTULO 2

Una de las características que se pueden observar al realizar un cultivo de tripomastigotes metacíclicos *in vitro* es la incapacidad de producir un cultivo que contenga este estadio morfológico de *T. cruzi* únicamente. Teniendo en cuenta lo anterior, y las características propias de este estudio, donde era necesario y determinante obtener muestras que únicamente presentaran tripomastigotes metacíclicos para la extracción de ARN, nos propusimos estandarizar un método sencillo y eficaz que permitiera la producción y purificación de este estadio, y que, además, no afectara las características infectivas y la viabilidad del parásito. Los resultados obtenidos mostraron que un cultivo en medio LIT a partir de una concentración de 1×10^7 epimastigotes/mL, seguido de una purificación por medio de una cromatografía en resina de sefarosa-DEAE permitían la obtención de los tripomastigotes metacíclicos puros.

Como producto de este capítulo se adjuntan el siguiente artículo científico:

- **Artículo 2:** Cruz-Saavedra L, Muñoz M, León C, Patarroyo MA, Arevalo G, Pavia P, Vallejo G, Carranza JC, Ramírez JD. Purification of *Trypanosoma cruzi* metacyclic trypomastigotes by ion exchange chromatography in sepharose-DEAE, a novel methodology for host-pathogen interaction studies. J Microbiol Methods. 2017 Nov;142:27-32. doi: 10.1016/j.mimet.2017.08.021. Epub 2017 Sep 1. PMID: 28865682.

Con fin de cumplir con el objetivo específico 2 inmerso en el capítulo 2, epimastigotes de *T. cruzi* previamente caracterizados como TcI fueron cultivados a partir de una concentración inicial de 1×10^7 epimastigotes/mL, se realizó el seguimiento de la concentración de los parásitos y de los estadios morfológicos del parásito presentes durante 10 días. A partir de los resultados obtenidos se determinó el tiempo de inicio de la metaciclogénesis, que correspondió al día donde se presentaba un aumento significativo en las formas tripomastigotes metacíclicos respecto al día control (Día 0).

En paralelo con los objetivos incluidos en esta tesis se realizó un análisis de los cambios en la expresión génica durante la metaciclogénesis de las DTUs TcI y TcII al ser expuestos a distintas temperaturas. Se realizó la comparación entre TcI y TcII expuestos a 26°C, temperatura empleada para los demás estudios parte de este capítulo, razón por la cual los datos obtenidos nos brindan los resultados sobre las diferencias en la metaciclogénesis entre TcI y TcII. Estos resultados fueron depositados es el artículo 3.

Como producto de este capítulo se adjuntan el siguiente artículo científico:

- **Artículo 3:** Cruz-Saavedra L, Muñoz M, Patiño LH, Vallejo GA, Guhl F, Ramírez JD.

Slight temperature changes cause rapid transcriptomic responses in *Trypanosoma cruzi* metacyclic trypomastigotes. Parasit Vectors. 2020 May 14;13(1):255. doi: 10.1186/s13071-020-04125-y. PMID: 32410662; PMCID: PMC7226949.

Con el fin de cumplir con el objetivo de este capítulo fue necesario implementar los resultados obtenidos a partir de los artículos 2 y 3. Cultivos de *T. cruzi* caracterizados previamente como TcI fueron realizados a partir de 1×10^7 epimastigotes/mL, transcurridos los días que habían sido previamente calculados como días de inicio de la metaciclogénesis para la DTU TcI se realizó la purificación de los tripomastigotes metacíclicos con la metodología implementada en el artículo 2. Los tripomastigotes metacíclicos obtenidos, al igual que a epimastigotes, se les realizó la extracción de ARN y la evaluación de calidad de este, y los ARNs que superaron las pruebas de calidad fueron enviados a secuenciación utilizando la plataforma Illumina Xten. Posteriormente, los reads obtenidos fueron procesados y se realizó en análisis de expresión diferencial y reconstrucción de vías de señalización.

Los resultados análisis para el análisis de la metaciclogénesis de TcI, se encuentran depositados en el siguiente artículo:

- **Artículo 4:** Cruz-Saavedra L, Vallejo GA, Guhl F, Messenger LA, Ramírez JD. Transcriptional remodeling during metacyclogenesis in *Trypanosoma cruzi* I. Virulence. 2020 Dec;11(1):969-980. doi: 10.1080/21505594.2020.1797274. PMID: 32715914; PMCID: PMC7549971.

CAPÍTULO 3

En respuesta al objetivo específico 3 en el capítulo 3, realizamos un análisis del ciclo de vida TcII, donde quisimos realizar una aproximación mayor, se siguió una metodología similar a la planteada para el capítulo 2 con el fin de obtener reads correspondientes a la expresión génica de los tripomastigotes metacíclicos de TcII, esta incluyo determinación de las curvas de metacíclogenesis (artículo 3 -figura 1b) y la purificación de los tripomastigotes mediante una cromatografía en sefarosa-DEAE (artículo 2), los resultados relacionados con esta parte de la metodología fueron previamente mencionados en el segundo capítulo en los artículos 2 y 3.

Por otro lado, y aprovechando la disponibilidad de los reads a partir de ARN de epimastigotes, tripomastigotes derivados de células y amastigotes de TcII en la base de datos de The European Nucleotide Archive (ENA) bajo el proyecto PRJNA25158, implementamos el primer análisis de ARNseq (hasta donde la literatura no lo permite conocer), donde no solamente se realiza la comparación entre la expresión de tripomastigotes metacíclicos y epimastigotes, sino que además, se realiza la comparación entre tripomastigotes metacíclicos y tripomastigotes derivados de células, dos estadios que han sido en algunos casos documentados bajo el mismo nombre y de los cuales no se conocen a ciencia cierta las diferencias en la expresión génica entre ellos, que además, podrían estar aportando a las propiedades biológicas exhibidas por estos estadios. Los

resultados para este análisis pueden ser encontrados en el artículo:

- **Artículo 5:** Cruz-Saavedra L, Vallejo GA, Guhl F, Ramírez JD. Transcriptomic changes across the life cycle of.*Trypanosoma cruzi* II. PeerJ. 2020 May 14;8:e8947. doi: 10.7717/peerj.8947. PMID: 32461822; PMCID: PMC7231504.

CAPÍTULO 1: Arquitectura genómica y diversidad genética de clones de *Trypanosoma cruzi* I (TcI).

Evidence of genomic plasticity in *Trypanosoma cruzi* I driven by aneuploidy and loss of heterozygosity

Lissa Cruz-Saavedra[a], Philipp Schwabl[b], Gustavo A. Vallejo[c], Julio C. Carranza[c], Marina Muñoz[a], Luz Helena Patino[a], Martin S. Llewellyn[b], Juan David Ramírez [a*].

[a]Centro de Investigaciones en Microbiología y Biotecnología-UR (CIMBIUR), Facultad de Ciencias Naturales, Universidad del Rosario, Bogotá, Colombia.

[b]Institute of Biodiversity, Animal Health & Comparative Medicine, University of Glasgow, Glasgow G12 8QQ, UK.

[c]Laboratorio de Investigación en Parasitología Tropical, Facultad de Ciencias, Universidad del Tolima, Ibagué, Colombia.

*Correspondence: juand.ramirez@urosario.edu.co

ABSTRACT

Trypanosoma cruzi, the agent of Chagas disease shows marked genetic diversity divided at least into six Discrete Typing Units (DTUs). High intra DTU genetic variability has been observed in the TcI, the most widely distributed DTU, where patterns of genomic diversity can provide information on ecological and evolutionary processes driving parasite population structure and genome organization. Genomic plasticity has been seen in *T. cruzi* reflected in chromosomal aneuploidies and rearrangement across multigene families. Weexplored genomic diversity among 18 Colombian *T. cruzi* I clones and 15 *T. cruzi* South American I strains. Our results confirm high genetical variability, heterozygosity and presence of a clade compatible with the TcI_{dom} genotype, described for strains from humans in Colombia and Venezuela. TcI showed high structural plasticity across the study region. Differential events of whole and segmental aneuploidy (SA) along chromosomes even between clones from the same strain were found and corroborated by the depth and allelic frequency. We detected loss of heterozygosity (LOH) events in different chromosomes, however, the size and location of segments under LOH varied between clones. Genes adjacent in SA and LOH breakpoints were evaluated, and retrotransposon hot spot genes flanked the beginning of SA. Our result suggests that *T. cruzi* genomes, like to those of Leishmania spp may be highly structurally unstable.

IMPORTANCE

The high genetic variability of *T. cruzi*'s TcIand its possible relationship with recombination events has been one of the great challenges in the study of this parasite. Recent genomic analyzes on this parasite demonstrated meiotic sex across its genome and multigene family's re-arrangement associated with recombination processes. We found genome evidence of high variability and plasticity in TcI clones, where events of chromosomal and segmental aneuploidy and loss of heterozygosity play an important role. Our findings are important to

support TcI high genetic variability, genomic plasticity and open new questions to understand the drivers of genomic structural instability present in this neglected parasite.

KEYWORDS *Trypanosoma cruzi*, TcI, genome, aneuploidy, segmental allele frequency, loss of heterozygosity

Trypanosoma cruzi is a flagellated protozoan that causes Chagas disease, which affects approximately 6 to 7 million people worldwide (1). This parasite present high genetic variability, which has allowed it to be classified into 6 Discrete Typing Units (DTUs), with *T. cruzi I* (TcI) being the most widely distributed DTU (2-4). *T. cruzi* I high genetic variability has been previously described using several approaches. In turn, the presence of a unique clonal genotype emerges associated with human infection in Colombia and Venezuela, known as TcI_{dom} (6-11).

For several years, *T. cruzi* genome has been thought to be highly plastic, even before the arrival of genome sequencing. Dvorak and colleagues clearly demonstrated substantial inter-clonal variation in DNA content as early as the 1980s employing cytometry strategies have been corroborate by more recent studies (12, 13). Analysis of *T. cruzi* genomes with micro-array technologies drew similar conclusions, with reports of substantial copy number variation and aneuploidy among closely related *T. cruzi* clones (14). Subsequent genomic studies, many based on a limited number of laboratory strains have confirmed high levels of genome plasticity in *T. cruzi* (15-17). Hi-C sequencing suggest that chromosomal locations and distributions of gene families, especially those that are highly repetitive and encode surface-expressed products, are difficult to predict and highly fluid in nature (15).

Genomic instability, principally aneuploidy, has been described in multiple microorganisms (18-22), as well as being widely reported in cancer (23). In some unicellular fungi and protozoa, genomic plasticity is thought be a means of adaption to environmental stress(19-21). Common manifestations of genomic plasticity include whole and segmental aneuploidy, as well as copy number variation. Trypanosomatids exercise little control over transcription (24). As such copy number can have profound consequences on gene expression, with important adaptive implications (25). The alternate mitotic and spindle assembly checkpoints (MACs, SACs) in trypanosomatids are considered basal to higher eukaryotes and could contribute to the high rate of aneuploidy observed in some species (26). Ploidy instability is particularly well-described in *Leishmania sp*., linked to drug resistance and metabolic plasticity (27, 28). Intriguingly, aneuploidy is infrequent or absent in *T. b. brucei* (29). In *T. cruzi* little is known about the frequency and adaptive significance aneuploidy, although naturally occurring aneuploids are increasingly reported (14, 15, 30, 31).

Trypanosoma cruzi has recently been demonstrated to undergo frequent genetic exchange (5, 30, 32). Reports of preponderant clonal evolution in this parasite where the recombination events are not frequent between the population to break clonal patterns, are a gross over-simplification based on antiquated genetic approaches (33, 34). In fact, *T. cruzi* DTU I, at least, appears to have a complex metapopulation structure with a mosaic of mating systems simultaneously present – clonal, sexual and parasexual (30). Recombination not only

provides a source of rapid phenotypic innovation, but can have fundamental impacts on genome structure – especially where parasexual and / or non-canonical meiosis are at play (e.g. 35). Aneuploidy observed in *Trypanosoma cruzi* could arise from just such processes (e.g 14, 30, 31). Experimental *T. cruzi* DTUI hybrids created, but never replicated, in the laboratory are thought to have arisen via parasexual genome fusion resulting in sub-tetraploid progeny (36). A gradual genomic fusion-then-loss mechanism similar to that observed in yeasts (37) has been proposed to explain patterns of aneuploidy observed in *T. cruzi* experimental hybrids (36).

To explore the diversity and drivers of genome plasticity in *T. cruzi*, we sequenced the genomes and explore the resultant karyotypes of 18 *T. cruzi* DTU I genomes from Colombia. Colombian clones were assessed alongside reference genomes from around South America. We found differences in TcI strains whole-genome phylogenetic marked per number of SNPs and heterozygosity that are not necessarily related to geographical and host isolation. Important events of aneuploidy around the whole and segmental parts of chromosomes, and events of LOH, were not necessarily represented in all the clones per strains. The results here described shows tremendous *T. cruzi* genomic plasticity.

RESULTS

Phylogenetic clustering and multiclonality

A total of 468,521 SNP sites were identified across all strains and clones which were included relative to the *T. cruzi* BrazilA4 reference genome. To evaluate taxonomic affinities within *T. cruzi* I, a phylogenetic tree was constructed using the UPGMA method. We included 15 *T. cruzi* clones isolated from different geographical locations of the Americas (blue lines) and 18 TcI clones generated from Colombian strains (color per strain) (Table S1). Tree topology correlated with geography, with most Colombian clones forming a discrete clade separate from strains of other countries. However, some exceptions were found in this analysis. The first of them corresponded with the Colombian cluster that included the strain Colombiana-Brazil and S1321 and X1081 clones, showing the highest number of SNPs compared to the reference and the lowest inbreeding coefficient (F). Interestingly Colombiana-Brazil and S1321 cluster together with between 3000 - 4000 different SNPs approximately, being the clone S1321_5 that have the less different (3250 SNPs) (Table S2, Fig 1B). Four clones of the CG strain (1-3, 5) clustered alongside TcI_{dom} clones X10462-P1C9 and X12422-P1C3, isolated from Venezuela (with robust bootstrap support (100%) (red square), with the highest F index and low number of SNPs (Fig. 1A). Bootstrap values higher than 80 are represented like a black circle in the tree.

Divergent clones within single hosts were observed, especially from a human sample (CG) where four clones were associated with $TcI_{dom,}$ as we previously described. While CG_4 was more closely linked with parasites of sylvatic origin D5, which is in correspondence with the cluster that shows a different number of SNPs and F index in comparison with the TcI_{dom} cluster, when we calculated the among of SNPs different between CG_4 and the other CG clones it was approximately 58000 SNPs (Fig. 1B, Table S2). No clear association between

the origin of the isolation (human, mammalian host and vector) and the phylogenetic groups was found across the full dataset, although the clade including 1321, X1081 and Colombiana-Brazil strains represented only sylvatic hosts (Fig. 1A).

Chromosomal Aneuploidy in *T. cruzi* I clones

Substantial somic heterogeneity (Fig 2A-B(light blue lines)), inferred from depth (light-blue lines), and validated using AF calculation (red and blue points) (Fig 2B), was observed in the TcI clones. Examples of alternate allele frequency plots based on karyotype estimates are shown in Figure 2B. Karyotype was not clearly correlated with phylogeny or geography (Fig 2A, Fig. S1). Instead, the clonal origin was an apparent driver of karyotype among some Colombian clones. Four of the CG clones, for example, shared a common gross karyotype (Fig. S2). A second karyotype is shared among some S1321 clones, D5 clones, CG_4 clone, and TDIM_1. Interestingly, the S1321_4 clone had different aneuploidy patterns (Fig. S2); however, we found changes between the clones from the same 'parental' strain in some chromosomes. D5 clones had split affinities with a common karyotype between D5 1, D5 3, and D5 4, and the remaining clone D5 2 similar to one of the CG (4) clone karyotypes. Third karyotype was showed by V2 and X12422-P1C3. X1081 showed an independent karyotype (Fig. S2). The most affected chromosomes concerning changes in somy during this analysis were chromosomes 24, 37, and 43 that showed tetraploid characteristics for most of the clones (Fig 2A). Other events of triploidy occurred in some clones to 4, 12, 19, 20, 28, 31, 33, 34 (Fig 2B). Chromosomes 35, 36, 38, 39, 40, 41, and 42 were excluded from the analysis given the percent of repeated content in the Brazil A4 reference genome and consequently, with a high masking.

Segmental aneuploidy in *Trypanosoma cruzi*

Divergent alternate allele frequency (AAF) distributions of Colombian TcI clones are consistent with the presence of segmental aneuploidy (SA) (diploid, triploid or tertaploid) (Fig. 3). Somy estimations were inferred from AAF distributions in combination with median read-depth variation. The chromosome showing the greatest of degree of segmental aneuploidy (and the longest tracts of consistently raised ploidy) was chromosome 1. The extent of SE on chromosome 1 was perhaps unsurprising considering that this chromosome has the largest areas well-mapped, non-repetitive sequence in which AAF could be evaluated. Two patterns of SA were found among the clones CG 1 and TDIM 1 (Fig. 3A). Consistent disomy was observed in most of the clones (Fig. S2). In the clone TDIM 1, however, both alternate allele frequency and read depth suggest segmental trisomy in Ch1 (Fig. 3A). Finally, we found AAF consistent with trisomic SA that was not reflected in the segmental depth increase to CG 1 clone (Fig. 3A). Among other clones several patterns of segmental aneuploidy among genetically similar clones of the same strain were observed.

Notably, segmental breakpoint locations were consistent within and among strains on chromosome 1, which led us to examine attributes and annotations of genes and sequences within these regions (Fig. 3B). To achieve this, two of longest segments were selected, i) 1bp- 608,394 bp, and finally, ii) 651,273 bp to 1,409,881 bp. We also explored a SA

breakpoint in the central section of this region at, 608,394 bp to 1,409,881 bp (Fig. 3B). We observed a large number of retrotransposon hot spots (RHS) in the flanking regions between these segments. Within these segments, RHS were also observed, alongside mucins, dispersed gene family proteins, ABC transporters, and ribosomal proteins (Fig. 3B).

We mapped our reads onto small scaffolds reported by Wang et al., 2021, and we noted correspondence between zones of SA reported by these authors and our own data (Table S2)

Differential loss of heterozygosity between clones of *T. cruzi* I suggest frequent mitotic gene conversion events

An analysis of loss of heterozygosity was performed for all the genomes in 10 kb windows, demonstrating the presence of LOH zones along the whole genome (Fig. 4A). LOH were found on disomic and trisomic chromosomes, indicating homozygous copies in the segments described below. We focused our analysis on the most extended segments with LOH, which were located on chromosomes 1, 4, 5, and 7 (Fig. 4B): In chromosome 1, we found LOH in four different segmental patterns in sample CG 4, Colombiana-brazil, FcHcl5, H1tx, H2, V2, and all the clones from strains D5 and X1081 (Fig. 4B); for chromosome 4, the LOH patterns were found in X12422-P1C3 and FcHc15, where LOH was covering the entire chromosome; the LOH patterns for chromosome 5 were mainly found in H1tx and X10462-P1C9; and for chromosome 7, only one LOH pattern was detected in all the clones of the D5 strain, CG 4 and X10462-P1C9.

The influence of repetitive regions and regions such as RHS in the patterns with LOH was assessed for the chromosomes mentioned above.Segmental LOH was identified on chromosome 1, again flanked by RHS. Our analysis did not show any other relationship between LOH and specific genes. In the case of the chromosome 4, we did not determine the genes that flanked the LOH area because it covers the whole chromosome. Finally, LOH segments in chromosomes 5 and 7 were flanked by genes encoding hypothetical proteins (Fig. S3).

DISCUSSION

Our analysis of 33 clones indicates a high level of genetic diversity of diversity in Colombian TcI, with some phylogeographic structuring and the presence of divergent clones within the same host or vector. After mapping to a recently assembled 3D reference genome (15), we were able to demonstrate substantial ploidy instability across the dataset, including several instances of segmental aneuploidy consistently with segmental aneuploidy breakpoints across multiple clones on chromosome 1, and also identified the presence of retrotransposon hotspots, which could have a role in driving genomic re-arrangements. Finally, widespread instanced of Loss of Heterozygosity (LOH) were detected and suggest an important role for gene conversion.

The results we observed corroborate previous findings associated with human infection clonal genotype TcI_{dom} at the genomic level (6, 8, 38, 39). A possible “bottleneck” event resulting in a decrease in its genetic variability has been hypothesized for this genotype, and

our results show low diversity and the lowest difference in comparison of SNPs to the reference genome coherent with the previous hypothesis. This could explain the similarities observed at a phylogenetic level between the strains within different geographical origins (6, 38, 40, 41).

Due to the ability of this DTU to circulate in domestic and sylvatic environments, genomic classification based on it has been reported. However, we did not find any strong association between host and origin (country) with phylogenetic relationships, maybe related to isolation time and geographical changes in the same country (5-8, 11). Our results support previous reports of multiclonality in TcI strains observed in sylvatic isolates related with high genetic variability, and emphasize the importance of evaluating single clones to evaluate the genetic variability (30, 40, 42). We believe that this process has drastically influenced the diversification upon the genome composition of circulating strains and could be reflected at the phylogenetic level. Studies in the murine model showed the impact in biological properties of multiclonal strains remarking its importance (43-46).

Changes in chromosomal somy appear to be well tolerated in trypanosomatids such as *Leishmania* and *T. cruzi* (31, 32). Ploidy plasticity is believed to be important in responding to environmental stress during the life cycle and precursors of mechanisms of resistance against treatment for some *Leishmania* species (23, 24). Our results show the presence of aneuploidy patterns for different chromosomes among TcI clones, consistent with previous genomic studies (Fig. 2) (15, 27-28, 30-31). How a disomic microorganism gains chromosomal mosaicism has been previously discussed including chromosomal segregation failure during mitosis and endoreplication. and meiosis processes such as: i) parasexual events that involved nuclear fusion followed by loss of chromosome copies, ii) failed or incomplete meiotic processes in the same manner that has been previously described for *Leishmania* as “meiosis-like”, iii) complete meiosis and posterior reduction in the chromosome copies. Given this possibility, it is important to highlight the recent evidence of meiotic sex in some populations of *T. cruzi* genomes (19, 27, 28, 30, 47-50). The Chromosome 24 was tetrasomic in all the clones evaluated, indicative of the presence of important genes to *T. cruzi* that require more than two copies as previously reported (15, 31). It is unknown how *T. cruzi* regulates aneuploidy processes per chromosome, considering the content of repetitive sequences; and therefore, studies to understand it are drastically needed. Our results suggest the influence of selective, differential environmental or temporal pressures as possible theoretical explanations by which specific chromosomes undergo aneuploidy as happens in many fungi taking into account that the machinery involved has reported in the *T. cruzi* genome with unknown function (47, 50, 51).

Genomic analysis of Brazil B4 strain (TcI) showed large allelic variations across the whole genome and are representative of genome sequences, such as alternative scaffolds that share high synteny with specific chromosomes (15). AAF was found on chromosome 1 between TcI clones flanked by RHS and contained families of repetitive gene protein sequences. However, the high number of hypothetical proteins avoid the understanding of the complete genomic organization of these segments (Fig. 3B). RHS has been recently studied in *T. cruzi*

where its sequences have retrotransposons insertion sites in their 5′ coding region with large hemizygous region and tandem amplification events (52, 53). Unequal crossing-over between non-sister homologous chromatids with retrotransposons involved, could affect large segments of the genome and could serve as the explanation for the origins of the trisomic segments in chromosome 1, where one of the copies is deleted resulting in hemizygous. Similar results have been demonstrated in *T. brucei*, where long regions of hemizygous segments affect VSG and other multigene families (54). The RHS is located after single strand cleavage sites that are necessary to activate core HR factors and make the DBS during HR which is essential for the survival of *T. cruzi* during its life cycle (55). It is reasonable to hypothesize that DBS could play an important role regarding the origins of RHS sequence generating AFF segments, but further studies are require to describe the mechanism (56-62).

Phenotypic diversity is rapidly driven by LOH and decreases in allelic diversity are associated with the appearance of recessive alleles that confer selective advantages in response to different kinds of environmental or temporal stressors (63). In yeast,recombination, repair of double strand DNA breaks, and/or chromosome segregation mechanisms are all associated with the appearance of LOH post host infection and other forms of *in vitro* stress and could related with LOH profiles observed in TcI clones (63, 64). Considering, the complex biological cycle of *Trypanosoma cruzi* that involves multiplevariations in environmental stressors, the LOH could have a very important role and serve as a checkpoint regulator. Therefore, we couldhypothesize that LOH profile variations arose from repair of a possible double strand DNA break as occurs in *Saccharomyces cerevisiae*. However, genomic analysis has focused on epimastigotes within the logarithmic phase and the genome from others stages have not been reported (65).

Previous studies described the increase of expression of some related-HR and non HR genes during metacyclogenesis and in epimastigotes from hybrid strains after exposure to irradiation that could be related with DNA double-strand break repair and derivate in recombination process (56, 58). In correlation with these results, analysis in Ecuadorian *T. cruzi* I genomes showed evidence of hybridization and meiotic recombination (30). It is important to note that LOH patterns are related with the presence of hybrids within these areas that are mainly derived from recombination events in *Candida spp* (66, 67). Our result could suggest a possible event of hybridization of the parents, which would lead to the formation of a lineage indicative of the LOH characteristics observed in this study. However, the only evidence of genetic exchange at *in vitro* level in *T. cruzi* has been reported in VERO cells with a nuclear fusion of trypomastigotes with different genomic profiles (36). Nevertheless, the machinery and the mechanism used by *T. cruzi* to carry out these processes are unknown, and no *in vivo* analysis have been performed to support these results (68).

Analysis of the 18 *T. cruzi* I clones' complete genome demonstrated the presence of high genomic plasticity within TcI populations. Considering segmental aneuploidy, one could infer that the origins of AF and LOH occurred through a recombination event throughout the course of sexual and asexual replication. It could provide a rationale as to the genomic

diversity that emerged throughout the course of evolution to help the parasite respond to different environmental stressors throughout the course of its life cycle. Higher recombination events have been related with this DTU in comparison with other species. Likewise, the presence of one of these processes in some subpopulations of *T. cruzi* would not be solely exclusive or an indication of the development of the other. We could assert that they would not be occurring constantly, as has previously been characterized for some fungi species (69-70). Future studies in *T. cruzi* should be focused on determining the mechanisms of action, signaling pathways, and stimuli required for the development of these processes, as well as their contribution to genomic changes, and the direct influence of these changes on the biology and virulence of the parasite.

MATERIALS AND METHODS

Maintenance of parasites: A total of 5 *Trypanosoma cruzi* strains isolated from different parts of Colombia, and previously characterized as TcI, were cultivated in liver infusion tryptose (LIT) medium supplemented with 10% fetal bovine serum and incubated at 26 ° C until the start of the test. The origin of the strains is found in Table S1.

Cell cloning - cell sorting: Multiclonality has already been described in *T. cruzi* strains (30, 40). Log phase epimastigote cultures of *T. cruzi* were washed in 1X PBS and maintained until the start of the flow cytometry protocol for cell sorting cloning. The parasites were drawn on the BD FACS Aria II equipment, using the BD FACSDiva ™ software (Becton, Dickinson Biosciences). In summary, 1 mL of epimastigotes in 1X PBS was drawn directly into 96-well plates at a concentration of one parasite per well and 50 µL of LIT medium supplemented with 10% fetal bovine serum and penicillin/streptomycin was immediately added to 2%. A total of 40 clones were generated for each strain, the above in order to increase the number of clone recoveries. The viability of the parasites was verified under an inverted microscope, when an increase in the concentration of the parasites was observed, LIT medium was added in volumes of 50 µL, when the culture exceeded 200 µL, it was massified in a 25 cm^3 culture box and maintained as previously described. Approximately five clones were selected for each strain. Each clone was genotyped using the algorithm proposed by Ramírez *et al*., 2010 (71). A total of 18 clones were finally selected for further analysis.

DNA extraction and sequencing: DNA extraction was performed from epimastigote cultures in LIT medium in the logarithmic phase at a concentration of approximately 1 X 10^6 parasites/mL. The parasites were washed twice with 1X PBS. The DNeasy Blood & Tissue kit from Qiagen was used (catalog No. 69504; Qiagen, Hilden, Germany). A volume of 200 µl of Buffer AL, 20 µl of proteinase K and 1 µL of RNAse A were added to the parasite pellet, the content was re-suspended and incubated at 36 ° C for 20 minutes in order to degrade the proteins and the RNA not required, followed by this, a second incubation was carried out at 56 ° C for 10 minutes, at the end of this time, the provider's protocol was followed. A total of 100 µL of DNA was obtained. The concentration and purity of DNA

was verified by means of a measurement in NanoDrop ™ 2000 / 2000c Spectrophtomers (ThermoFisher scientific), a concentration greater than 1 mg / mL and a value of 2 ± 2 for the 260/280 and 230/260 indices. They were considered successful, and the integrity of the DNA was evaluated by means of a 2% agarose gel electrophoresis. The extracted DNA that met all the mentioned quality parameters was sent to Novogene Bioinformatics Technology Co., Ltd, Beijing, China, for sequencing using Illumina's HiSeq X-Ten system platform, mate-paired libraries were built using end repair (350-bp insert size) and subject to paired-end sequencing (2 × 150-bp read length). The reads obtained were filtered by adapter contamination, > 10% uncertain nucleotides, or> 50% low-quality nucleotides (base quality <5).

DNA mapping and variant calling: The quality of the reads obtained for the 18 sequenced genomes was evaluated using the fastQC software (https://www.bioinformatics.babraham.ac.uk/projects/fastqc). The sequenced genomes were assembled using the BWA-mem v0.7.3 software (Burrows-Wheeler Aligner) under the default parameters, using the *T. cruzi* – Brazil A4v49 genome as reference (15, 72). Subsequently, the samtools sort v0.1.18 tool was used to sort the alignments, followed by the marking of the PCR-duplicates by Picard v1.85(73). SNPs analysis was performed with Genome Analysis Toolkit (GATK) v3.7.0 using the HaplotypeCaller option (74). The output files obtained for each of the clone genomes were linked using GATK GenotypeGVCFs. The obtained vcf file was filtered by depth (DP <10 /> 500), quality of the reads (QUAL <1500), and finally, the selectType option of GATK was used to obtain the SNPs. Additionally, bedtools intersect was used to place a virtual mappability mask in order to exclude the variants present in unreliably mappable regions from the Brazil A4v49 reference genome, following the protocol performed by Schwabl et al., 2019 (30). On the other hand, to determine the SNPs present at the mitochondrial level, the same methodology previously mentioned was followed using the kinetoplast maxicircle sequence for Brazil A4as the reference genome available in Genbank FJ203996.1 using the default parameters in GATK. The reads per sample per chromosome calculation were made using samtools view options -f 1 -F 12.

Phylogenetic reconstruction: The vcf file that contain the information for the SNPs present in the sequenced genomes for all the clones regarding the nuclear genome and the kinetoplast maxicircle (mitochondrial) genome of Brazil A4were used to create multifasta file using vcf-to-tab, excluding sites with missing information (--max-missing option). MAFFT v7.271 was used to perform the alignment (75). The reconstruction of nuclear and mitochondrial phylogenies was performed by UPGMA clustering in IQ-TREE v1.5.4, using an initial search for the best substitution model applied to the sequences and 1000 ultrafast bootstrap replicates (76). The files were viewed in FigTree v1.4.3 and edited in the Interactive Tree of Life (iToL) tool (77). Values of heterozygocity were determined using vcftools -het option that calculated the F index. The count of SNPs was executed with bcftools view options -c1 -H . A total of 15 nuclear sequences corresponding to TcI reference genomes isolated from different geographical points of America were included in Table S1.

Determination of chromosomal somy: For the determination of somy, the standardized protocol by Schwabl et al, 2019 was used (30). Briefly, the Samtools depth tool v0.1.18 was used to determine the average depth for 1 kb windows along each of the chromosomes from the .bam files obtained from the mapping by BWA, followed by this the median of the averages was calculated for the previously obtained windows (78). Finally, the estimation of the somy was made dividing the calculated median between the 40th percentile and multiplying by two. The results obtained were graphical using the heatmap.2 function available in the R v3.6.3 software.

Allelic frequency and loss of heterozygosity (LOH): The data corresponding to the allelic frequency (AF) were purified in txt files from the SNPs file using vcftools and SelectVariants - VariantsToTable of GATK for the genome of each one of the clones, and plotted using the plot function of R (73), in disomic patterns the AF is reflected in a heterozygosity radius of 0 or 1 for homozygous SNPs and 0.5 for heterozygous SNPs, when there is a trisomic pattern a heterozygosity radius of close to 0.66 and 0.33 is observed, and in tetrasomic patterns the radius of heterozygosity is close to 0.25 and 0.75. For LOH determination, the vcf file containing the information for SNPs was separated into SNPs, positions and individuals using vcftools. The above files were used as input files in R v3.6.3 software, where data.table, stringr, ape, phangorn packages were used. Heterozygous, homozygous distinct to the reference, and homozygous SNPs equal to the reference genome were determined for each position. SNPs present in hard-to-map regions of the reference genome were excluded from the analysis. The number of SNPs per chromosome were plotted using 10 kb windows using R plot.

Identification of the genes: The IDs for the genes present in regions that exhibited changes in the allelic frequency - relevant depth and areas with LOH, were extracted from the ggf file for the Brazil A4 v49 reference genome and subjected to the TriTrypDB tool from EupathDB (79). using an initial search in the Brazil A4 v49 (2018) genome followed by a gene orthology analysis in Brazil A4 (15), the above, in order to cover data on genes noted as coding for nonspecific proteins. The list of genes present in these areas was obtained and purified by means of dynamic tables in Excel.

SUPPLEMENTAL MATERIAL

Fig. S1. Chromosomal Aneuploidy in *T. cruzi* I clones – Dendogram.

Fig. S2. Allelic frequency and depth per all chromosomes to all *Trypanosoma cruzi* I included in the study.

PDF files per clone

Fig. S3. Annotation gene of segment with loss of heterozygosity on chromosome 1, 4, 5 and 7.

TIFF file

Table. S1. Strain - Clones provenance.

DOCX file

Table. S3. SNPs differences between clones and strains.

Table. S3. Number of reads present in segmental allelic frequency patterns on contig describe by Wang *et al*., 2021 that had synteny to chromosome 1

XLS file

ACKNOWLEDGMENTS

We thank Luisa Berna and João Cunha for their suggestions during bioinformatic analysis. Cruz-Saavedra thanks her mom for support and push her to be better researcher and person and encourage her to fulfill her dreams.

REFERENCES

1. OMS. Climate change and health. 2019.
2. Zingales B, Andrade SG, Briones MR, Campbell DA, Chiari E, Fernandes O, et al. A new consensus for *Trypanosoma cruzi* intraspecific nomenclature: second revision meeting recommends TcI to TcVI. Mem Inst Oswaldo Cruz. 2009;104(7):1051-4.
3. Zingales B, Miles MA, Campbell DA, Tibayrenc M, Macedo AM, Teixeira MM, et al. The revised *Trypanosoma cruzi* subspecific nomenclature: rationale, epidemiological relevance and research applications. Infect Genet Evol. 2012;12(2):240-53.
4. Zingales B. *Trypanosoma cruzi* genetic diversity: Something new for something known about Chagas disease manifestations, serodiagnosis and drug sensitivity. Acta Trop. 2018;184:38-52.
5. Ramírez JD, Guhl F, Messenger LA, Lewis MD, Montilla M, Cucunuba Z, et al. Contemporary cryptic sexuality in *Trypanosoma cruzi* . Mol Ecol. 2012;21(17):4216-26.
6. Ramírez JD, Tapia-Calle G, Guhl F. Genetic structure of *Trypanosoma cruzi* in Colombia revealed by a High-throughput Nuclear Multilocus Sequence Typing (nMLST) approach. BMC Genet. 2013;14:96.
7. Herrera C, Bargues MD, Fajardo A, Montilla M, Triana O, Vallejo GA, et al. Identifying four *Trypanosoma cruzi* I isolate haplotypes from different geographic regions in Colombia. Infection, Genetics and Evolution. 2007;7(4):535-9.
8. Herrera C, Guhl F, Falla A, Fajardo A, Montilla M, Adolfo Vallejo G, et al. Genetic variability and phylogenetic relationships within *Trypanosoma cruzi* I isolated in Colombia based on miniexon gene sequences. Journal of parasitology research. 2009;2009.
9. Llewellyn MS, Rivett-Carnac JB, Fitzpatrick S, Lewis MD, Yeo M, Gaunt MW, et al. Extraordinary *Trypanosoma cruzi* diversity within single mammalian reservoir hosts implies a mechanism of diversifying selection. Int J Parasitol. 412011. p. 609-14.
10. León CM, Hernández C, Montilla M, Ramírez JD. Retrospective distribution of *Trypanosoma cruzi* I genotypes in Colombia. Mem Inst Oswaldo Cruz. 2015;110(3):387-93.
11. Ramírez JD, Montilla M, Cucunubá ZM, Floréz AC, Zambrano P, Guhl F. Molecular epidemiology of human oral Chagas disease outbreaks in Colombia. PLoS Negl Trop Dis. 2013;7(2):e2041.

12. Dvorak JA, Hall TE, Crane MS, Engel JC, McDaniel JP, Uriegas R. *Trypanosoma cruzi* : flow cytometric analysis. I. Analysis of total DNA/organism by means of mithramycin-induced fluorescence. J Protozool. 1982 Aug;29(3):430-7. doi: 10.1111/j.1550-7408.1982.tb05427.x. PMID: 6182288.
13. Lewis MD, Llewellyn MS, Gaunt MW, Yeo M, Carrasco HJ, Miles MA. Flow cytometric analysis and microsatellite genotyping reveal extensive DNA content variation in *Trypanosoma cruzi* populations and expose contrasts between natural and experimental hybrids. Int J Parasitol. 2009 Oct;39(12):1305-17. doi: 10.1016/j.ijpara.2009.04.001. Epub 2009 Apr 22. PMID: 19393242; PMCID: PMC2731025.
14. Minning TA, Weatherly DB, Flibotte S, Tarleton RL. Widespread, focal copy number variations (CNV) and whole chromosome aneuploidies in *Trypanosoma cruzi* strains revealed by array comparative genomic hybridization. BMC Genomics. 2011 Mar 7;12:139. doi: 10.1186/1471-2164-12-139. PMID: 21385342; PMCID: PMC3060142.
15. Wang W, Peng D, Baptista RP, Li Y, Kissinger JC, Tarleton RL. Strain-specific genome evolution in *Trypanosoma cruzi* , the agent of Chagas disease. PLoS Pathog. 2021 Jan 28;17(1):e1009254. doi: 10.1371/journal.ppat.1009254. PMID: 33508020; PMCID: PMC7872254.
16. Díaz-Viraqué F, Pita S, Greif G, de Souza RCM, Iraola G, Robello C. Nanopore Sequencing Significantly Improves Genome Assembly of the Protozoan Parasite *Trypanosoma cruzi* . Genome Biol Evol. 2019 Jul 1;11(7):1952-1957. doi: 10.1093/gbe/evz129. PMID: 31218350; PMCID: PMC6640297.
17. Talavera-López C, Messenger LA, Lewis MD, Yeo M, Reis-Cunha JL, Matos GM, Bartholomeu DC, Calzada JE, Saldaña A, Ramírez JD, Guhl F, Ocaña-Mayorga S, Costales JA, Gorchakov R, Jones K, Nolan MS, Teixeira SMR, Carrasco HJ, Bottazzi ME, Hotez PJ, Murray KO, Grijalva MJ, Burleigh B, Grisard EC, Miles MA, Andersson B. Repeat-Driven Generation of Antigenic Diversity in a Major Human Pathogen, *Trypanosoma cruzi* . Front Cell Infect Microbiol. 2021 Mar 3;11:614665. doi: 10.3389/fcimb.2021.614665. PMID: 33747978; PMCID: PMC7966520.
18. Bennett RJ, Forche A, Berman J. Rapid Mechanisms for Generating Genome Diversity: Whole Ploidy Shifts, Aneuploidy, and Loss of Heterozygosity. Cold Spring Harb Perspect Med. 42014.
19. Bussotti G, Gouzelou E, Cortes Boite M, Kherachi I, Harrat Z, Eddaikra N, et al. *Leishmania* Genome Dynamics during Environmental Adaptation Reveal Strain-Specific Differences in Gene Copy Number Variation, Karyotype Instability, and Telomeric Amplification. MBio. 2018;9(6).
20. Gilchrist C, Stelkens R. Aneuploidy in yeast: Segregation error or adaptation mechanism? Yeast. 362019. p. 525-39.
21. Selmecki A, Forche A, Berman J. Aneuploidy and Isochromosome Formation in Drug-Resistant Candida albicans. Science. 2006;313(5785):367-70.
22. Wertheimer NB, Stone N, Berman J. Ploidy dynamics and evolvability in fungi. Philos Trans R Soc Lond B Biol Sci. 3712016.
23. Ben-David U, Amon A. Context is everything: aneuploidy in cancer. Nat Rev Genet. 2020 Jan;21(1):44-62. doi: 10.1038/s41576-019-0171-x. Epub 2019 Sep 23. PMID: 31548659.
24. Clayton C. Regulation of gene expression in trypanosomatids: living with polycistronic transcription. Open Biol. 2019 Jun 28;9(6):190072. doi: 10.1098/rsob.190072. Epub 2019 Jun 5. PMID: 31164043; PMCID: PMC6597758.
25. Ubeda JM, Raymond F, Mukherjee A, Plourde M, Gingras H, Roy G, Lapointe A, Leprohon P, Papadopoulou B, Corbeil J, Ouellette M. Genome-wide stochastic adaptive DNA amplification at direct and inverted DNA repeats in the parasite *Leishmania*. PLoS Biol. 2014 May

20;12(5):e1001868. doi: 10.1371/journal.pbio.1001868. PMID: 24844805; PMCID: PMC4028189.
26. Akiyoshi B, Gull K. Discovery of unconventional kinetochores in kinetoplastids. Cell. 2014;156(6):1247-1258. doi:10.1016/j.cell.2014.01.049
27. Patino LH, Imamura H, Cruz-Saavedra L, Pavia P, Muskus C, Méndez C, et al. Major changes in chromosomal somy, gene expression and gene dosage driven by SbIII in *Leishmania braziliensis* and *Leishmania panamensis*. Sci Rep. 92019.
28. Dumetz F, Imamura H, Sanders M, Seblova V, Myskova J, Pescher P, et al. Modulation of Aneuploidy in *Leishmania donovani* during Adaptation to Different *In Vitro* and *In Vivo* Environments and Its Impact on Gene Expression. mBio. 82017.
29. Almeida LV, Coqueiro-Dos-Santos A, Rodriguez-Luiz GF, McCulloch R, Bartholomeu DC, Reis-Cunha JL. Chromosomal copy number variation analysis by next generation sequencing confirms ploidy stability in *Trypanosoma brucei* subspecies. Microb Genom. 2018 Oct;4(10):e000223. doi: 10.1099/mgen.0.000223. Epub 2018 Sep 27. PMID: 30256189; PMCID: PMC6249438.
30. Schwabl P, Imamura H, Broeck FVd, Costales JA, Maiguashca-Sánchez J, Miles MA, et al. Meiotic sex in Chagas disease parasite *Trypanosoma cruzi* . Nature Communications. 2019;10(1):1-14.
31. Reis-Cunha JL, Baptista RP, Rodrigues-Luiz GF, Coqueiro-Dos-Santos A, Valdivia HO, de Almeida LV, Cardoso MS, D'Ávila DA, Dias FHC, Fujiwara RT, Galvão LMC, Chiari E, Cerqueira GC, Bartholomeu DC. Whole genome sequencing of *Trypanosoma cruzi* field isolates reveals extensive genomic variability and complex aneuploidy patterns within TcII DTU. BMC Genomics. 2018 Nov 13;19(1):816. doi: 10.1186/s12864-018-5198-4. PMID: 30424726; PMCID: PMC6234542.
32. Messenger LA, Miles MA. Evidence and importance of genetic exchange among field populations of *Trypanosoma cruzi* . Acta Trop. 2015;151:150-5.
33. Tibayrenc M, Ayala FJ. The population genetics of *Trypanosoma cruzi* revisited in the light of the predominant clonal evolution model. Acta Trop. 2015;151:156-65.
34. Tibayrenc M, Ayala FJ. How clonal are *Trypanosoma* and *Leishmania*? Trends Parasitol. 2013;29(6):264-9.
35. Hickman MA, Paulson C, Dudley A, Berman J. Parasexual Ploidy Reduction Drives Population Heterogeneity Through Random and Transient Aneuploidy in *Candida albicans*. Genetics. 2015;200(3):781-794. doi:10.1534/genetics.115.178020
36. Gaunt MW, Yeo M, Frame IA, Stothard JR, Carrasco HJ, Taylor MC, et al. Mechanism of genetic exchange in American trypanosomes. Nature. 2003;421(6926):936-9.
37. Bennett RJ. The parasexual lifestyle of *Candida albicans.* Curr Opin Microbiol. 2015;28:10-17. doi:10.1016/j.mib.2015.06.017
38. Llewellyn MS, Miles MA, Carrasco HJ, Lewis MD, Yeo M, Vargas J, et al. Genome-scale multilocus microsatellite typing of *Trypanosoma cruzi* discrete typing unit I reveals phylogeographic structure and specific genotypes linked to human infection. PLoS pathogens. 2009;5(5):e1000410.
39. Cura CI, Mejía-Jaramillo AM, Duffy T, Burgos JM, Rodriguero M, Cardinal MV, et al. *Trypanosoma cruzi* I genotypes in different geographical regions and transmission cycles based on a microsatellite motif of the intergenic spacer of spliced-leader genes. Int J Parasitol. 2010;40(14):1599-607.

40. Villa LM, Guhl F, Zabala D, Ramírez JD, Urrea DA, Hernández DC, et al. The identification of two *Trypanosoma cruzi* I genotypes from domestic and sylvatic transmission cycles in Colombia based on a single polymerase chain reaction amplification of the spliced-leader intergenic region. Mem Inst Oswaldo Cruz. 2013;108(7):932-5.
41. Costales JA, Kotton CN, Zurita-Leal AC, Garcia-Perez J, Llewellyn MS, Messenger LA, et al. Chagas disease reactivation in a heart transplant patient infected by domestic *Trypanosoma cruzi* discrete typing unit I (TcI DOM). Parasites & vectors. 2015;8(1):435.
42. Valadares HM, Pimenta JR, Segatto M, Veloso VM, Gomes ML, Chiari E, et al. Unequivocal identification of subpopulations in putative multiclonal *Trypanosoma cruzi* strains by FACs single cell sorting and genotyping. PLoS neglected tropical diseases. 2012;6(7).
43. Cruz L, Vivas A, Montilla M, Hernández C, Flórez C, Parra E, et al. Comparative study of the biological properties of *Trypanosoma cruzi* I genotypes in a murine experimental model. Infect Genet Evol. 2015;29:110-7.
44. Hernández C, Cucunubá Z, Parra E, Toro G, Zambrano P, Ramírez JD. Chagas disease (*Trypanosoma cruzi*) and HIV co-infection in Colombia. Int J Infect Dis. 2014;26:146-8.
45. Hernández C, Cucunubá Z, Flórez C, Olivera M, Valencia C, Zambrano P, et al. Molecular diagnosis of Chagas disease in Colombia: parasitic loads and discrete typing units in patients from acute and chronic phases. PLoS neglected tropical diseases. 2016;10(9):e0004997.
46. Burgos JM, Diez M, Vigliano C, Bisio M, Risso M, Duffy T, et al. Molecular identification of *Trypanosoma cruzi* discrete typing units in end-stage chronic Chagas heart disease and reactivation after heart transplantation. Clin Infect Dis. 2010;51(5):485-95.
47. Sterkers Y, Lachaud L, Crobu L, Bastien P, Pagès M. FISH analysis reveals aneuploidy and continual generation of chromosomal mosaicism in Leishmania major. Cell Microbiol. 2011;13(2):274-83.
48. Seervai RNH, Jones SK, Hirakawa MP, Porman AM, Bennett RJ. Parasexuality and Ploidy Change in Candida tropicalis. Eukaryot Cell. 122013. p. 1629-40.
49. Lee HO, Davidson JM, Duronio RJ. Endoreplication: polyploidy with purpose. Genes Dev. 2009;23(21):2461-77.
50. Inbar E, Shaik J, Iantorno SA, Romano A, Nzelu CO, Owens K, et al. Whole genome sequencing of experimental hybrids supports meiosis-like sexual recombination in *Leishmania*. PLoS Genet. 152019.
51. Sasaki M, Tischfield SE, van Overbeek M, Keeney S. Meiotic Recombination Initiation in and around Retrotransposable Elements in *Saccharomyces cerevisiae*. PLoS Genet. 92013.
52. Bernardo WP, Souza RT, Costa-Martins AG, Ferreira ER, Mortara RA, Teixeira MMG, et al. Genomic Organization and Generation of Genetic Variability in the RHS (Retrotransposon Hot Spot) Protein Multigene Family in *Trypanosoma cruzi* . Genes. 2020;11(9).
53. Bringaud F, Biteau N, Melville SE, Hez S, El-Sayed NM, Leech V, et al. A new, expressed multigene family containing a hot spot for insertion of retroelements is associated with polymorphic subtelomeric regions of Trypanosoma brucei. Eukaryotic cell. 2002;1(1).
54. Callejas S, Leech V, Reitter C, Melville S. Hemizygous subtelomeres of an African trypanosome chromosome may account for over 75% of chromosome length. Genome research. 2006;16(9).
55. Marcelo SdS. DNA Double-Strand Breaks: A Double-Edged Sword for Trypanosomatids | Cell and Developmental Biology. Frontiers in Cell and Developmental Biology. 2021.
56. Alves CL, Repoles BM, da Silva MS, Mendes IC, Marin PA, Aguiar PHN, et al. The recombinase Rad51 plays a key role in events of genetic exchange in *Trypanosoma cruzi* . Sci Rep. 2018;8(1):13335.

57. Ramirez JL. An Evolutionary View of *Trypanosoma cruzi* Telomeres. Frontiers in cellular and infection microbiology. 2020;9

58. Cruz-Saavedra L, Vallejo GA, Guhl F, Ramírez JD. Transcriptomic changes across the life cycle of *Trypanosoma cruzi* II. PeerJ. 2020;8.
59. Farmer S, Hong EJE, Leung WK, Argunhan B, Terentyev Y, Humphryes N, et al. Budding Yeast Pch2, a Widely Conserved Meiotic Protein, Is Involved in the Initiation of Meiotic Recombination. PLoS One. 72012.
60. Akematsu T, Fukuda Y, Garg J, Fillingham JS, Pearlman RE, Loidl J. Post-meiotic DNA double-strand breaks occur in Tetrahymena, and require Topoisomerase II and Spo11. eLife. 62017.
61. Forche A, Alby K, Schaefer D, Johnson AD, Berman J, Bennett RJ. The Parasexual Cycle in *Candida albicans* Provides an Alternative Pathway to Meiosis for the Formation of Recombinant Strains. PLoS Biol. 62008.
62. Lam I, Mohibullah N, Keeney S. Sequencing Spo11 Oligonucleotides for Mapping Meiotic DNA Double-Strand Breaks in Yeast. Methods Mol Biol. 2017;1471:51-98.
63. Abbey D, Hickman M, Gresham D, Berman J. High-Resolution SNP/CGH Microarrays Reveal the Accumulation of Loss of Heterozygosity in Commonly Used *Candida albicans* Strains. G3 (Bethesda, Md). 2011;1(7).
64. Andersen MP, Nelson ZW, Hetrick ED, Gottschling DE. A genetic screen for increased loss of heterozygosity in *Saccharomyces cerevisiae*. Genetics. 2008;179(3).
65. Daigaku Y, Mashiko S, Mishiba K, Yamamura S, Ui A, Enomoto T, Yamamoto K. et al. Loss of heterozygosity in yeast can occur by ultraviolet irradiation during the S phase of the cell cycle. Mutation research. 2006;600(1-2).
66. Berry ASF, Salazar-Sanchez R, Castillo-Neyra R, Borrini-Mayori K, Chipana-Ramos C, Vargas-Maquera M, et al. Sexual reproduction in a natural *Trypanosoma cruzi* population. PLoS Negl Trop Dis. 2019;13(5):e0007392.
67. Wang JM, Bennett RJ, Anderson MZ. The Genome of the Human Pathogen *GAUNRT* Is Shaped by Mutation and Cryptic Sexual Recombination. mBio. 2018;9(5).

68. El-Sayed NM, Myler PJ, Bartholomeu DC, Nilsson D, Aggarwal G, Tran AN, et al. The genome sequence of *Trypanosoma cruzi* , etiologic agent of Chagas disease. Science. 2005;309(5733):409-15.
69. Forche A, Alby K, Schaefer D, Johnson AD, Berman J, Bennett RJ. The Parasexual Cycle in Candida albicans Provides an Alternative Pathway to Meiosis for the Formation of Recombinant Strains. PLoS Biol. 62008.
70. de Massy B. Initiation of meiotic recombination: how and where? Conservation and specificities among eukaryotes. Annu Rev Genet. 2013;47:563-99.
71. Ramírez JD, Guhl F, Rendón LM, Rosas F, Marin-Neto JA, Morillo CA. Chagas cardiomyopathy manifestations and *Trypanosoma cruzi* genotypes circulating in chronic Chagasic patients. PLoS Negl Trop Dis. 2010 Nov 30;4(11):e899. doi: 10.1371/journal.pntd.0000899. PMID: 21152056; PMCID: PMC2994916.
72. Li H, Durbin R. Fast and accurate short read alignment with Burrows-Wheeler transform. Bioinformatics. 2009 Jul 15;25(14):1754-60. doi: 10.1093/bioinformatics/btp324. Epub 2009 May 18. PMID: 19451168; PMCID: PMC2705234.
73. DePristo MA, Banks E, Poplin R, Garimella KV, Maguire JR, Hartl C, Philippakis AA, del Angel G, Rivas MA, Hanna M, McKenna A, Fennell TJ, Kernytsky AM, Sivachenko AY, Cibulskis K, Gabriel SB, Altshuler D, Daly MJ. A framework for variation discovery and genotyping using next-generation DNA sequencing data. Nat Genet. 2011 May;43(5):491-8. doi: 10.1038/ng.806. Epub 2011 Apr 10. PMID: 21478889; PMCID: PMC3083463.

74. McKenna A, Hanna M, Banks E, Sivachenko A, Cibulskis K, Kernytsky A, Garimella K, Altshuler D, Gabriel S, Daly M, DePristo MA. The Genome Analysis Toolkit: a MapReduce framework for analyzing next-generation DNA sequencing data. Genome Res. 2010 Sep;20(9):1297-303. doi: 10.1101/gr.107524.110. Epub 2010 Jul 19. PMID: 20644199; PMCID: PMC2928508.
75. Katoh K, Rozewicki J, Yamada KD. MAFFT online service: multiple sequence alignment, interactive sequence choice and visualization. Brief Bioinform. 2019 Jul 19;20(4):1160-1166. doi: 10.1093/bib/bbx108. PMID: 28968734; PMCID: PMC6781576.
76. Nguyen LT, Schmidt HA, von Haeseler A, Minh BQ. IQ-TREE: a fast and effective stochastic algorithm for estimating maximum-likelihood phylogenies. Mol Biol Evol. 2015 Jan;32(1):268-74. doi: 10.1093/molbev/msu300. Epub 2014 Nov 3. PMID: 25371430; PMCID: PMC4271533.
77. Letunic I, Bork P. Interactive Tree Of Life (iTOL) v4: recent updates and new developments. Nucleic Acids Res. 2019 Jul 2;47(W1):W256-W259. doi: 10.1093/nar/gkz239. PMID: 30931475; PMCID: PMC6602468.
78. Li H, Handsaker B, Wysoker A, Fennell T, Ruan J, Homer N, Marth G, Abecasis G, Durbin R; 1000 Genome Project Data Processing Subgroup. The Sequence Alignment/Map format and SAMtools. Bioinformatics. 2009 Aug 15;25(16):2078-9. doi: 10.1093/bioinformatics/btp352. Epub 2009 Jun 8. PMID: 19505943; PMCID: PMC2723002.
79. Warrenfeltz S, Basenko EY, Crouch K, Harb OS, Kissinger JC, Roos DS, Shanmugasundram A, Silva-Franco F. EuPathDB: The Eukaryotic Pathogen Genomics Database Resource. Methods Mol Biol. 2018;1757:69-113. doi: 10.1007/978-1-4939-7737-6_5. PMID: 29761457; PMCID: PMC7124890.

A

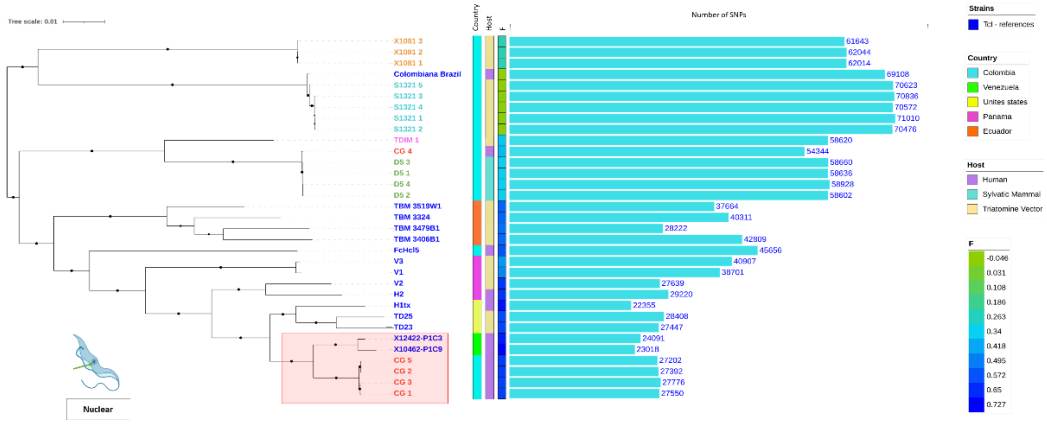

B

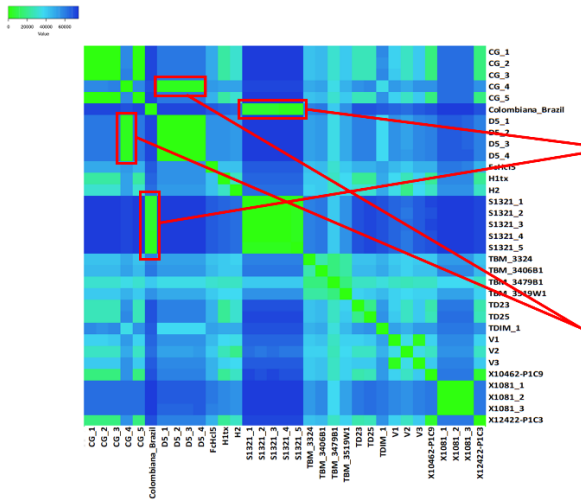

Sample 1	Sample 2	Number of SNPs
Colombiana_Brazil	S1321_1	4083
Colombiana_Brazil	S1321_2	4064
Colombiana_Brazil	S1321_3	4060
Colombiana_Brazil	S1321_4	3924
Colombiana_Brazil	S1321_5	3250

Sample 1	Sample 2	Number of SNPs
CG_4	D5_1	2396
CG_4	D5_2	2373
CG_4	D5_3	2406
CG_4	D5_4	2389

Fig. 1. Phylogenetic reconstruction of TcI. A. Phylogenetic reconstruction from *Trypanosoma cruzi* I genomes isolated from America. Blue color: TcI reference clones, Different colors: Colombian TcI clones per strains generated in this study. Country origin is represented with different colors, homozygosity values in the heatmap format and SNPs number in the barplot format. The corresponding clade with the TcI_{dom} genotype is indicated in the phylogeny cover by red square. B. SNPs differences per clones and strains.

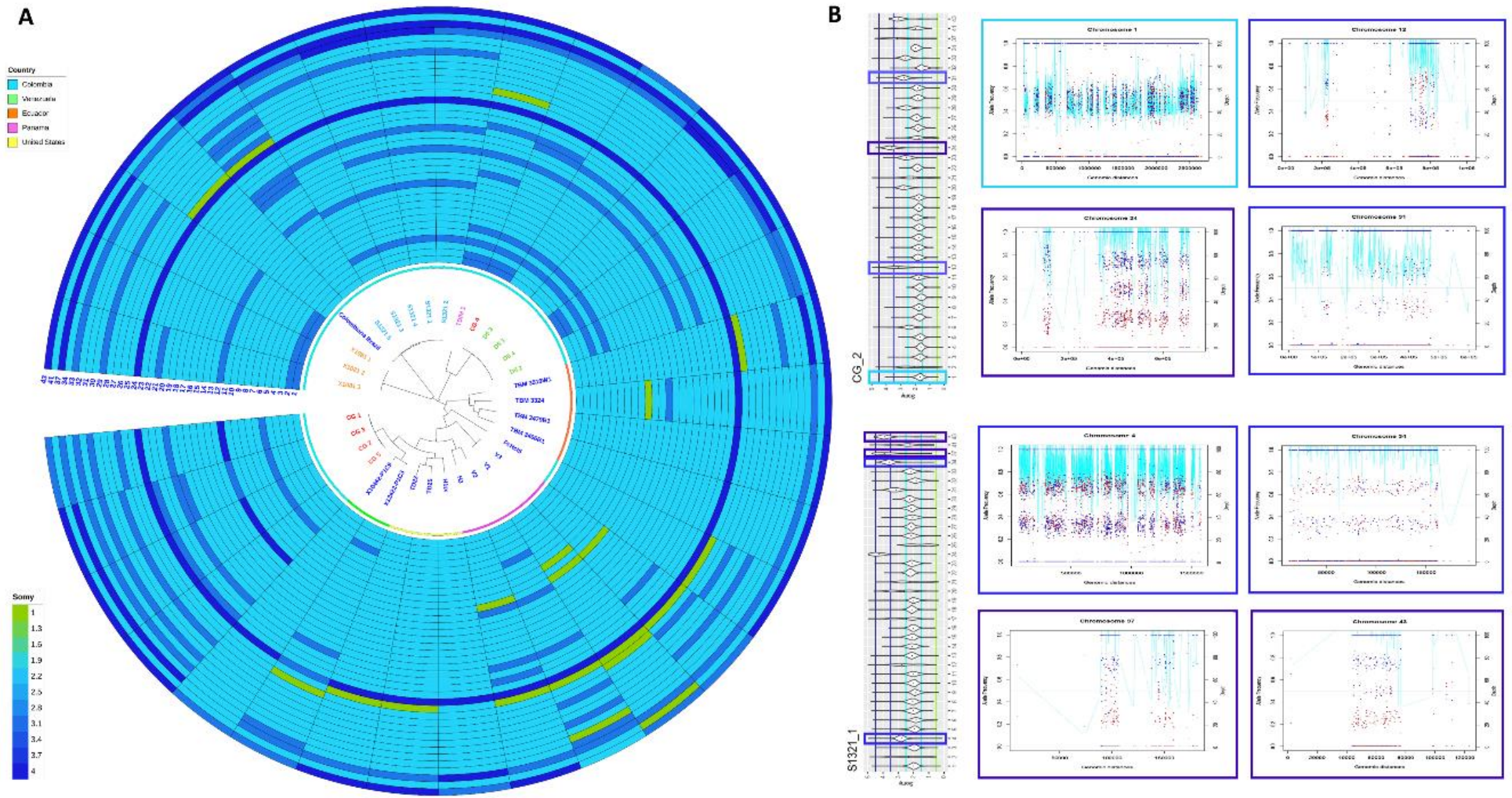

Fig. 2. Chromosomal Aneuploidy in *T. cruzi* I clones. A. The heatmap shows the ploidy calculated from the depth per chromosome for each of the TcI clones. Reference clones and sequenced clones for this study are noted. B. Depth (light blue lines) and Allelic frequencies (read and blue points) for the chromosomes.

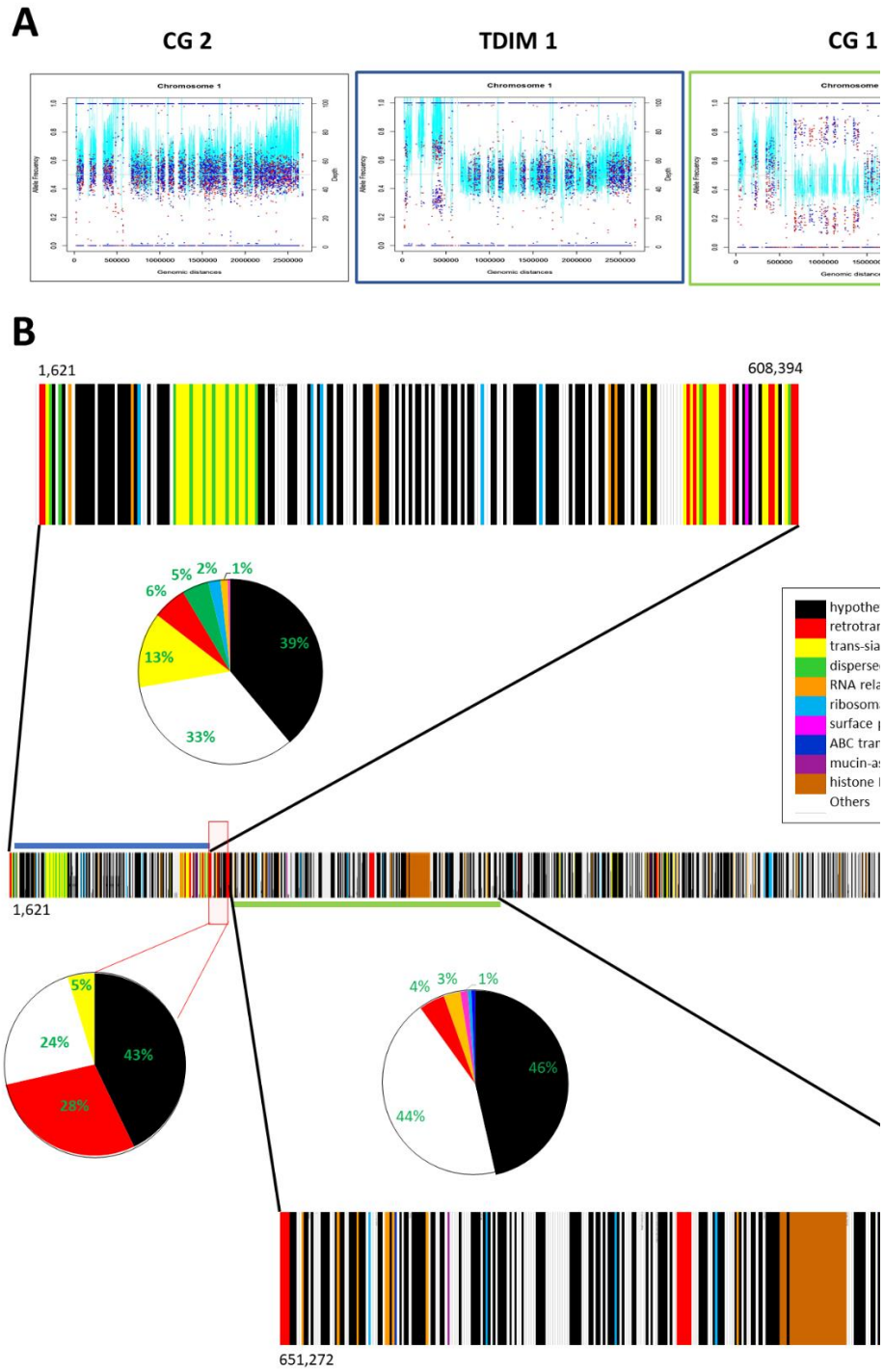

Fig. 3. Segmental modifications in allelic frequency and depth of chromosome 1 and gene anotiations. A. The graph shows the patterns of segmental allelic frequency and depth observed in the TcI clones evaluated. B. Gen annotations.

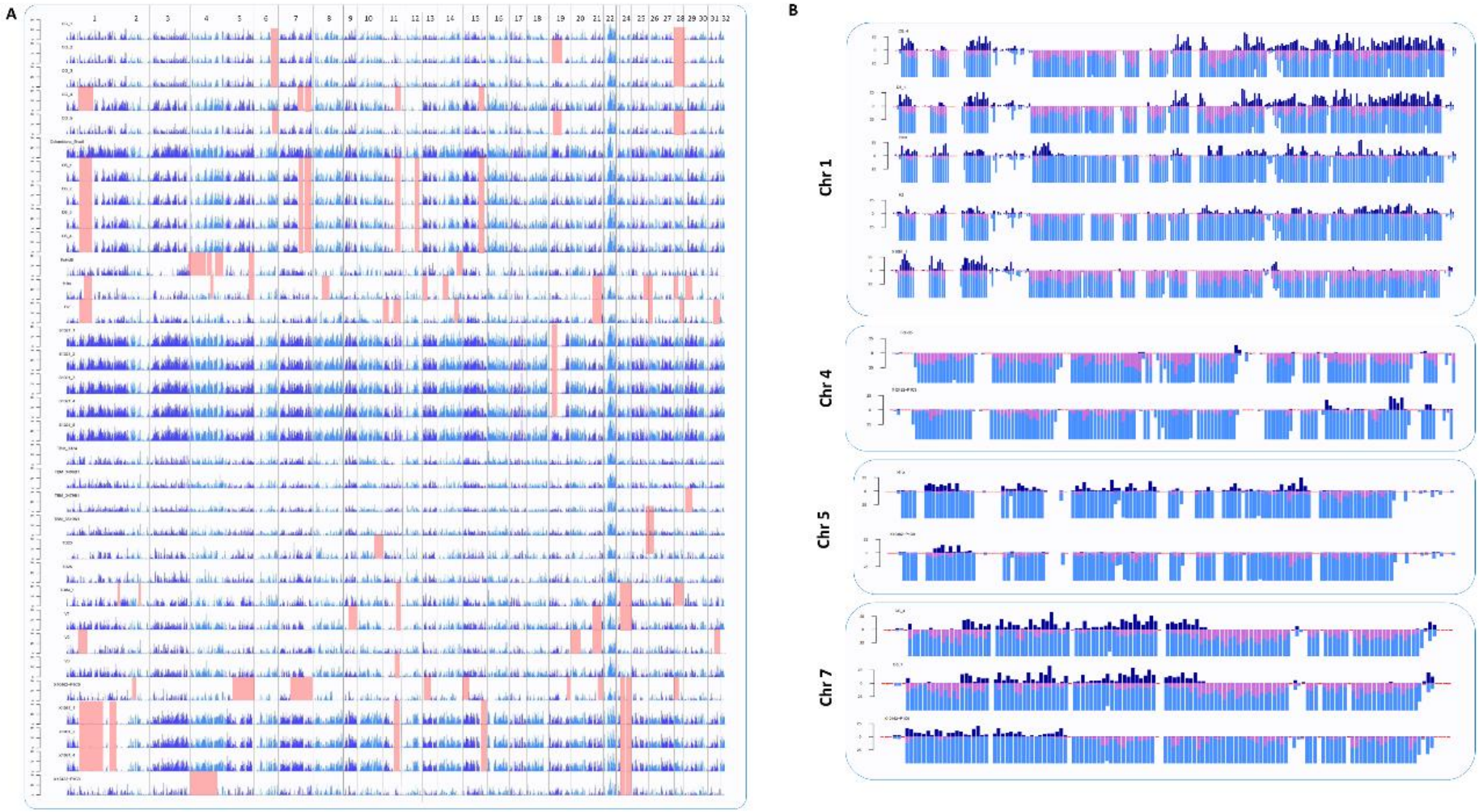

Fig. 4. Differential loss of heterozygosity between clones of *T. cruzi* I. A. presence of heterozygous **SNPs in the first 34 chromosmes, red squared symbolize areas with LOH. B.** The bar graph shows the heterozygous SNPs above the Y axis (dark blue), homozygous SNPs below the Y axis, in two groups, not present in the genome. reference (pink), present in the reference genome (light blue).

CAPÍTULO 2: Perfiles de expresión génica de *Trypanosoma cruzi* I durante el proceso de metaciclogénesis *in vitro.*

Journal of Microbiological Methods 142 (2017) 27–32

Contents lists available at ScienceDirect

Journal of Microbiological Methods

journal homepage: www.elsevier.com/locate/jmicmeth

Purification of *Trypanosoma cruzi* metacyclic trypomastigotes by ion exchange chromatography in sepharose-DEAE, a novel methodology for host-pathogen interaction studies

Lissa Cruz-Saavedra[a], Marina Muñoz[a], Cielo León[a], Manuel Alfonso Patarroyo[b,c], Gabriela Arevalo[b,c], Paula Pavia[d], Gustavo Vallejo[e], Julio César Carranza[e], Juan David Ramírez[a,*]

[a] Universidad del Rosario, Facultad de Ciencias Naturales y Matemáticas, Programa de Biología, Grupo de Investigaciones Microbiológicas-UR (GIMUR), Bogotá, Colombia
[b] Molecular Biology and Immunology Department, Fundación Instituto de Inmunología de Colombia (FIDIC), Bogotá, Colombia
[c] Universidad del Rosadio, School of Medicine and Health Sciences, Bogotá, Colombia
[d] Unidad de Investigación Cientifica, Subdirección de Docencia e Investigación, Hospital Militar Central, Bogotá, Colombia
[e] Laboratorio de Investigaciones en Parasitología Tropical-LIPT, Universidad del Tolima, Ibague, Colombia

ARTICLE INFO

Keywords:
Trypanosoma cruzi
Metacyclic trypomastigotes
Chromatography
Sepharose-DEAE
Culture

ABSTRACT

Metacyclic trypomastigotes are essential for the understanding of the biology of *Trypanosoma cruzi*, the agent of Chagas disease. However, obtaining these biological stages in axenic medium is difficult. Techniques based on charge and density of the parasite during different stages have been implemented, without showing a high efficiency in the purification of metacyclic trypomastigotes. So far, there is no protocol implemented where sepharose-DEAE is used as a resin. Therefore, herein we tested its ability to purify metacyclic trypomastigotes in Liver Infusion Triptose (LIT) medium cultures. A simple, easy-to-execute and effective protocol based on ion exchange chromatography on Sepharose-DEAE resin for the purification of *T. cruzi* trypomastigotes is described. *T. cruzi* strains from the Discrete Typing Units (DTUs) I and II were used. The strains were harvested in LIT medium at a concentration of 1×10^7 epimastigotes/mL. We calculated the time of trypomastigotes increment (TTI). Based on the data obtained, Ion exchange chromatography was performed with DEAE-sepharose resin. To verify the purity and viability of the trypomastigotes, a culture was carried out in LIT medium with subsequent verification with giemsa staining. To evaluate if the technique affected the infectivity of trypomastigotes, *in vitro* assays were performed in Vero cells and *in vivo* in ICR-CD1 mice. The technique allowed the purification of metacyclic trypomastigotes of other stages of *T. cruzi* in a percentage of 100%, a greater recovery was observed in cultures of 12 days. There were differences regarding the recovery of metacyclic trypomastigotes for both DTUs, being DTU TcI the one that recovered a greater amount of these forms. The technique did not affect parasite infectivity *in vitro* or/and *in vivo*.

1. Introduction

The kinetoplastid parasite *Trypanosoma cruzi* is the etiologic agent of Chagas disease, a tropical pathology that affects around 8 million people around the world (http://www.who.int/mediacentre/factsheets/fs340/en/). This parasite exhibits remarkable genetic variability and is subdivided into at least 6 discrete typing units (DTUs): *T. cruzi* I–VI and a recent described genotype associated to bats (TcBat) (Zingales et al., 2009; Brenière et al., 2016). These DTUs are associated with different clinical manifestations, epidemiological cycles of transmission and geographical regions (Hernández et al., 2016).

T. cruzi has a complex life cycle that occurs among humans, mammalian reservoirs and triatomine insects of the subfamily Reduviidae, displaying several morphological stages with distinct antigenic characteristics (Tyler and Engman, 2001). One of the most important processes during its life cycle is metacyclogenesis, which is defined as the transformation of replicative epimastigotes into infective metacyclic trypomastigotes (Kollien and Schaub, 2000). They develop in the rectum of the triatomine, and are implicated in the transmission of the parasite to the vertebrate host (Avila et al., 2003; Garcia et al., 2010).

T. cruzi infective metacyclic trypomastigotes have been fundamental for the understanding of the biology of the parasite, as well as for the

* Corresponding author.
E-mail address: juand.ramirez@urosario.edu.co (J.D. Ramírez).

http://dx.doi.org/10.1016/j.mimet.2017.08.021
Received 25 July 2017; Received in revised form 24 August 2017; Accepted 24 August 2017
Available online 01 September 2017

infection of cells and insects. Some methods are available to recover pure metacyclic trypomastigotes from axenic media such as Liver Infusion Tryptose (LIT), Triatomine Artificial Urine (TAU) and M16. Pure (100%) metacyclic trypomastigotes cannot be obtained using such media and as a result, cultures containing epimastigote stages are obtained (Camargo, 1964; Abegg et al., 2017). Therefore, in the eve of Next Generation Sequencing era and the new technologies that have arisen to conduct host-pathogen interaction studies, it is pivotal to have an easy, fast and reliable tool to purify total metacyclic trypomastigotes in the sample (Camargo, 1964; Castanys et al., 1984). Among them, density separation with percoll (Castanys et al., 1984; Rimoldi et al., 1986), and separation techniques based on the differential plasma membrane charge between epimastigotes and trypomastigotes using ion exchange chromatography with resins such as cellulose-DEAE, dE − 52 and sephadex, have been developed for the purification of metacyclic trypomastigotes (Abbassy et al., 1972; Gutteridge et al., 1978; Chao and Dusanic, 1984). These methods include the purification of blood and intracellular forms of *T. cruzi* (Gutteridge et al., 1978; Schmatz and Murray, 1981; de Sousa and 33, 1983).

The extensive use of chromatography has permitted purifying metacyclic trypomastigotes for the association of specific molecules expressed on this parasite stage membrane that are either involved in cell invasion (mainly transialidases as the gp82 and gp90), insect epithelial cell invasion and adhesion to gastric mucin (Neira et al., 2003; Manque et al., 2000; Bayer-Santos et al., 2013), effective drug evaluation for the different *T. cruzi* stages (Orrego et al., 2014; Villamizar et al., 2017) and molecular characterization of membrane protein families from metacyclic trypomastigotes involved in invasion and resistance (Martins et al., 2015; Cestari and Ramirez, 2010). This methodology has also been employed to purify parasite proteins such as alkaline kinase, coimmunoprecipitation between CK2 proteins and tubulin, as well as extracting proteins expressed in tissues infected with the parasite (Morris et al., 1990; Santana et al., 1992; de Lima et al., 2006). Moreover, it has been also used to obtain *Trypanosoma evansi* antigens (Camargo et al., 2004), *Fasciola hepatica* hemoproteins and some bacterial antigens from *Escherichia coli* and virulence factors from *Helicobacter pylori* (McGonigle and Dalton, 1995; Sigdel et al., 2004; Shih et al., 2013; Hong et al., 2017). However, to date, no protocol has been reported where sepharose-DEAE is used as a resin for *T. cruzi*. Based on the above-mentioned data, and considering the necessity of purifying metacyclic trypomastigotes. The aim of this work was to describe a simple, easy and effective protocol based on ion exchange chromatography in sepharose-DEAE resin for the purification of *T. cruzi* metacyclic trypomastigotes.

2. Materials and methods

2.1. Parasites - metacyclogenesis curves

A total of 1×10^8 epimastigotes/mL from the MDID/BR/84/DM28 (TcI), and MHOM/BR/53/Y (TcII) strains were cultured in LIT medium supplemented with 5% inactivated fetal calf serum, 5% CO_2 at 26 °C. The concentration of parasites was determined daily by Neubauer chamber and the discrimination between stages (epimastigotes and trypomastigotes) was evaluated in Giemsa stained slides. This allowed the differentiation of these stages based on the location of the kinetoplast, nucleus and modifications in the flagellum. Epimastigotes present a compact nucleus in the middle of the cytoplasm, a kinetoplast located in the anterior part of the parasite, and just after this is observed the flagellum. On the other hand, metacyclic trypomastigotes show an elongated nucleus, kinetoplast located in the posterior part of the parasite and finally a flagellum that surrounds the cytoplasm of the parasite from the posterior to the anterior section. With the data obtained during approximately 12 days, curves of metacyclogenesis were performed and the day where a significant increase of trypomastigote forms was recorded with respect to day 0. This was defined as time of trypomastigotes increment (TTI). A total of 3 replicates (3 cultures) for each of the strains were used to avoid bias in the evaluation of metacyclogenesis.

2.2. Purification of metacyclic trypomastigotes

The ion exchange chromatography technique on sepharose membrane-DEAE was standardized to obtain a medium of pure metacyclic trypomastigotes (free of epimastigotes), as follows:

The stationary phase corresponded to the DEAE sepharose resin and the mobile one to PBS plus 4.5% glucose (PBG). A pH = 8.0 is required for the compound coupled to the DEAE-sepharose to maintain a negative charge. Subsequently, 2 mL of DEAE-sepharose were added to a column that allowed the flow of PBG (the resin was equilibrated to pH 8 by adding 30 mL of PBG). The pH of the column was verified before further development of the technique. A total of three replicates of epimastigote-trypomastigote cultures from each of the strains (MDID/BR/84/DM28 (TcI), and MHOM/BR/53/Y (TcII)) that were on the TTI day were used from 10 mL cultures in LIT medium, and were centrifuged at 2500 rpm. The supernatant was discarded and the pellet obtained was resuspended in PBG, and further centrifugation was performed to remove residues from the LIT medium that could interfere with the chromatography. The supernatant was discarded again and the pellet was retained. Finally, the parasites were suspended in 5 mL of PBG, and transferred to the equilibrated DEAE column. 5 mL of eluate were collected and then centrifuged, the supernatant was discarded with a Pasteur pipette to prevent loss of trypomastigotes of the pellet preserving 1 mL of the content. In order to confirm the results, a total of 3 replicates were performed, the replicates made were analyzed by the methodologies Sections 2.3 and 2.4 described in this article. The procedure described above was performed for each of the three replicates of both strains.

2.3. Giemsa staining and quantification of trypomastigotes

The parasites obtained were quantified in a Neubauer chamber and Giemsa staining was performed to evaluate the efficiency in the recovery of trypomastigotes (discriminating between the parasite stages present). For the quantification of trypomastigotes obtained, a 1:10 dilution was made with 10 μL of the eluate obtained and 90 μL of PBG. An aliquot of 10 μL of the dilution was dispensed in the Neubauer chamber. Reading was performed by counting the parasites present in the 4 quadrants of the chamber, followed by the calculation of the average of total parasites on the number of quadrants, and multiplying this result by 10,000 and the dilution used, which in this case corresponds to 10. The evaluation and differentiation between *T. cruzi* stages was carried out using the previously described methodology by observing the kinetoplast, nucleus and flagellum. The concentration of trypomastigotes before and after the purification was calculated with the data obtained.

2.4. Cultivation in LIT medium

One of the characteristics that *T. cruzi* exhibits is the replication ability only present in the amastigote and epimastigote stages (Tyler and Engman, 2001). Therefore, a culture of the final eluate in LIT medium supplemented with 5% fetal bovine serum was performed for 8 days to evaluate the purity of the trypomastigotes collected in the eluate. If there were epimastigotes in the eluate, this could represent evidence of concentration increase and subsequently presence of pure epimastigotes in the LIT culture.

2.5. Cell culture

Infections in VERO semiconfluent cells (Vero (ATCC® CCL-81™) were performed to verify *in vitro* susceptibility of Vero cells to infection

with TcI and TcII metacyclic trypomastigotes. Approximately 700,000 cells/mL were infected with 4,000,000 parasites/mL of each strain and maintained in 25 cm^2 flasks at 37 °C with 5% CO_2. The first culture replacement with Dulbecco's Modified Eagle Medium (DMEM) supplemented with 10% SFB was performed on the second day of infection and thereafter every five days. The cultures were observed daily under inverted microscopy in the search for amastigotes or trypomastigotes. A total of three replicates were employed.

2.6. Infection in mice

A set of four Twenty-six-day ICR-CD1 mice were infected intraperitoneally with a 1×10^6 trypomastigotes of each of the strains to test the infectivity of trypomastigotes *in vivo* (two replicates per strain). The biomodels were maintained at the animal facility of the Universidad de Los Andes, Colombia, under biosecurity standards, macroambient conditions, humidity 60% ± 5, temperature 20 °C ± 2, ventilation of 10 to 15 changes per hour, housed in type T3 stainless steel cages of 48 cm of length, 26 cm of width and 16 cm of height, with a capacity of 3 animals per cage, supply of water and food *ad libitum*, following the principles for the experimentation with animals stipulated in the Bioterium and following national and international regulations. To evaluate the parasitemia, 50 μL of blood were obtained from the animal's tail, during 16, 30 and 45 days of testing, obtaining three samples per mouse and a total of 6 samples per strain (2 replicates). The samples obtained were submitted to extraction of DNA using the Roche High Pure PCR Template Preparation Kit, followed by a quantitative qPCR, following the protocol of Duffy et al., 2012.

2.7. Statistic analyses

The data obtained were tabulated in Excel 2015 for the performance of the metacyclogenesis curve using 2 replicates per strain. The graphs corresponding to the metacyclogenesis curve, as well as the statistical analyses (normality, ANOVA and multiple comparisons between the production of trypomastigotes during the different days of the metacyclogenesis curve), were performed in the GraphPad Prism 6 software.

3. Results and discussion

3.1. Parasites - metacyclogenesis curve

The concentration of parasites used (1×10^8) induced the metacyclogenesis of epimastigotes from day 1 post culture (DPC) for both strains (Fig. 1), which could be related to a nutritional stress and a redox status caused by the decrease of nutrients generated by the high concentration of parasites in the medium. Nutritional stress is considered a prime factor that triggers the metacyclogenesis of the parasite, due to the activation of enzymes such as adenylate cyclase and subsequent increase of cAMP in the medium (Nogueira et al., 2015; Hamedi et al., 2015; Shaw et al., 2016). However, considering that these trypomastigotes may correspond to an earlier culture, the TTI was estimated. Both strains exhibited an increase in metacyclogenesis from 4 DPC (Fig. 1A). Despite this, when performing the ANOVA test and the analysis of multiple comparisons, statistically significant differences were only observed with TTI from 8 DPC for the MDID/BR/84/DM28 (TcI) strain (Fig. 1B), and 6 DPC for the MHOM/BR/53/Y strain (TcII) (Fig. 1C), with lower concentrations of transformed trypomastigotes for the TcI strain. These results could be related to the genetic and biological differences that have been observed between these DTUs, and are most likely associated with the fundamental role played by the parasite membrane (Abegg et al., 2017). It should be noted that the MHOM/BR/53/Y strain maintained a constant trypomastigote concentration from TTI day.

3.2. Purification of metacyclic trypomastigotes

One of the characteristic features of epimastigote and trypomastigote stages is the difference in plasma membrane charge, as has been previously demonstrated in several studies (Abbassy et al., 1972; Gutteridge et al., 1978). We decided to test the purification of metacyclic trypomastigotes from a culture in LIT medium, which also had abundant epimastigotes (Fig. 1D–E), using the DEAE-sepharose affinity chromatography technique, where DEAE bound to the resin has a high positive charge. This compound captures the epimastigotes due to the formation of an electrostatic ionic bond between the DEAE and the parasite membrane. The trypomastigotes do not present this charge and pass through the resin and can be recovered in the eluate. The ion exchange chromatography with DEAE sepharose resin allowed the separation of 100% pure metacyclic trypomastigotes from the epimastigote stages under the conditions mentioned above. The results were obtained from visualizing three replicates of 200 parasites in one Giemsa-colored slide and daily observation for a period of 8 days of an eluate culture in LIT medium (Fig. 2C–D). Another parameter analyzed was the recovery of trypomastigotes; for this purpose, the amount of trypomastigotes before and after the separation were determined. It was observed that the technique allowed the recovery of a smaller number of trypomastigotes compared to those that were initially in the LIT media and that these differences were higher for the MHOM/BR/53/Y strain (Fig. 2A). The differential expression of some transialidases such as gp82 and gp90 among different strains has been demonstrated, which could be related to lower levels of sialic acid in the membrane that would lead to a modification in the membrane charge. Considering that the sialic acid is the main contributor to the membrane charge of the parasite and related to the infectivity capacity of *T. cruzi*, differences in the parasite yield obtained after purification were expected between strains (Franchin et al., 1997). However, we did not observe epimastigotes (stages with negative charge), in the obtained eluate which could indicate an increase in the negative charge of MHOM/BR/53/Y strain trypomastigotes and therefore an increase in the affinity for the resin, which could explain the low concentrations of trypomastigotes obtained in the eluate, confirming the high biological differences that could be associated with differences in the plasma membrane (Neira et al., 2003; Manque et al., 2000; Bayer-Santos et al., 2013).

The changes in the recovery of trypomastigotes observed when performing the technique could be due to the presence of immature stages of metacyclic trypomastigotes that still possess epimastigote characteristics like membrane charge and could be retained by the sepharose resin – DEAE (Kollien and Schaub, 2000). The Sepharose - DEAE chromatography resulted in a greater recovery of trypomastigote under these conditions (Fig. 2B) using parasites corresponding to 12 DPC. This was probably due to complete differentiation into metacyclic trypomastigotes. These results confirm the remodeling that the parasite undergoes in the plasma membrane, that is most likely associated with the function exerted by the trypomastigote stages and its relation with the infective capacity (Serrano et al., 1995; de Andrade et al., 1991; Schenkman et al., 1993; Chaves et al., 1993; Yoshida et al., 1997). Finally, we decided to evaluate some parameters and conditions that allow an efficient set-up for the technique. An optimal volume of 2 mL DEAE-sepharose was found for a 10 mL column; resin saturation was observed when 1×10^9 parasites/mL were loaded, allowing the passage of epimastigotes; moreover, the maximum recovery volume (eluate obtained) was 5 mL, since a larger volume would allow the passage of epimastigotes.

3.3. In vitro and in vivo evaluation

Considering that the metacyclic trypomastigotes correspond to the infective stage of the parasite, we decided to evaluate if the DEAE-sepharose chromatography could affect this characteristic. An *in vitro* test was performed to solve this concern in VERO cells and *in vivo* in ICR-

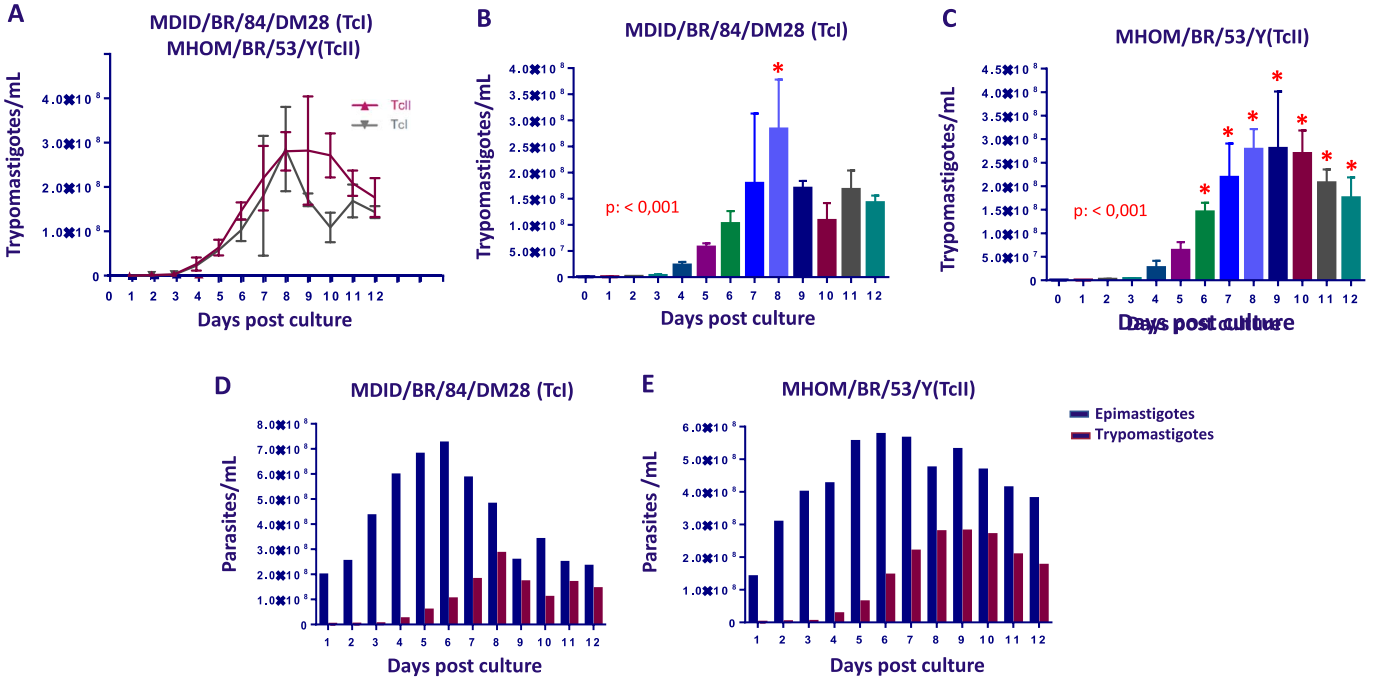

Fig. 1. Metacyclogenesis *in vitro*. A. Metacyclogenesis Curves TcI and TcII. B. TcI metacyclic trypomastigotes. C. TcII Metacyclic trypomastigotes. D. Comparison of epimastigotes and TcI metacyclic trypomastigotes. E. Comparison of epimastigotes and TcI metacyclic trypomastgiotes. The results were statistically significant when $p < 0.05$. The results were obtained using 3 replicates.

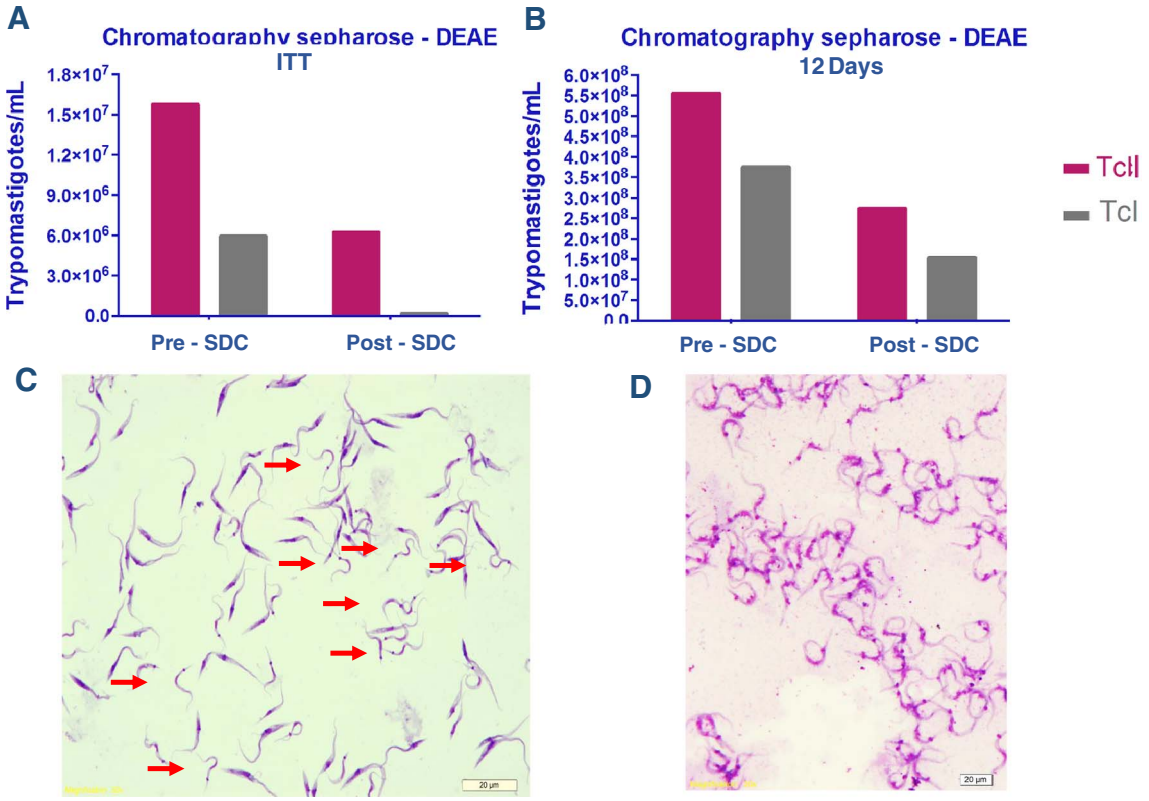

Fig. 2. Sepharose Chromatography - DEAE. A. Chromatography day time of trypomastigotes increment (TTI). B. Chromatography day 12, C. Metacyclic trypomastigotes and epimastigotes in Liver Infusion Tryptose (LIT) medium. B. Trypomastigotes obtained by chromatography in sepharose-DEAE.

CD1 mice. The *in vitro* analysis showed the ability of trypomastigotes of the TcI (MDID/BR/84/DM28) and TcII (MHOM/BR/00/Y) strains to develop, where amastigote nests and free trypomastigotes were observed at 11 days of infection (Fig. 3A–B). When the *in vivo* infectivity evaluation of both strains was carried out, both mice were positive by qPCR; one of the mice infected with the MHOM/BR/00/Y strain showed a decrease in motor activity, piloerection and finally death. The samples were positive for *T. cruzi* from day 16 until the end of the test

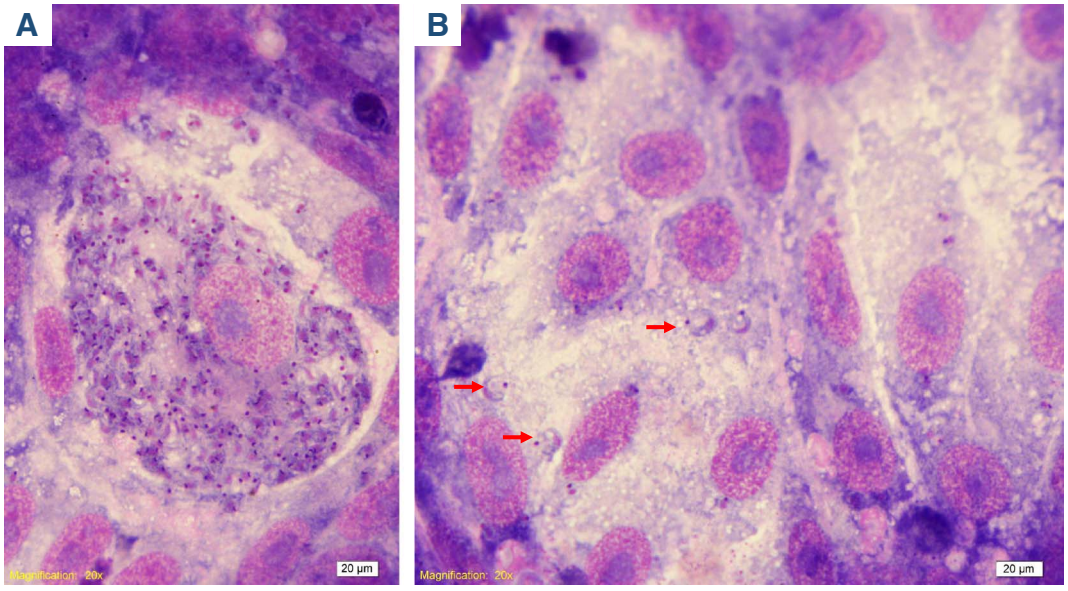

Fig. 3. *In vitro* and *in vivo* evaluation. A. Amastigotes of *T. cruzi* in Vero cells. B. Peripheral blood trypomastigotes in Vero cells.

(16, 30, 45 days). These results are related to the age of the mice and the development of a potent immune system. One of the major disadvantages presented by the chromatography techniques previously described with cellulose-DEAE and the sephadex, was the decrease in the infective capacity of the obtained trypomastigotes (Abbassy et al., 1972; Chao and Dusanic, 1984). In the present study our results have shown that the trypomastigotes obtained by DEAE-sepharose maintain their infectivity both *in vivo* and *in vitro*.

4. Conclusions

The methodology herein described allowed the complete purification of metacyclic trypomastigotes cultured in LIT medium which contained epimastigote forms prior to purification. The technique allowed a greater recovery of fully differentiated metacyclic trypomastigotes. The infectivity of trypomastigotes was not affected either *in vitro* or *in vivo*. This technique is a fast and efficient alternative for purifying metacyclic trypomastigote stages with a high purity and also without affecting their infectivity, which represents a technique of great utility in the study of specific characteristics of this parasite stage and also for the comprehension of the *T. cruzi* life cycle and studies related to host-pathogen interactions.

Acknowledgements

This work was funded by the Fondo Nacional de Financiamiento para la ciencia, la tecnología y la innovación Francisco José de Caldas, Departamento Administrativo de Ciencia, Tecnología e Innovación (Colciencias), award number FP44842-063-2015.

References

Abbassy, S.N., Seed, T.M., Kreier, J.P., 1972. Isolation of the trypomastigote form of *Trypanosoma cruzi* from a mixture of the trypomastigotes and epimastigote forms of the parasite by use of a DEAE-cellulose column. J. Parasitol. 58, 631–632.

Abegg, C.P., Abreu, A.P., Silva, J.L., Araújo, S.M., Gomes, M.L., Ferreira, É.C., Toledo, M.J., 2017. Polymorphisms of blood forms and in vitro metacyclogenesis of *Trypanosoma cruzi* I, II, and IV. Exp. Parasitol. 176, 8–15 (doi: 10.1016/j.exppara.2017.02.013).

de Andrade, A.F., Esteves, M.J., Angluster, J., Gonzales-Perdomo, M., Goldenberg, S., 1991. Changes in cell-surface carbohydrates of *Trypanosoma cruzi* during metacyclogenesis under chemically defined conditions. J. Gen. Microbiol. 137 (12), 2845–2849 (PubMed PMID: 1791438).

Avila, A.R., Dallagiovanna, B., Yamada-Ogatta, S.F., Monteiro-Góes, V., Fragoso, S.P., Krieger, M.A., Goldenberg, S., 2003. Stage-specific gene expression during *Trypanosoma cruzi* metacyclogenesis. Genet. Mol. Res. 31 (2(1)), 159–168 (Review. PubMed PMID: 12917812).

Bayer-Santos, E., Cunha-e-Silva, N.L., Yoshida, N., Franco da Silveira, J., 2013. Expression and cellular trafficking of GP82 and GP90 glycoproteins during *Trypanosoma cruzi* metacyclogenesis. Parasit. Vectors 6, 127. http://dx.doi.org/10.1186/1756-3305-6-127.

Brenière, S.F., Waleckx, E., Barnabé, C., 2016. Over six thousand *Trypanosoma cruzi* strains classified into Discrete Typing Units (DTUs): attempt at an inventory. PLoS Negl. Trop. Dis. 10 (8), e0004792 (doi:10.1371/journal.pntd.0004792).

Camargo, E.P., 1964. Growth and differentiation in *Trypanosoma cruzi*. I. Origin of metacyclic trypano-somes in liquid media. Rev. Inst. Med. Trop. 6, 93–100.

Camargo, R.E., Uzcanga, G.L., Bubis, J., 2004. Isolation of two antigens from *Trypanosoma evansi* that are partially responsible for its cross-reactivity with *Trypanosoma vivax*. Vet. Parasitol. 13 (123(1–2)), 67–81 (PubMed PMID: 15265572).

Castanys, S., Osuana, A., Camarro, F., Ruiz-Perez, L.M., 1984. Purification of metacyclic forms of *Trypanosoma cruzi* by Percoll discontinuous gradient centrifugation. Z. Parasitenkd. 70, 443–449.

Cestari, I., Ramirez, M.I., 2010. Inefficient complement system clearance of *Trypanosoma cruzi* metacyclic trypomastigotes enables resistant strains to invade eukaryotic cells. Gruner AC, ed. PLoS ONE 5 (3), e9721 (doi:10.1371/journal.pone).

Chao, D., Dusanic, D.G., 1984. Comparative studies of the isolation of metacyclic trypomastigotes of *Trypanosoma cruzi* by DEAE ion exchange chromatography. Zhonghua Min. Guo Wei Sheng Wu Ji Mian Yi Xue Za Zhi 17 (3), 146–152 (PubMed PMID: 6391853).

Chaves, L.B., Briones, M.R., Schenkman, S., 1993. Trans-sialidase from *Trypanosoma cruzi* epimastigotes is expressed at the stationary phase and is different from the enzyme expressed in trypomastigotes. Mol. Biochem. Parasitol. 61 (1), 97–106 (PubMed PMID: 8259137).

De Lima, A.R., Medina, R., Uzcanga, G.L., Noris Suárez, K., Contreras, V.T., Navarro, M.C., Arteaga, R., Bubis, J., 2006. Tight binding between a pool of the heterodimeric alpha/beta tubulin and a protein kinase CK2 in *Trypanosoma cruzi* epimastigotes. Parasitology 132 (Pt 4), 511–523.

Duffy, T., Cura, C.I., Ramirez, J.C., Abate, T., Cayo, N.M., Parrado, R., et al., Schijman, A.G., 2012. Analytical performance of a multiplex real-time PCR assay using TaqMan probes for quantification of *Trypanosoma cruzi* satellite ADN in blood samples. PLoS Negl. Trop. Dis. 7 (1), e2000 (10.1371/journal.pntd.0002000).

Franchin, G., Pereira-Chioccola, V.L., Schenkman, S., Rodrigues, M.M., 1997. Passive transfer of a monoclonal antibody specific for a sialic acid-dependent epitope on the surface of *Trypanosoma cruzi* trypomastigotes reduces infection in mice. Infect. Immun. 65 (7), 2548–2554.

Garcia, E.S., Genta, F.A., de Azambuja, P., Schaub, G.A., 2010. Interactions between intestinal compounds of triatomines and *Trypanosoma cruzi*. Trends Parasitol. 26 (10), 499–505 (doi: 10.1016/j.pt.2010.07.003. Review. PubMed PMID: 20801082).

Gutteridge, W.E., Cover, B., Gaborak, M., 1978. Isolation of blood and intracellular forms of *Trypanosoma cruzi* from rats and other rodents and preliminary studies of their metabolism. Parasitology 76, 159–176.

Hamedi, A., Botelho, L., Britto, C., Fragoso, S.P., Umaki, A.C., Goldenberg, S., Bottu, G., Salmon, D., 2015. In vitro metacyclogenesis of *Trypanosoma cruzi* induced by starvation correlates with a transient adenylyl cyclase stimulation as well as with a constitutive upregulation of adenylyl cyclase expression. Mol. Biochem. Parasitol. 200 (1–2), 9–18 (doi: 10.1016/j.molbiopara.2015.04.002. Epub Apr 23. PubMed PMID: 25912925).

Hernández, C., Cucunubá, Z., Flórez, C., Olivera, M., Valencia, C., et al., Ramírez, J.D., 2016. Molecular diagnosis of chagas disease in Colombia: parasitic loads and discrete typing units in patients from acute and chronic phases. PLoS Negl. Trop. Dis. 10 (9),

e0004997 (doi:10.1371/journal.pntd.0004997).
Hong, Z.-W., Yang, Y.-C., Pan, T., Tzeng, H.-F., Fu, H.-W., 2017. Differential effects of DEAE negative mode chromatography and gel-filtration chromatography on the charge status of Helicobacter pylori neutrophil-activating protein. Ho PL, ed. PLoS ONE 12 (3), e0173632 (doi:10.1371/journal.pone.0173632).
Kollien, A.H., Schaub, G.A., 2000. The development of *Trypanosoma cruzi* in triatominae. Parasitol. Today 16 (9), 381–387.
Manque, P.M., Eichinger, D., Juliano, M.A., Juliano, L., Araya, J.E., Yoshida, N., 2000. Characterization of the cell adhesion site of *Trypanosoma cruzi* metacyclic stage surface glycoprotein gp82. Mansfield JM, ed. Infect. Immun. 68 (2), 478–484.
Martins, N.O., de Souza, R.T., Cordero, E.M., Cortez, D., Cortez, C., da Silveira, J.F., et al., 2015. Molecular characterization of a novel family of *Trypanosoma cruzi* surface membrane proteins (TcSMP) involved in mammalian host cell invasion. PLoS Negl. Trop. Dis. 9 (11), e0004216 (doi:10.1371/journal.pntd.0004216).
McGonigle, S., Dalton, J.P., 1995. Isolation of Fasciola hepatica haemoglobin. Parasitology 111 (Pt 2), 209–215 (PubMed PMID: 7675536).
Morris, S.A., Wittner, M., Weiss, L., Hatcher, V.B., Tanowitz, H.B., Bilezikian, J.P., Gordon, P.B., 1990. Extracellular matrix derived from *Trypanosoma cruzi* infected endothelial cells directs phenotypic expression. J. Cell. Physiol. 45 (2), 340–346 (PubMed PMID: 1700983).
Neira, I., Silva, F,.A., Cortez, M., Yoshida, N., 2003. Involvement of *Trypanosoma cruzi* metacyclic trypomastigote surface molecule gp82 in adhesion to gastric mucin and invasion of epithelial cells. Infect. Immun. 71 (1), 557–561 (doi:10.1128/IAI.71.1.557-561.2003).
Nogueira, N.P., Saraiva, F.M.S., Sultano, P.E., Cunha, P.R.B.B., Laranja, G.A.T., Paes, M.C., et al., 2015. Proliferation and differentiation of *Trypanosoma cruzi* inside its vector have a new trigger: redox status. PLoS ONE 10 (2), e0116712 (doi:10.1371/journal.pone.0116712).
Orrego, P.R., Olivares, H., Cordero, E.M., Bressan, A., Cortez, M., Araya, J.E., et al., 2014. A cytoplasmic new catalytic subunit of calcineurin in *Trypanosoma cruzi* and its molecular and functional characterization. PLoS Negl. Trop. Dis. 8 (1), e2676 (doi:10.1371/journal.pntd.0002676).
Rimoldi, M.T., Katzin, V.J., González Cappa, S.M., de Bracco, M.M., 1986. Isolation by Percoll gradient centrifugation and radiolabeling of bloodstream forms of *Trypanosoma cruzi*. Rev. Argent. Microbiol. 18 (1), 41–44 (PubMed PMID: 3120241).
Santana, J.M., Grellier, P., Rodier, M.H., Schrevel, J., Teixeira, A., 1992. Purification and characterization of a new 120 kDa alkaline proteinase of *Trypanosoma cruzi*. Biochem. Biophys. Res. Commun. 30 (187(3)), 1466–1473 (PubMed PMID: 1417823).
Schenkman, R.P., Vandekerckhove, F., Schenkman, S., 1993. Mammalian cell sialic acid enhances invasion by *Trypanosoma cruzi*. Infect. Immun. 61 (3), 898–902.
Schmatz, D.M., Murray, P.K., 1981. *Trypanosoma cruzi*: selective isolation of pure trypomastigotes from cultured muscle cells. J. Parasitol. 67 (4), 517–521 (PubMed PMID: 7021789).
Serrano, A.A., Schenkman, S., Yoshida, N., Mehlert, A., Richardson, J.M., Ferguson, M.A., 1995. The lipid structure of the glycosylphosphatidylinositol-anchored mucin-like sialic acid acceptors of *Trypanosoma cruzi* changes during parasite differentiation from epimastigotes to infective metacyclic trypomastigote forms. J. Biol. Chem. 10 (270(45)), 27244–27253 (PubMed PMID: 7592983).
Shaw, A.K., Kalem, M.C., Zimmer, S., 2016. Mitochondrial gene expression is responsive to starvation stress and developmental transition in *Trypanosoma cruzi*. mSphere 1 (2), e00051–16 (doi:10.1128/mSphere.00051-16).
Shih, K.-S., Lin, C.-C., Hung, H.-F., Yang, Y.C., Wang, C.A., Jeng, K.C., Fu, H.W., 2013. One-step chromatographic purification of *Helicobacter pylori* neutrophil-activating protein expressed in *Bacillus subtilis*. PLoS ONE 8 (4), e60786 (doi:10.1371/journal.pone.0060786).
Sigdel, T.K., Cilliers, R., Gursahaney, P.R., Crowder, M.W., 2004. Fractionation of soluble proteins in *Escherichia coli* using DEAE-, SP-, and phenyl sepharose chromatographies. J. Biomol. Tech. 15 (3), 199–207.
de Sousa, M.A., 1983. A simple method to purify biologically and antigenically preserved bloodstream trypomastigotes of *Trypanosoma cruzi* using DEAE-cellulose columns. Mem. Inst. Oswaldo Cruz 78 (3), 317–333 (PubMed PMID: 6361445).
Tyler, K.M., Engman, D.M., 2001a. The life cycle of *Trypanosoma cruzi* revisited. Int. J. Parasitol. 31 (5-6), 472–481 (Review. PubMed PMID: 11334932).
Villamizar, L.H., Cardoso, M., de Andrade, J., Teixeira, M.L., Soares, M.J., 2017. Linalool, a Piper aduncum essential oil component, has selective activity against *Trypanosoma cruzi* trypomastigote forms at 4 °C. Mem. Inst. Oswaldo Cruz 112 (2), 131–139 (doi:10.1590/0074-02760160361).
Yoshida, N., Dorta, M.L., Ferreira, A.T., Oshiro, M.E., Mortara, R.A., Acosta-Serrano, A., Favoreto Júnior, S., 1997. Removal of sialic acid from mucin-like surface molecules of *Trypanosoma cruzi* metacyclic trypomastigotes enhances parasite-host cell interaction. Mol. Biochem. Parasitol. 84 (1), 57–67 (PubMed PMID: 9041521).
Zingales, B., Andrade, S.G., Briones, M.R.S., Campbell, D.A., Chiari, E., Fernandes, O., et al., 2009. A new consensus for *Trypanosoma cruzi* intraspecific nomenclature: second revision meeting recommends TcI to TcVI. Mem. Inst. Oswaldo Cruz 104, 1051–1054.

Parasites & Vectors

RESEARCH Open Access

Slight temperature changes cause rapid transcriptomic responses in *Trypanosoma cruzi* metacyclic trypomastigotes

Lissa Cruz-Saavedra[1], Marina Muñoz[1], Luz Helena Patiño[1], Gustavo A. Vallejo[2], Felipe Guhl[3] and Juan David Ramírez[1*]

Abstract

Background: Severe changes in temperature can affect the behavior and ecology of some infectious agents. *Trypanosoma cruzi* is a protozoan that causes Chagas disease. This parasite has high genetic variability and can be divided into six discrete typing units (DTUs). *Trypanosoma cruzi* also has a complex life-cycle, which includes the process of metacyclogenesis when non-infective epimastigote forms are differentiated into infective metacyclic trypomastigotes (MT). Studies in triatomines have shown that changes in temperature also affect the number and viability of MT.

Methods: The objective of this study was to evaluate how temperature affects the transcriptional profiles of *T. cruzi* I and II (TcI and TcII) MT by exposing parasites to two temperatures (27 °C and 28 °C) and comparing those to normal culture conditions at 26 °C. Subsequently, RNA-seq was conducted and differentially expressed genes were quantified and associated to metabolic pathways.

Results: A statistically significant difference was observed in the number of MT between the temperatures evaluated and the control, TcII DTU was not strongly affected to exposure to high temperatures compared to TcI. Similar results were found when we analyzed gene expression in this DTU, with the greatest number of differentially expressed genes being observed at 28 °C, which could indicate a dysregulation of different signaling pathways under this temperature. Chromosome analysis indicated that chromosome 1 harbored the highest number of changes for both DTUs for all thermal treatments. Finally, gene ontology (GO) analyses showed a decrease in the coding RNAs involved in the regulation of processes related to the metabolism of lipids and carbohydrates, the evasion of oxidative stress, and proteolysis and phosphorylation processes, and a decrease in RNAs coding to ribosomal proteins in TcI and TcII, along with an increase in the expression of surface metalloprotease GP63 in TcII.

Conclusions: Slight temperature shifts lead to increased cell death of metacyclic trypomastigotes because of the deregulation of gene expression of different processes essential for the TcI and TcII DTUs of *T. cruzi*.

Keywords: *Trypanosoma cruzi*, DTUs, Temperature, Metacyclic trypomastigotes, RNAseq, Transcriptomic

Background

It is estimated that during the last 130 years there has been an increase of 0.85 °C in the global temperature, with the biggest changes observed during the last few decades [1]. Temperature changes affect host-pathogen interactions, vector distributions, transmission, and in

*Correspondence: juand.ramirez@urosario.edu.co
[1] Grupo de Investigaciones Microbiológicas-UR (GIMUR), Departamento de Biología, Facultad de Ciencias Naturales, Universidad del Rosario, Bogotá, Colombia
Full list of author information is available at the end of the article

some cases even the life-cycle of pathogens, mainly for vector-borne diseases such as dengue, malaria, leishmaniasis, and Chagas disease [2–11].

Triatomines (Hemiptera: Reduviidae) are the vectors of Chagas disease, an endemic pathology caused by *Trypanosoma cruzi*. Studies analyzing the effects of temperature shifts on the distribution of Chagas disease vectors have shown variable results, ranging from a possible decrease in the number of human infections to an increased risk of infection [5, 12, 13]. Studies on the impact of temperature shifts (28 °C and 30 °C) on the life-cycle of *Rhodnius prolixus*, a main vector of Chagas disease, have found that an increase in temperature decreases the transmission of the parasite, increases the ratio of feeding and reproduction, and affects the process of metacyclogenesis in the vector in the first 10 days of infection, when 26 °C is used as a control [14]. Similarly, studies of the phenol-oxidase system in the vector, which is involved in immunity against invading pathogens, have shown decreased levels at high temperatures, thus affecting both *T. cruzi* infection and vector survival [15]. This suggests that triatomine biology and the parasite life-cycle are directly affected by slight temperature shifts.

Trypanosoma cruzi shows high genetic variability and is classified into six discrete typing units (DTUs), associated with different epidemiological cycles, hosts, vectors, and clinical manifestations [16, 17]. In addition, this parasite has a complex life-cycle involving four stages during its passage between mammalian hosts such as humans and triatomine vectors. One of the most important steps in the life-cycle of *T. cruzi* occurs in the rectal ampulla of the vector and involves the transformation of non-infective replicative epimastigote forms into infective metacyclic trypomastigotes (MT) [18]. This process is called metacyclogenesis and involves morphological, biochemical, genetic, and transcriptional changes essential for progression of the parasite's life-cycle [18–20]. The factors that promote metacyclogenesis are yet to be fully elucidated; however, nutritional stress increases the levels of adenylate cyclase expression and cAMP concentrations stimulate the expression of genes involved in autophagy, which is essential for the progression of this process. Some metabolic changes that have been detected in metacyclogenesis are related to the presence of oxidized proteins, the activation of enzymes involved in the metabolism of carbon and nitrogen as a source of energy, and the activation of mitochondrial enzymes, such as cytochrome, in response to nutritional stress [21–23]. Some of the changes in the parasite during this process are related to structural modifications of the kinetoplast, elongation of the nucleus, and an increase in heterochromatin, together these changes relate to the decrease in mRNA expression in MT forms [18, 24]. The success of the metacyclogenesis process depends on the expression of certain specific genes, such as those encoding methionine peptidase I (Met I), surface metalloprotease GP82, surface metalloprotease GP90, and MT-specific proteins, as well as other genes such as the *Tclmp4* gene associated with a ribonucleoprotein involved in the processing of the S40 subunit, which is important in progression of the cell-cycle [25, 26]. Transcriptomic analysis using RNAseq technology has been useful in understanding the gene remodeling that occurs in *T. cruzi* during infection, in identifying genes expressed differentially between the three stages of this parasite, and in evaluating the gene profiles between virulent and non-virulent clones [27–31]. However, until now, the transcriptional profiles of *T. cruzi* have not been evaluated when MT are exposed to different temperatures. Therefore, the objective of this study was to assess whether slight and short-term changes in temperature affect the gene transcription of *T. cruzi* MT.

Methods

Epimastigote culture

Cultures of epimastigotes of the strains MHOM/CO/04/MG (TcI) and MHOM/BR/53/Y (TcII) were maintained by weekly passage in liver infusion tryptose (LIT) medium supplemented with 10% fetal bovine serum. These strains were selected as these have been previously used in *in vivo* studies in murine models and triatomines, they are fully characterized and provide a suitable set of biological strains for *in vitro* studies [14]. For verification of the DTU, DNA extraction was performed from cultures of epimastigotes in logarithmic phase for both strains using the DNeasy kit (Cat. # 69504; Qiagen, Hilden, Germany), followed by conventional PCR directed to the spliced-leader intergenic region (SL-IR) as reported elsewhere [32]. The obtained products were subjected to electrophoresis on a 2% agarose gel, with expected band sizes of 300 bp for TcII and 350 bp for TcI.

Calculation of MTs per day

To determine the day at which the number of MTs emerged, we calculated the number of MTs as previously described [33]. Epimastigotes in exponential growth phase, genotyped previously as TcI (MHOM/CO/04/MG) and TcII (MHOM/BR/53/Y), were washed twice with phosphate-buffered saline (1× PBS) and centrifuged at 10,000× *rpm*, then 1×10^7 epimastigotes were cultivated in LIT medium supplemented with 5% fetal bovine serum at temperatures of 26 °C, 27 °C and 28 °C. These temperatures were selected based on an estimated temperature increase of 0.85 °C during recent decades and a previous report in *R. prolixus* [14]. To avoid a bias related to a possible inadequate initial concentration

of epimastigotes, all tests were carried out from the same initial inoculum and placed in different incubators according to the required temperature. The cultures were kept for 10 days, considering that we wanted to obtain pure MT cultures. The verification of temperature maintenance in the incubators was carried out twice a day during the entire study period. The concentration of parasites was calculated using a Neubauer chamber, in order to determine the epimastigotes and trypomastigotes that were viable; the mobility of parasites was used as a discrimination parameter and only mobile forms were included in the count. The number of epimastigotes (EP) and metacyclic trypomastigotes (MT) was determined microscopically on slides fixed with 100% methanol with 10% Giemsa stain. For each slide, 300 fields were analyzed under an optical microscope (40×). Three biological replicates for each experiment were included, as well as three technical replicates for each biological replicate to decrease any operator errors.

Statistical analysis

The data relating to the concentration of parasites and the determination of stages were tabulated in Microsoft Excel. The determination of stages was normalized as a percentage that included two factors: the percentage of MT and the percentage of EP. These data were applied to the concentration of parasites to determine the specific concentration for each morphological stage in each individual experiment. To evaluate whether the data showed a normal distribution, a Shapiro-Wilk test was carried out, followed by (provided the obtained data did not follow a normal distribution) a Kruskall-Wallis test and the analysis of Dunn's multiple comparisons to determine the day of emergence of metacyclic forms (EMD). This day was selected as the first day when statistically significant changes were observed in the concentration of MT compared with the control (day 0). The data were also used to generate a calculation of MTs per day. Finally, the comparison between DTUs was performed using a non-parametric Friedman test followed by an analysis of multiple comparisons. All analyses were performed using GraphPad Prism 7.4 software using $P < 0.05$ as the cut-off for significance.

Purification of metacyclic trypomastigotes

To evaluate the expression of MT genes during EMD when the parasites were subjected to different temperatures (26 °C, 27 °C and 28 °C), RNA extraction from TcI (MHOM/CO/04/MG) and TcII (MHOM/BR/53/Y) was performed. As we previously reported [33], cultures of *T. cruzi* contain a mix of EP and MT stages during EMD. To obtain a pure MT sample, we developed sepharose ion exchange chromatography according to our previously reported protocol [33]. After which, the samples were washed twice with 1× PBS and the stage was verified under a microscope.

RNA extraction and sequencing

In order to stabilize the MT after purification by means of sepharose-DEAE resin chromatography, the MT obtained were washed twice with 1× PBS, and incubated in LIT medium without supplements for 2 h. MT purified by sepharose ion exchange chromatography were subjected to RNA extraction. The RNA was extracted from 24 samples (i.e. two DTUs at three temperatures, with two biological replicates and two technical replicates) using a RNeasy Plus Mini Kit (Qiagen) following the manufacturer's protocol. The quality of the RNA obtained was evaluated on an agarose gel and the concentration, as well as other parameters such as the 260/280 index and the 230/260 index, were measured by nanodrop spectrophotometry. The RNAs that showed typical RNA bands, had concentrations higher that 1 mg/ml, and a 260/280 index close to 2 were selected for total RNA sequencing.

The selected RNAs were sent to Novogene Bioinformatics Technology Co., Ltd. (Beijing, China) for sequencing using the Illumina HiSeq X-TEN platform. The strand-specific TrueSeq RNAseq Library Prep with an insert size of 350 bp was selected to prepare the RNA libraries, and the size of each read was 2 × 150 bp. The read quality was verified using fastqc software (http://www.bioinformatics.babraham.ac.uk/projects/fastqc/). In summary, parameters such as per base quality score, per base sequence GC content, Kmer content (among others) were evaluated.

Mapping and transcript quantification

The raw sequence reads, for the 24 transcriptomes included in this study, had an average of 70,630,112 bases and a standard deviation of 20,976,808.33 bases. The results for each of the treatments and replicates are available in Additional file 1: Table S1.

The fasta file for the *T. cruzi* Sylvio X10-1 genome was downloaded from the Eupath TriTryp database (https://tritrypdb.org/tritrypdb/) and Bowtie version 2 software was used as a reference index (Additional file 2: Table S2). Then 24 paired-end samples were individually aligned using TopHat version v2.1.0 and default parameters [34]. Similarly, the gtf file deform annotated genome of *T. cruzi* Sylvio X10-1 was downloaded from the Eupath TriTryp database and was used to perform transcript assembly from the reads obtained from the alignment by TopHat (Additional file 2: Table S2). The software Cufflinks version v2.0.2 (http://cole-trapnell-lab.github.io/cufflinks/) was used for this task and the "u" parameter (multi-read correlation) was included. Once the mapping process was

completed, the union of the gff files obtained using the Cuffmerge tool of Cufflinks was made using the "g" and "s" options, and different files were created to analyze the differences in expression between replicates, different temperatures for the same DTU, and finally, between DTUs at the same temperature [34].

Differential expression and ontology analysis

Cuffdiff was used to evaluate the differential expression of genes between DTUs and temperatures [34]. The normalized expression was calculated using FPKM (fragments per kilobase of exon per million fragments mapped), and comparisons between genes expressed at 27 °C and 28 °C and the 26 °C control were made for each of the DTUs. Genes that presented a Q-value (*P*-value corrected) less than or equal to 0.05 were considered to be differentially expressed. The same protocol was followed to evaluate the differential expression between replicates of samples and DTUs for each of the temperatures. The *CummeRbund* software package in R was used to visualize the output files obtained from the Cuffdiff analysis and for the generation of graphs [35]. To make a biological inference and determine the protein products encoded for each of the DEGs, and to analyze the enzymes that could be encoded by these same genes, the list of upregulated and downregulated genes obtained by the statistical analysis of Cuffdiff were analyzed using the EupathDB TriTryp online tool (https://tritrypdb.org/tritrypdb/), and the lists of DEGs for each treatment were submitted. The output files were selected based on the analysis of the gene ontological terms (GO terms) for each of these genes, and the tables obtained were recorded in Microsoft Excel for further analysis [36, 37]. Dynamic tables were constructed to quantify the number of upregulated and downregulated genes for each of the GO terms and the results were used to construct graphs. Ten biological process GO terms with the greatest number of genes were selected.

Results

Increase in temperature affects the emergence of metacyclic trypomastigotes in *Trypanosoma cruzi* I and II *in vitro*

The emergence of MT was evaluated in *T. cruzi* MHOM/CO/04/MG (TcI) and MHOM/BR/53/Y (TcII) cultures over 10 days (Fig. 1a). Nutritional stress is one of the main factors that promotes metacyclogenesis in *T. cruzi*, and previous studies have demonstrated the presence of MT in cultures grown in LIT medium when a high concentration of parasites was used as the inoculum. We used these previously described culture conditions and protocol to calculate the MT per day in this study [33]. No MT were observed on day 0, but low concentrations of MT were detected from day 1 in most of the treatment conditions, except for TcI incubated at 27 °C (MT observed from day 2). The highest concentrations of MT (6×10^8 trypomastigotes/ml on average) were observed on day 7 for TcI incubated at 26 °C, whereas the concentration of MT for TcII under the same conditions was 2.8×10^8 trypomastigotes/ml on day 8 (Fig.1b, c). The concentration of MT decreased at temperatures of 27 °C and 28 °C for both DTUs, with a maximum of 6.0×10^7 and 1.7×10^7 trypomastigotes/ml being detected, respectively, with the highest concentrations of MT observed on day 10 (Fig. 1a, b, e). Similar behavior was observed for TcII incubated at 27 °C and 28 °C, with maximum concentrations of 8.5×10^7 and 1.3×10^7 trypomastigotes/ml on day 10 (Fig. 1b, d, e). As previously mentioned, MT concentrations were higher for TcI compared with TcII in most of the experiments (Fig. 2c, d, e); however, we found the opposite behavior for TcII at 27 °C on day 10, with higher concentrations of MT compared with TcI at 27 °C; despite this, no statistically significant difference was observed on this day. We performed normality analysis using the Shapiro-Wilk test for the data obtained from each of the treatments and the results showed that some samples did not follow a normal distribution. We therefore used non-parametric analysis for statistical evaluation of our data. To determine the day of emergence of metacyclic forms (EMD), we performed a Kruskall-Wallis test followed by an analysis of Dunn's multiple comparisons, using day 0 (0 trypomastigotes/ml) as the control. The EMD for the TcI cultured at 26 °C occurred 4 days post-culture (DPC), compared with 6 DPC for TcII at the same temperature (Fig. 1b). When the temperature was increased to 27 °C, the EMD occurred at 8 DPC for TcI and 6 DPC for TcII, and at 28 °C, the EMD was 8 and 5 DPC for TcI and TcII, respectively. Samples from the EMD were used for RNA extraction for each of the treatments (Fig. 1c, d, e). Differences between the temperatures and DTUs were analyzed by Friedman's non-parametric tests and the results revealed statistically significant differences between the treatments ($P < 0.0001$, $df = 6$). To analyze these differences in greater detail, Dunn's multiple comparisons were performed and no differences were detected between the DTUs treated at the same temperature. However, following Kolmogorov-Smirnov analysis, a difference between the TcI at 26 °C and TcII at 26 °C treatments was detected ($P = 0.0233$). Furthermore, a difference was detected between the parasites treated at 26 °C (control) and 28 °C for both DTUs ($P \leq 0.001$).

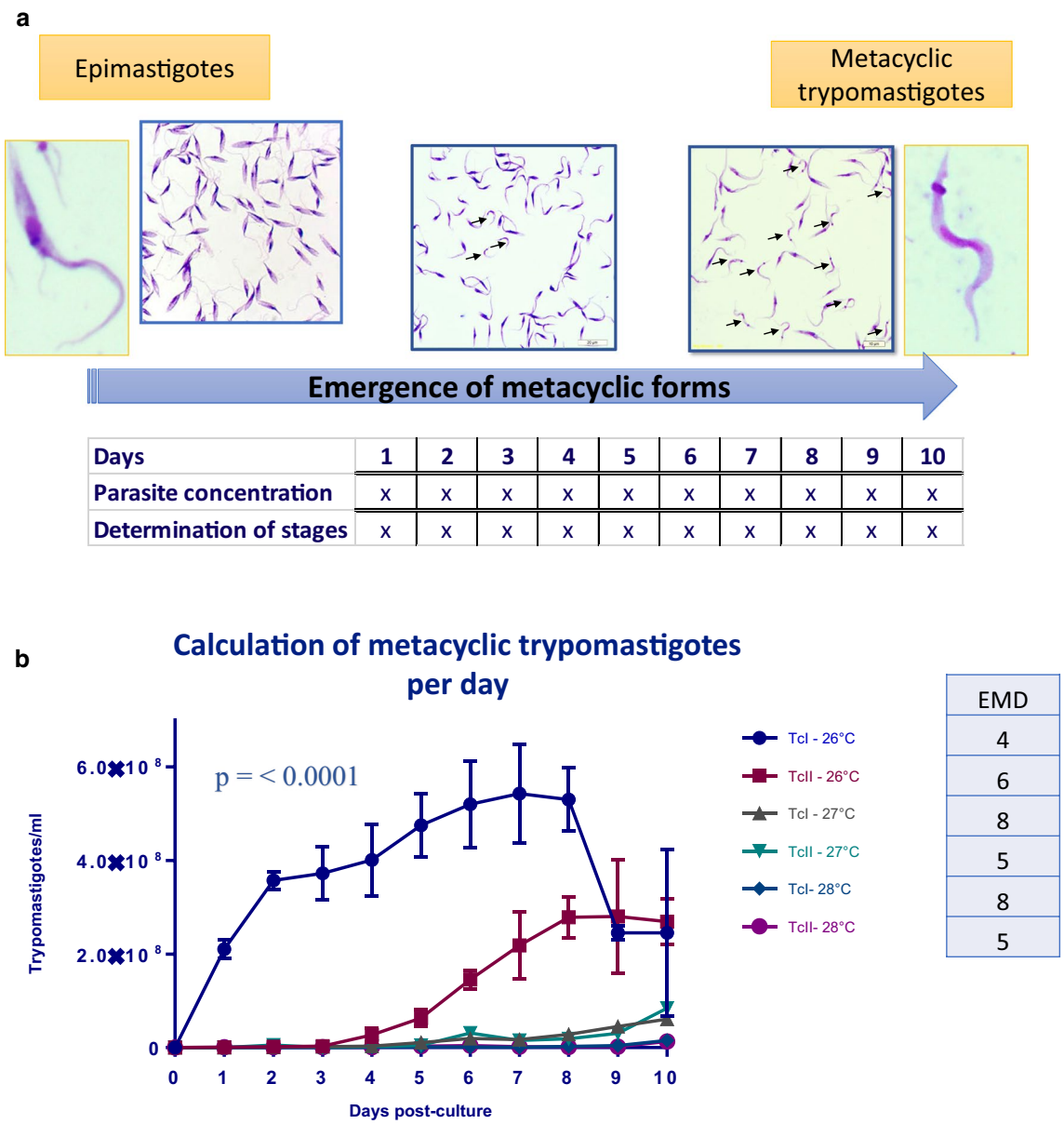

Fig. 1 Increase in temperature affects the emergence of metacyclic trypomastigotes in *Trypanosoma cruzi* I and II *in vitro*. **a** Process of generation of emergence of metacyclic curves for *T. cruzi*. **b** Calculation of metacyclic trypomastigotes per day of all discrete typing units (DTUs) and temperatures. The observed *P*-value corresponds to the comparison between DTUs and temperatures. The emergence of metacyclic forms day (EMD) for each of the DTUs is shown next to the legends. The arrows indicate the nuclei of MTs

Changes in temperature increase and decrease gene transcription in MT of *T. cruzi* I and II

The concentration, purity and integrity of the extracted RNAs was verified, only the RNAs that passed the quality threshold for all these parameters were sent to sequencing. Additional file 3: Figure S1 shows the integrity RNA bands in agarose gels, RNA concentrations and the 260/280 index. The RNAs from two biological replicates and two technical replicates for each treatment were assembled and compared with the reference genome Sylvio/X10 (Additional file 2: Table S2). No differences were detected between the replicates of TcI and TcII at any of the temperatures (Additional file 4: Figure S2a, b). Differential expression analysis did not show strong variability between the genes expressed among replicates for many of the genes according to the Q-values (*P*-value corrected) $P \geq 0.05$ when Cuffdiff analysis was performed.

A total of 11,154 genes were compared for TcI at 26 °C and 27 °C, and 11,185 genes were compared for TcI at 26 °C and 28 °C. For TcII the comparison between 26 °C and 27 °C included 5884 and in the case of 26 °C and 28 °C the number of genes corresponded to 13,187. On the other hand, the comparison between DTUs at 26 °C had 10,984 genes, for 27 °C there were 9300 genes, and finally, for 28 °C 9777 genes. Differential expression analysis revealed that the MT of TcI and TcII exposed to different temperatures showed differences in the expression of genes when compared with the control at 26 °C by Cuffdiff analysis (Fig. 2a, b, Additional file 5: Table S3). Similarly, differences in gene expression were assessed for DTUs at each of the temperatures (Fig. 2c–e); however, a smaller

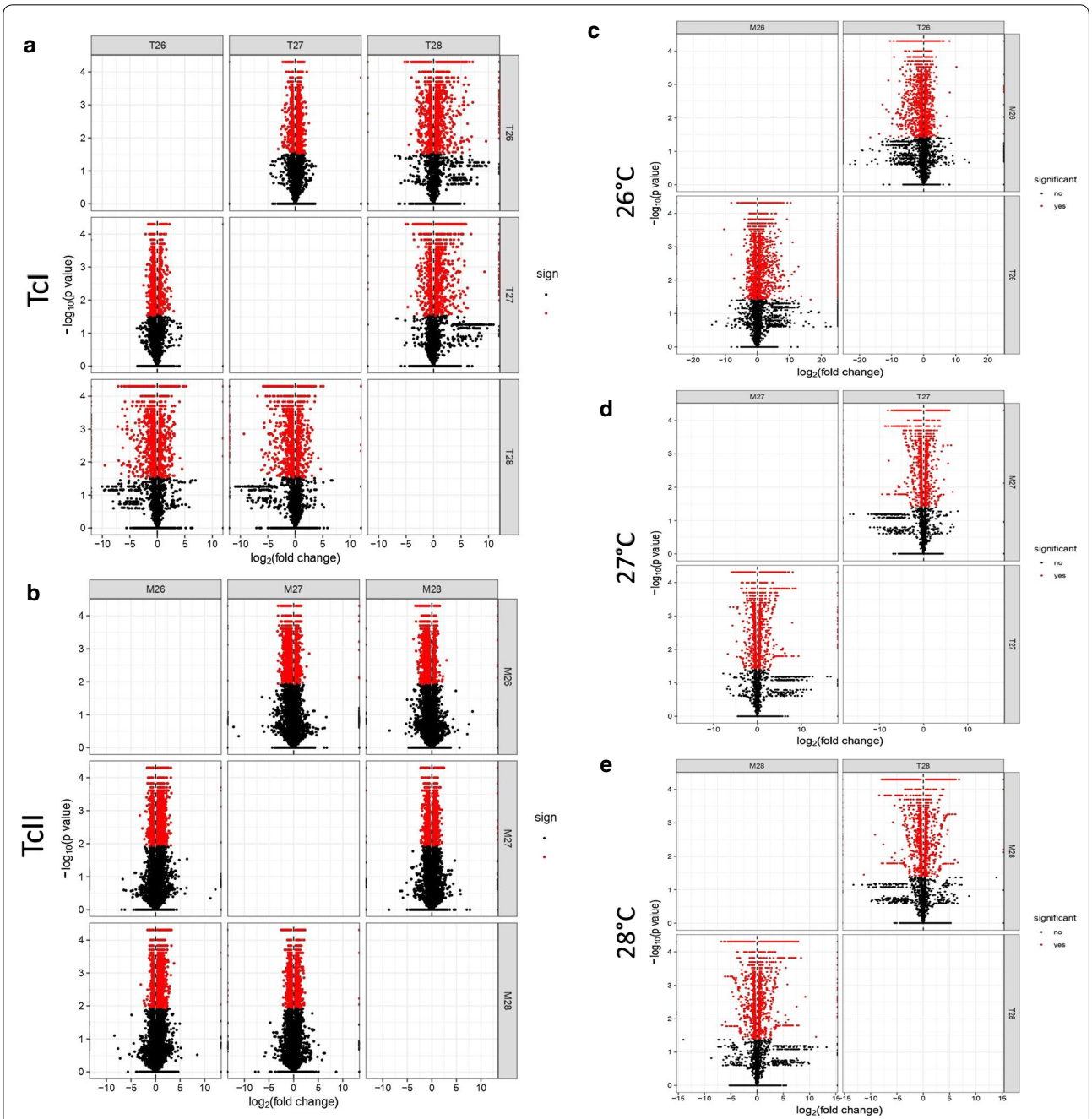

Fig. 2 Volcano matrix of DEGs in the metacyclic trypomastigotes of *Trypanosoma cruzi* I and II. The differentially expressed genes (DEGs) are shown in red. Fold changes are shown on the X-axis and *P*-values are shown on the Y-axis. **a** DEGs for TcI at different temperatures. **b** DEGs for TcII at different temperatures. **c** DEGs for TcI and TcII exposed to 26 °C. **d** DEGs for TcI and TcII exposed to 27 °C. **e** DEGs for TcI and TcII exposed to 28 °C

number of genes were observed when differences between MT treated with different temperatures but belonging to the same DTU were analyzed. This characteristic was even more marked when the comparison was made between DTUs that were exposed to 27 °C and 28 °C (Fig. 2d, e).

The TcI DTU had a greater number of downregulated genes in MT exposed to temperatures of 27 °C and 28 °C compared with the control at 26 °C, different to what was observed for 27 °C compared with 28 °C. The number of genes upregulated in TcII MT was higher for parasites exposed to 28 °C than 27 °C compared with the TcII control at 26 °C (Fig. 3a). For TcII DTU, the response to increased temperature was mainly marked by an upregulated gene expression, where the highest number of upregulated genes was observed for TcII at 28 °C (Fig. 3a).

We evaluated the presence of shared genes between different temperature treatments for each DTU. Out of a total of 10,114 expressed genes, TcI at 26 °C shared 8818 genes with TcI at 27 °C and 9251 genes with TcI at 28 °C, and TcI at 27 °C and TcI at 28 °C shared 9711 genes (Fig. 3b). The number of genes shared between TcII at 26 °C and 27 °C was 6588, and 6668 genes were shared with TcII at 28 °C, the number of genes shared between TcII at 27 °C and 28 °C was 6768. The temperature at which the greatest number of genes were expressed for TcI DTU was 28 °C (Fig. 3b).

We evaluated whether there were differences between the number of upregulated and downregulated genes among the different chromosomes, and quantified the differentially expressed genes (DEGs) in each of the chromosomes for each DTU when exposed to a range of temperatures. Chromosome 1 had the highest number of upregulated and downregulated genes for the two DTUs at all of the temperatures evaluated. Many of the DEGs were found in the MT exposed to 28 °C, with DTU TcII presenting the greatest number of changes and showing an interesting pattern of downregulation, with 165 genes downregulated on chromosome 1, 96 genes downregulated on chromosome 5, 120 genes downregulated on chromosome 37, and 98 genes downregulated on chromosome 11, in addition to various changes in the remaining chromosomes. Similarly, when the upregulated genes were evaluated by chromosome, TcII at 28 °C had an average of 100 to > 300 genes expressed in the majority of chromosomes from 1 to 21; however, the greatest number of upregulated genes corresponded to TcII at 27 °C, and no upregulated genes were observed for TcI at 28 °C, as previously observed (Fig. 3c).

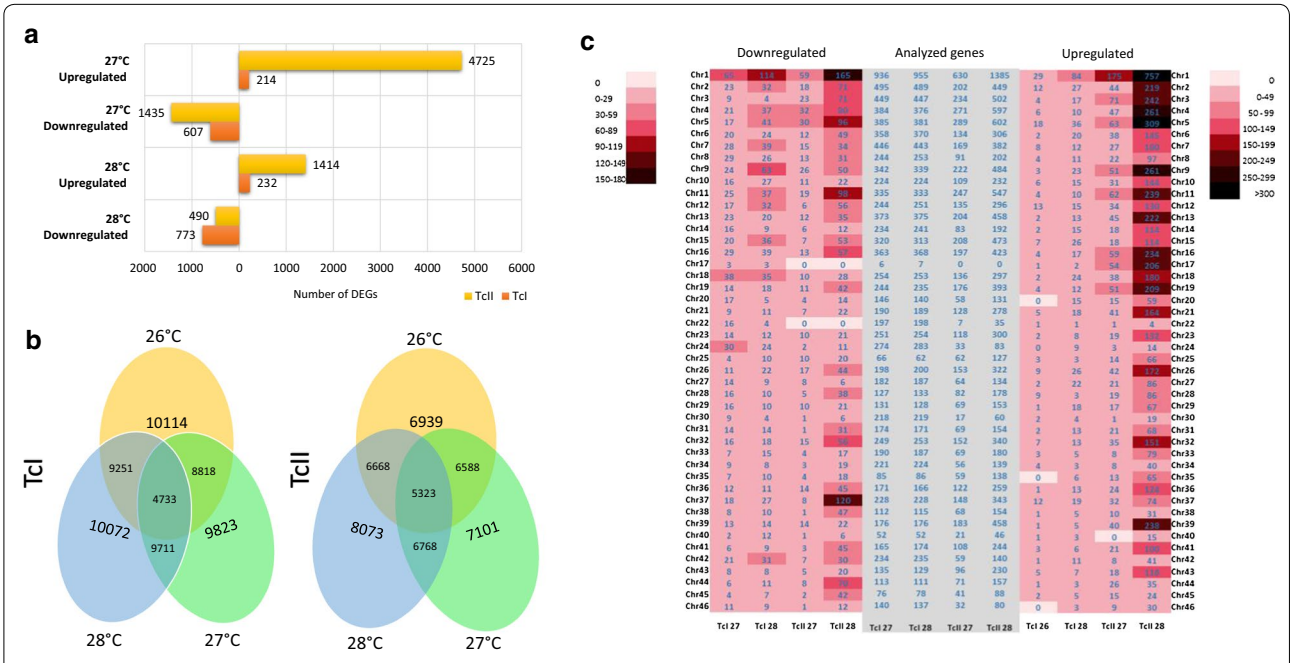

Fig. 3 DEGs in the metacyclic trypomastigotes of *Trypanosoma cruzi* I and II. **a** Number of differentially expressed genes (DEGs). The graph shows the number of downregulated and upregulated genes for each of the exposure temperatures and indicates the total number of genes under these conditions (next to bars) and the number of genes per fold-change. **b** Venn diagram with DEGs shared between temperatures treatments for each DTU. **c** Heat map showing downregulated and upregulated genes per chromosome and the number of genes analyzed in each comparison

Differentially expressed genes were associated with molecular processes that play an important role during thermal stress

The IDs for each of the downregulated and upregulated genes in each of the treatments evaluated here were submitted to the Tritryp gene database of EupathDB and gene ontology analysis was performed for each DTU and temperature (Additional files 6, 7, 8: Tables S4, S5, S6). Of the downregulated genes, 607 for TcI at 27 °C and 773 for TcI at 28 °C were subjected to analysis; of these, a total of 463 and 625 GO terms, respectively, were obtained. Large percentages of the genes were associated with molecular processes. Of note, many genes related to oxidoreductase activity in TcI at 28 °C were downregulated, which is an important part of the metacyclogenesis process, and as a consequence, of the emergence of MTs. Similarly, when the terms associated with biological processes were evaluated, downregulation of genes involved in oxidation-reduction processes was observed at both temperatures (Fig. 4b, c). A total of 214 and 232 overexpressed genes in TcI at 27 °C and 28 °C, respectively, were evaluated for the ontological terms. The results for this group of genes showed a total of 406 GO terms for 27 °C and 427 for 28 °C. The highest percentage of ontology terms corresponded to molecular processes, and these results were similar to those found for downregulated genes in TcI (Fig. 4a). Ontology terms relating to proteolysis processes and the phosphorylation of proteins were also observed at both temperatures, as well as genes relating to the motor activity of microtubules (Fig. 4b, c).

The most differentially upregulated and downregulated genes were associated with molecular processes based on the GO ontology for both temperatures used in TcII. A total of 1435 and 490 downregulated genes were obtained at 27 °C and 28 °C, respectively; these were associated with 541 and 625 GO terms, respectively. Downregulated genes associated with GO terms involved with oxidation-reduction processes and oxidoreductase activity were found at both temperatures (Fig. 5b, c). A total of 1414 and 4725 genes were upregulated in TcII at 27 °C and 28 °C, respectively; of these, we found associations with 977 and 1713 GO terms, respectively, including terms associated with the upregulation of transport mediators by vesicles (Fig. 5b, c). Some of the processes with the largest number of DEGs are described below.

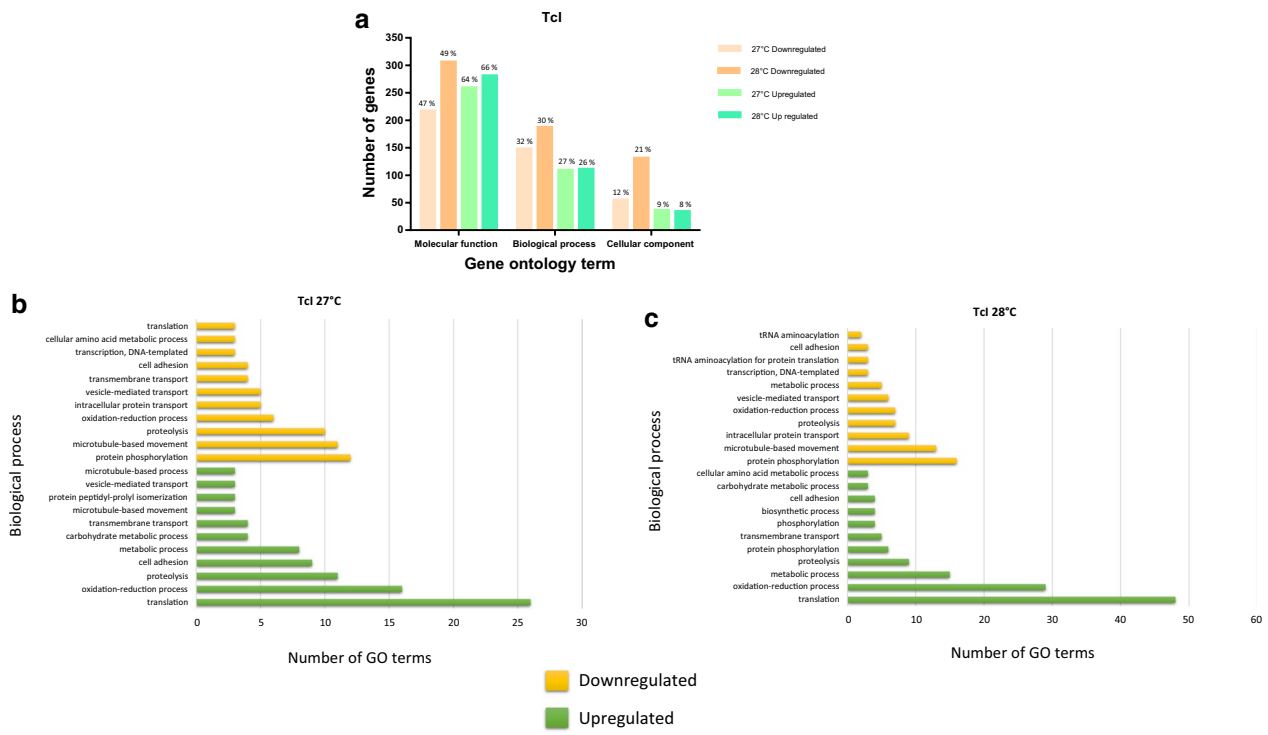

Fig. 4 Gene ontology terms associated with the DEGs for *Trypanosoma cruzi* I. **a** Number and percentage of downregulated and upregulated genes for each discrete typing unit (DTU) and the gene ontology (GO) terms. **b** Ten GO terms with the greatest number of differentially expressed genes (DEGs) for biological processes in the MT of TcI exposed to 27 °C. **c** Ten GO terms with the highest number of DEGs for biological processes in the MT of TcI exposed to 28 °C

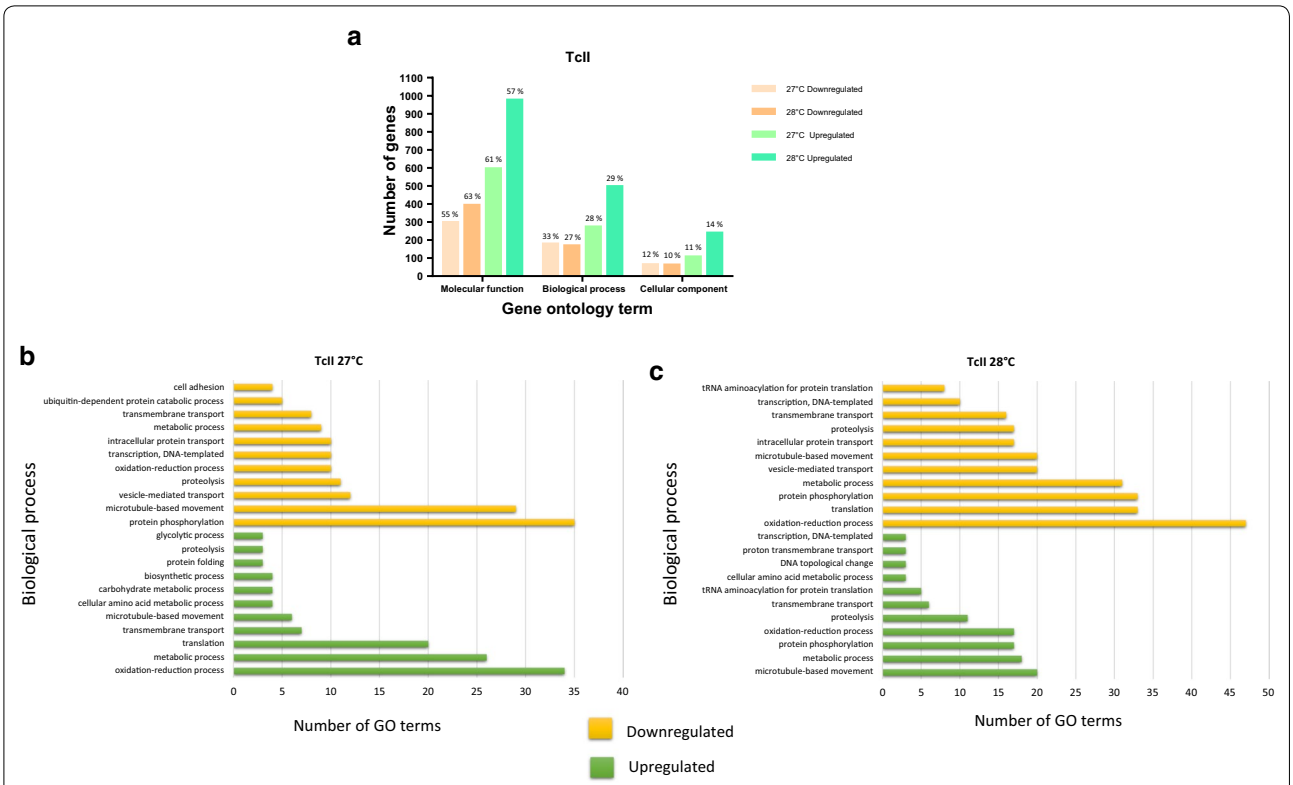

Fig. 5 Gene ontology terms associated with the DEGs for *Trypanosoma cruzi* II. **a** Number and percentage of downregulated and upregulated genes for each discrete typing unit (DTU) and the gene ontology (GO) terms. **b** Ten GO terms with the greatest number of differentially expressed genes (DEGs) for biological processes in the MT of TcII exposed to 27 °C. **c** Ten GO terms with the highest number of DEGs for biological processes in the MT of TcII exposed to 28 °C

Metabolism

A high degree of regulation was observed for genes involved in the metabolism of lipids in the MT when exposed to different temperatures. The treatment with the most DEGs are involved in lipid metabolism was TcII at 27 °C with 10 downregulated genes, followed by TcI at 28 °C with 8 downregulated genes and TcI at 27 °C with 6 downregulated genes when compared to TcI at 26 °C (Additional files 6, 7: Table S4, S5). Common genes altered in all of these treatments were TcSYL_0078950 and TcSYL_0103620 annotated under the terms lipid metabolic process and oxidation-reduction process, respectively. In addition, genes involved in the synthesis of some amino acids, dependent on this metabolic pathway, such as arginine (TcSYL_0201940) for TcII at 27 °C and proline (TcSYL_0201810) for TcI at 28 °C, were downregulated (Additional file 6: Table S4). The downregulation of a gene associated with the tetrahydrofolate biosynthetic process (log2-fold_change: − 158.836, TcSYL_0078950) in TcI at 27 °C was also detected (Additional file 6: Table S4).

The coding transcript for the hexokinase enzyme (TcSYL_0169190-TcSYL_0169200) showed a decrease in expression for all of the treatments compared with the control. Similarly, the transcript for lactate/malate dehydrogenase with the alpha/beta C-terminal domain (TcSYL_0122290) was upregulated for all treatments except for TcII at 28 °C. Aldose 1-epimerase (TcSYL_0046290) was upregulated in MT exposed to 27 °C and in TcII at 28 °C. Similar results were found for the transcript encoding glucosamine-6-phosphate isomerases/6-phosphogluconolactonase, which was upregulated for TcI at 27 °C and TcII at 28 °C (TcSYL_0165520) (Additional files 6, 7: Table S4, S5). A more in-depth analysis of glucose metabolism revealed a decrease in expression levels for genes involved in the GO terms "glucose 6-phosphate metabolic process" and "cellular glucose homeostasis" for TcI at 28 °C and TcII at 27 °C; however, the genes for the same GO terms were upregulated for TcII at 28 °C (Additional file 6: Table S4). The transcript TcSYL_0000660 coding for 6-phosphofructo-2-kinase involved in the GO fructose metabolic process was upregulated in most of the treatments except for TcI at 27 °C (Additional files 6, 7: Table S4, S5).

Oxidoreduction

One of the processes most affected by the exposure of MT to different temperatures was oxidoreduction. A total of 15 transcripts for TcI at 27 °C, 29 transcripts for TcI at 28 °C, 34 transcripts for TcII at 27 °C and 17 transcripts for TcII at 28 °C corresponded to downregulated genes involved in the reduction-oxidation process. In addition, a small number of upregulated genes related to the reduction-oxidation process was detected for TcI at 27 °C (5 transcripts), TcI at 28 °C (7 transcripts) and TcII at 27 °C (10 transcripts); however, 47 transcripts were detected for TcII at 28 °C (Additional files 6, 7, 8: Tables S4, S5, S6). The products for each of the downregulated and upregulated genes are available in Additional file 8: Table S6, including different types of oxidoreductases, peroxidases, hydrogenases and cytochrome B oxidases involved in this pathway.

TcI showed downregulation in the expression of genes mainly responsible for the management of oxidative stress in parasites incubated at 27 °C. Among these genes were quinone reductase (NADPH), fumarate reductase (NADH), and cytochrome *c* oxidase, as well as amino acid kinases and peptidases, which are indispensable for obtaining energy in the parasite during part of metacyclogenesis. TcI exposed to 28 °C showed a decrease in the expression of proteins responsible for the regulation of oxidative stress, similar to the results at 27 °C, but also showed decreased expression of other proteins such as cytochrome-b5 reductase and alcohol dehydrogenase (Additional file 8: Table S6), which indicates that the differential expression of these proteins may be a consequence of the exposure of MT to high temperatures.

Proteins related to proteolysis

Proteins related to proteolysis play an important role in the regulation, maintenance, and progression of the life-cycle of *T. cruzi*. Our results revealed the regulation of genes coding for proteins of some important families related to these processes (Additional files 6, 7, 8: Tables S4, S5, S6). The predominant family of proteins that were regulated included leishmanolysin or GP63, and a total of 8 genes were downregulated and 4 were upregulated for TcI at 27 °C, 4 were downregulated and 3 were upregulated for TcI at 28 °C, no genes were downregulated but 4 were upregulated for TcII at 27 °C, and 3 were downregulated and 8 were upregulated for TcI at 28 °C (Additional files 6, 7: Table S4, S5). It is important to note that although genes encoding proteins within this family were both upregulated and downregulated, none of the genes ID showed both of these outcomes indicating the specific up- or downregulation of specific GP63 proteins (Additional file 9: Table S7).

The M32 metallopeptidase family of proteins showed different expression patterns between treatments. Two transcripts were upregulated for TcI at 27 °C and downregulated for TcI at 28 °C (TcSYL_0019490 and TcSYL_0138670), TcSYL_0138680 being the only gene that was downregulated for TcI at 28 °C. Regarding TcII, transcripts TcSYL_0019490 and TcSYL_0138670 were downregulated in MT exposed to both temperatures (Additional file 9: Table S7).

The calpain family of cysteine proteases was another family of proteins regulated in MT under different temperatures. The transcripts TcSYL_0080730, TcSYL_0080800, TcSYL_0080820 and TcSYL_0146610 were upregulated in TcI at 27 °C, whereas for TcII at 27 °C only the TcSYL_0146610 gene was upregulated, and TcII at 28 °C showed a decrease in the expression of TcSYL_0080820 and TcSYL_0146610 genes, and an increase in expression of TcSYL_0063550 (Additional file 9: Table S7).

Finally, both thermal treatments triggered the overexpression of ubiquitin-2-like Rad60 SUMO-like (TcSYL_0109300) protein in TcII. In addition, a series of proteases were expressed differentially in some of the treatments. When evaluating TcI at 28 °C, transcript TcSYL_0075250 coding for the cytosol aminopeptidase family was downregulated, whereas TcSYL_0202010 (M16C-associated peptidase) was upregulated (Additional file 6: Table S4). For TcII at 27 °C, TcSYL_0013180 (prolyl oligopeptidase family) was overexpressed. Finally, for TcII at 28 °C, TcSYL_0171200 (serine carboxypeptidase) was upregulated (Additional file 9: Table S7).

Proteins related to phosphorylation

The transcripts TcSYL_0114970 (chromosome 18) and TcSYL_0171180 (chromosome 36), both annotated as protein kinase domains, were downregulated for TcI at 27 °C, and simultaneously, a total of 12 protein kinase domain transcripts were upregulated. For TcI at 28 °C, 6 genes coding for protein kinase domains were downregulated and 12 genes were upregulated. For TcII, the same genes were downregulated and 34 were upregulated in the MT exposed to 27 °C, and 16 were downregulated and 41 were upregulated in the MT exposed to 28 °C (Additional file 10: Table S8).

Translation

One of the most disturbed processes when evaluating the GO for the DEGs in the MT exposed to different temperatures was translation. A total of 26 transcripts related to the process of translation were downregulated for TcI at 27 °C and 48 transcripts were downregulated for TcI at 28 °C, compared with 6 upregulated transcripts for

27 °C and 5 upregulated transcripts for 28 °C. The results obtained for TcII showed similar patterns, especially when evaluating MT exposed to 27 °C, when 24 genes were downregulated and 6 genes were upregulated. By contrast, for TcII at 28 °C, 8 genes were downregulated and 7 genes were upregulated (Additional file 6: Table S4, Additional file 7: Table S5).

The family of ribosomal proteins were the most affected transcripts in MT after exposure to high temperatures, with 26 transcripts upregulated for TcI at 27 °C, 44 transcripts upregulated for TcI at 28 °C, 18 transcripts upregulated for TcII at 27 °C and only two transcripts upregulated for TcII at 28 °C. The complete list of DEGs is available in Additional file 7: Table S5. Transcripts TcSYL_0010030 (KH domain) and TcSYL_0103320 (KOW motif) were downregulated in TcI at 28 °C and TcII at 27 °C, tRNA synthetases of class I (M) (TcSYL_0170460) was overexpressed in TcI for both treatments and two transcripts coding for tRNA synthetases of class I (I, L, M and V) (TcSYL_0090210 and TcSYL_0140390) and two transcripts coding for mitochondrial small ribosomal subunit Rsm22 (TcSYL_0048380 and TcSYL_0048390) were upregulated in TcI at 27 °C. For TcI at 28 °C, there was an increase in the expression of TcSYL_0166880 and TcSYL_0202360, both coding for tRNA synthetases of class II (D, K and N) (Additional file 11: Table S9). Finally, the upregulated genes in TcII at 27 °C encoded families of ribosomal proteins L4/L1 (TcSYL_0003330), S4 (TcSYL_0011150), L2 (TcSYL_0013860) and L14p/L23e (TcSYL_0046720), whereas these genes were downregulated in the other treatments. In addition, upregulation of the RNA polymerase I-associated factor PAF67 (TcSYL_0113260) was observed in TcII at 27 °C (Additional file 11: Table S9).

Vesicle-mediated transport

Genes involved in vesicle-mediated transport were downregulated in three of the four evaluated treatments (TcI 27 °C, TcII 27 °C, TcII 28 °C) with respect to the control. The coding transcript for vesicle-mediated transport (TcSYL_0091630) was downregulated in TcII at 27 °C and 28 °C, as were genes involved in the transport of ions (TcSYL_0109340), metal ions (TcSYL_0178120), cations (TcSYL_0174330), chloride ions (TcSYL_0111950) and hydrogen ions (TcSYL_0181420). The transport of some macromolecules essential for the parasite was also affected in TcI at 27 °C and TcII at 28 °C, with a decrease in the expression of the genes TcSYL_0146190 (protein transport) and TcSYL_0047800 (nucleoside transmembrane transport) (Additional files 6, 7: Table S4, S5).

A greater number of upregulated genes observed in TcII than in TcI when exposed to different temperatures

When DTUs were compared between the different temperature treatments, the ontology with the highest number of downregulated and upregulated genes was related to molecular processes. When comparing between DTUs at 26 °C, a total of 957 terms were downregulated in TcII compared to TcI and 810 terms were upregulated in the same comparison, this being the only temperature where the number of downregulated genes was higher than that of upregulated genes. A decrease in the expression of structural components of ribosomes and integral components of the membrane and cytoplasm was observed in TcII compared with TcI, in addition to an increase in the expression of genes that encode DNA binding proteins for this DTU (Additional file 8: Table S6). The results obtained at 27 °C revealed 1427 downregulated genes and 1274 regulated genes, and consistent with the results at 26 °C, there was a decrease in the expression of genes coding for integral components of the membrane and cytoplasm, in addition to an increase in the expression of genes encoding nucleic acid binding proteins (Additional file 12: Table S10). Finally, the highest temperature evaluated in this study (28 °C) showed a total of 1210 downregulated and 1943 upregulated terms between DTUs. Ontological terms related to proteolysis and integral membrane components were found downregulated for this analysis, whereas the upregulated ontological terms that contributed most to this comparison were related to DNA binding (Additional file 12: Table S10).

Discussion

The results of this study show how slight changes in temperature affect the gene expression of two of the most important DTUs of *T. cruzi* (Fig. 2, Additional file 5: Table S3). Herein, we observed how temperature decreased the concentration of MT and slowed transformation, as evident when evaluating the EMD (Fig. 1). Similar results were observed when the effect of temperature on the metacyclogenesis of *T. cruzi* in *R. prolixus* was evaluated, confirming that the parasite maintains the same biological characteristics in studies both *in vivo* and *in vitro* [14]. When TcII was exposed to 28 °C, this temperature affected the concentration of MT when compared with 26 °C for the same DTU but it was significantly downregulated in TcI at 28 °C, potentially indicating resistance in the DTU of TcII at high temperatures. The EMD for TcII at 28 °C was lower than that of TcII at 26 °C, confirming the resistance of TcII when exposed to high temperatures (Fig. 1). Previous studies evaluating the metacyclogenesis process and presence of MTs *in vivo* showed similar results suggesting that TcII

parasites have adapted to high temperatures [14]. Differences between these DTUs during metacyclogenesis have already been reported in other *in vitro* studies, where the concentration of MT was higher compared with TcI and TcIV DTUs following exposure to high temperatures [38]. Despite this, we observed regulation of the expression of different genes between parasites treated with different temperatures and between DTUs treated at the same temperature, with fewer genes regulated between DTUs treated at the same temperature, especially for 27 °C and 28 °C (Fig. 2 a, Additional file 5: Table S3). This characteristic indicates that at higher temperatures or even under stress conditions, the parasite could decrease the expression of single genes by DTUs and increase the expression of genes associated with cell stress for cell survival purposes; however, further in-depth studies are required to confirm this, that include a greater number of biological replicates.

The analyses performed here showed that chromosome 1 harbored the majority of DEGs (Fig. 2c). Interestingly, despite the fact that the length of this chromosome exceeds 3 Mb, it comprises a higher number of housekeeping genes, unlike other chromosomes that contain a large number of repetitive genes encoding surface proteins [39]. On the other hand, the presence in the *T. cruzi* genome of a compartment core that mainly includes conserved and disruptive genes that cover most of the repetitive coding sequences for surface proteins, influence the unequal grouping of these proteins throughout the genome and of course on each of the chromosomes [40]. Structural changes, including copy number variations (CNV) and single nucleotide polymorphisms, have been observed in response to environmental stimuli and as a consequence of genomic adaptations [41, 42]. Based on these results, we hypothesize that *T. cruzi* may display the same characteristic of genomic adaptation to the environment, and that consequently, in response to thermal stress, may generate structural variations as a result of genetic changes on chromosomes 1 and 3. The ability to generate mutations as a consequence of oxidative stress has already been proven in this parasite and oxidative stress is believed to be the main trigger for the generation of genetic mutations during metacyclogenesis of *T. cruzi*, indicating the ability of this parasite to adapt to environmental stresses [43]. However, genomic studies to assess the effect of temperature or other stress stimuli on the genome of this parasite are required to support this premise including a better annotation of the available *T. cruzi* genomes.

Genes involved in the glucose 6-phosphate metabolic process and cellular glucose homeostasis were also upregulated in TcI at 28 °C and TcII at 27 °C (Additional files 6, 7: Table S4, S5). One of the enzymes involved in this process, glucose-6-phosphate dehydrogenase, whose function is to catalyze one of the first reactions in the pentose phosphate pathway and consequently produce NADPH, plays an essential role during infection and the defense against oxidative stress, which is why it has also been used in the study of therapeutic targets [44, 45]. Therefore, the decrease in the expression of proteins involved in the processes in which tetrahydrofolate acid and glucose 6-phosphate play a role, may have a strong influence on the cell death that occurs in the MT of TcI at 28 °C and TcII at 27 °C, and also on the survival of TcII at 28 °C when these genes are upregulated.

Oxidative stress is associated with cell death; however, under normal conditions, *T. cruzi* has the ability to cope with oxidative stress by producing a large number of antioxidant proteins and DNA repair proteins [46–49]. Our results showed a decrease in the expression of a large number of genes involved in these processes, such as quinone reductase (NADPH), fumarate reductase (NADH), cytochrome *c* oxidase and alcohol dehydrogenase, with these genes being more highly expressed in parasites exposed to 27 °C (Additional file 8: Table S6). However, even more interesting is the massive increase in the number of downregulated genes relating to oxidative stress in TcI at 27 °C and 28 °C and in TcII at 27 °C, compared with the increase in upregulated genes related to this process in TcII at 28 °C (Additional file 8: Table S6). These findings may explain the decrease in the concentration of MT at these temperatures as a result of cell death due to uncontrolled oxidative stress and the possible resistance of MT of TcII at 28 °C when exposed to this same source of stress, potentially illustrating the ability of this parasite to manage oxidative stress and increase of expression of genes linked to this process.

The differential expression of protein kinases during metacyclogenesis has been reported [46]. In our study, an increase in the number of genes coding for these proteins was found at all of the temperatures tested for both DTUs when compared with the control; however, the most dramatic change was exhibited by TcII, with 34 and 41 upregulated genes being observed at 27 °C and 28 °C, respectively (Additional file 10: Table S8), indicating the strong influence of these proteins in this DTU as a response to thermal stress. However, the reference genome used here for mapping does not allow us to determine the type of kinases expressed; a more in-depth study of the sequences of differentially expressed transcripts may provide insight into the specific function of the proteins to be translated. The presence of mitogen-activated protein kinases (MAPKs) in *T. cruzi* and their participation in evasion of the immune system has been reported, and many of these proteins play a role the stress response in other eukaryotes. For example, the Smp38

MAPK has been reported to be involved in the regulation of homeostasis in *Schistosoma mansoni* under oxidative stress, which is one of the main stimuli of metacyclogenesis, and may not therefore be affected by exposure to high temperatures. Protein kinases with this type of function may be upregulated in TcII as a contingency mechanism for this type of cellular stress [50, 51].

One of the characteristics of metacyclogenesis is an increase in transcription and translation followed by a decrease in the forms of MT. This is a consequence of the exposure of *T. cruzi* to nutrient-deficient medium, which leads to higher energy requirements that are achieved mainly by protein degradation and post-translational regulation. We therefore propose that when parasites are subjected to similar types of stress, such as temperature, this same behavior may be triggered in the parasite [25, 52]. Our findings revealed a drastic decrease in the expression of a large number of genes coding for members of the ribosome family in three of the four thermal treatments (Additional file 11: Table S9). This indicated that the decrease in the expression of constitutive ribosomal proteins, and as a consequence the synthesis of new ribosomes, is related to the exacerbated decrease in translation in TcI at 27 °C and 28 °C and TcII at 27 °C and the presence of MT forms with these particular characteristics (Additional file 11: Table S9). The presence of ribosomal profiles in which different ribosomal proteins are combined, has already been observed in *Toxoplasma gondii* and *T. cruzi* as a mechanism for translational control between different stages and for the translation of virulence factors [53]. Studies where the expression of ribosomal proteins was analyzed showed the decrease in translation efficiency in MT compared to EP for the same strain; these results demonstrate the importance of these proteins in gene regulation between different stages of the parasite, and could give us an indication of the regulation of specific profiles of ribosomal proteins in response to any type of stress, especially considering the distinctive regulation of expression that trypanosomatids present compared to other eukaryotes [54]. The decrease in transcripts of ribosomal proteins found in our study may be related to a specific profile of translational regulation associated with the response to thermal stress; however, a more detailed study is needed to confirm this.

Metalloproteases (GP63) are a family of glycosylphosphatidylinositol (GPI)-labeled proteins present in trypanosomatids whose main function is associated with virulence. Transcriptomic analyzes have shown the presence of a group of these proteins that are expressed throughout the parasite life-cycle, while approximately the remaining 50% are stage-specific [28]. Suggesting specific functions between members of this protein family, the increase in the expression of GP63 in TcII could suggest the presence of a specific group of GP63, active in response to heat stress in this DTU, with a possible influence in quick response to stress conditions. On the other hand, the importance of GP63 has been observed during the adherence of *T. cruzi* to the intestine of the vector and the binding to host cells during infection in the host, considering our results, it could be inferred that TcII when exposed at high temperatures could acquire advantages in transmission and infection and, therefore, in the progression of its life-cycle [55–57]. However, a characterization study of the GP63 class expressed in TcII must be performed in order to know the type of response to thermal stress present in this DTU.

One of the limitations of this study was that the exposure of the parasite to different temperatures was only performed for one incubation time. This was because MT do not have the capacity for replication, so it was impossible to continue their culture in axenic medium. One of our results showed an increase in genes expressed from chromosome 1; however, complete genome analysis was not performed for the parasites exposed to different temperatures, which may have provided further insights. One of the characteristics of *T. cruzi* is that its genome is largely comprised of repetitive sequences that mostly code for families of multigenic proteins. This feature makes it difficult to assemble sequenced genomes and the only reference genome currently available is for the TcI DTU, which is at the level of chromosome assembly. Our study was conducted using this genome and this is why special care had to be taken when analyzing the differential expression of genes in TcII. In some cases, manual checks were needed to avoid bias, so the availability of a reference genome for this DTU would facilitate the analysis and assembly process for future analyses for TcII. Differences between strains of the same DTU have been observed at both genomic and biological levels; although our results cannot be fully extrapolated to all populations of TcI and TcII strains, they provide a first approach to a better comprehension of the influence of temperature stress on gene expression of MT that had not been previously evaluated. Future studies must be conducted to unravel the influence of temperature on gene expression including a greater number of strains by DTU.

Conclusions

Our study showed that temperature affects *T. cruzi* I and II MT through regulation of the expression of genes coding for proteins involved in the metabolism of lipids and carbohydrates, the evasion of oxidative stress, proteolysis and phosphorylation processes, and also, the decrease of ribosomal proteins involved in translation, leading to cell death. However, DTU TcII exhibited greater resistance to thermal stress and greater survival, and an increase in

genes linked to the handling of oxidative stress and the expression of the GP63 protein was detected. This could be due to an early response to these stress conditions in the TcII DTU; the results obtained for the count of MT where from day 6 at 27 °C and on day 5 at 28 °C showed a higher concentration of MT compared to TcI. The main objective of this study was to evaluate the changes in transcriptomic profiles in TcI and TcII MT when they are subjected to thermal stress. Subsequent studies should focus on assessing how transcriptomic profiles change by using specific temperatures to which the parasites are exposed during their passage through the vector. The presence of differential stress responses in these DTUs during emergence of MT could explain the biological differentiation exhibited by these DTUs in the host, and could also indicate a possible change in the distribution and epidemiology of these DTUs with environmental temperature increases.

Supplementary information

Supplementary information accompanies this paper at https://doi.org/10.1186/s13071-020-04125-y.

Additional file 1: Table S1. The number of raw sequence reads for the fastaq files obtained from the sequencing of MTs.

Additional file 2: Table S2. Files of the *T. cruzi* reference genome Sylvio X10-2 with links for access to the fasta and gff *T. cruzi* Sylvio X10-2 reference files.

Additional file 3: Figure S1. RNA Quality analysis.

Additional file 4: Figure S2. Differential comparison between technical and biological replicates.

Additional file 5: Table S3. Differentially expressed genes for MT of TcI and TcII using the cuffdiff tool of cufflinks.

Additional file 6: Table S4. Gene ontology (GO) terms for the genes downregulated and upregulated for MT of TcI for both treatment temperatures.

Additional file 7: Table S5. Gene ontology (GO) terms for the genes downregulated and upregulated for MT of TcII for both treatment temperatures.

Additional file 8: Table S6. Oxidation reduction process. Gene IDs and the products for the downregulated and upregulated genes involved in oxidation reduction process for MT of TcI and TcII for both treatment temperatures.

Additional file 9: Table S7. Proteolysis process. Gene IDs and the products for the downregulated and upregulated genes involved in proteolysis process for MT of TcI and TcII.

Additional file 10: Table S8. Phosphorylation protein process. Gene IDs and the products for the downregulated and upregulated genes involved in phosphorylation protein process for MT of TcI and TcII.

Additional file 11: Table S9. Translation process. Gene IDs and the products for the downregulated and upregulated genes involved in translation process for MT of TcI and TcII.

Additional file 12: Table S10. Gene ontology (GO) terms for the downregulated and upregulated genes for the comparison between MT of TcI and TcII for each temperature.

Abbreviations

DTU: discrete typing unit; MT: metacyclic trypomastigote; EP: epimastigotes; cAMP: cyclic amino acid phosphate; RNA: ribonucleic acid; mRNA: messenger ribonucleic acid; GP: glicoprotein; BMD: the beginning of metacyclogenesis day; DPC: days post-culture; GO: gene ontology.

Acknowledgments

We thank Martin Llewellyn and Philipp Shwabl for their support with the bioinformatic analysis. We thank Kate Fox, DPhil, from Edanz Group (https://www.edanzediting.com/ac) for editing a draft of this manuscript.

Authors' contributions

LCS performed biological analysis, RNA extraction, bioinformatics analysis and drafted the manuscript. MM and LHP supported the biological and bioinformatic analysis. GV contributed to the generation of *T. cruzi* strains and designed this project. FG contributed to the design of the study. JDR designed the study, coordinated the biological and bioinformatic analysis and wrote the manuscript. All authors read and approved the final manuscript.

Funding

This study was funded by the Departamento Administrativo de Ciencia, Tecnología e Innovación COLCIENCIAS, project 120465843375 contract 063-2015 (http://www.colciencias.gov.co/node/1119) to FG, GAV and JDR. The funders played no role in the study design, data collection and analysis, the decision to publish, or preparation of the manuscript. LC was funded by DIRECCIÓN ACADÉMICA (Becas de pasantías doctorales). JDR is a Latin American fellow in the Biomedical Sciences, supported by The Pew Charitable Trusts.

Availability of data and materials

Data supporting the conclusions of this article are included within the article and its additional files. All data employed in this manuscript are available in the European Nucleotide Archive (ENA) under PRJEB33521 project (https://www.ebi.ac.uk/ena/data/view/PRJEB33521).

Ethics and consent to participate

Not applicable.

Consent for publication

Not applicable.

Competing interests

The authors declare that they have no competing interests.

Author details

[1] Grupo de Investigaciones Microbiológicas-UR (GIMUR), Departamento de Biología, Facultad de Ciencias Naturales, Universidad del Rosario, Bogotá, Colombia. [2] Laboratorio de Investigaciones en Parasitología Tropical, Facultad de Ciencias, Universidad del Tolima, Ibagué, Colombia. [3] Centro de Investigaciones en Microbiología y Parasitología Tropical (CIMPAT), Facultad de Ciencias, Universidad de Los Andes, Bogotá, Colombia.

Received: 24 January 2020 Accepted: 8 May 2020
Published online: 14 May 2020

References

1. Edenhofer O, R Pichs-Madruga Y, Sokona,E, Farahani, S, Kadner, K, Seyboth, A, et al. IPCC, Summary for policymakers. In: Climate change 2014: mitigation of climate change. Contribution of Working Group III to the fifth assessment report of the intergovernmental panel on climate change. https://www.ipcc.ch/site/assets/uploads/2018/05/SYR_AR5_FINAL_full_wcover.pdf. 2014. Accessed 12 Nov 2019.
2. Bayoh MN, Lindsay SW. Effect of temperature on the development of the aquatic stages of *Anopheles gambiae sensu stricto* (Diptera: Culicidae). Bull Entomol Res. 2003;93:375–81.
3. Bi Y, Yu W, Hu W, Lin H, Guo Y, Zhou XN, et al. Impact of climate variability on *Plasmodium vivax* and *Plasmodium falciparum* malaria in Yunnan Province, China. Parasit Vectors. 2013;6:357.

4. Butterworth MK, Morin CW, Comrie AC. An analysis of the potential impact of climate change on dengue transmission in the southeastern United States. Environ Health Perspect. 2017;25:579–85.
5. Caminade C, McIntyre KM, Jones AE. Impact of recent and future climate change on vector-borne diseases. Ann N Y Acad Sci. 2019;1436:157–73.
6. Carmona-Castro O, Moo-Llanes DA, Ramsey JM. Impact of climate change on vector transmission of *Trypanosoma cruzi* (Chagas, 1909) in North America. Med Vet Entomol. 2018;32:84–101.
7. Ceccarelli S, Rabinovich JE. Global climate change effects on Venezuela's vulnerability to Chagas disease is linked to the geographic distribution of five triatomine species. J Med Entomol. 2015;52:1333–43.
8. González C, Wang O, Strutz SE, González-Salazar C, Sánchez-Cordero V, Sarkar S. Climate change and risk of leishmaniasis in North America: predictions from ecological niche models of vector and reservoir species. PLoS Negl Trop Dis. 2010;19:e585.
9. McMichael AJ, Haines A. Global climate change: the potential effects on health. BMJ. 1997;315:805–9.
10. Morin CW, Comrie AC, Ernst K. Climate and dengue transmission: evidence and implications. Environ Health Perspect. 2013;121:1264–72.
11. Peterson AT, Campbell LP, Moo-Llanes DA, Travi B, Gonzalez C, Ferro MC, et al. Influences of climate change on the potential distribution of *Lutzomyia longipalpis sensu lato* (Psychodidae: Phlebotominae). Int J Parasitol. 2017;47:667–74.
12. Garza M, Feria Arroyo TP, Casillas EA, Sanchez-Cordero V, Rivaldi CL, Sarkar S. Projected future distributions of vectors of *Trypanosoma cruzi* in North America under climate change scenarios. PLoS Negl Trop Dis. 2014;58:e2818.
13. Medone P, Ceccarelli S, Parham PE, Figuera A, Rabinovich JE. The impact of climate change on the geographical distribution of two vectors of Chagas disease: implications for the force of infection. Philos Trans R Soc Lond B Biol Sci. 2015;5(370):20130560.
14. Tamayo LD, Guhl F, Vallejo GA, Ramírez JD. The effect of temperature increase on the development of *Rhodnius prolixus* and the course of *Trypanosoma cruzi* metacyclogenesis. PLoS Negl Trop Dis. 2018;12:e0006735.
15. González-Rete B, Salazar-Schettino PM, Bucio-Torres MI, Córdoba-Aguilar A, Cabrera-Bravo M. Activity of the prophenoloxidase system and survival of triatomines infected with different *Trypanosoma cruzi* strains under different temperatures: understanding Chagas disease in the face of climate change. Parasit Vectors. 2019;12:219.
16. Zingales B, Andrade SG, Briones MR, Campbell DA, Chiari E, Fernandes O, et al. A new consensus for *Trypanosoma cruzi* intraspecific nomenclature: second revision meeting recommends TcI to TcVI. Mem Inst Oswaldo Cruz. 2009;104:1051–4.
17. Zingales B, Miles MA, Campbell DA, Tibayrenc M, Macedo AM, Teixeira MM, et al. The revised *Trypanosoma cruzi* subspecific nomenclature: rationale, epidemiological relevance and research applications. Infect Genet Evol. 2012;12:240–53.
18. Gonçalves CS, Ávila AR, de Souza W, Motta MCM, Cavalcanti DP. Revisiting the *Trypanosoma cruzi* metacyclogenesis: morphological and ultrastructural analyses during cell differentiation. Parasit Vectors. 2018;6(11):83.
19. Hamedi A, Botelho L, Britto C, Fragoso SP, Umaki AC, Goldenberg S, et al. *In vitro* metacyclogenesis of *Trypanosoma cruzi* induced by starvation correlates with a transient adenylyl cyclase stimulation as well as with a constitutive upregulation of adenylyl cyclase expression. Mol Biochem Parasitol. 2015;200:9–18.
20. Vanrell MC, Losinno AD, Cueto JA, Balcazar D, Fraccaroli LV, Carrillo C, et al. The regulation of autophagy differentially affects *Trypanosoma cruzi* metacyclogenesis. PLoS Negl Trop Dis. 2017;11:e0006049.
21. Cardoso J, Lima CDP, Leal T, Gradia DF, Fragoso SP, Goldenberg S, et al. Analysis of proteasomal proteolysis during the *in vitro* metacyclogenesis of *Trypanosoma cruzi*. PLoS One. 2011;6:e21027.
22. Fampa P, Santos AL, Ramirez MI. *Trypanosoma cruzi*: ubiquity expression of surface cruzi-pain molecules in TCI and TCII field isolates. Parasitol Res. 2010;107:443–7.
23. Tyler KM, Engman DM. The life cycle of *Trypanosoma cruzi* revisited. Int J Parasitol. 2001;31:472–81.
24. Hernandez R, Cevallos AM, Nepomuceno-Mejia T, Lopez-Villasenor I. Stationary phase in *Trypanosoma cruzi* epimastigotes as a preadaptive stage for metacyclogenesis. Parasitol Res. 2012;111:509–14.
25. Avila AR, Dallagiovanna B, Yamada-Ogatta SF, Monteiro-Góes V, Fragoso SP, Krieger MA, et al. Stage-specific gene expression during *Trypanosoma cruzi* metacyclogenesis. Genet Mol Res. 2003;2:159–68.
26. Parodi-Talice A, Monteiro-Goes V, Arrambide N, Avila AR, Duran R, Correa A, et al. Proteomic analysis of metacyclic trypomastigotes undergoing *Trypanosoma cruzi* metacyclogenesis. J Mass Spectrom. 2007;42:1422–32.
27. Belew AT, Junqueira C, Rodrigues-Luiz GF, Valente BM, Oliveira AER, Polidoro RB, et al. Comparative transcriptome profiling of virulent and non-virulent *Trypanosoma cruzi* underlines the role of surface proteins during infection. PLoS Pathogens. 2017;13:e1006767.
28. Berná L, Chiribao ML, Greif G, Rodriguez M, Alvarez-Valin F, Robello C. Transcriptomic analysis reveals metabolic switches and surface remodeling as key processes for stage transition in *Trypanosoma cruzi*. PeerJ. 2017;5:e3017.
29. Houston-Ludlam GA, Belew AT, El-Sayed NM. Comparative transcriptome profiling of human foreskin fibroblasts infected with the Sylvio and Y strains of *Trypanosoma cruzi*. PLoS One. 2016;11:e0159197.
30. Li Y, Shah-Simpson S, Okrah K, Belew AT, Choi J, Caradonna KL, et al. Transcriptome remodeling in *Trypanosoma cruzi* and human cells during intracellular infection. PLoS Pathogens. 2016;12:e1005511.
31. Udoko AN, Johnson CA, Dykan A, Rachakonda G, Villalta F, Mandape SN, et al. Early regulation of profibrotic genes in primary human cardiac myocytes by *Trypanosoma cruzi*. PLoS Negl Trop Dis. 2016;10:e0003747.
32. Souto RP, Fernandes O, Macedo AM, Campbell DA, Zingales B. DNA markers define two major phylogenetic lineages of *Trypanosoma cruzi*. Mol Biochem Parasitol. 1996;83:141–52.
33. Cruz-Saavedra L, Munoz M, Leon C, Patarroyo MA, Arevalo G, Pavia P, et al. Purification of *Trypanosoma cruzi* metacyclic trypomastigotes by ion exchange chromatography in sepharose-DEAE, a novel methodology for host-pathogen interaction studies. J Microbiol Methods. 2017;142:27–32.
34. Trapnell C, Pachter L, Salzberg SL. TopHat: discovering splice junctions with RNA-seq. Bioinformatics. 2009;25:1105–11.
35. Trapnell C, Roberts A, Goff L, Pertea G, Kim D, Kelley DR, et al. Differential gene and transcript expression analysis of RNA-seq experiments with TopHat and Cufflinks. Nat Protoc. 2012;7:562–78.
36. Aurrecoechea C, Barreto A, Basenko EY, Brestelli J, Brunk BP, Cade S, et al. EuPathDB: the eukaryotic pathogen genomics database resource. Nucleic Acids Res. 2017;45:D581–91.
37. Warrenfeltz S, Basenko EY, Crouch K, Harb OS, Kissinger JC, Roos DS, et al. EuPathDB: the eukaryotic pathogen genomics database resource. Methods Mol Biol. 2018;1757:69–113.
38. Kollien AH, Schaub GA. The development of *Trypanosoma cruzi* in triatominae. Parasitol Today. 2000;16:381–7.
39. Callejas-Hernández F, Rastrojo A, Poveda C, Gironès N, Fresno M. Genomic assemblies of newly sequenced *Trypanosoma cruzi* strains reveal new genomic expansion and greater complexity. Sci Rep. 2018;8:14631.
40. Bussotti G, Gouzelou E, Cortes Boite M, Kherachi I, Harrat Z, Eddaikra N, et al. *Leishmania* genome dynamics during environmental adaptation reveal strain-specific differences in gene copy number variation, karyotype instability, and telomeric amplification. MBio. 2018;9:e01399–418.
41. Berná L, Rodriguez M, Chiribao ML, et al. Expanding an expanded genome: long-read sequencing of *Trypanosoma cruzi*. Microb Genom. 2018;4:e000177.
42. Torres-Silva CF, Repolês BM, Ornelas HO, Macedo AM, Franco GR, Junho Pena SD, et al. Assessment of genetic mutation frequency induced by oxidative stress in *Trypanosoma cruzi*. Genet Mol Biol. 2018;41:466–74.
43. Reis-Cunha JL, Bartholomeu DC. *Trypanosoma cruzi* genome assemblies: challenges and milestones of assembling a highly repetitive and complex genome. Methods Mol Biol. 2019;1955:1–22.
44. Igoillo-Esteve M, Cazzulo JJ. The glucose-6-phosphate dehydrogenase from *Trypanosoma cruzi*: its role in the defense of the parasite against oxidative stress. Mol Biochem Parasitol. 2006;149:170–81.
45. Maugeri DA, Cannata JJ, Cazzulo JJ. Glucose metabolism in *Trypanosoma cruzi*. Essays Biochem. 2011;51:15–30.
46. Amorim JC, Batista M, da Cunha ES, Lucena ACR, Lima CP, Sousa K, et al. Quantitative proteome and phosphoproteome analyses highlight the adherent population during *Trypanosoma cruzi* metacyclogenesis. Sci Rep. 2017;29(7):9899.

47. Machado-Silva A, Cerqueira PG, Grazielle-Silva V, Gadelha FR, Peloso Ede F, Teixeira SM, et al. How *Trypanosoma cruzi* deals with oxidative stress: antioxidant defence and DNA repair pathways. Mutat Res Rev Mutat Res. 2016;767:8–22.
48. Ryter SW, Kim HP, Hoetzel A, Park JW, Nakahira K, Wang X, et al. Mechanisms of cell death in oxidative stress. Antioxid Redox Signal. 2007;9:49–89.
49. Zou Y, Liu Q, Yang X, Huang HC, Li J, Du LH, et al. Label-free monitoring of cell death induced by oxidative stress in living human cells using terahertz ATR spectroscopy. Biomed Opt Express. 2018;9:14–24.
50. Avelar Ld GA, Gava SG, Neves RH, Silva MCS, Araújo N, Tavares NC, et al. Smp38 MAP kinase regulation in *Schistosoma mansoni*: roles in survival, oviposition, and protection against oxidative stress. Front Immunol. 2019;24:10–21.
51. Soares-Silva M, Diniz FF, Gomes GN, Bahia D. The mitogen-activated protein kinase (MAPK) pathway: role in immune evasion by trypanosomatids. Front Microbiol. 2016;24(7):183.
52. Ferreira LR, Dossin Fde M, Ramos TC, Freymuller E, Schenkman S. Active transcription and ultrastructural changes during *Trypanosoma cruzi* metacyclogenesis. Ann Acad Bras Cienc. 2008;80:157–66.
53. León CM, Hernández C, Montilla M, Ramírez JD. Retrospective distribution of *Trypanosoma cruzi* I genotypes in Colombia. Mem Inst Oswaldo Cruz. 2015;110:387–93.
54. Smircich P, Eastman G, Bispo S, Duhagon M, Guerra-Slompo E, Garat B, et al. Ribosome profiling reveals translation control as a key mechanism generating differential gene expression in *Trypanosoma cruzi*. BMC Genomics. 2015;16:s443.
55. Rebello KM, Uehara LA, Ennes-Vidal V, et al. Participation of *Trypanosoma cruzi* gp63 molecules on the interaction with *Rhodnius prolixus*. Parasitology. 2019;146:1075–82.
56. Kulkarni MM, Olson CL, Engman DM, McGwire BS. *Trypanosoma cruzi* GP63 proteins undergo stage-specific differential posttranslational modification and are important for host cell infection. Infect Immun. 2009;77:2193–200.
57. Cuevas IC, Cazzulo JJ, Sánchez DO. gp63 homologues in *Trypanosoma cruzi:* surface antigens with metalloproteinase activity and a possible role in host cell infection. Infect Immun. 2003;71:5739–49.

Publisher's Note

VIRULENCE
2020, VOL. 11, NO. 1, 969–980
https://doi.org/10.1080/21505594.2020.1797274

Taylor & Francis
Taylor & Francis Group

RESEARCH PAPER

OPEN ACCESS Check for updates

Transcriptional remodeling during metacyclogenesis in *Trypanosoma cruzi* I

Lissa Cruz-Saavedra [a], Gustavo A. Vallejo[b], Felipe Guhl[c], Louisa A. Messenger[d], and Juan David Ramírez [a]

[a]Grupo de Investigaciones Microbiológicas-UR (GIMUR), Departamento de Biología, Facultad de Ciencias Naturales, Universidad del Rosario, Bogotá, Colombia; [b]Laboratorio de Investigaciones en Parasitología Tropical, Facultad de Ciencias, Universidad del Tolima, Ibagué, Colombia; [c]Centro de Investigaciones en Microbiología y Parasitología Tropical (CIMPAT), Facultad de Ciencias, Universidad de Los Andes, Bogotá, Colombia; [d]London School of Hygiene and Tropical Medicine, London, UK

ABSTRACT

Metacyclogenesis is one of the most important processes in the life cycle of *Trypanosoma cruzi*. In this stage, noninfective epimastigotes become infective metacyclic trypomastigotes. However, the transcriptomic changes that occur during this transformation remain uncertain. Illumina RNA-sequencing of epimastigotes and metacyclic trypomastigotes belonging to *T. cruzi* DTU I was undertaken. Sequencing reads were aligned and mapped against the reference genome, differentially expressed genes between the two life cycle stages were identified, and metabolic pathways were reconstructed. Gene expression differed significantly between epimastigotes and metacyclic trypomastigotes. The cellular pathways that were mostly downregulated during metacyclogenesis involved glucose energy metabolism (glycolysis, pyruvate metabolism, the Krebs cycle, and oxidative phosphorylation), amino acid metabolism, and DNA replication. By contrast, the processes where an increase in gene expression was observed included those related to autophagy (particularly Atg7 and Atg8 transcripts), corroborating its importance during metacyclogenesis, endocytosis, by an increase in the expression of the AP-2 complex subunit alpha, protein processing in the endoplasmic reticulum and meiosis. Study findings indicate that in *T. cruzi* metacyclic trypomastigotes, metabolic processes are decreased, and expression of genes involved in specific cell cycle processes is increased to facilitate transformation to this infective stage.

ARTICLE HISTORY
Received 30 March 2020
Revised 24 June 2020
Accepted 7 July 2020

KEYWORDS
Trypanosoma cruzi; metacyclic trypomastigotes; epimastigotes; transcriptomic; pathways

Introduction

Trypanosoma cruzi is a protozoan parasite that causes Chagas disease and is a serious public health problem in the Americas [1]. *T. cruzi* has a complex life cycle that alternates between triatomine insects and mammalian hosts, such as humans [2]. The parasite adopts four morphological forms that allows it to adapt to different microenvironmental stresses experienced during distinct life cycle stages [3].

The *T. cruzi* life cycle in mammals begins when metacyclic trypomastigotes (MTs), an infectious form, present in the vector's feces reach peripheral blood through the skin wound caused by the triatomine during a blood meal and infect mononuclear cells, such as monocytes. In mononuclear cells, MTs differentiate into amastigotes, which are non-mobile replicative forms that undergo multiple rounds of division until finally transforming into cell-derived trypomastigotes (CDTs). The latter lyses the cells and migrate to infect other cells or tissues for which they have a high tropism [2,3]. The *T. cruzi* life cycle in insects begins when a triatomine bug ingests blood from mammals with CDTs circulating in the peripheral blood, which then differentiate into noninfective replicative epimastigotes (EPs). When the EPs reach the insect's midgut, they continue migrating through the intestine, undergoing multiple rounds of replication until finally reaching the rectal ampulla, where they transform into MTs [2,3]. Metacyclogenesis is the process by which noninfective EPs transform into infectious MTs. Although some of the events carried out during metacyclogenesis remain unclear, the main stimulus is exposure of EPs to a poor nutritional environment that is rich in redox stress, leading to increased adenylate cyclase activity and consequent rise of intracellular cAMP levels in the parasite [4,5].

Metacyclogenesis is one of the most important and essential steps in the *T. cruzi* life cycle, in which a set of morphological, transcriptomic, proteomic, and metabolic changes allows the parasite to prepare for successful infection [6]. The most relevant morphological changes include modifying the position and shape of the nucleus and kinetoplast, which are associated with increased heterochromatin, followed by lengthening of the flagellum

CONTACT Juan David Ramírez juand.ramirez@urosario.edu.co
Supplemental data for this article can be accessed here.

and elongation of the cytoplasm [7]. During this process, the proteome and phosphoproteome regulate proteins involved in transcription process, transialidases, mucin-associated surface proteins (MASPs), and dispersed gene family 1 (DGF-1) proteins, 12–24 hours after adhesion of EPs to the vector's rectal cuticle [8]. Increased expression of mutagenic proteins has also been reported, including gp82s, calpain, and cruzipain, which are all involved in MT infectivity [9,10]. Regarding metabolic changes, increased proteolysis and metabolism, in response to redox stress, has been observed; these processes strongly influence metacyclogenesis and autophagy regulation [4,11–13].

Two previous studies have been carried out to understand genetic expression in EPs and MTs. The first of these performed by Minning *et al.*, using microarrays, demonstrated an abundance of mRNA related to the morphological stage of *T. cruzi* during its life cycle, finding in MTs an upregulation of transcripts encoding transialidases and in EPs an increase in the expression of genes that participate in the histidine-to-glutamate pathway [14]. By comparison, analyses performed by Smircich *et al.*, using SOLiD RNA-seq, confirmed the variation in expression profiles between EPs and MTs, characterized by an increase in the expression of genes mainly related to virulence (transialidases) [15]. To date, RNA-seq has been used to evaluate gene expression in EPs, amastigotes, and CDTs. Transcriptome remodeling occurs in these three morphological forms, with EPs characterized by highly expressed genes associated with energy metabolism, CDTs with evasion of the host immune system and membrane proteins, and amastigotes with genes involved in regulating the cell cycle [16]. These findings highlight the importance of modifying RNA expression profiles among different morphological forms of *T. cruzi*, enabling the parasite to adapt to the microenvironments it is exposed to during its life cycle [14,16]. In addition, transcriptomic analysis of EPs during growth curves has shown that during late-stage stationary phase, in response to nutritional stress, overall transcriptional expression decreases, while pre-adaptive upregulation of transialidases, nuclear-associated genes and those involved in flagellum processing occurs to enable transformation to the metacyclic form [17]. However, in this study, the EP and MT stages were not separated; thus, the authors could not determine which parasite stage contributed particular transcripts [17]. Other studies have focused on the relationship between transcriptomics of both the host cell and parasite, as well as virulence genes and remodeling during infection; however, these studies have thus far excluded the MT transcriptome [18–22].

Metacyclogenesis comprises a set of essential changes during the *T. cruzi* life cycle, which are crucial to facilitate the infection process and survival of the parasite outside the vector, as well as potentially contribute to differential virulence between strains. To date, there is still a paucity of information regarding the modifications the *T. cruzi* transcriptome undergoes during metacyclogenesis. Therefore, this study was conducted to evaluate the gene expression profiles of *Trypanosoma cruzi* I during metacyclogenesis *in vitro*.

Results

Metacyclogenesis curve

The MT concentration increased from day 1 post-culture in the three replicates evaluated, with an average concentration of 2.9×10^8 trypomastigotes/mL. The highest MT concentration corresponded to an average of 5.35×10^8 trypomastigotes/mL on day 7 post-culture; however, from day 7 onwards, the number of MTs decreased until reaching an average MT concentration of 1.75×10^8 trypomastigotes/mL after 10 days post-infection (Figure S1). Analysis of data normality for the three biological replicates indicated a normal distribution. Thus, an analysis of variance (ANOVA) was performed, followed by multiple comparisons, which showed a difference between replicates. An ANOVA was performed to determine the first day of metacyclogenesis, which corresponded with day 4 post-culture (Figure S1).

Gene expression profiles of epimastigotes and metacyclic trypomastigotes

RNA-sequencing of the eight transcriptomes included in this study generated an average of 56,997,358.81 and 21,980,185.92 sequencing reads (standard deviations of 6,350,528.951 and 1,377,905.656) for MTs and EPs, respectively. The results for each of the treatments and replicates are available in Table S1. The differentially expressed genes (DEGs) showed no statistically significant differences between the MT biological replicates (Figure S2B). However, we detected 18 DEGs corresponding to EPs, which differed among biological replicates. These genes were eliminated from the analysis to avoid bias when comparing the MT and EP profiles (Figure S2A). The DEGs differed significantly in MTs when compared with EPs; 250 DEGs were downregulated, and 251 were upregulated for the intersect between cufflinks and DESeq2 (Figure 1, Table S2). A heatmap showing the 50 genes that were the most down- and upregulated, and their respective logfold changes, is shown in Figure S3.

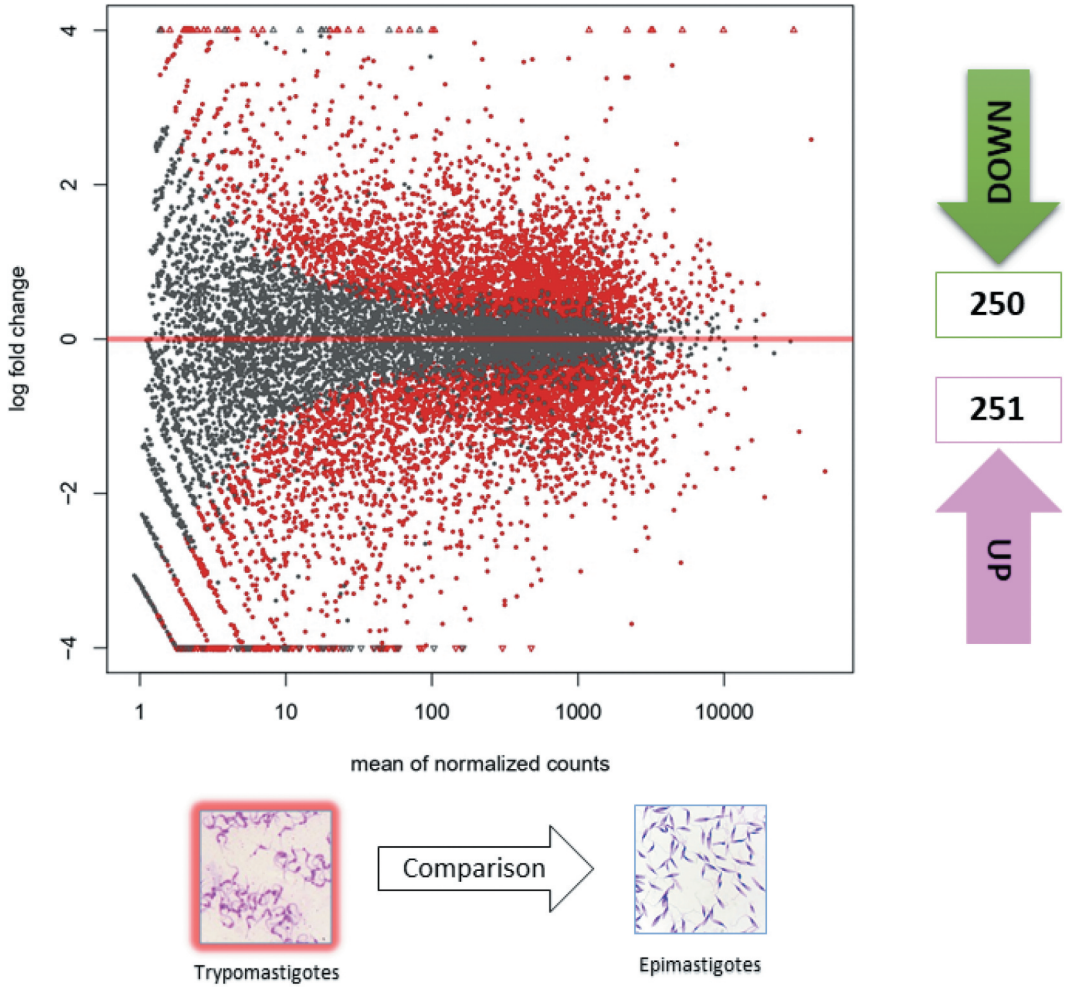

Figure 1. Gene expression of epimastigotes and metacyclic trypomastigotes. Volcano matrix to compare differentially expressed genes (DEGs) between metacyclic trypomastigotes (MTs) and epimastigotes (EPs), indicating the total number of down- and upregulated DEGs in metacyclic trypomastigotes.

Gene ontology analysis

A total of 209 ontological terms were downregulated and 164 upregulated in MTs compared to EPs. The ontology that represented the highest number of down- and upregulated terms was related to molecular functions (65% and 58%, respectively), followed by biological processes, which had a greater proportion of downregulated genes (38%) compared to upregulated (33%), and finally, cellular components, with six terms downregulated and 11 upregulated (Figure 2, Table S3). Considering the importance of cellular processes throughout the *T. cruzi* life cycle and of course in metacyclogenesis and based on the objective of this study, we continued to describe in greater depth the cellular processes identified. The ontological term that grouped the largest number of downregulated genes corresponded to oxidation-reduction process (n = 15), followed by proteolysis (n = 9), and cell redox homeostasis, cellular amino acid metabolic process and transmembrane transport (with three genes each). By comparison, the proportion of upregulated genes with related ontological terms was lower, with proteolysis being the term that grouped the largest number of genes (n = 6), followed by cell adhesion (n = 5) and oxidation-reduction process (4) (Figure 2).

Metabolic pathway reconstruction

From the GO terms, we selected the FASTA files and reconstructed the metabolic pathways, corresponding to the most down- and upregulated genes.

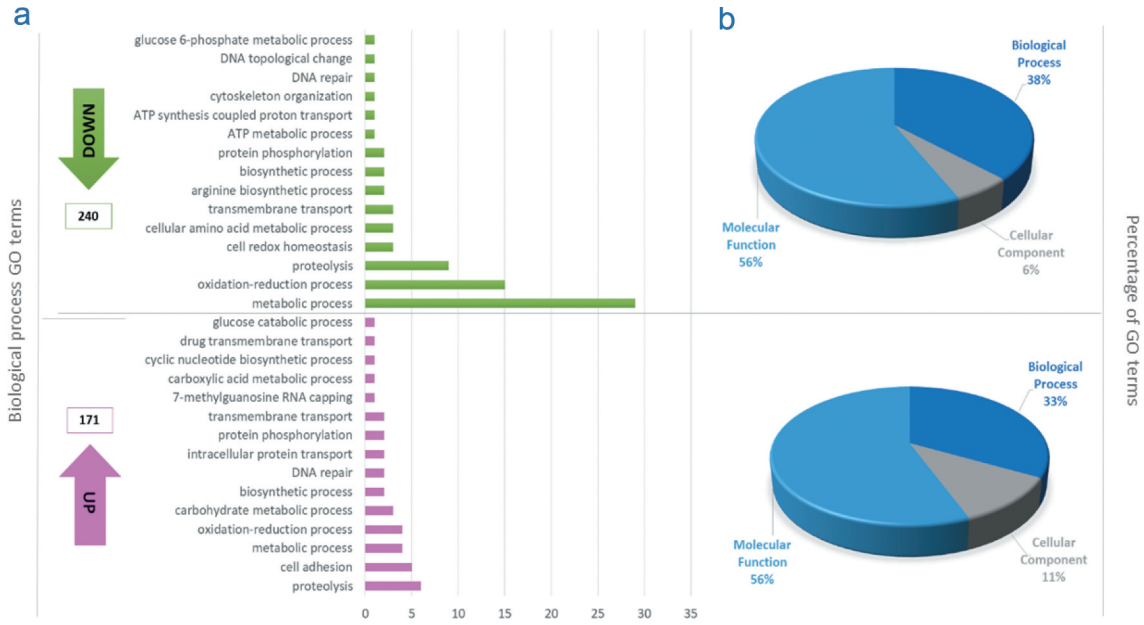

Figure 2. Gene ontology terms. (a) Gene ontology terms corresponding to the 15 most down and upregulated biological process from differential expressed genes obtained when were compared metacyclic trypomastigotes with epimastigotes; The ontological terms for the downregulated genes are in green and the ontological terms for the upregulated genes in pink. (b) Total proportions of ontology terms downregulated (upper) and upregulated (lower).

Glucose energy processes

In MTs, six genes were downregulated for glycolysis, including the enzymes phosphoglucomutase (EC 5.4.2.2-TcSYL_0046700), glucokinase (EC 2.7.1.2), glyceraldehyde-3-phosphate dehydrogenase (EC 1.2.1.12-TcSYL_0011690), pyruvate dehydrogenase E2 component dihydrolipoamide acetyltransferase (EC 2.3.1.12-TcSYL_00734), aldehyde dehydrogenase (NAD+) (EC 1.2.1.3-TcSYL_0140060), and alcohol dehydrogenase 1/7 (EC 1.1.1.1). In addition, aldose 1-epimerase (EC 5.1.3.3-TcSYL_0172170) and 2,3-bisphosphoglycerate-independent phosphoglycerate mutase (EC 5.4.2.12-TcSYL_0108730) were upregulated (Figure 3).

Glucose degradation produces pyruvate via the glycolytic pathway. Three genes were upregulated in pyruvate metabolism, with malate dehydrogenase (oxaloacetate-decarboxylating) (EC 1.1.1.38-TcSYL_0047970) exclusively related to pyruvate metabolism (Figure 3). Pyruvate metabolism allows acetyl-CoA formation, which is necessary for Krebs cycle progression; two genes involved in pyruvate metabolism/Krebs cycle were downregulated, pyruvate dehydrogenase E2 component (dihydrolipoamide acetyltransferase) (EC:2.3.1.12-TcSYL_0073490) and dihydrolipoamide dehydrogenase (EC:1.8.1.4-TcSYL_0111890), and two genes involved in the pyruvate metabolism/Krebs cycle were upregulated, fumarate hydratase, class I (EC 4.2.1.2-T40S), and malate dehydrogenase (EC 1.1.1.37) (Figure 3)

Amino acid metabolism

Next, we evaluated the differential metabolism of amino acids in MTs.

For alanine, aspartate, and glutamate metabolism, three genes were downregulated and one was upregulated. The downregulated genes corresponded to alanine transaminase (EC 2.6.1.2-TcSYL_0178360), glutamate dehydrogenase (NADP+) (EC 1.4.1.4-TcSYL_0074000) and 1-pyrroline-5-carboxylate dehydrogenase (EC 1.2.1.88-TcSYL_0001430); aspartate aminotransferase, cytoplasmic (EC: 2.6.1.1-TcSYL_0131200) was upregulated.

For glycine, serine and threonine metabolism, three genes were downregulated: glycine hydroxymethyltransferase (EC: 2.1.2.1 – TcSYL_0027590), dihydrolipoamide dehydrogenase (EC: 1.8.1.4-TcSYL_0111890) and glycine C-acetyltransferase (EC: 2.3. 1.29-TcSYL_0103590); and one upregulated: 2,3-bisphosphoglycerate-independent phosphoglycerate mutase (EC: 5.4.2.12- TcSYL_0108730). For tyrosine metabolism, tyrosine aminotransferase (EC:2.6.1.5-TcSYL_0012630), alcohol dehydrogenase 1/7 (EC:1.1.1.1), and 4-hydroxy-2-oxoheptanedioate aldolase (EC:4.1.2.52- TcSYL_0019630) were downregulated and aspartate aminotransferase, cytoplasmic (EC:2.6.1.1-TcSYL_0131200) was upregulated.

Regarding cysteine and methionine metabolism, three genes were downregulated; 5′-methylthioadenosine phosphorylase (EC 2.4.2.28-TcSYL_0163070) is expressed only

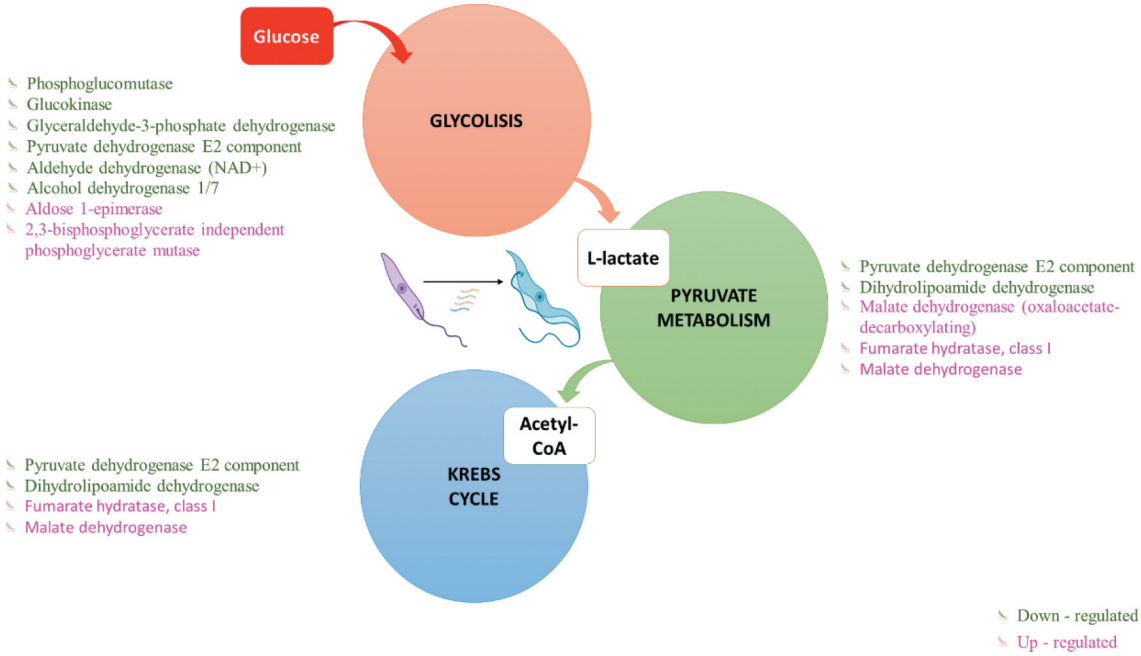

Figure 3. Glucose energy processes. Differentially expressed genes (DEGs) in Metacyclic trypomastigotes in comparison with epimastigotes in the metabolism of glycolysis, pyruvate, and the Krebs cycle (downregulated genes in green and upregulated genes in pink).

in the metabolism of cysteine and methionine, and S-adenosylmethionine synthetase (EC 2.5.1.6-TcSYL_0140680), and tyrosine aminotransferase (2.6.1.5-TcSYL_0012630) are also related to other metabolic pathways. In addition, three genes were upregulated: aspartate aminotransferase, cytoplasmic (EC 2.6.1.1-TcSYL_0131200), thiosulfate/3-mercaptopyruvate sulfurtransferase (EC:2.8.1.1 2.8.1.2-TcSYL_0079450) and malate dehydrogenase (K00026).

Finally, down- and upregulated genes related to valine, leucine, and isoleucine degradation were increased. Two downregulated genes were dihydrolipoamide dehydrogenase (EC 1.8.1.4-TcSYL_0111890) and 2-oxoisovalerate dehydrogenase E2 component (dihydrolipoyl transacylase) (EC 2.3.1.168-TcSYL_0062200); only one gene expressed in this pathway was upregulated: 3-methylcrotonyl-CoA carboxylase alpha subunit (EC 6.4.1.4-TcSYL_0057610).

Cellular processes

Consistent with the morphological modifications that *T. cruzi* undergoes during metacyclogenesis, three genes related to regulation of the actin cytoskeleton were upregulated: phosphatidylinositol-4,5-bisphosphate 3-kinase catalytic subunit alpha/beta/delta (EC: 2.7.1.153 – TcSYL_0025520), actin-related protein 2/3 complex, subunit 5, and serine/threonine-protein phosphatase PP1 catalytic subunit (EC: 3.1.3.16-TcSYL_0044050). Endocytosis-related genes were also increased in expression, with two genes upregulated from this process: AP-2 complex subunit alpha (TcSYL_0201950) and ARP 2/3 actin-related protein 2/3 complex, subunit 1A/1. Likewise, protein processing in the endoplasmic reticulum was upregulated (protein transport protein SEC61 subunit alpha, calreticulin (TcSYL_0030690), and DnaJ homolog subfamily A member 1). Previous studies have demonstrated the importance of autophagy activation as a stimulus for metacyclogenesis, and the presence of the autophagy protein TcAtg8 that triggers metacyclogenesis under conditions of nutritional depression [13]. In this study, two genes in this process were upregulated: ubiquitin-like modifier-activating enzyme Atg7 (TcSYL_0008790) and GABA (A) receptor-associated protein Atg8 (TcSYL_0079440) (Figure 4).

DNA processes

Two RNA-encoding proteins involved in DNA replication were downregulated, corresponding to proliferating cell nuclear antigen (PCNA-TcSYL_0064140) and replication C subunit 3/5 (TcSYL_0116350); cell cycle cyclin-dependent kinase regulatory subunit CKS1

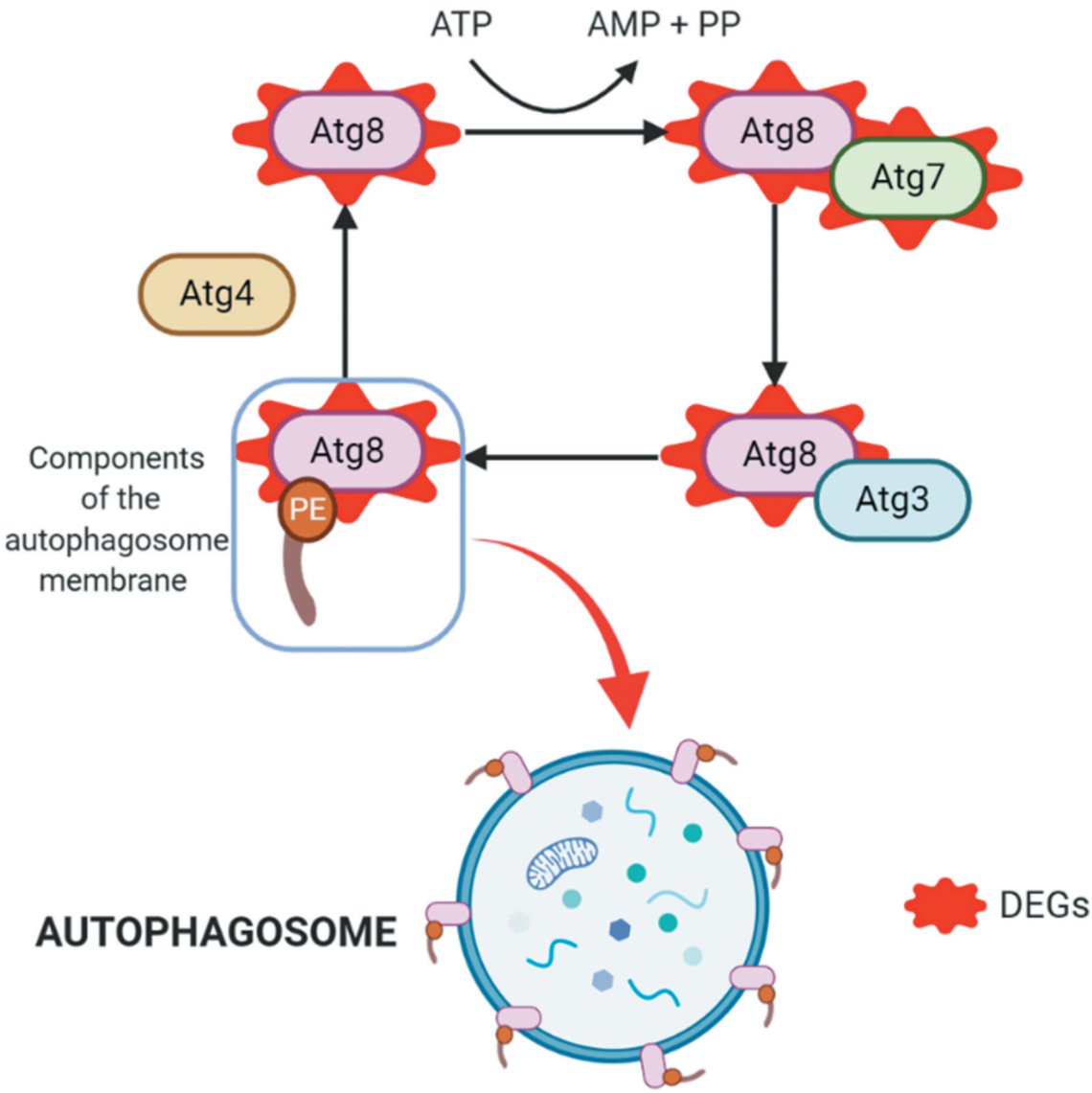

Figure 4. Autophagy process. Upregulated DEGs in autophagy (in red). The cysteine protease Atg4 cuts the arginine residue in the C-terminal part of Atg8, and immediately Atg8 is transferred to Atg7 and Atg3, and finally to the substrate phosphatidylethanolamine (PE); this complex (Atg8-PE) is part of the autophagosome membrane components.

(TcSYL_0112190) and MDR1 cohesin complex subunit SCC1 (TcSYL_0162370) were also downregulated. Two genes were upregulated which are involved in meiosis, adenylate cyclase (Cyr1) (TcSYL_0107750) and serine/threonine-protein phosphatase PP1 catalytic subunit (Glc7); however, these genes are not specific to this process and participate in other metabolic pathways (TcSYL_0044050).

Discussion

T. cruzi presents a peculiar transcriptional control, where polycistron mRNAs that include genes that are not necessarily related, are transcribed by RNA polymerase II. mRNA maturation involves a process of trans-splicing, with gene expression being regulated at a posttranscriptional level [23]. This complex process suggests the need to unveil the transcriptomic features of this parasite in terms of understanding its biology per se.

One of the most important processes in the life cycle of *T. cruzi* is metacyclogenesis. This process allows the parasite to acquire all necessary metabolic and structural features to differentiate from a noninfective (EPs) to an infective stage (MTs) and overcome the harsh environmental changes the parasite faces throughout its life cycle [6]. Previous studies have evaluated how starvation, redox stress, proteome

modifications, the phosphoproteome, and expression of proteins involved in virulence, are the main stimuli in inducing metacyclogenesis [4–6,10,12]. This study was conducted to evaluate transcriptome remodeling in MTs with respect to EPs using RNA-seq. The MT transcriptome differed significantly from the EP transcriptome, results that have previously been observed using microarrays and SOLiD RNA-seq [14,15]. This was expected because of the morphological and biochemical differences exhibited by MTs, including the modified shape of the nucleus and kinetoplast, changes in chromatin compaction, repositioning of the flagellum–kinetoplast complex, decreases in reservosome size and an increase in specific proteins related to virulence and infective capacity [7,22].

We found that one of the most affected metabolic pathways in MTs was energy metabolism from glucose, in which we identified downregulated genes in glycolysis, pyruvate metabolism, the Krebs cycle, and oxidative phosphorylation. These genes are likely downregulated because of the different nutritional requirements of MTs. This observation was verified by comparing EP transcriptomes in logarithmic phase and EPs in stationary phase, which indicated that regulation of these processes influences the parasite's adaptation to microenvironments under nutritional stress (Figure 3) [4,11]. In *T. cruzi*, glycosomes are organelles that have the enzymatic content of different metabolic pathways, thus allowing compartmentalization of different processes [24]. Previous studies in *T. brucei* have shown a decrease in the glycolytic pathway glycosomes in the infective form of the parasite in the vector, allowing the parasite a rapid regulation of the metabolism in response to low glucose environments [13]. An increase in the number of down-regulated genes in MTs, the infective form of *T. cruzi* present in the vector, is consistent with these findings; however, the presence of genes coding for fumarate hydratase, class I and malate dehydrogenase up-regulated in MTs, both enzymes being involved in the glycolytic branch and active as a consequence of a decrease in pyruvate synthesis, which would possibly explain the down-regulation of pyruvate hydrogenase observed in MTs [25]. The activation of the glycolytic arm and its relationship with the decrease in pyruvate has already been previously documented in *T. cruzi* CDTs in response to the presence of a cell matrix, the results observed here could infer the presence of these regulatory processes in other stages of *T. cruzi* but future mechanistic studies must be conducted to fulfill this hypothesis [26].

Amino acids play important roles in the parasite lifecycle, including in processes related to survival, death, differentiation, and evasion of the host immune system [27]. One characteristic of the MT transcriptome was decreased amino acid metabolism, which may be a consequence of starvation faced by the parasite. In addition, the activation of amino acid catabolism as an energy and carbon source has been demonstrated in epimastigotes in the stationary phase, allowing this metabolic plasticity to adapt to the nutritional conditions it faces [11]. Triatomine artificial urine medium is used in some studies to initiate metacyclogenesis *in vitro* and is supplemented with amino acids such as proline, glutamate, and aspartate, equally present at the distal portion of the triatomine's [28]. Previous studies have shown the importance of L-proline in energy metabolism during metacyclogenesis in addition to its role during oxidative stress and against other different abiotic and biotic stresses [29]. This may indicate that during this phase of the *T. cruzi* life cycle, although these amino acids are not synthesized, the parasite can use previously synthesized reserves. Future Analysis of the amino acid composition during metacyclogenesis and in mature MTs could shed light on amino acid regulation during these stages of the *T. cruzi* life cycle [30]. In contrast, upregulation of the genes involved in synthesizing methionine and cysteine showed a variable expression. Studies of trypanosomatids, such as *Trypanosoma brucei brucei* and *Crithidia fasciculata*, have shown that these parasites can recycle methionine from methylthioadenosine, a product derived from the polyamine synthetic pathway found in EP reservosomes in *T. cruzi*, which may explain its availability in MTs [31,32].

Autophagy allows *T. cruzi* to withstand nutritional stress during metacyclogenesis and amastigogenesis [13,33,34]. The autophagy process involves (Atg)-related proteins and begins when the cysteine protease Atg4 cuts the arginine residue in the C-terminal part of Atg8, and immediately, the protein Atg8 is transferred to Atg7 and later to Atg3, to finally be transferred to the substrate phosphatidylethanolamine (PE). This complex (Atg8-PE) is a principal part of the autophagosome membrane components, making Atg8 one of the best autophagy markers [13]. We found two upregulated genes involved in autophagy, including Atg7 (Figure 4). One upregulated gene was Atg7. Although this gene has not been previously studied in *T. cruzi*, it functions by interrupting autophagy in the bloodstream stages of *Trypanosoma brucei*; thus, it is possible that Atg7 fulfills a similar function in *T. cruzi* MTs. The presence of both Atg7 and Atg8 confirms the importance of autophagy during metacyclogenesis, future studies should conduct longer sequential RNA-seq analyses to further investigate how autophagy is exploited by MTs and characterize the autophagy-related genes that are expressed (Figure 4) [13,35].

Endocytosis in *T. cruzi* is restricted to two specialized invaginations around the base of the flagellum; these are the flagellar pocket membrane and the cytostome, the latter being present only in the replicative forms of the parasite (EPs and AMs) [36]. In this study, upregulated

genes included AP-2 complex subunit alpha (AP-2), a clathrin-associated protein. Within this gene family, AP-1 decreases the proliferation and differentiation of EP into MTs, while AP-3 is essential for *T. brucei* growth and virulence [37]. Previous studies evaluated AP-2 expression in EPs and CDTs of *T. cruzi*; thus, we verified the ID TcSYL_0201950 that codes for this protein in our dataset (Table S2). We observed that although EPs express this protein, its expression is greater in MTs [38,39]. To what extent the increased expression of this protein can confer certain properties to MTs remains unknown, but these results suggest that MT expression levels are regulated to modify an entire metabolic pathway. Endocytosis, in addition to being an important process in regulating the parasite's nutritional requirements, may play a role in regulating the transport of proteins involved in other MT functions such as virulence; these proteins may be previously synthesized and carried to the membrane by endocytosis and vacuole-linked transport.

A recent genomics study of *T. cruzi* reported meiotic sex as a mechanism of genetic exchange; however, the ability for recombination in *T. cruzi* has been heavily debated over the past few decades, and the population of this parasite has been mainly characterized as clonal [40–44]. MT transcriptome analysis demonstrated the presence of two upregulated genes associated with meiosis, and bioinformatics studies of the sequenced genomes have demonstrated that 40–60% of the human/yeast signaling pathway involved in meiosis in trypanosomatids, such as *Leishmania* and *Trypanosoma*, is conserved [42]. This is the first study where the expression of genes related to meiosis in some stage of *T. cruzi* has been demonstrated, despite this, the genes found may participate in other cellular processes, which is why there is no absolute certainty of activating the meiotic process during metacyclogenesis [45]. Despite this, the absence of other specific meiotic proteins could be related to the time at which the RNA was extracted from the MTs (4 days); daily monitoring of gene expression for additional days could provide more information about this cellular process. Intriguingly, the first report of genetic exchange in *T. cruzi* showed that this biological process occurs in CDTs in Vero cells, suggesting the presence of meiosis-related proteins during some parts of the *T. cruzi* life cycle [46]. One of the upregulated genes was the adenylate cyclase (Cyr1), which induces the production of cAMP in response to redox stress; *in vitro* analyses have shown an increase in the levels of this enzyme during metacyclogenesis. Furthermore, the receptor-type adenylate cyclase putative gene has been reported to be upregulated in mature MTs, which together suggests the importance of this enzyme in metacyclogenesis [4,14]. Future studies should examine the transcriptome of the entire *T. cruzi* life cycle to determine which stage has the capacity for recombination and to determine the true recombination mechanism(s) used by *T. cruzi*. This particular analysis was conducted on TcI (*T. cruzi* I) strains, and other DTUs (Discrete typing units) and their capacity for recombination should also be considered.

Materials and methods

Parasite culture and metacyclogenesis curve

EPs of the *T. cruzi* strain MHOM/CO/04/MG (*T. cruzi* I) were cultured in liver infusion tryptose medium (LIT) supplemented with 10% fetal bovine serum at 26°C. We followed a previously described protocol to construct metacyclogenesis curves [47]. In summary, three biological replicates were used, and 1×10^8 EP/mL in the logarithmic phase were cultured in LIT medium supplemented with 10% fetal bovine serum. The parasites were quantified by counting in a Neubauer chamber daily for 10 days, and this process was repeated three times. Slides of the parasites were stained with 10% Giemsa and observed under optical microscopy to visually identify EP and MT forms. Three hundred parasites were classified as EP or MT based on the locations of the nucleus and kinetoplast and on the elongated flagellum in MTs. Three hundred cells were counted per sample. The results were tabulated in Excel over 10 days.

Determining the first day of metacyclogenesis and statistical analysis

To determine the beginning of metacyclogenesis, we obtained the daily MT concentration from the total parasite concentration and the percentage of trypomastigotes observed on the Giemsa-stained slides. We used three replicates to determine the concentration of trypomastigotes in the sample. A Shapiro–Wilk test was performed to observe normality for the MT data. A Kruskal–Wallis test followed by Dunn's multiple comparison test were used to determine the first day of metacyclogenesis, which corresponded to the day on which the MT number was significantly increased. Graphs were constructed based on the number of MTs and EPs per day. Statistical analyses were performed and graphs were constructed using GraphPad Prism, version 7.4 (GraphPad Software Inc., La Jolla, CA, USA).

Purification of MTs and RNA extraction

EP/MT cultures in LIT medium were selected on the previously calculated first day of metacyclogenesis to purify the MTs; the parasites were washed twice with 1X phosphate-buffered saline (PBS); then, resin-exchange sepharose-DEAE chromatography was performed following the protocol described by Cruz-Saavedra *et al*. 2017 [47]. The eluate containing trypomastigotes was obtained, then washed again with 1X PBS, and RNA was extracted using the RNeasy Plus Mini Kit (Qiagen, Düsseldorf, Germany) following the manufacturer's protocols. RNA quality and quantity was evaluated using three parameters: integrity by 2% agarose gel electrophoresis, 1 mg/mL concentration using NanoDrop™ 2000/2000 c spectrophotometers (Thermo Fisher Scientific Inc., CA, USA) and purity using indexes 260/280 and 230/260, which each were ~2.0. To compare gene expression profiles from the MTs against the EPs, we extracted RNA from the logarithmic phase for EPs from a culture in LIT, which was washed twice with PBS; then, the aforementioned RNA extraction protocol was followed.

Preparation of the libraries and RNA sequencing

Extracted RNA was sent to Novogene Bioinformatics Technology Co., Ltd., Beijing, China, to construct the libraries and for sequencing using the Illumina HiSeq X-TEN platform. As an initial step, prior to library preparation, the commercial company verified the RNA quality using an agarose gel and Qubit analysis; only samples that passed these quality controls were included in the sequencing run. To construct the libraries, the extracted RNA was enriched using oligo-beads (dT), and rRNA was removed using a Ribo-Zero kit (Illumina, California, United states). Finally, RNA was randomly fragmented using a fragmentation buffer. The cDNA was produced using a strand-specific TrueSeq RNA-seq Library Prep kit (Illumina, California, United states), following the supplier's instructions. RNA libraries were prepared with an insert size of 350 bp. The size of each read was 2 × 150 bp. Read quality was analyzed using FastQC software (https://www.bioinformatics.babraham.ac.uk/projects/fastqc), which considered 10 parameters, including per base sequence quality, per sequence GC content, and Kmer content. In order to improve the quality of the reads, Novogene performed filtering of low-quality reads to remove those that had adapters, reads containing N > 10% (N represents a base that cannot be determined), and those with low-quality scores (Qscore ≤5). Finally, FastQC analysis was performed again using the previously mentioned parameters based on the filtered reads. Two biological replicates and two technical replicates were included per experiment.

Mapping and differential expression analysis

Eight paired-end samples, corresponding to two biological replicates and two technical replicates per stage were individually aligned using TopHat – v2.1.0 version, which uses bowtie as an alignment engine but has the ability to recognize splicing sites. TopHat was run using default parameters, and the FASTA file of the reference genome of *Trypanosoma cruzi* Sylvio X10-1 version 43, available in EupathDB, was obtained to assemble the samples [48,49]. Differential expression analysis was performed using two methods: cufflinks and HTseq/DESeq2. The bam files obtained from the TopHat assembly were used for mapping in Cufflinks, the gff annotation file of the *T. cruzi* reference genome, Sylvio X10-1 – 43 version, also available in EupathDB, was used to obtain the location of genes in the reference genome. Next, the cuffmerge tool under the "g" and "s" options was used to join files, including those to compare the replicates for each stage (EPs and MTs) and between stages. Finally, differentially expressed genes (DEGs) were identified using the cuffdiff tool, including the parameters "-p", "L", and "u." Fragments per kilobase of exon per million fragments mapped (FPKM) was used to normalize the expression, the *p*-value was calculated from the log2 fold change obtained, and finally, the value was obtained from the correction of the *p*-value. Genes that presented a *q*-value <0.05 were considered statistically significant [3,49]. Regarding the second methodology used, the Python Toolbox HTseq-count tool was used to transform genetic depth information into a count of readings by gene overlapping using the gff annotation file of the *T. cruzi* reference genome, Sylvio X10-1-43 version; .txt output files were obtained for each replicate for each stage (EPs and MTs) [50]. The DESeq Bioconductor package version 1.26.0 was used to determine DEGs, data normalization was performed using the median of ratios method, and the default parameters were followed; transcripts with a log2 fold change >2 and that presented a statistically significant differential expression (*p*adj = <0.05) were selected [51]. DEGs identified by Cufflinks and DESeq2 were classified as downregulated or upregulated. Outputs of both methodologies were compared and selected gene IDs, identified with both tools, were submitted to the virtual tool Venny 2.1, and taken forward for analysis [52].

Gene ontology and pathway reconstruction

The gene IDs for down- and upregulated DEGs, obtained from both Cufflink and DESeq2, were submitted to the EupathDB TriTrip online tool in two different lists to obtain the gene ontology (GO) terms for enrichment analysis [53,54]. To reconstruct protein pathways, a FASTA output file was obtained from the IDs of the down- and upregulated DEGs submitted to EupathDB with protein-coding sequences. Each gene FASTA file was subjected to the KEGG Automatic Annotation Server (KAAS) tool, selecting the homology search algorithm GHOSTX and the GENES dataset for kinetoplasts available in the manually curated KEGG GENES database [55,56]. The html file obtained was analyzed under the "Pathway" map option to search the pathways that presented a greater KEGG orthology from the DEGs. This tool allowed maps for each differentially regulated pathway to be predicted [55]. KAAS annotates genes by comparing them against the cured KEGG bases using algorithms such as BLAST or GHOSTX; the results are grouped according to the metabolic pathways in which they are activated allowing them to be visualized graphically. The Biorender tool was used (https://biorender.com/) to reconstruct the autophagy metabolic pathway.

Conclusions

In conclusion, transcriptomic gene expression differed significantly between *T. cruzi* EPs and MTs. In MTs processes related to ATP production from glucose were downregulated, including pathways for glycolysis, pyruvate metabolism, and the Krebs cycle, likely in response to increased nutritional stress. Changes to the microenvironmental composition may act as a stimulus for increased endocytosis in *T. cruzi* in response to nutrient deprivation, which in turn promotes endocytosis to transport virulence-related proteins in MTs, such as Gp82 and Gp90. In addition, during metacyclogenesis, energy deficiency leads to a decrease in amino acid metabolism, which may be compensated by increased availability of reservosomes, to provide these amino acids and essential proteins for MTs. Autophagy-related genes are also upregulated, while those involved in DNA replication are downregulated, to facilitate transformation to a nonreplicative form. Future studies should also consider parasitic genetic diversity (DTUs); improved understanding of DNA editing throughout the *T. cruzi* lifecycle will be pivotal for the development of novel drugs and potential vaccines to reduce the current burden of Chagas disease.

Acknowledgments

We thank Philipp Shwabl for his assistance in bioinformatics analysis.

Disclosure statement

The authors declare there are no competing interests.

Author contributions

LCS performed the biological analysis, RNA extraction from metacyclic trypomastigotes and epimastigotes, performed the bioinformatics analysis, and drafted the manuscript. GV contributed to generating the *T. cruzi* strain. FG contributed to designing the study. LAM assisted with manuscript drafting. JDR designed the study, coordinated the biological and bioinformatics analyses, and wrote the manuscript. All authors read and approved the final manuscript.

Data availability

All data employed in this paper are available in the European Nucleotide Archive (ENA) under PRJEB33521 study accession (https://www.ebi.ac.uk/ena/data/view/PRJEB33521).

Funding

We thank the Departamento Administrativo de Ciencia, Tecnología e Innovación COLCIENCIAS for funding the project 120465843375, contract 063-2015 (http://www.colciencias.gov.co/node/1119) for FG, GAV, and JDR. The funders played no role in the study design, data collection, and analysis, publishing decision, or manuscript preparation. We thank DIRECCIÓN ACADÉMICA (Becas de pasantías doctorales) for financing the scholarship for LCS. Juan David Ramírez González, PhD. is a Latin American fellow in the Biomedical Sciences, supported by The Pew Charitable Trusts.

ORCID

Lissa Cruz-Saavedra http://orcid.org/0000-0002-2383-0686
Juan David Ramírez http://orcid.org/0000-0002-1344-9312

References

[1] OMS. Climate change and health. World Health Organization; 2019.
[2] Tyler KM, Engman DM. The life cycle of Trypanosoma cruzi revisited. Int J Parasitol. 2001;31(5–6):472–481.
[3] Goldenberg S, Avila AR. Aspects of Trypanosoma cruzi stage differentiation. Adv Parasitol. 2011;75:285–305.
[4] Hamedi A, Botelho L, Britto C, et al. In vitro metacyclogenesis of Trypanosoma cruzi induced by starvation correlates with a transient adenylyl cyclase stimulation as well as with a constitutive upregulation of adenylyl

cyclase expression. Mol Biochem Parasitol. 2015;200 (1–2):9–18.
[5] Nogueira NP, Saraiva FM, Sultano PE, et al. Proliferation and differentiation of Trypanosoma cruzi inside its vector have a new trigger: redox status. PLoS One. 2015;10(2):e0116712.
[6] Contreras VT, Morel CM, Goldenberg S. Stage specific gene expression precedes morphological changes during Trypanosoma cruzi metacyclogenesis. Mol Biochem Parasitol. 1985;14(1):83–96.
[7] Gonçalves CS, Ávila AR, de Souza W, et al. Revisiting the Trypanosoma cruzi metacyclogenesis: morphological and ultrastructural analyses during cell differentiation. Parasit Vectors. 2018;11(1):83.
[8] Amorim JC, Batista M, da Cunha ES, et al. Quantitative proteome and phosphoproteome analyses highlight the adherent population during Trypanosoma cruzi metacyclogenesis. Sci Rep. 2017;7(1):9899.
[9] Bayer-Santos E, Cunha-e-Silva NL, Yoshida N. Franco da Silveira J. Expression and cellular trafficking of GP82 and GP90 glycoproteins during Trypanosoma cruzi metacyclogenesis. Parasit Vectors. 2013;6:127.
[10] Ennes-Vidal V, Menna-Barreto RFS, Santos ALS, et al. MDL28170, a calpain inhibitor, affects Trypanosoma cruzi metacyclogenesis, ultrastructure and attachment to Rhodnius prolixus midgut. PLoS One. 2011;6(4): e18371.
[11] Barisón MJ, Rapado LN, Merino EF, et al. Metabolomic profiling reveals a finely tuned, starvation-induced metabolic switch in Trypanosoma cruzi epimastigotes. J Biol Chem. 2017;292 (21):8964–8977.
[12] Cardoso J, Lima CDP, Leal T, et al. Analysis of proteasomal proteolysis during the in vitro metacyclogenesis of Trypanosoma cruzi. PLoS One. 2011;6(6):e21027.
[13] Vanrell MC, Losinno AD, Cueto JA, et al. The regulation of autophagy differentially affects Trypanosoma cruzi metacyclogenesis. PLoS Negl Trop Dis. 2017;11 (11):e0006049.
[14] Minning TA, Weatherly DB, Atwood J 3rd, et al. The steady-state transcriptome of the four major life-cycle stages of *Trypanosoma cruzi*.BMC Genomics. 2009;10 (1):370. [cited 2009 Aug 7].
[15] Smircich P, Eastman G, Bispo S, et al. Ribosome profiling reveals translation control as a key mechanism generating differential gene expression in *Trypanosoma cruzi*. BMC Genomics. 2015;16(1):443. [Published 2015 Jun 9].
[16] Berná L, Chiribao ML, Greif G, et al. Transcriptomic analysis reveals metabolic switches and surface remodeling as key processes for stage transition. Peer J. 2017;5:e3017.
[17] Dos Santos CMB, Ludwig A, RL K, et al. Trypanosoma cruzi transcriptome during axenic epimastigote growth curve. Mem Inst Oswaldo Cruz. 2018;113(5).
[18] Belew AT, Junqueira C, Rodrigues-Luiz GF, et al. Comparative transcriptome profiling of virulent and non-virulent Trypanosoma cruzi underlines the role of surface proteins during infection. PLoS Pathog. 2017;13(12):e1006767.
[19] Houston-Ludlam GA, Belew AT, El-Sayed NM. comparative transcriptome profiling of human foreskin fibroblasts infected with the Sylvio and Y strains of Trypanosoma cruzi. PLoS One. 2016;11(8):e0159197.
[20] Li Y, Shah-Simpson S, Okrah K, et al. Transcriptome remodeling in Trypanosoma cruzi and human cells during intracellular infection. PLoS Pathog. 2016;12 (4):e1005511.
[21] Udoko AN, Johnson CA, Dykan A, et al. Early regulation of profibrotic genes in primary human cardiac myocytes by Trypanosoma cruzi. PLoS Negl Trop Dis. 2016;10(1):e0003747.
[22] Avila AR, Dallagiovanna B, Yamada-Ogatta SF, et al. Stage-specific gene expression during Trypanosoma cruzi metacyclogenesis. Genet Mol Res. 2003;2 (1):159–168.
[23] Developmental KS. Regulation of gene expression in the absence of transcriptional control: the case of kinetoplastids. Mol Biochem Parasitol. 2012;181:2.
[24] Michels P, Bringaud F, Herman M, et al. Metabolic functions of glycosomes in Trypanosomatids. Biochim Biophys Acta. 2006;1763(12):1463–1477.
[25] Quiñones W, Acosta H, Gonçalves CS, et al. Structure, properties, function of glycosomes in *Trypanosoma cruzi*. Front Cell Infect Microbiol. 2020;10:25.
[26] Mattos EC, Canuto G, Manchola NC, et al. Reprogramming of Trypanosoma cruzi metabolism triggered by parasite interaction with the host cell extracellular matrix. PLoS Negl Trop Dis. 2019 Feb 6;13(2):e0007103.
[27] Marchese L, Nascimento Jde F, Damasceno FS, et al. The uptake and metabolism of amino acids, and their unique role in the biology of pathogenic trypanosomatids. Pathogens. 2018;7(2):36.
[28] Barrett F, Friend W. Differences in the concentration of free amino acids in the haemolymph of adult male and female *Rhodnius Prolixus*. Comp Biochem Physiol B. 1975;52:3.
[29] Contreras VT, Salles JM, Thomas N, et al. In vitro differentiation of Trypanosoma cruzi under chemically defined conditions. Mol Biochem Parasitol. 1985;16 (3):315–327.
[30] Paes LS, Suárez Mantilla B, Zimbres FM, et al. Proline dehydrogenase regulates redox state and respiratory metabolism in Trypanosoma cruzi. PLoS One. 2013;8 (7):e69419.
[31] Berger BJ, Dai WW, Wang H, et al. Aromatic amino acid transamination and methionine recycling in trypanosomatids. Proc Natl Acad Sci USA. 1996;93 (9):4126–4130.
[32] Sant'Anna C, Nakayasu ES, Pereira MG, et al. Subcellular proteomics of Trypanosoma cruzi reservosomes. Proteomics. 2009;9(7):1782–1794.
[33] Maeda FY, Cortez C, Yoshida N. Cell signaling during Trypanosoma cruzi invasion. Front Immunol. 2012;3:361.
[34] Salassa BN, Romano PS. Autophagy: A necessary process during the Trypanosoma cruzi life-cycle. Virulence. 2019;10:460–469.
[35] Proto WR, Jones NG, Coombs GH, et al. Tracking autophagy during proliferation and differentiation of Trypanosoma brucei. Microb Cell. 2014;1:9–20.
[36] Brosson S, Fontaine F, Vermeersch M, et al. Specific endocytosis blockade of *Trypanosoma cruzi* exposed to

a Poly-LAcNAc binding lectin suggests that lectin-sugar interactions participate to receptor-mediated endocytosis. PLoS One. 2016;11(9):e0163302.
[37] Huang G, Fang J, Sant'Anna C, et al. Adaptor protein-3 (AP-3) complex mediates the biogenesis of acidocalcisomes and is essential for growth and virulence of Trypanosoma brucei*. J Biol Chem. 2011;286:36619–36630.
[38] Kalb LC, Frederico YCA, Boehm C, et al. Conservation and divergence within the clathrin interactome of Trypanosoma cruzi. Sci Rep. 2016;6:31212.
[39] Moreira CN, Batista CM, Fernandes JC, et al. Knockout of the gamma subunit of the AP-1 adaptor complex in the human parasite Trypanosoma cruzi impairs infectivity and differentiation and prevents the maturation and targeting of the major protease cruzipain. PLoS One. 2017;12(7):e0179615.
[40] Berry ASF, Salazar-Sanchez R, Castillo-Neyra R, et al. Sexual reproduction in a natural Trypanosoma cruzi population. PLoS Negl Trop Dis. 2019;13(5):e0007392.
[41] Ramirez JD, Llewellyn MS. Reproductive clonality in protozoan pathogens–truth or artefact? Mol Ecol. 2014;23(17):4195–4202.
[42] Schwabl P, Imamura H, Van den Broeck F, et al. Meiotic sex in Chagas disease parasite Trypanosoma cruzi. Nat Commun. 2019;10(1):3972.
[43] Tibayrenc M, Ayala FJ. The population genetics of Trypanosoma cruzi revisited in the light of the predominant clonal evolution model. Acta Trop. 2015;151:156–165.
[44] Tibayrenc M, Ayala FJ. A misleading description of the predominant clonal evolution model in Trypanosoma cruzi. Acta Trop. 2018;187:13–14.
[45] Genois MM, Paquet ER, Laffitte MCN, et al. DNA repair pathways in trypanosomatids: from DNA repair to drug resistance. Microbiol Mol Biol Rev. 2014;78:40–73.
[46] Gaunt MW, Yeo M, Frame IA, et al. Mechanism of genetic exchange in American trypanosomes. Nature. 2003;421(6926):936–939.
[47] Cruz-Saavedra L, Munoz M, Leon C, et al. Purification of Trypanosoma cruzi metacyclic trypomastigotes by ion exchange chromatography in sepharose-DEAE, a novel methodology for host-pathogen interaction studies. J Microbiol Methods. 2017;142:27–32.
[48] Trapnell C, Pachter L, Salzberg SL. TopHat: discovering splice junctions with RNA-Seq. Bioinformatics. 2009;25(9):1105–1111.
[49] Trapnell C, Roberts A, Goff L, et al. Differential gene and transcript expression analysis of RNA-seq experiments with TopHat and Cufflinks. Nat Proto. 2012;7(3):562–578. .
[50] Anders S, Pyl PT, Huber W. HTSeq—a Python framework to work with high-throughput sequencing data. Bioinformatics. 2015;31:166–169.
[51] Love MI, Huber W, Anders S. Moderated estimation of fold change and dispersion for RNA-seq data with DESeq2. Genome Biol. 2014;15(12):550.
[52] Oliveros JC. Venny. An interactive tool for comparing lists with Venn's diagrams; 2007-2015. https://bioinfogp.cnb.csic.es/tools/venny/index.html.
[53] Aurrecoechea C, Barreto A, Basenko EY, et al. EuPathDB: the eukaryotic pathogen genomics database resource. Nucleic Acids Res. 2017;45(D1):D581–d591.
[54] Warrenfeltz S, Basenko EY, Crouch K, et al. EuPathDB: the eukaryotic pathogen genomics database resource. Methods Mol Biol. 2018;1757:69–113.
[55] Moriya Y, Itoh M, Okuda S, et al. KAAS: an automatic genome annotation and pathway reconstruction server. Nucleic Acids Res. 2007;35(Web Server issue):W182–185.
[56] Suzuki S, Kakuta M, Ishida T, et al. GHOSTX: an improved sequence homology search algorithm using a query suffix array and a database suffix array. PLoS One. 2014;9(8):e103833.

CAPÍTULO 3: Remodelación en la expresión génica durante el ciclo de vida de *Trypanosoma cruzi* II.

Transcriptomic changes across the life cycle of *Trypanosoma cruzi II*

Lissa Cruz-Saavedra[1], Gustavo A. Vallejo[2], Felipe Guhl[3] and Juan David Ramírez[1]

[1] Grupo de Investigaciones Microbiológicas-UR (GIMUR), Departamento de Biología, Facultad de Ciencias Naturales, Universidad del Rosario, Bogota, Colombia
[2] Laboratorio de Investigación en Parasitología Tropical, Facultad de Ciencias, Universidad del Tolima, Ibagué, Colombia
[3] Centro de Investigaciones en Microbiología y Parasitología Tropical (CIMPAT), Facultad de Ciencias, Universidad de Los Andes, Bogota, Colombia

ABSTRACT

Trypanosoma cruzi is a flagellated protozoan that causes Chagas disease; it presents a complex life cycle comprising four morphological stages: epimastigote (EP), metacyclic trypomastigote (MT), cell-derived trypomastigote (CDT) and amastigote (AM). Previous transcriptomic studies on three stages (EPs, CDTs and AMs) have demonstrated differences in gene expressions among them; however, to the best of our knowledge, no studies have reported on gene expressions in MTs. Therefore, the present study compared differentially expressed genes (DEGs), and signaling pathway reconstruction in EPs, MTs, AMs and CDTs. The results revealed differences in gene expressions in the stages evaluated; these differences were greater between MTs and AMs-PTs. The signaling pathway that presented the highest number of DEGs in all the stages was associated with ribosomes protein profiles, whereas the other related pathways activated were processes related to energy metabolism from glucose, amino acid metabolism, or RNA regulation. However, the role of autophagy in the entire life cycle of *T. cruzi* and the presence of processes such as meiosis and homologous recombination in MTs (where the expressions of SPO11 and Rad51 plays a role) are crucial. These findings represent an important step towards the full understanding of the molecular basis during the life cycle of *T. cruzi*.

Subjects Genomics, Microbiology, Parasitology
Keywords *Trypanosoma cruzi*, Metacyclic trypomastigotes, Epimastigotes, Trypomastigotes, Transcriptomic, Pathways

INTRODUCTION

Trypanosoma cruzi is a flagellated protozoan that causes Chagas disease, and it is estimated to affect approximately 8 million individuals worldwide (*OMS, 2019*; *Rassi & De Rezende, 2012*). *T. cruzi* has a complex life cycle comprising four well-differentiated morphological stages—epimastigote (EP), amastigote (AM), cell-derived trypomastigote (CDT) and metacyclic trypomastigote (MT), that circulate among several mammals, such as humans and vectors from the Reduviidae family (*Goldenberg & Avila, 2011*).

The life cycle of *T. cruzi* in vectors initiates when an insect consumes it from a mammal that possesses the CDT stage in the peripheral blood. CDTs are characterized by their

Submitted 22 November 2019
Accepted 19 March 2020
Published 14 May 2020

Corresponding author
Juan David Ramírez,
juand.ramirez@urosario.edu.co

Academic editor
Erika Braga

Additional Information and Declarations can be found on page 21

DOI **10.7717/peerj.8947**

mobility and inability to replicate. They migrate through the insect gut until they reach the midgut where they replicate and differentiate into mobile EPs. Subsequently, EPs move through the intestine while undergoing multiple rounds of replication via binary fission. Finally, in the rectal blister of the insect and because of nutritional stress, EPs adhere to the perimicrovilar film of the epithelial cells of the insect and transform into MTs, which are the infectious stages of *T. cruzi*. They are characterized by their mobility but not replication. MTs are dejected with the feces of the insect to infect other mammals (*Goldenberg & Avila, 2011*; *Teixeira et al., 2012*). The process through which EPs transform into MTs is called metacyclogenesis, and it involves multiple changes in the parasite such as modifications in nucleus and the kinetoplast location, increases in heterochromatin, elongation of the cytoplasm, increases in the flagellum pocket in the cytoplasm, and increases in the expressions of proteins mainly associated with virulence (e.g., transialidase-like GP63, mucins and mucin-associated surface proteins (MASP)) (*Avila et al., 2003*; *Bayer-Santos et al., 2013*; *Contreras, Morel & Goldenberg, 1985*; *Ferreira et al., 2008*).

On the other hand, the life cycle of *T. cruzi* in mammals initiates when MTs that are dejected in the feces of the insect reach the bloodstream of mammals either through laceration generated by the bite of the insect or via other routes such as oral, transfusion, congenital, or laboratory accidents, and they subsequently infect mononucleated or epithelial cells near the infection site. Once in the bloodstream, the parasites inside the white cells differentiate into nonmobile replicative forms called AMs via a process called amastigogenesis. Similar to EPs, AMs undergo multiple rounds of replication and finally they differentiate into nonreplicative mobile forms—CDTs, which lyse the cell and migrate through the bloodstream to invade other mononucleated cells and/or tissues for which they have a high tropism (e.g., the heart, esophagus, colon and adipose tissue as well as the nervous tissue in some cases). The progression of infection in these tissues is directly responsible for the clinical manifestations of Chagas disease (*Cruz et al., 2015*; *Cucunubá et al., 2016*; *Ferreira et al., 2011*; *Goldenberg & Avila, 2011*; *Hernández et al., 2014*).

Recently, the importance of autophagy in controlling the life cycle of *T. cruzi* has been described (*Salassa & Romano, 2019*). Studies have indicated that the activation of this metacyclogenesis process is triggered by autophagy, and although its participation has been inferred during the entire life cycle of *T. cruzi*, the regulatory mechanism of this process in all the stages of *T. cruzi* is unknown to date (*Salassa & Romano, 2019*; *Vanrell et al., 2017*). However, one of the great uncertainties during the life cycle of this parasite is associated with gene regulation, particularly considering polycistronic transcription and the absence of transcription initiation sites where most of the regulatory processes occur at the post-transcriptional level. Some studies have demonstrated the influence in the expression profiles of ribosomal proteins between MTs and EPs, nevertheless, similar to the role of autophagy, to date, the changes in the life cycle of this parasite have not been completely elucidated (*Smircich et al., 2015*). These are only a few processes that are believed to play a relevant role in the life cycle of *T. cruzi*; however, previous studies have demonstrated transcriptomic level differences using next-generation

sequencing in EPs, CDTs and AMs. However, transcriptomic level differences in CDTs and MTs, which are two stages with similar morphological characteristics (in which some stages of the *T. cruzi* life cycle are considered to perform the same function), remain unknown. Moreover, to the best of our knowledge, studies comparing EPs and MTs and investigating how metacyclogenesis influences the infective properties and metabolism in MTs have not been conducted to date (*Belew et al., 2017*; *Berná et al., 2017*; *Dos Santos et al., 2018*; *Houston-Ludlam, Belew & El-Sayed, 2016*; *Li et al., 2016*).

Therefore, there is a current need to comprehend gene regulation in the life cycle of *T. cruzi* and transcriptional profiles at different stages of this parasite to understand the pathogenicity and ability of this parasite to adapt to different microenvironments. Therefore, the objectives of the present study were to evaluate differentially expressed genes (DEGs) in MTs, CDTs, AMs and EPs in *T. cruzi* II, mainly focusing on processes such as autophagy, ribosomal profiling, and other processes (such as meiosis and homologous recombination (HR)) that have not yet been fully described in *T. cruzi*.

METHODS

Parasite cultures

Epimastigote cultures of the strain MHOM/BR/53/Y were maintained in a liver infusion tryptose medium (LIT) supplemented with 10% fetal bovine serum. When an abundant logarithmic phase culture was obtained, a protocol standardized by our group was followed (*Cruz-Saavedra et al., 2017*). Briefly, an EP culture of 1×10^7 cells was prepared and incubated at 26 °C. Six days post-culture, the time needed for the appearance of MT due to nutritional stress and the purification of MTs via ion-exchange chromatography of sepharose-DEAE were investigated according to the protocol of *Cruz-Saavedra et al. (2017)*. MTs obtained in the eluate were washed twice with 1X phosphate-buffered saline (PBS), and their morphological stages were verified by observation under an optical microscope.

RNA extraction and RNA sequencing

RNA was extracted from purified MTs using the RNeasy Plus Mini Kit (Qiagen, Hilden, Germany) according to the manufacturer's protocol. The concentration and quality of the obtained RNA were evaluated by measurements using a nanodrop. A concentration greater than 1 mg/mL and a 260/280 index of 2 ± 2 were acceptable. In addition, the integrity of the obtained RNA was verified by electrophoresis on an agarose gel. RNAs that met these parameters were sent for sequencing to Novogene Bioinformatics Technology Co., Ltd., Beijing, China, using the Illumina HiSeq X-TEN platform, Novogene performed a verification of the RNA quality on Qubit Assays and electrophoresis on agarose gels. Strand-specific TrueSeq RNAseq Library Prep with an insert size of 350 bp was selected to prepare RNA libraries, and the size of each read was 2 × 150 bp. In addition, in order to guarantee the quality of the reads that will be used in the analysis, the reads containing adapters, reads containing $N > 10\%$ (N represents the base cannot be determined) and reads containing low quality (Qscore <= 5) base which is over 50% of the total base were all removed. This procedure is part of the technical service performed

by Novogene Bioinformatics Technology. From the filtered file, according to the parameters mentioned previously, the quality of these reads was determined using the fastQC software (http://www.bioinformatics.babraham.ac.uk/projects/fastqc/). In summary, parameters such as per base quality score, per base sequence, GC content and Kmer content were evaluated (Table S1).

Obtaining the reads of EPs and CDTs

Twelve paired-end reads for the EPs, CDTs and AMs of the strain MHOM/BR/53/Y resulting from sequencing on the Illumina HiSeq 1000 platform were available and obtained from the European Nucleotide Archive (ENA) under the PRJNA251583 and PRJNA251582 projects. PRJNA251583 was submitted to the ENA database on 1 June 2015, by Host-Pathogen Genomics Laboratory, University of Maryland (HPGL-UMD), and the results obtained were published in the article entitled "Comparative Transcriptome Profiling of Human Foreskin Fibroblasts Infected with the Sylvio and Y Strains of *T. cruzi* " (*Houston-Ludlam, Belew & El-Sayed, 2016*). On the other hand, PRJNA251583 was submitted to the ENA database on 1 January 2015, by Host-Pathogen Genomics Laboratory-University of Maryland (HPGL-UMD), and as a result the paper "Transcriptome Remodeling in *T. cruzi* and Human Cells during Intracellular Infection" (*Li et al., 2016*). The information about the files used is available in Table S1. After downloading these files, the reads were verified using the fastQC software and the abovementioned parameters (Table S1).

Differential expression mapping and analysis

Twelve paired-end reads files obtained for MTs, EPs, AMs and CDTs (three biological replicates per stage), were aligned using the read alignment program TopHat version v2.1.0 under default parameters. TopHat uses as an alignment engine "bowtie" but also has the ability to review unallocated reads and align them using the information on splicing junctions. To perform the analysis Tophat was provided of the reference genome of SylvioX10-1 of *T. cruzi* in the TriTrypDB-46_TcruziSylvioX10-1 version available in EupathDB. The reference genome was obtained and indexed using the bowtie2-build option, and it was used to perform the assembly, only mapped reads were considered for subsequent analysis. Files obtained from the TopHat output were used for mapping in Cufflink (*Trapnell, Pachter & Salzberg, 2009*), whereas those obtained from the previously described assembly were used for the gene coordinates in the gff file TriTrypDB-46_TcruziSylvioX10-1 available in EupathDB to obtain the gene coordinates in the reference genome and matched against the reference gff annotation using the cufflinks tool.

Subsequently, a comparison between the biological replicates for each stage and between the organisms in each stage (MT, EP and CDT) was performed using the cuffmerge tool. Finally, fragments per kilobase of exon per million fragments mapped (FPKM) was used to normalize the RNA expression. The fold changed was calculated for each comparison, considering a q-value of <0.05 for determining shortfall deviation risks, differential gene expressions were calculated using the cuffdiff tool under the number

of threads (p), labels (L) and multi-read-correct (u) options, finally, the FDR-adjusted *p*-value (*q*-value) correction was performed (*Trapnell, Pachter & Salzberg, 2009*; *Trapnell et al., 2012*). Additionally, all data were plotted using the CummeRbund software package R, including Volcano graph, Multi-Dimensional Scaling (MDS) plot, heat maps, and Shannon divergence or Jensen–Shannon distance (JS distance) analysis (*Trapnell et al., 2012*).

Gene ontology and pathway reconstruction

From the tables obtained when performing differential expression analysis in cuffdiff, which also contained the information of the down-regulated and up-regulated DEGs IDs when comparing gene expression among MTs and AMs, MTs and CDTs and MTs and EPs (Table S2, gene column). We constructed lists of DEGs IDs and these were submitted to the EupathDB TriTryp online tool in six different files; two per stage comparison (down-up-regulated). Two files were obtained for each comparison and type of expression (down-up regulated) from the analysis in the EupathDB TriTryp tool. The first one contained the list with the gene ontology terms for the DEGs that were subsequently deposited in Table S3, these were obtained using the download-function prediction-GO terms tool, and a second, corresponding to a FASTA file containing the coding sequence for each of the DEGs (q value < 0.05) that was used as input for the Kyoto Encyclopedia of Genes and Genomes (KEGG) Automatic Annotation Server (KAAS) tool, for that purpose the tool used was download-FASTA. Six FASTA files in total were obtained, these files were used as input files for reconstructing signaling pathways in KAAS (*Aurrecoechea et al., 2017*; *Warrenfeltz et al., 2018*). Each gene FASTA file (six) was submitted to the KAAS tool, the GHOSTX homology search algorithm and the GENES dataset for kinetoplastids available in the manually curated KEGG GENES database. KAAS is a manual annotator that allows using the information from the FASTA files to determine the genes that encode these sequences by means of alignment against the databases available in KEGG that contain the information of trypanosomatids genes, and subsequently, perform a reconstruction of the signaling pathways, in which these genes are participating. Based on this strategy, we performed the reconstruction of signaling pathways from DEGs (*Aurrecoechea et al., 2017*; *Moriya et al., 2007*). The html file obtained was analyzed under the "Pathway" map option to search the pathways that presented a greater KEGG. This tool allowed predicting the mapping for each differentially regulated pathway and grouped them according to the signaling pathways in which they are activated, thus allowing their graphical visualization. The Adobe Photoshop CC software was used to condense all the data obtained into a single graph, which included down-regulated and up-regulated genes in the three biological stages (*Moriya et al., 2007*). In addition, Excel lists were generated for all the data produced by KAAS to compare the down-regulated pathways between MTs and AMs, MTs and CDTs and between MTs and EPs as well as the number of differentially regulated genes. Subsequently, the data were plotted for 15 pathways that presented the highest number of down-regulated and up-regulated DEGs in each comparison.

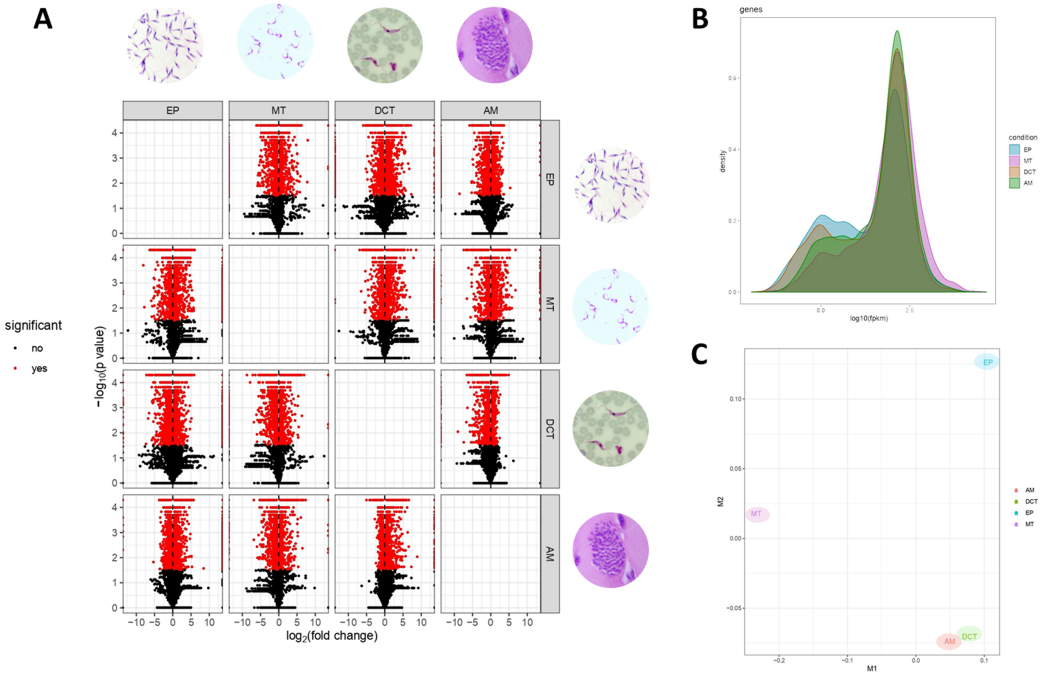

Figure 1 Gene expression in epimastigotes, CDTs, amastigotes and metacyclic trypomastigotes. (A) Volcano plot comparing differentially expressed genes (DEGs) among epimastigotes, amastigotes, cell-derived trypomastigotes, and metacyclic trypomastigotes. (B) The distribution analysis of FPKM values across epimastigotes, amastigotes, cell-derived trypomastigotes, and metacyclic trypomastigotes. (C) Multi-Dimensional Scaling plot (MDS) across epimastigotes, amastigotes, cell-derived trypomastigotes, and metacyclic trypomastigotes. Full-size DOI: 10.7717/peerj.8947/fig-1

RESULTS

Differential gene expression during the life cycle of *T. cruzi*

The raw sequence reads, for the 12 transcriptomes included in this study, had an average of 41442480,75 bases and a standard deviation of 16660041,89 bases. The results for each of the treatments and replicates are available in Table S1. No differences were detected between the replicates of AMs, CDTs, EPs and MTs (Fig. S1).

Differences in gene expressions were observed among the three stages of *T. cruzi* (Fig. 1A). When CDTs were compared with MTs, 2,108 genes were down-regulated and 1,972 were up-regulated, whereas when EPs were compared with MTs, 1,739 were down-regulated and 2,188 were up-regulated, and AMs compared to MTs, 1,732 were down-regulated and 1,917 were up-regulated (Table S2). The distribution analysis of FPKM values across individual samples revealed that transcriptomes with the highest number of genes and the highest FPKM value corresponded to MTs, followed by AMs and CDTs, whereas the lowest FPKM value was observed for EPs and MTs (Fig. 1B). The Multi-Dimensional Scaling (MDS) plot shows a greater dissimilarity between MTs, EPs, maintaining this when comparing the transcriptome of the previous stages with AMs and CDTs, on the contrary, of AMs and CDTs have a high similarity between them (Fig. 1C). Interestingly, the Jensen–Shannon divergence or JS distance analysis revealed that the lowest differentiation value was 0.147 between AMs and CDT, followed by 0.212

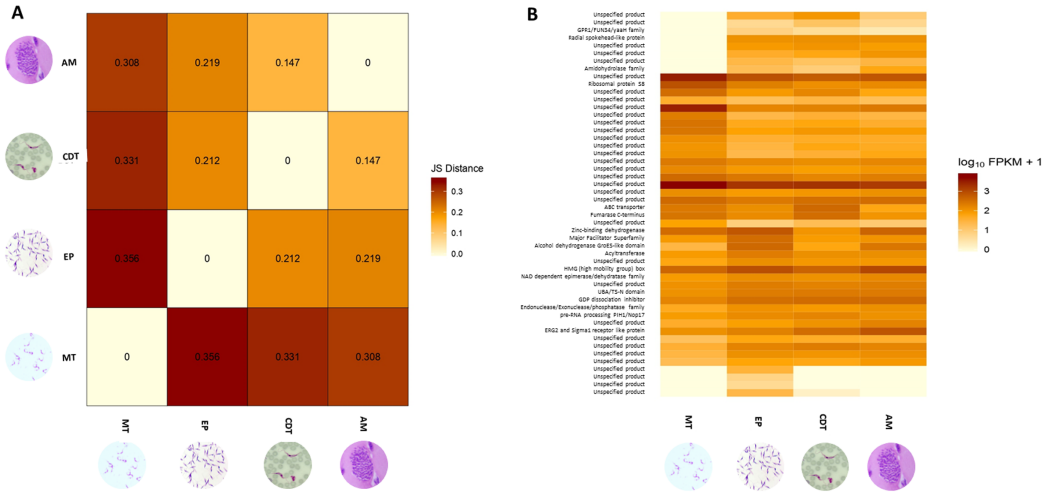

Figure 2 Analysis of differentially expressed genes (DEGs). (A) Jensen–Shannon distance (JS distance) analysis among epimastigotes, amastigotes, cell-derived trypomastigotes, and metacyclic trypomastigotes. (B) The 50 most up-regulated DEGs among epimastigotes, amastigotes, cell-derived trypomastigotes and metacyclic trypomastigotes. Full-size DOI: 10.7717/peerj.8947/fig-2

between EPs and CDTs, 0.308 between AMs and MTs, 0.331 between CDTs and MTs, and finally, 0.353 between EPs and CDTs, indicating that the similarity between MTs and CDTs is not as high as that suggested previously (Fig. 2A).

An analysis of the 50 most down and up-regulated DEGs among the three stages of *T. cruzi* revealed that 33 of these genes encoded for unspecified products, and the remaining 17 genes for different functions, including the ABC transporter, preRNA processing PIH1/Nop17, ribosomal protein S8, and GPR1/FUN34/yaaH family (Fig. 2B). Therefore, to determine if these genes are associated with any specific signaling pathway, we reconstructed the signaling pathways in KAAS. However, we found only two genes associated with ribosomal coding for the small subunit ribosomal protein S15Ae (TcSYL_0001610) and the large subunit ribosomal protein LP1 (TcSYL_0000480), whereas the other signaling pathways had only one DEG. Of note, one of these pathways was associated with HR and the coding gene for topoisomerase (DNA) II binding protein 1 (TcSYL_0001820), which is specific to this process.

Differentially regulated signaling pathways

To determine the signaling pathways associated with DEGs, the results obtained in KAAS were used, which included the signaling pathways and the number of DEGs. Data analysis was performed using Excel and six comparisons were evaluated: down-regulated genes in AMs vs. CDTs, up-regulated genes in AMs vs. CDTs, down-regulated genes in MTs vs. CDTs, up-regulated genes in MTs vs. CDTs, down-regulated genes in MTs vs. EPs, and up-regulated genes in EPs vs. MTs. The data corresponding to the gene ontology is shown in Table S3. In all the groups, the pathway with the highest number of DEGs was associated with ribosomes. A total of 45 genes in this pathway were down-regulated and 17 were up-regulated in MTs compared with those in CDTs.

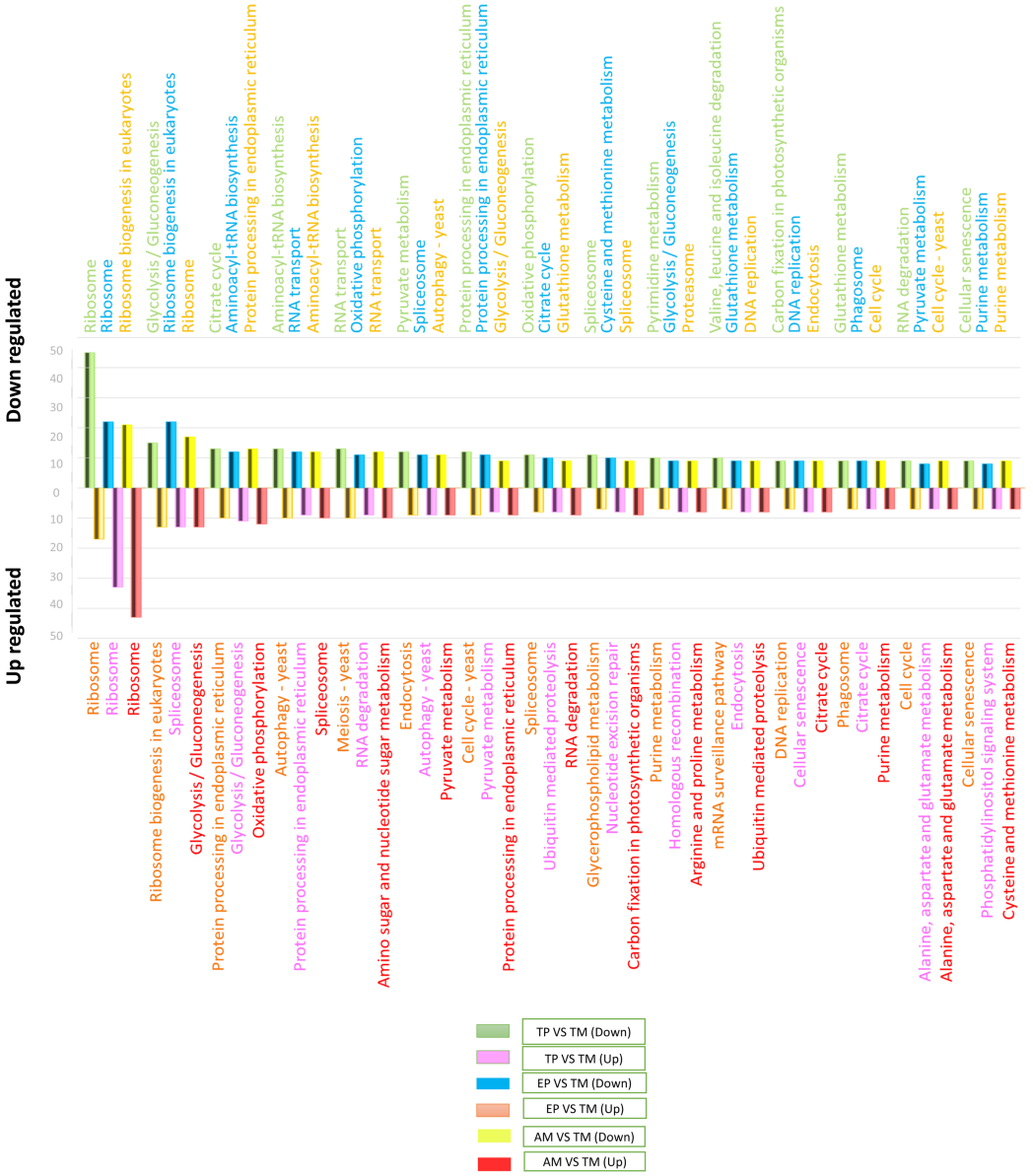

Figure 3 The 15 most differentially regulated pathways. Comparison of the down-regulated (green) and up-regulated (pink) pathways between metacyclic trypomastigotes and cell-derived trypomastigotes. Comparison of the down-regulated (blue) and up-regulated (orange) pathways between metacyclic trypomastigotes and epimastigotes. Comparison of the down-regulated (yellow) and up-regulated (red) pathways between metacyclic trypomastigotes and amastigotes.

Full-size DOI: 10.7717/peerj.8947/fig-3

In contrast, when gene expression was compared between MTs and EPs, the number of up-regulated DEGs was greater (n = 33) than the number of down-regulated genes (n = 22), and 17 genes were down-regulated and 43 up-regulated between MTs and AMs (Fig. 3). Furthermore, the signaling pathway for ribosome biogenesis in eukaryotes was up-regulated only in MTs compared with that in CDTs and AMs (n = 13, 21) and it was down-regulated in MTs compared with that in EPs (n = 22) (Fig. 3).

The signaling pathway for endocytosis presented seven down-regulated and nine upregulated genes when MTs were compared with CDTs, nine downregulated between MTs and AMs, and eight down-regulated and up-regulated genes when MTs were compared with EPs. The production of phagosomes exhibited similar expression patterns with seven down-regulated and up-regulated genes when MTs were compared with CDTs and nine down-regulated and five up-regulated genes when MTs were compared with EPs. However, these results were not found when comparing between MTs and AMs.

On the other hand, in comparison with the signaling pathways associated with energy metabolism, the signaling pathway for glycolysis exhibited 15 down-regulated and four up-regulated genes in MTs compared with that in CDTs, nine down-regulated and 12 up-regulated genes in MTs compared with that in AMs and 10 down-regulated and 11 up-regulated genes in MTs compared with that in EPs. The signaling pathway for the pyruvate metabolism, which produces pyruvate, was also differentially regulated. Overall, 12 genes were down-regulated and four were up-regulated between MTs and CDTs, whereas nine genes were down-regulated and eight were up-regulated between MTs and EPs, and nine up-regulated genes between MTs and AMs. Acetyl-CoA is produced from pyruvate, and this molecule is necessary for citric acid or Krebs cycle. As expected, the signaling pathway for Krebs cycle was also differentially regulated; the number of down-regulated and up-regulated genes was 13 and five, respectively, in MTs compared with CDTs, whereas the number of down-regulated and up-regulated genes was 11 and seven, respectively, in MTs compared with EPs, and seven genes were up-regulated when comparing MTs and AMs. Finally, from the NADH molecules produced in Krebs cycle, the available H+ is used to produce ATP during oxidative phosphorylation, which is the main source of energy in most cells. We observed 11 down-regulated genes and four up-regulated genes that were differentially expressed in this pathway in MTs vs. CDTs, 12 down-regulated and six up-regulated genes in MTs vs. EPs, and 10 up-regulated genes in MTs vs. AMs (Fig. 3). The metabolisms of purines and pyrimidines were also differentially regulated; 10 genes were down-regulated and two were up-regulated in MTs compared with those in CDTs for pyrimidine metabolism. Conversely, when comparing this same stage (MT) with EP, the number of up-regulated genes was greater (n = 6) than the number of down-regulated genes (n = 3), however, the same results were not observed for the comparison between MTs and AMs. Similarly, the number of genes associated with purine metabolism was quite similar for all the stages, wherein the gene numbers ranged from 6 to 8, unlike the comparison between MTs and AMs where only 7 up-regulated genes were observed (Fig. 3).

One of the most important processes in the life cycle of *T. cruzi* is related to the posttranscriptional regulation of this parasite, particularly the transcriptional characteristics of the down-regulated and up-regulated genes in *T. cruzi*. In the RNA-associated pathways, 13 genes were down-regulated and 12 were up-regulated between MTs and CDTs and six were down-regulated, five were up-regulated between MTs and EPs and 12 were up-regulated to MTs and AMs. In contrast, the signaling pathway responsible for RNA degradation exhibited 9 down-regulated and three upregulated genes

between MTs and CDTs. However, the opposite was observed between MTs and EPs, where the number of overregulated genes (n = 9) was greater than the number of down-regulated genes (n = 5), similar results were observed for MTs and AMs where nine up-regulated genes were found. The mRNA surveillance pathway was mainly up-regulated (n = 7 genes) in MTs compared with that in CDTs. However, three down-regulated genes were also detected, and the numbers were much closer to those observed in the downregulation, with eight down-regulated and four up-regulated genes (Fig. 3).

Several signaling pathways related to amino acids metabolisms were differentially regulated. One of the signaling pathways with the highest number of DEGs was the aminoacyl-tRNA biosynthesis pathway, where 13 and 15 genes were down-regulated between MTs and CDTs and between MTs and EPs, respectively, and six and five genes were up-regulated, respectively, in contrast, just 12 genes were down-regulated to MTs and AMs. In the valine signaling pathway degrading leucine and isoleucine, 10 genes were down-regulated and two were up-regulated between MTs and CDTs. In the comparison between MTs and EPs, a different expression response was observed where four genes were down-regulated and four were up-regulated. Similarly, the amino sugar and nucleotide sugar metabolism pathways were down-regulated in MTs compared with those in CDTs, with a total of eight down-regulated genes and two up-regulated between them. In contrast, a comparison between MTs and EPs showed six up-regulated and three down-regulated genes in MTs and a comparison between MTs and AMs nine up-regulated genes. Glutathione comprises three amino acids: glutamate, cysteine and glycine. The down-regulation of nine genes and the overregulation of six genes related to their metabolism were observed between MTs and CDTs. When MTs were compared with EPs, similar results were observed where nine genes were down-regulated and five were up-regulated and when we compared MTs and AMs nine genes were down-regulated, suggesting the importance of this molecule in the life cycle of *T. cruzi* (Fig. 3).

Finally, one of the altered processes that did not show differential expression was protein processing in the endoplasmic reticulum. A total of 12 genes were down-regulated and 10 genes were up-regulated between CDTs and MTs, whereas 11 were down-regulated and nine were up-regulated between MTs and CDTs and 13 up-regulated genes between MTs and AMs, indicating the importance of this pathway throughout the life cycle of the parasite. Another route with similar expression characteristics was related to spliceosomes, where 11 and eight genes were down-regulated and up-regulated between MTs and CDTs, respectively, and 11 and 13 were down-regulated and up-regulated between MTs and EPs and finally, nine were down-regulated and 10 up-regulated between MTs and AMs (Fig. 3).

Reconstruction of signaling pathways

Based on the number of DEGs present in the differentially regulated signaling pathways and the importance of these factors in the life cycle of *T. cruzi*, we decided to reconstruct the signaling pathways and the genes present in them that were differentially regulated in MTs compared with those in CDTs and EPs.

Autophagy

Autophagy has recently been associated with the control and differentiation of the life cycle of *T. cruzi*. Therefore, we decided to evaluate the changes in gene expressions that occurred among the life cycle stages. The regulation process with the highest number of up-regulated genes was observed when MTs were compared with CDTs and MTs compared with AMs. These genes included GABA (A) receptor-associated protein (ATG8-TcSYL_0079440) and ubiquitin-like-conjugating enzyme ATG3 (TcSYL_0114940). They were up-regulated between MTs and EPs, and MTs and AMs for the gene encoding inositol-hexakisphosphate 5-kinase (KCS1-EC: 2.7.4.21). On the other hand, two genes were down-regulated between MTs and CDTs and up-regulated between MTs and EPs and MTs and AMs. These were serine palmitoyltransferase (LCB1/2-EC: 2.3.1.50-TcSYL_0132770) and eukaryotic translation initiation factor 2-alpha kinase 4 (Gcn2-EC: 2.7.11.1-TcSYL_0075610). The translation initiation factor 2 subunit 1 was down-regulated in MTs compared with that in CDTs, EPs, AMs. The serine/threonine-protein kinase mTOR (TOR-EC: 2.7.11.1-TcSYL_0047210) and vacuolar protein sorting-associated protein 45 (VSP45-TcSYL_0011600) were up-regulated in MTs compared with those in CDTs and EPs and down-regulated in MTs between AMs. Lipase ATG15 (ATG15-EC: 3.1.1.3) and actin-related protein 2 (ARP2/3) were up-regulated in MTs compared with that in CDTs, whereas they were down-regulated in MTs compared with those in EPs and MTs compared with AMs. The genes coding for vesicle-fusing ATPase (SEC18 - TcSYL_0110800) and alpha-soluble NSF attachment protein (SEC17 - TcSYL_0118420) showed different expression profiles. The former was up-regulated between MTs and CDTs between MTs and EPs and down-regulated between MTs and AMs and between MTs and EPs; the latter was down-regulated between MTs and CDTs, between MTs and AMs and between MTs and EPs and they were up-regulated between MTs and EPs. The Lipase ATG15 (TcSYL_0196430) were down-regulated between MTs and EPs, and between MTs and AMs and up-regulated in MTs and CDT. Finally, the phosphatidylinositol 3-kinase gene (EC: 2.7.1.137) was differentially regulated in all the comparisons (VSP34 - TcSYL_0103210) (Fig 4).

Ribosomal profiles

As mentioned previously, one of the signaling pathways that presented the greatest number of down-regulated and up-regulated DEGs in the three life cycle stages of *T. cruzi* was associated with ribosomes. Previous studies have demonstrated the importance of ribosomal profiles as a possible mechanism of posttranscriptional regulation. To determine the specific genes with differential expressions and if they were shared between stages and the types of expression (up or down), the data obtained by KAAS shown in Fig. 4 was condensed. The results showed that small subunit ribosomal proteins S20e (TcSYL_0042980), S3e (TcSYL_0010030), SAe (TcSYL_0121230), and large subunit ribosomal proteins L17e (TcSYL_0048680), L14e (TcSYL_0200830), and L37e (TcSYL_0138350) were down-regulated only in MTs compared with those in CDTs and up-regulated in MTs compared with AMs. S19e (TcSYL_0045890) and L22e (TcSYL_0005370) were only down-regulated in MTs compared with those in CDTs.

A

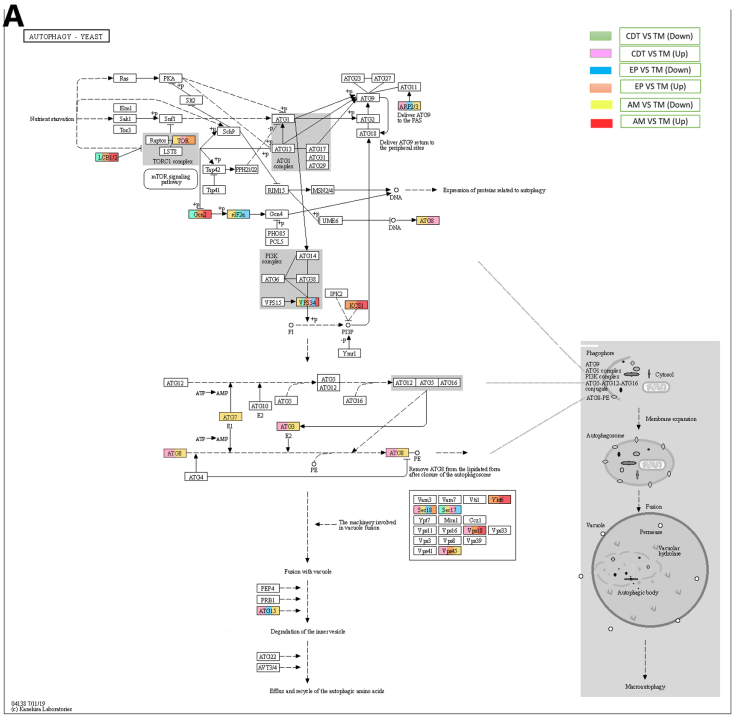

B

Genes	Metacyclic trypomastigotes – cell derived trypomastigotes		Metacyclic trypomastigotes - epimastigotes		Metacyclic trypomastigotes - Amastigotes	
	COMPARISON					
	Down-regulated	Up-regulated	Down-regulated	Up-regulated	Down-regulated	Up-regulated
origin recognition complex subunit 1 (ORC1)		✓			✓	
cyclin-dependent kinase (CDC28)		✓				
serine/threonine-protein phosphatase 2A regulatory subunit A (PPP2R1)		✓			✓	
serine/threonine-protein phosphatase PP1 catalytic subunit (Glc7)	✓			✓		✓
meiotic recombination protein SPO11		✓		✓		
structural maintenance of chromosome 1 (SMC1)			✓		✓	
cell cycle checkpoint protein (RAD17)	✓			✓		✓
DNA replication licensing factor MCM2	✓			✓		
DNA replication licensing factor MCM3					✓	
DNA replication genes Licensing factor MCM4	✓			✓		
DNA replication licensing factor MCM5			✓			
DNA replication licensing factor MCM6		✓	✓		✓	
mitotic spindle assembly checkpoint protein MAD2		✓	✓		✓	
cohesin complex subunit SA-1/2 (IRR1)		✓	✓		✓	
serine / threonine-protein kinase mTOR		✓		✓	✓	
adenylate cyclase (Cyr1)	✓	✓	✓	✓		✓
anaphase-promoting complex subunit 1 (APC1)	✓	✓	✓	✓		✓

Figure 4 Autophagy processes. (A) Comparison of the down-regulated (green) and up-regulated (pink) pathways between metaciclic trypomastigotes and cell derived trypomastigotes. Comparison of the down-regulated (blue) and up-regulated (orange) pathways between metacyclic trypomastigotes and epimastigotes. Comparison of the down-regulated (yellow) and up-regulated (red) pathways between metacyclic trypomastigotes and amastigotes. (B) Table of down- and up-regulated genes between metacyclic trypomastigotes and amastigotes, cell derived trypomastigotes, epimastigotes. The pathway annotation pipeline using KAAS for KEGG pathway assignments was used to reconstruct the pathways and was modified to include down- and up-regulated genes (*Kanehisa & Goto, 2000*). Full-size DOI: 10.7717/peerj.8947/fig-4

The small subunit ribosomal protein S11e (TcSYL_0118400) and large subunit ribosomal protein L10Ae (TcSYL_0014830) were down-regulated in MTs compared with those in EPs and AMs compared with MTs. No other differentially regulated gene showed this characteristic of exclusivity between expression classes in the stages of *T. cruzi*. However, some genes were down-regulated in MTs compared with those in CDTs and up-regulated in MTs compared with those in EPs and AMs. These genes included large subunit ribosomal proteins L3e (TcSYL_0045960), L8e (TcSYL_0203300), L9e (TcSYL_0140530), L19e (TcSYL_0078610), L5e (TcSYL_0115310), L34e (TcSYL_0015800), LP0 (TcSYL_0083010), L10e (TcSYL_0147240), L13e (TcSYL_0001000), L15e (TcSYL_0140770), L35Ae (TcSYL_0045350), L44e (TcSYL_0088040), L36e (TcSYL_0074510), and L38e (TcSYL_0001390) and small subunit ribosomal proteins S15e (TcSYL_0201640), S4e (TcSYL_0089620), S15Ae (TcSYL_0001610), S18e (TcSYL_0113930), S14e (TcSYL_0140720), S9e (TcSYL_0114280), S5e (TcSYL_0074870), S6e (TcSYL_0115180), S26e (TcSYL_0043730), S27e (TcSYL_0014810), and S27Ae (TcSYL_0113470). In contrast, a group of genes up-regulated in MTs compared with those in CDTs and down-regulated in MTs compared with those in EPs and AMs was also observed among the large subunit ribosomal proteins L4e (TcSYL_0003330), L23Ae (TcSYL_0078780), L32e (TcSYL_0115140), L13Ae (TcSYL_0050090), and L6e (TcSYL_0009100) and the

A

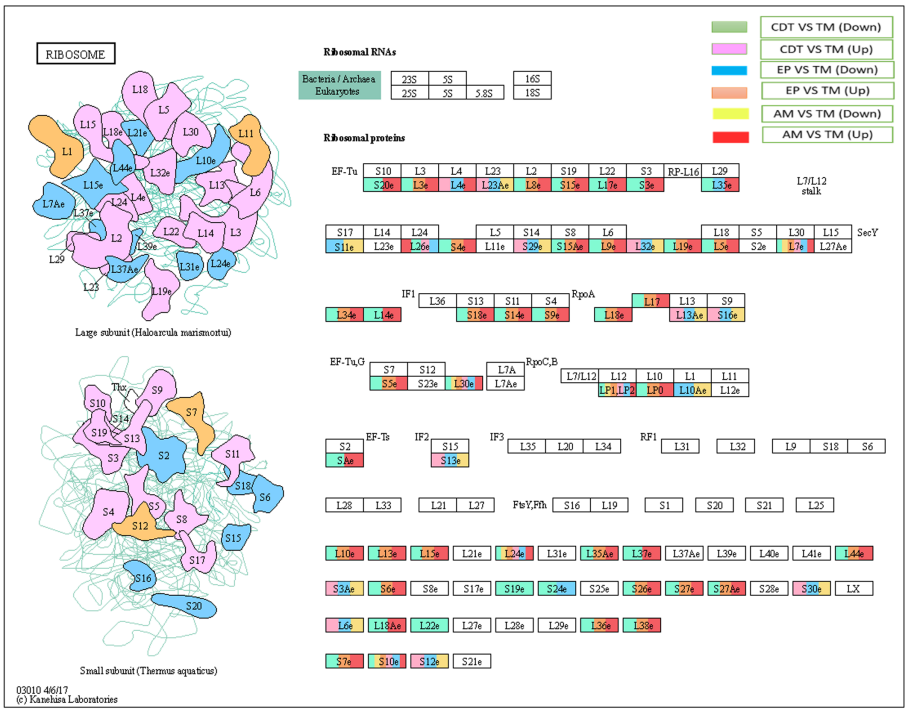

B

	COMPARISON					
	Metacyclic trypomastigotes - cell derived trypomastigotes		Metacyclic trypomastigotes - epimastigotes		Metacyclic trypomastigotes - Amastigotes	
Genes	Down-regulated	Up-regulated	Down-regulated	Up-regulated	Down-regulated	Up-regulated
S19e	✓					
L22e	✓					
S20e	✓					✓
S3e	✓					✓
SAe	✓					✓
L17e	✓					✓
L14e	✓					✓
L37e	✓					✓
L18Ae	✓					✓
S11e			✓		✓	
L10Ae			✓		✓	
L17	✓			✓		✓
L3e	✓			✓		✓
L8e	✓			✓		✓
L9e	✓			✓		✓
L19e	✓			✓		✓
L5e	✓			✓		✓
L34e	✓			✓		✓
LP0	✓			✓		✓
L10e	✓			✓		✓
L13e	✓			✓		✓
L15e	✓			✓		✓
L35Ae	✓			✓		✓
L44e	✓			✓		✓
L36e	✓			✓		✓
L38e	✓			✓		✓
S15e	✓			✓		✓
S4e	✓			✓		✓
S15Ae	✓			✓		✓
S18e	✓			✓		✓
S14e	✓			✓		✓
S9e	✓			✓		✓
S5e	✓			✓		✓
S6e	✓			✓		✓
S26e	✓			✓		✓
S27e	✓			✓		✓
S27Ae	✓			✓		✓
S7e	✓			✓		✓
L4e		✓	✓			✓
L23Ae		✓	✓		✓	
L32e		✓	✓		✓	
L13Ae		✓	✓		✓	
L6e		✓	✓		✓	
S29e		✓	✓		✓	
S16e		✓	✓		✓	
S13e		✓	✓		✓	
S3Ae		✓	✓		✓	
S30e		✓	✓		✓	
S12e		✓	✓		✓	
L35e	✓		✓			✓
L18e	✓		✓			✓
S24e	✓		✓			
L26e	✓	✓	✓			✓
L7e	✓	✓	✓	✓	✓	✓
L30e	✓	✓	✓	✓	✓	✓
LP1-LP2	✓	✓	✓	✓	✓	✓
L24e	✓	✓	✓	✓	✓	✓
S10e	✓	✓	✓	✓	✓	✓

Figure 5 Ribosomal profiles. (A) Comparison of the down-regulated (green) and up-regulated (pink) pathways between metacyclic trypomastigotes and cell derived trypomastigotes. Comparison of the down-regulated (blue) and up-regulated (orange) pathways between metacyclic trypomastigotes and epimastigotes. Comparison of the down-regulated (yellow) and up-regulated (red) pathways between metacyclic trypomastigotes and amastigotes. (B) Table of down- and up-regulated genes between metaciclic trypomastigotes and amastigotes, cell derived trypomastigotes, epimastigotes. The pathway annotation pipeline using KAAS for KEGG pathway assignments was used to reconstruct the pathways and was modified to include down-regulated and up-regulated genes (Kanehisa & Goto, 2000). Full-size DOI: 10.7717/peerj.8947/fig-5

small subunit ribosomal proteins S29e (TcSYL_0180240), S16e (TcSYL_0023130), S13e (TcSYL_0087830), S3AE (TcSYL_0132400), S30e (TcSYL_0168900), and S12e (TcSYL_0108040), except L4e (TcSYL_0003330) that was up-regulated in MTs between AMs. Large subunit ribosomal proteins L35e (TcSYL_0156520) and L18e (TcSYL_0005640) and small subunit ribosomal protein S24e (TcSYL_0073760) were down-regulated in both MTs vs. CDTs and MTs vs. EPs and up-regulated in MTs vs. AMs. The coding gene for large subunit ribosomal protein L26e (TcSYL_0103320) was not up-regulated in MTs compared with that in EPs, but was differentially regulated for the other comparisons and up-regulated to MTs between AMs. Finally, some genes were present in all regulation processes and in all stages. These included the large subunit ribosomal proteins L7e (TcSYL_0022670), L30e (TcSYL_0132850), LP1-LP2 (TcSYL_0050180), and L24e (TcSYL_0074880) and the small subunit ribosomal protein S10e (TcSYL_0114020) (Fig. 5).

Meiosis process

Meiosis was one of the pathways in which we did not expect to find differential regulation during the *T. cruzi* life cycle. A total of 10 genes were up-regulated in MTs compared with those in CDTs, and 4 of these up-regulated genes were exclusively expressed in this stage, including origin recognition complex subunit 1 (ORC1 - TcSYL_0076530), cyclin-dependent kinase (CDC28-EC: 2.7.11.22 - TcSYL_0171170), serine/threonine-protein phosphatase 2A regulatory subunit A (PP2A - TcSYL_0110840), and the meiosis meiotic recombination protein SPO11 specific protein (K10878-TcSYL_0014080) genes. When the reads that encode to SPO11 obtained for each stage were compared, 36.2295 reads were obtained for CDTs and 60.2713 reads were obtained for MTs. Likewise, of the genes mentioned ORC1 and PP2A were down-regulated in AMs compared with MTs. No gene was found to be exclusively down-regulated between these two stages. When comparing MTs with EPs, the structural maintenance of chromosome 1 (SMC1 - TcSYL_0117100) and DNA replication licensing factor MCM5 (EC: 3.6.4.12 - TcSYL_0047860) genes were down-regulated in this process, likewise, SMC1 was down-regulated between AMs and MTs, but no exclusive up-regulated gene was observed. Serine/threonine-protein phosphatase PP1 catalytic subunit (PP1C – GLC - 7-EC: 3.1.3.16 - TcSYL_0044050), cell cycle checkpoint protein (RAD17-EC: 3.1.11.2 - TcSYL_0111040), DNA replication licensing factor MCM2 (EC: 3.6.4.12 - TcSYL_0044110), and DNA replication genes licensing factor MCM4 (EC: 3.6.4.12 - TcSYL_0155930) were down-regulated in MTs compared with those in CDTs, and they were up-regulated in MTs compared with those in EPs. Similarly, RAD17 and PP1 were down-regulated between AMs and MTs. Mitotic spindle assembly checkpoint protein MAD2 (TcSYL_0019360), cohesin complex subunit SA-1/2 (IRR1 - TcSYL_0010920), and DNA replication licensing factor MCM6 (EC: 3.6.4.12 - TcSYL_0181360) were up-regulated in MTs compared with those in CDTs, and they were down-regulated in MTs compared with those in EP and between MTs and AMs. DNA replication licensing factor MCM3 (TcSYL_0086540) was down-regulated in MTs compared with that in AMs. The serine/threonine-protein kinase mTOR (EC: 2.7.11.1-TPR2 - TcSYL_0047210) gene was up-regulated in MTs compared with that in CDTs and in MTs compared with that in EPs and down-regulated between MTs and AMs. Finally, adenylate cyclase (Cyr 1 - EC: 4.6.1.1 - TcSYL_0083140) and anaphase-promoting complex subunit 1 (APC1 - TcSYL_0139430) were down-regulated and up-regulated for all the comparisons, excepting between AMs and MTs where they only were down-regulated (Fig. 6).

Homologous recombination

In conjunction with the meiosis process, the signaling pathway for HR was regulated, DNA polymerase delta subunit 1 (POLD1-EC: 2.7.7.7 - TcSYL_0197030) and DNA topoisomerase III (TOP3-EC: 5.6.2.1 - TcSYL_0001820) were up-regulated in MTs compared with those in EPs, and DNA repair and recombination protein RAD54 and RAD54-like protein (EC: 3.6.4.- (TcSYL_0047980) were down-regulated in MTs compared with those in EPs and up-regulated between AMs and MT. The double-strand break (DSB) repair protein MRE11 (TcSYL_0085330), DNA repair protein RAD51

A

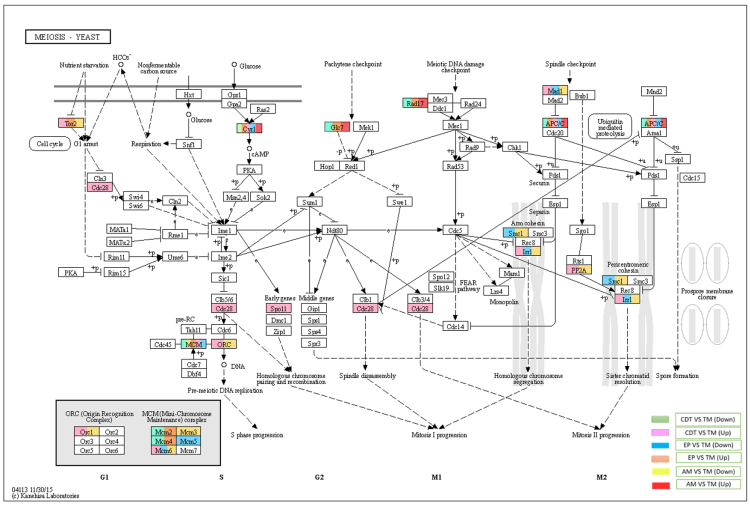

B

Genes	Metacyclic trypomastigotes – cell derived trypomastigotes		Metacyclic trypomastigotes - epimastigotes		Metacyclic trypomastigotes - Amastigotes	
	Down-regulated	Up-regulated	Down-regulated	Up-regulated	Down-regulated	Up-regulated
origin recognition complex subunit 1 (ORC1)		✓			✓	
cyclin-dependent kinase (CDC28)		✓				
serine/threonine-protein phosphatase 2A regulatory subunit A (PPP2R1)		✓			✓	
serine/threonine-protein phosphatase PP1 catalytic subunit (Glc7)	✓			✓		✓
meiotic recombination protein SPO11		✓		✓		
structural maintenance of chromosome 1 (SMC1)			✓		✓	
cell cycle checkpoint protein (RAD17)	✓			✓		✓
DNA replication licensing factor MCM2	✓			✓		
DNA replication licensing factor MCM3					✓	
DNA replication genes Licensing factor MCM4	✓			✓		
DNA replication licensing factor MCM5			✓			
DNA replication licensing factor MCM6		✓	✓		✓	
mitotic spindle assembly checkpoint protein MAD2		✓	✓		✓	
cohesin complex subunit SA-1/2 (IRR1)		✓	✓		✓	
serine / threonine-protein kinase mTOR		✓		✓	✓	
adenylate cyclase (Cyr1)	✓	✓	✓	✓		✓
anaphase-promoting complex subunit 1 (APC1)	✓	✓	✓	✓		✓

Figure 6 Meiosis processes. (A) Comparison of the down-regulated (green) and up-regulated (pink) pathways between metacyclic trypomastigotes and cell derived trypomastigotes. Comparison of the down-regulated (blue) and up-regulated (orange) pathways between metacyclic trypomastigotes and epimastigotes. Comparison of the down-regulated (yellow) and up-regulated (red) pathways between metacyclic trypomastigotes and amastigotes. (B) Table of down- and up-regulated genes between metacyclic trypomastigotes and amastigotes, cell derived trypomastigotes, epimastigotes. The pathway annotation pipeline using KAAS for KEGG pathway assignments was used to reconstruct the pathways and was modified to include down-regulated and up-regulated genes (Kanehisa & Goto, 2000). Full-size DOI: 10.7717/peerj.8947/fig-6

(TcSYL_0043760), and homologous topoisomerase (DNA) II binding protein 1 (TOPBP1-TcSYL_0001820) specific recombination protein were down-regulated in MTs compared with those in CDTs, and they were up-regulated in MTs compared with those in EPs and RAD51 and TOPBP1 were up-regulated between MTs and AMs. The results obtained for TOPBP1 were verified by observing that the log2 changes (fold-change) were −1.27163 and 1.71369, respectively. Replication factor A1 (RPA - TcSYL_0179190) was down-regulated in MTs compared with that in CDTs, it was down-regulated and up-regulated in MTs compared with that in EPs and down and up-regulated between MTs and AMs, whereas DNA polymerase I (Dpol-EC: 2.7.7.7 - TcSYL_0091960) was down-regulated and up-regulated in MTs compared with that in TPs, up-regulated in MTs compared with that in EP and down-regulated between MTs and AMs. Finally, DNA repair protein RAD50 (TcSYL_0043690) was found to be down-regulated and up-regulated in all the comparisons of *T. cruzi* stages, with the exception of MTs compared to AMs where it was not observed up-regulated (Fig. 7).

DISCUSSION

Processes related to energy metabolism (e.g., glycolysis, the pyruvate metabolism, the Krebs cycle, and oxidative phosphorylation) were differentially regulated among the four stages and were mainly down-regulated in MTs, with a greater difference observed in comparison with CDTs (Fig. 3). Metacyclogenesis is characterized by a response to strong nutritional stress stimulus, which continues in the MT stage, where energy metabolism is based on the degradation of proteins and not on glucose. However, we did not expect

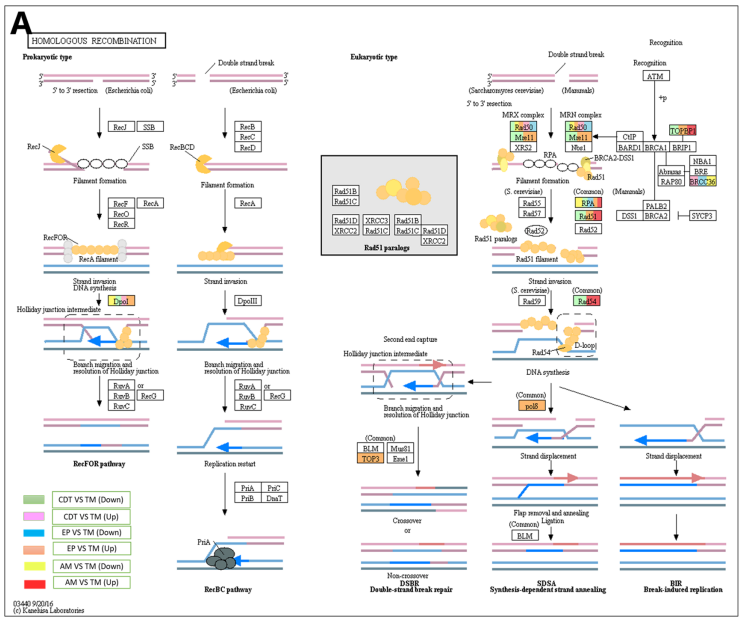

B

	COMPARISON					
	Metacyclic trypomastigotes - cell derived trypomastigotes		Metacyclic trypomastigotes - epimastigotes		Metacyclic trypomastigotes – Amastigotes	
Genes	Down-regulated	Up-regulated	Down-regulated	Up-regulated	Down-regulated	Up-regulated
DNA polymerase delta subunit 1 (POLD1)				✓		
DNA topoisomerase III (TOP3)				✓		
DNA repair and recombination protein RAD54			✓			
RAD54-like protein			✓			✓
double-strand break repair protein MRE11	✓			✓		
DNA repair protein RAD51	✓			✓		✓
BRCA1/BRCA2-containing complex subunit 3		✓	✓		✓	
homologous topoisomerase (DNA) II binding protein 1 (TOPBP1)	✓			✓		✓
replication factor A1 (RPA)	✓		✓	✓	✓	✓
DNA polymerase I (Dpol)	✓	✓		✓	✓	
DNA repair protein RAD50	✓	✓	✓	✓	✓	

Figure 7 Homologous recombination processes. (A) Comparison of the down-regulated (green) and up-regulated (pink) pathways between metacyclic trypomastigotes and cell derived trypomastigotes. Comparison of the down-regulated (blue) and up-regulated (orange) pathways between metacyclic trypomastigotes and epimastigotes. Comparison of the down-regulated (yellow) and up-regulated (red) pathways between metacyclic trypomastigotes and amastigotes. (B) Table of down- and up-regulated genes between metacyclic trypomastigotes and amastigotes, cell derived trypomastigotes, epimastigotes. The pathway annotation pipeline using KAAS for KEGG pathway assignments was used to reconstruct the pathways and was modified to include down-regulated and up-regulated genes (Kanehisa & Goto, 2000).

Full-size DOI: 10.7717/peerj.8947/fig-7

that the greatest difference in signaling pathways would be between MTs and CDTs, which maybe because of the manner in which CDTs acquire glucose. During intracellular infection, AMs obtain glucose from the host cell; moreover, even a decrease in the disposition process decreases the replication of amastigotes even after the differentiation into CDTs and the release of CDTs into the bloodstream. CDTs can use the substrate directly and because blood has more glucose than the rectal blister of the insect (where MTs are found), the parasite can activate energy generation from this substrate. In contrast to MTs, an increase in glucose in the infected organs and a decrease in plasma were observed, which suggests the importance of this metabolism during the AM–CDT cycle. However, we had no information about the entire curve of differentiation between these stages and at what time this metabolic differentiation occurs, and the observed results show that there is not a great difference with respect to the energetic metabolism between AMs and CDTs, later analyzes could be focused in the analysis of available reads of amastigote RNA at different times of cell culture (*Contreras, Morel & Goldenberg, 1985*; *Hamedi et al., 2015*; *Kalem et al., 2018*).

The signaling pathway related to RNA degradation was mainly down-regulated in MTs compared with that in CDTs, and it was up-regulated in MTs compared with that in EPs and AMs, thus demonstrating an inversely proportional relationship with the mRNA surveillance pathway. These results are of great importance considering the polycistron characteristics of *T. cruzi* where RNA regulation occurs mainly at the posttranscriptional

level, and mechanisms such as RNA degradation and survival contribute greatly to its regulation mainly in stages with replicative characteristics (Fig. 3) (*Clayton & Shapira, 2007*; *Martinez-Calvillo et al., 2010*). During metacyclogenesis, there is a decrease in transcription and an increase in heterochromatin in the parasite in response to the energy deficiency it encounters. Thus, the maintenance of the proteome is generated mainly from previously transcribed RNA and is stored or free in the cytoplasm of the parasite. Conversely, it occurs in EPs where their energy metabolism is high and also presents an active replication, which requires a continuous increase of the cellular proteome and where the previously mentioned mechanisms will regulate the expression (*Avila et al., 2003*; *Barisón et al., 2017*). Therefore, we can infer that *T. cruzi* uses this tool as a source of proteome modification among the morphological stages. Another mechanism of post-transcriptional regulation is directly related to the availability and degradation of amino acids, the latter being the main form of energy in MTs (*Avila et al., 2003*). Although several amino acid metabolism genes were down-regulated and up-regulated, we did not identify a clear gene expression profile among the life cycle stages of *T. cruzi* (Fig. 3). However, glutathione specifically gained our attention. This molecule comprises three amino acids—glutamate, cysteine, and glycine—and was mainly down-regulated in MTs compared with that in CDTs, AMs and EPs. Glutathione is used by the parasite as trypanothione peroxidase (an antioxidant enzyme that performs detoxification) which is formed from two glutathione molecules linked to spermidine groups through the NH2 bonds of the latter and is considered a virulence factor that allows the parasite to evade the immune system (*Piacenza et al., 2013*). Thus, the presence of this down-regulated compound in MTs compared with that in CDTs could be related to the role of CDTs to evade the host immune system, whereas its increase in the EPs and AMs could be related to the avoidance of oxidative stress in the vector and inside the cell. This mechanism gives the parasite the ability to escape the host's immune system or the oxidative stress present in the vector. Considering that oxidative stress mechanisms are necessary stimuli for differentiation processes such as metacyclogenesis and amastigogenesis, where EPs, AMs and CDTs are mainly exposed, would explain the higher expression of glutathione in these stages compared with that observed in MTs (*Barisón et al., 2017*; *Nogueira et al., 2015*; *Tyler & Engman, 2001*).

The importance of autophagy during the life cycle of *T. cruzi* and in the metacyclogenesis process has been recently suggested (*Salassa & Romano, 2019*; *Vanrell et al., 2017*). The expression of this signaling pathway was differentially regulated in all the comparisons. When reconstructing this signaling pathway and determining the DEGs, the differential expression of ATG8 was demonstrated, which is associated with one of the main autophagy process markers. It was up-regulated in MTs compared with that in EPs and up-regulated between MTs and AMs. Previous studies evaluating autophagy during metacyclogenesis demonstrated the presence of this protein during starvation, which is the main stimulus for metacyclogenesis, which would explain the decrease in its expression in amastigotes where starvation is not one of the main characteristics (*Vanrell et al., 2017*). Despite this, ATG3 was also up-regulated between MTs and EPs and down-regulated between MTs and AMs. ATG3 has been associated with ATG8

lipidation for autophagosome formation in encysting *Acanthamoeba*, where its presence was related to the absence of the ATG8 complex and a decrease in encysting. The presence of this up-regulated protein in MTs suggests its relationship with the completion of metacyclogenesis and the lipidation of ATG8 and the ATG8 complex formed during this process. However, because ATG8 was also up-regulated, its presence is not clear (*Moon et al., 2011*). On the other hand, the presence of ATG3 in *Toxoplasma gondi* is associated with the maintenance of mitochondrial homeostasis during cell division. However, MTs are not replicative, and the AMs that correspond to the replicative forms present the RNA coding for this down-regulated protein; therefore, it is possible that this protein may have different functions or specific functions in parasites or that this process is maintained as a result of nutritional stress present during metacyclogenesis and not because of cell division (*Besteiro et al., 2011*). ATG15 is a lipase whose function is to lyse the membrane of the autophagic body inside the lysosome for the functioning of both the compartments. This protein was up-regulated in MTs compared with that in EPs, and it was down-regulated in MTs compared with that in EPs and AMs. Although ATG15 has not been studied in depth in parasites, the reason for the differential expression profile between AMs–EPs and CDTs in comparison with MTs is not known. Therefore, we decided to evaluate the genes present in this signaling pathway with the same expression profile and found the coding gene for sec17. Sec17 is an α-SNAP protein belonging to SNARE proteins (soluble N-ethylmaleimide-sensitive factor adapting proteins receptors) related to intracellular trafficking in eukaryotes, such as trypanosomatids (*Datta et al., 2018*; *Murungi et al., 2014*). Analysis of the SNARE proteins in *T. brucei* has demonstrated their differential regulation during the life cycle of this parasite, indicating its importance in the differentiation of the parasite and thus explaining the differential expression profile observed here (*Koumandou et al., 2008*).

The pathway with the highest number of differentially regulated genes in all the comparisons (down-regulated and up-regulated) and stages of *T. cruzi* was related to ribosomes. However, we want to highlight the presence of related expression profiles with genes coding for specific ribosomal proteins between the parasitic stages (Fig. 5). A total of 80 ribosomal proteins have been described in eukaryotes. Similarly, the presence of ribosomal profiles in *T. cruzi* has been previously reported as a mechanism of posttranscriptional regulation in EPs and MTs. Despite this, the ribosomal profiles between AMs, CDTs and MTs have not been compared (*Dalla Venezia et al., 2019*; *Nardelli et al., 2007*; *Smircich et al., 2015*). Differential ribosomal profiles between the stages of *T. brucei* have been previously reported (*Jensen et al., 2014*; *Vasquez et al., 2014*). Consistent with these results, the concept of specialized ribosomes, which could determine translational activity in response to different types of stimuli related to status, development, environment, and pathologies, has recently been formulated (*Dalla Venezia et al., 2019*). Modifications in rRNA such as 2′-O ribose-methylation, pseudouridylation, and base methylation are associated with the function of the ribosome. However, it is not known if these rRNA modifications are related to any specific group of ribosomal proteins. Studies on these rRNAs modifications and their relationship with ribosomal proteins should be conducted to corroborate this hypothesis. The results of our

study suggest the presence of a group of ribosomal proteins common to all the stages of *T. cruzi* as well as another group of proteins that are down-regulated or up-regulated between the replicative (AMs–EPs) and not replicative stages (CDTs) that could regulate the presence of proteomes specialized between the stages and confer the specific functions they exhibit (Fig. 5). However, an analysis at the proteomic level where ribosomal proteins between replicative and non-replicative stages are evaluated must be performed in order to corroborate the hypothesis proposed here.

Meiosis is one of the processes that has not been described in *T. cruzi* to date, unlike that in other trypanosomatids such as *T. brucei*, where a sexual exchange is known to occur through this form of cell reproduction (*Peacock et al., 2014*). Despite this, analyses at the level of single genetic markers, multilocus sequence typing (MLST), and complete genome sequencing have demonstrated the presence of genes involved in meiosis as well as events compatible with genetic exchange through a meiotic process (*Berry et al., 2019*; *El-Sayed et al., 2005*; *Franzén et al., 2011*; *Messenger & Miles, 2015*; *Ramírez et al., 2012*; *Schwabl et al., 2019*). The results obtained here demonstrated the presence of several down-regulated and up-regulated genes among the life cycle stages of *T. cruzi* related to this process. As shown in Fig. 6, only four genes were up-regulated in MTs compared with those in CDTs and SPO11 was one of the up-regulated genes. SPO11 is a specific meiosis gene, and its function is to mediate the onset of recombination and generate double chain breaks in homologous chromosomes during prophase I of meiosis I (*Genois et al., 2014*). To the best of our knowledge, MTs have not been associated with sexual exchange processes such as meiosis, and the only study on this process was conducted in VERO cells, where *T. cruzi* clones transfected with different antibiotics demonstrated the parasite's ability to generate clones resistant to both antibiotics, in addition, the analysis of these clones revealed genomic characteristics generated as a result of nuclear hybridization and subsequent recombination characteristic of a meiosis process, however, the results obtained for the gene expression of AMs do not show the presence of up-regulated genes related to the process of meiosis (*Gaunt et al., 2003*). Therefore, to generate a reduction in ploidy through meiosis, studies on *Candida albicans* and *Giardia intestinalis* have demonstrated the ability of proteins, such as SPO11 reprogramming, to perform recombination processes during an alternative process of parasexuality, which could explain the overregulation of this protein at this stage (*Carpenter et al., 2012*; *Forche et al., 2008*; *Poxleitner et al., 2008*). On the other hand, "the meiosis toolkit" requires the expression of specific genes and genes that encode for proteins associated with DNA repair and other functions necessary in this process. Although we failed to detect other meiosis-specific DEGs, coding genes for proteins, such as Cdc28, Orc1, Apc1, Smc1, Rad17 and several Mcm proteins, were identified. The latter exhibited an inversely proportional gene regulation between MTs and CDTs, between MTs and AMs and between MTs and EPs. Cyclin-dependent kinase Cdc28 is necessary for meiosis initiation events, such as replication and recombination, and Orc1 is a component of the origin recognition complex. Cdc28 and Orc1 along with SPO11 participate in the formation of meiotic DNA DSBs. If we had observed the upregulation of these proteins only in MTs, we could assume that the recombination process was occurring at this stage and that it

required the presence of this machinery. However, we cannot be sure that it is associated with the entire meiosis process (Fig. 6) (*Akematsu et al., 2017*; *Benjamin et al., 2003*; *Farmer et al., 2012*; *Vader et al., 2011*). Similarly, the Mcm proteins, which are a complex of seven replicative helicases, are joined via a dimer (Mcm3-5) and a trimer (Mcm4-6-7) that are connected by Mcm2. In our results, Mcm was up-regulated in MTs compared with that in CDTs, which together with SPO11, Cd28 and ORC1 indicate its participation in sexual exchange processes with MTs. It also suggests the ability of these seven proteins to differentially regulate the stages of *T. cruzi* and indicates its relationship with different processes involved in the protein conformation of the complete Mcm (*Santosa et al., 2013*). Future in vivo studies on cultured cells and triatomines are warranted to determine the true ability of *T. cruzi* to perform meiosis and identify the correct life stage regulating this process.

Based on the meiosis results and the regulation mainly associated with the initiation of meiosis, we decided to investigate the gene expressions among the stages of *T. cruzi* in the signaling pathway for HR. Our analysis revealed differentiation in the gene regulation of Rad proteins (Fig. 7). The following genes were identified to be up-regulated in MTs compared with those in CDTs: Rad50, MRE11 and TOPBP1, RPA, the recombinase Rad51, POLD1 and TOPO3. Rad54 was down-regulated, and with similar genetic expression, Rad50, TOPBP1, RPA, POLD1 and Rad54 when comparing the MTs with the AMs, these results demonstrate the activation of a large part of the proteins involved in the HR pathway in MTs. In addition, it is important to highlight that TOPBP1 was identified among the 50 most overregulated genes in this study, which further highlights the importance of this signaling pathway. Studies on *T. cruzi* have demonstrated a relationship between high levels of Rad51 and the presence of hybrids in the CL–Brener strain, suggesting a possible relationship between these proteins and HR in this parasite (*Alves et al., 2018*). Further studies on MTs evaluating the genes involved in HR are necessary to confirm this result and its possible relationship with genetic exchange processes other than meiosis, such as parasexuality. One of the limitations of this study is associated with the reads obtained from a sequencing performed in previous years. Subsequent studies must focus on the follow-up of a strain or clone of *T. cruzi* throughout its life cycle in the same period of time to reduce possible external variables.

CONCLUSIONS

From the results obtained here, we can conclude that there is a difference in gene expression among the stages of *T. cruzi*. Considering the regulation of energy metabolism from glucose, the maintenance and survival of mRNA, the participation of the autophagy processes, not only as stimuli in the metacyclogenesis but also as processes present throughout the parasite's life cycle, and the ribosomal profiles among the stages, we can infer its importance in the posttranscriptional regulation and proteome found in the different stages of *T. cruzi*. We can also infer a genetic exchange process in the MTs where SPO11 and Rad51 play a fundamental role in the development of DSBs and HR. To the best of our knowledge, this is the first study where RNA sequencing was used as a

tool to analyze the expression profiles present in MTs and their respective comparison with all stages of *T. cruzi* cycle. The results obtained here open a window of knowledge toward processes and pathways of signaling regulated in the infectious stage of the parasite and the life cycle of *T. cruzi* in general. The response to different microenvironments and types of stress during their life cycle provides an opportunity to control the transmission of this parasite and improve our understanding of the drivers of *T. cruzi* cell biology.

ACKNOWLEDGEMENTS

We thank Martin Llewellyn and Philipp Shwabl for their assistance in bioinformatics analysis.

ADDITIONAL INFORMATION AND DECLARATIONS

Funding

The Departamento Administrativo de Ciencia, Tecnología e Innovación COLCIENCIAS funded the project 120465843375, contract 063-2015 for Felipe Guhl, Gustavo A. Vallejo and Juan David Ramírez. DIRECCIÓN ACADÉMICA (Becas de pasantías doctorales) financed Lissa Cruz-Saavedra's work in this study through a scholarship. Juan David Ramírez González is a Latin American fellow in the Biomedical Sciences, whose work in this study was supported by The Pew Charitable Trusts. The funders had no role in study design, data collection and analysis, decision to publish, or preparation of the manuscript.

Grant Disclosures

The following grant information was disclosed by the authors:
Departamento Administrativo de Ciencia, Tecnología e Innovación COLCIENCIA: 120465843375.
DIRECCIÓN ACADÉMICA (Becas de pasantías doctorales).
The Pew Charitable Trusts.

Competing Interests

The authors declare that they have no competing interests.

Author Contributions

- Lissa Cruz-Saavedra conceived and designed the experiments, performed the experiments, analyzed the data, prepared figures and/or tables, authored or reviewed drafts of the paper, and approved the final draft.
- Gustavo A. Vallejo analyzed the data, authored or reviewed drafts of the paper, and approved the final draft.
- Felipe Guhl analyzed the data, authored or reviewed drafts of the paper, and approved the final draft.
- Juan David Ramírez conceived and designed the experiments, performed the experiments, analyzed the data, prepared figures and/or tables, authored or reviewed drafts of the paper, and approved the final draft.

Data Availability

The following information was supplied regarding data availability:

Data is available at the European Nucleotide Archive (ENA): PRJNA251583 (SAMEA5925497) and PRJEB33521 (SAMEA5925496, SAMEA5925498).

Supplemental Information

Supplemental information for this article can be found online at http://dx.doi.org/10.7717/peerj.8947#supplemental-information.

REFERENCES

Akematsu T, Fukuda Y, Garg J, Fillingham JS, Pearlman RE, Loidl J. 2017. Post-meiotic DNA double-strand breaks occur in *Tetrahymena*, and require Topoisomerase II and Spo11. *eLife* **6**:e26176 DOI 10.7554/eLife.26176.

Alves CL, Repoles BM, Da Silva MS, Mendes IC, Marin PA, Machado CR, Aguiar PHN, Da Silva Santos S, Franco GR, Macedo AM, Pena SDJ, De Oliveira Andrade L, Guarneri AA, Tahara EB, Elias MC, Machado CR. 2018. The recombinase Rad51 plays a key role in events of genetic exchange in *Trypanosoma cruzi*. *Scientific Reports* **8(1)**:13335 DOI 10.1038/s41598-018-31541-z.

Aurrecoechea C, Barreto A, Basenko EY, Brestelli J, Brunk BP, Cade S, Crouch K, Doherty R, Falke D, Fischer S, Gajria B, Harb OS, Heiges M, Hertz-Fowler C, Hu S, Iodice J, Kissinger JC, Lawrence C, Li W, Pinney DF, Pulman JA, Roos DS, Shanmugasundram A, Silva-Franco F, Steinbiss S, Stoeckert CJ Jr, Spruill D, Wang H, Warrenfeltz S, Zheng J. 2017. EuPathDB: the eukaryotic pathogen genomics database resource. *Nucleic Acids Research* **45(D1)**:D581–D591 DOI 10.1093/nar/gkw1105.

Avila AR, Dallagiovanna B, Yamada-Ogatta SF, Monteiro-Góes V, Fragoso SP, Krieger MA, Goldenberg S. 2003. Stage-specific gene expression during Trypanosoma cruzi metacyclogenesis. *Genetics and Molecular Research* **2(1)**:159–168.

Barisón MJ, Rapado LN, Merino EF, Furusho Pral EM, Mantilla BS, Marchese L, Nowicki C, Silber AM, Cassera MB. 2017. Metabolomic profiling reveals a finely tuned, starvation-induced metabolic switch in *Trypanosoma cruzi* epimastigotes. *Journal of Biological Chemistry* **292(21)**:8964–8977 DOI 10.1074/jbc.M117.778522.

Bayer-Santos E, Cunha-e-Silva NL, Yoshida N, Franco da Silveira J. 2013. Expression and cellular trafficking of GP82 and GP90 glycoproteins during Trypanosoma cruzi metacyclogenesis. *Parasit Vectors* **6**:127 DOI 10.1186/1756-3305-6-127.

Belew AT, Junqueira C, Rodrigues-Luiz GF, Valente BM, Oliveira AER, Polidoro RB, Zuccherato LW, Bartholomeu DC, Schenkman S, Gazzinelli RT, Burleigh BA, El-Sayed NM, Teixeira SMR, Taylor M. 2017. Comparative transcriptome profiling of virulent and non-virulent *Trypanosoma cruzi* underlines the role of surface proteins during infection. *PLOS Pathogens* **13(12)**:e1006767 DOI 10.1371/journal.ppat.1006767.

Benjamin KR, Zhang C, Shokat KM, Herskowitz I. 2003. Control of landmark events in meiosis by the CDK Cdc28 and the meiosis-specific kinase Ime2. *Genes & Development* **17**:1524–1539 DOI 10.1101/gad.1101503.

Berná L, Chiribao ML, Greif G, Rodriguez M, Alvarez-Valin F, Robello C. 2017. Transcriptomic analysis reveals metabolic switches and surface remodeling as key processes for stage transition in *Trypanosoma cruzi*. *PeerJ* **5(3)**:e3017 DOI 10.7717/peerj.3017.

Berry ASF, Salazar-Sanchez R, Castillo-Neyra R, Borrini-Mayori K, Chipana-Ramos C, Vargas-Maquera M, Ancca-Juarez J, Náquira-Velarde C, Levy MZ, Brisson D, Chagas Disease Working Group in Arequipa. 2019. Sexual reproduction in a natural Trypanosoma cruzi population. *PLOS Neglected Tropical Diseases* **13(5)**:e0007392 DOI 10.1371/journal.pntd.0007392.

Besteiro S, Brooks CF, Striepen B, Dubremetz JF. 2011. Autophagy protein Atg3 is essential for maintaining mitochondrial integrity and for normal intracellular development of *Toxoplasma gondii* Tachyzoites. *PLOS Pathogens* **7(12)**:e1002416 DOI 10.1371/journal.ppat.1002416.

Carpenter ML, Assaf ZJ, Gourguechon S, Cande WZ. 2012. Nuclear inheritance and genetic exchange without meiosis in the binucleate parasite *Giardia intestinalis*. *Journal of Cell Science* **125(10)**:2523–2532 DOI 10.1242/jcs.103879.

Clayton C, Shapira M. 2007. Post-transcriptional regulation of gene expression in trypanosomes and leishmanias. *Molecular and Biochemical Parasitology* **156(2)**:93–101 DOI 10.1016/j.molbiopara.2007.07.007.

Contreras VT, Morel CM, Goldenberg S. 1985. Stage specific gene expression precedes morphological changes during Trypanosoma cruzi metacyclogenesis. *Molecular and Biochemical Parasitology* **14(1)**:83–96 DOI 10.1016/0166-6851(85)90108-2.

Cruz L, Vivas A, Montilla M, Hernández C, Flórez C, Parra E, Ramírez JD. 2015. Comparative study of the biological properties of *Trypanosoma cruzi* I genotypes in a murine experimental model. *Infection, Genetics and Evolution* **29**:110–117 DOI 10.1016/j.meegid.2014.11.012.

Cruz-Saavedra L, Muñoz M, León C, Patarroyo MA, Arevalo G, Pavia P, Vallejo G, Carranza JC, Ramírez JD. 2017. Purification of *Trypanosoma cruzi* metacyclic trypomastigotes by ion exchange chromatography in sepharose-DEAE, a novel methodology for host-pathogen interaction studies. *Journal of Microbiological Methods* **142**:27–32 DOI 10.1016/j.mimet.2017.08.021.

Cucunubá ZM, Okuwoga O, Basáñez MG, Nouvellet P. 2016. Increased mortality attributed to Chagas disease: a systematic review and meta-analysis. *Parasites & Vectors* **9(1)**:42 DOI 10.1186/s13071-016-1315-x.

Dalla Venezia N, Vincent A, Marcel V, Catez F, Diaz JJ. 2019. Emerging role of eukaryote ribosomes in translational control. *International Journal of Molecular Sciences* **20(5)**:1226 DOI 10.3390/ijms20051226.

Datta SP, Jana K, Mondal A, Ganguly S, Sarkar S. 2018. Multiple paralogues of α-SNAP in *Giardia lamblia* exhibit independent subcellular localization and redistribution during encystation and stress. *Parasites & Vectors* **11(1)**:539 DOI 10.1186/s13071-018-3112-1.

Dos Santos CMB, Ludwig A, Kessler RL, De Cássia Pontello Rampazzo R, Inoue AH, Krieger MA, Pavoni DP, Probst CM. 2018. Trypanosoma cruzi transcriptome during axenic epimastigote growth curve. *Memórias do Instituto Oswaldo Cruz* **113(5)**:921 DOI 10.1590/0074-02760170404.

El-Sayed NM, Myler PJ, Bartholomeu DC, Nilsson D, Aggarwal G, Tran AN, Ghedin E, Worthey EA, Delcher AL, Blandin G, Westenberger SJ, Caler E, Cerqueira GC, Branche C, Haas B, Anupama A, Arner E, Aslund L, Attipoe P, Bontempi E, Bringaud F, Burton P, Cadag E, Campbell DA, Carrington M, Crabtree J, Darban H, Da Silveira JF, De Jong P, Edwards K, Englund PT, Fazelina G, Feldblyum T, Ferella M, Frasch AC, Gull K, Horn D, Hou L, Huang Y, Kindlund E, Klingbeil M, Kluge S, Koo H, Lacerda D, Levin MJ, Lorenzi H, Louie T, Machado CR, McCulloch R, McKenna A, Mizuno Y, Mottram JC, Nelson S, Ochaya S, Osoegawa K, Pai G, Parsons M, Pentony M, Pettersson U, Pop M, Ramirez JL, Rinta J, Robertson L, Salzberg SL, Sanchez DO, Seyler A, Sharma R, Shetty J, Simpson AJ,

Sisk E, Tammi MT, Tarleton R, Teixeira S, Van Aken S, Vogt C, Ward PN, Wickstead B, Wortman J, White O, Fraser CM, Stuart KD, Andersson B. 2005. The genome sequence of Trypanosoma cruzi, etiologic agent of Chagas disease. *Science* **309(5733)**:409–415 DOI 10.1126/science.1112631.

Farmer S, Hong EJ, Leung WK, Argunhan B, Terentyev Y, Humphryes N, Toyoizumi H, Tsubouchi H. 2012. Budding Yeast Pch2, a widely conserved meiotic protein, is involved in the initiation of meiotic recombination. *PLOS ONE* **7(6)**:e39724.

Ferreira AV, Segatto M, Menezes Z, Macedo AM, Gelape C, De Oliveira Andrade L, Nagajyothi F, Scherer PE, Teixeira MM, Tanowitz HB. 2011. Evidence for *Trypanosoma cruzi* in adipose tissue in human chronic Chagas disease. *Microbes and Infection* **13(12–13)**:1002–1005 DOI 10.1016/j.micinf.2011.06.002.

Ferreira LR, Dossin FDM, Ramos TC, Freymuller E, Schenkman S. 2008. Active transcription and ultrastructural changes during Trypanosoma cruzi metacyclogenesis. *Anais Da Academia Brasileira De Ciencias* **80(1)**:157–166 DOI 10.1590/S0001-37652008000100011.

Forche A, Alby K, Schaefer D, Johnson AD, Berman J, Bennett RJ. 2008. The parasexual cycle in candida albicans provides an alternative pathway to meiosis for the formation of recombinant strains. *PLOS Biology* **6(5)**:e110 DOI 10.1371/journal.pbio.0060110.

Franzén O, Ochaya S, Sherwood E, Lewis MD, Llewellyn MS, Miles MA, Andersson B. 2011. Shotgun sequencing analysis of *Trypanosoma cruzi* I Sylvio X10/1 and comparison with *T. cruzi* VI CL Brener. *PLOS Neglected Tropical Diseases* **5(3)**:e984 DOI 10.1371/journal.pntd.0000984.

Gaunt MW, Yeo M, Frame IA, Stothard JR, Carrasco HJ, Taylor MC, Mena SS, Veazey P, Miles GAJ, Acosta N, De Arias AR, Miles MA. 2003. Mechanism of genetic exchange in American trypanosomes. *Nature* **421(6926)**:936–939 DOI 10.1038/nature01438.

Genois MM, Paquet ER, Laffitte MCN, Maity R, Rodrigue A, Ouellette M, Masson JY. 2014. DNA repair pathways in trypanosomatids: from dna repair to drug resistance. *Microbiology and Molecular Biology Reviews* **78(1)**:40–73 DOI 10.1128/MMBR.00045-13.

Goldenberg S, Avila AR. 2011. Aspects of *Trypanosoma cruzi* stage differentiation. *Advances in Parasitology* **75**:285–305.

Hamedi A, Botelho L, Britto C, Fragoso SP, Umaki ACS, Goldenberg S, Bottu G, Salmon D. 2015. In vitro metacyclogenesis of Trypanosoma cruzi induced by starvation correlates with a transient adenylyl cyclase stimulation as well as with a constitutive upregulation of adenylyl cyclase expression. *Molecular and Biochemical Parasitology* **200(1–2)**:9–18 DOI 10.1016/j.molbiopara.2015.04.002.

Hernández C, Cucunubá Z, Parra E, Toro G, Zambrano P, Ramírez JD. 2014. Chagas disease (*Trypanosoma cruzi*) and HIV co-infection in Colombia. *International Journal of Infectious Diseases* **26**:146–148 DOI 10.1016/j.ijid.2014.04.002.

Houston-Ludlam GA, Belew AT, El-Sayed NM. 2016. Comparative transcriptome profiling of human foreskin fibroblasts infected with the sylvio and Y strains of *Trypanosoma cruzi*. *PLOS ONE* **11(8)**:e0159197 DOI 10.1371/journal.pone.0159197.

Jensen BC, Ramasamy G, Vasconcelos EJR, Ingolia NT, Myler PJ, Parsons M. 2014. Extensive stage-regulation of translation revealed by ribosome profiling of *Trypanosoma brucei*. *BMC Genomics* **15**:911 DOI 10.1186/1471-2164-15-911.

Kalem MC, Gerasimov ES, Vu PK, Zimmer SL. 2018. Gene expression to mitochondrial metabolism: Variability among cultured *Trypanosoma cruzi* strains. *PLOS ONE* **13(5)**:e0197983.

Kanehisa M, Goto S. 2000. KEGG: Kyoto encyclopedia of genes and genomes. *Nucleic Acids Research* **28(1)**:27–30.

Koumandou VL, Natesan SKA, Sergeenko T, Field MC. 2008. The trypanosome transcriptome is remodelled during differentiation but displays limited responsiveness within life stages. *BMC Genomics* **9(1)**:298.

Li Y, Shah-Simpson S, Okrah K, Belew AT, Choi J, Caradonna KL, Padmanabhan P, Ndegwa DM, Temanni MR, Corrada BH, El-Sayed NM, Burleigh BA, Bravo HC. 2016. Transcriptome remodeling in *Trypanosoma cruzi* and human cells during intracellular infection. *PLOS Pathogens* **12(4)**:e1005511 DOI 10.1371/journal.ppat.1005511.

Martinez-Calvillo S, Vizuet-de-Rueda JC, Florencio-Martinez LE, Manning-Cela RG, Figueroa-Angulo EE. 2010. Gene expression in trypanosomatid parasites. *Journal of Biomedicine and Biotechnology* **2010(2)**:525241 DOI 10.1155/2010/525241.

Messenger LA, Miles MA. 2015. Evidence and importance of genetic exchange among field populations of *Trypanosoma cruzi*. *Acta Tropica* **151**:150–155 DOI 10.1016/j.actatropica.2015.05.007.

Moon EK, Chung DI, Hong Y, Kong HH. 2011. Atg3-mediated lipidation of Atg8 is involved in encystation of *Acanthamoeba*. *Korean Journal of Parasitology* **49(2)**:103–108 DOI 10.3347/kjp.2011.49.2.103.

Moriya Y, Itoh M, Okuda S, Yoshizawa AC, Kanehisa M. 2007. KAAS: an automatic genome annotation and pathway reconstruction server. *Nucleic Acids Research* **35(Web Server)**:W182–W185 DOI 10.1093/nar/gkm321.

Murungi E, Barlow LD, Venkatesh D, Adung'a VO, Dacks JB, Field MC, Christoffels A. 2014. A comparative analysis of trypanosomatid SNARE proteins. *Parasitology International* **63(2)**:341–348 DOI 10.1016/j.parint.2013.11.002.

Nardelli SC, Avila AR, Freund A, Motta MC, Manhães L, De Jesus TC, Schenkman S, Fragoso SP, Krieger MA, Dallagiovanna B. 2007. Small-subunit rRNA processome proteins are translationally regulated during differentiation of *Trypanosoma cruzi*. *Eukaryotic Cell* **6(2)**:337–345 DOI 10.1128/EC.00279-06.

Nogueira NP, Saraiva FM, Sultano PE, Cunha PR, Laranja GA, Justo GA, Sabino Kátia CC, Coelho MGP, Rossini A, Atella GC, Paes MC, Knight M. 2015. Proliferation and differentiation of *Trypanosoma cruzi* inside its vector have a new trigger: redox status. *PLOS ONE* **10(2)**:e0116712 DOI 10.1371/journal.pone.0116712.

OMS. 2019. Climate change and health. *Available at https://www.who.int/news-room/fact-sheets/detail/climate-change-and-health*.

Peacock L, Bailey M, Carrington M, Gibson W. 2014. Meiosis and haploid gametes in the pathogen *Trypanosoma brucei*. *Current Biology* **24(2)**:181–186 DOI 10.1016/j.cub.2013.11.044.

Piacenza L, Peluffo G, Alvarez MN, Martínez A, Radi R. 2013. *Trypanosoma cruzi* antioxidant enzymes as virulence factors in chagas disease. *Antioxidants & Redox Signaling* **19(7)**:723–734 DOI 10.1089/ars.2012.4618.

Poxleitner MK, Carpenter ML, Mancuso JJ, Wang CJ, Dawson SC, Cande WZ. 2008. Evidence for karyogamy and exchange of genetic material in the binucleate intestinal parasite *Giardia intestinalis*. *Science* **319(5869)**:1530–1533 DOI 10.1126/science.1153752.

Ramírez JD, Guhl F, Messenger LA, Lewis MD, Montilla M, Cucunuba Z, Miles M, Llewellyn MS. 2012. Contemporary cryptic sexuality in *Trypanosoma cruzi*. *Molecular Ecology* **21(17)**:4216–4226 DOI 10.1111/j.1365-294X.2012.05699.x.

Rassi A, De Rezende JM. 2012. American trypanosomiasis (Chagas disease). *Infectious Disease Clinics* **26(2)**:275–291.

Salassa BN, Romano PS. 2019. Autophagy: a necessary process during the *Trypanosoma cruzi* life-cycle. *Virulence* **10(1)**:460–469 DOI 10.1080/21505594.2018.1543517.

Santosa V, Martha S, Hirose N, Tanaka K. 2013. The fission yeast minichromosome maintenance (MCM)-binding protein (MCM-BP), Mcb1, regulates MCM function during prereplicative complex formation in DNA replication. *Journal of Biological Chemistry* **288(10)**:6864–6880 DOI 10.1074/jbc.M112.432393.

Schwabl P, Imamura H, Van den Broeck F, Costales JA, Maiguashca-Sánchez J, Miles MA, Andersson B, Grijalva MJ, Llewellyn MS. 2019. Meiotic sex in Chagas disease parasite *Trypanosoma cruzi*. *Nature Communications* **10(1)**:3972 DOI 10.1038/s41467-019-11771-z.

Smircich P, Eastman G, Bispo S, Duhagon MA, Guerra-Slompo EP, Garat B, Goldenberg S, Munroe DJ, Dallagiovanna B, Holetz F, Sotelo-Silveira JR. 2015. Ribosome profiling reveals translation control as a key mechanism generating differential gene expression in *Trypanosoma cruzi*. *BMC Genomics* **16(1)**:443 DOI 10.1186/s12864-015-1563-8.

Teixeira DE, Benchimol M, Crepaldi PH, de Souza W. 2012. Interactive multimedia to teach the life cycle of *Trypanosoma cruzi*, the causative agent of chagas disease. *PLOS Neglected Tropical Diseases* **6(8)**:e1749 DOI 10.1371/journal.pntd.0001749.

Trapnell C, Pachter L, Salzberg SL. 2009. TopHat: discovering splice junctions with RNA-Seq. *Bioinformatics* **25(9)**:1105–1111 DOI 10.1093/bioinformatics/btp120.

Trapnell C, Roberts A, Goff L, Pertea G, Kim D, Kelley DR, Pimentel H, Salzberg SL, Rinn JL, Pachter L. 2012. Differential gene and transcript expression analysis of RNA-seq experiments with TopHat and Cufflinks. *Nature Protocols* **7(3)**:562–578 DOI 10.1038/nprot.2012.016.

Tyler KM, Engman DM. 2001. The life cycle of Trypanosoma cruzi revisited. *International Journal for Parasitology* **31(5–6)**:472–481 DOI 10.1016/S0020-7519(01)00153-9.

Vader G, Blitzblau HG, Tame MA, Falk JE, Curtin L, Hochwagen A. 2011. Protection of repetitive DNA borders from self-induced meiotic instability. *Nature* **477(7362)**:115–119 DOI 10.1038/nature10331.

Vanrell MC, Losinno AD, Cueto JA, Balcazar D, Fraccaroli LV, Carrillo C, Romano PS. 2017. The regulation of autophagy differentially affects *Trypanosoma cruzi* metacyclogenesis. *PLOS Neglected Tropical Diseases* **11(11)**:e0006049 DOI 10.1371/journal.pntd.0006049.

Vasquez JJ, Hon CC, Vanselow JT, Schlosser A, Siegel TN. 2014. Comparative ribosome profiling reveals extensive translational complexity in different *Trypanosoma brucei* life cycle stages. *Nucleic Acids Research* **42**:3623–3637 DOI 10.1093/nar/gkt1386.

Warrenfeltz S, Basenko EY, Crouch K, Harb OS, Kissinger JC, Roos DS, Shanmugasundram A, Silva-Franco F. 2018. EuPathDB: the eukaryotic pathogen genomics database resource. *Methods in Molecular Biology* **1757**:69–113 DOI 10.1007/978-1-4939-7737-6_5.

6. CONCLUSIONES

Capítulo 1:

- Los clones TcI colombianos de *T. cruzi* presentan una estructura filogenética única, correlacionada con una alta variabilidad genética y patrones variados de heterocigocidad, donde adicionalmente se pueden presentar cepas multiclonales con características genéticas diferenciales.
- Se corrobora la presencia del genotipo TcI_{dom} asociado a la infección en humanos en Colombia y Venezuela, con una menor diferenciación en relación con la cepa de referencia Brazil-B4, y un índice F alto.
- Se observan patrones de aneuploidía diferenciales entre los clones colombianos evaluados que no necesariamente se mantienen entre los clones de cada cepa, siendo esta característica corroborada por medio del análisis de la profundidad y la frecuencia alélica.
- Patrones de frecuencia alélica segmental diferencial entre clones e intra-cepas de *T. cruzi* fueron observados para el cromosoma 1. Genes codificantes para "Retrotransposon Hot Spot" (RHS) fueron encontrados flanqueando los segmentos que presentaban características triploides.
- Regiones con pérdida de heterocigosidad (LOH) fueron observadas en varios cromosomas entre e intra-cepa los cuales cubrían la extensión total del cromosoma en algunos casos. No se encontró relación entre LOH y las regiones repetitivas, o genes en específico.

Capítulo 2:

- La metodología planteada con el fin de purificar tripomastigotes metacíclicos a partir de cultivos mixtos con epimastigotes, permitió la purificación de los tripomastigotes metacíclicos sin alterar su infectividad después de realizado el procedimiento a un nivel *in vitro* e *in vivo*. La estandarización de esta técnica provee a la comunidad científica una alternativa rápida y eficiente para purificar tripomastigotes metacíclicos, siendo de gran utilidad en el estudio de características específicas de este estadio del parásito, contribuyendo a la comprensión del ciclo de vida *T. cruzi.*
- Hasta donde la literatura lo permite, este es el primer estudio donde se evalúan los genes regulados diferencialmente entre epimastigotes y tripomastigotes metacíclicos. Una diferencia en la expresión génica entre estos estadios fue claramente observada para la DTUs TcI.
- Se logró determinar la importancia de vías relacionadas con las proteínas ribosomales con perfiles específicos durante la metaciclogénesis de TcI.

- Las principales vías de señalización reguladas diferencialmente estuvieron relacionadas con procesos del metabolismo energético a partir de glucosa, metabolismos de los aminoácidos, endocitosis y mantenimiento y supervivencia del ARN. Así mismo, de gran importancia fue observar la participación de la autofagia en la regulación de metaciclogénesis, la presencia de perfiles diferenciales entre todos los estadios relacionados con ARNs codificantes para proteínas ribosomales, procesos relacionados con el ADN y celulares. La continuación a este estudio debe ser enfocada no solamente en corroborar que los genes descritos se están transcribiendo, sino que además están siendo traducidos a proteínas.

Capítulo 3:

- Los análisis permitieron observar las diferencias a nivel de expresión génica entre los estadios presentes en el del ciclo de vida de TcII.
- Se logró determinar la importancia de vías relacionadas con las proteínas ribosomales con perfiles específicos a lo largo de todo el ciclo de vida de TcII. Mostrando adicionalmente, una clara diferencia en los perfiles de expresión de tripomastigotes derivados de células y tripomastigotes metacíclicos, lo que corrobora la regulación diferencial entre ambos estadios.
- Al igual que para el capítulo 2, las principales vías de señalización más reguladas tenían relación con procesos del metabolismo energético a partir de glucosa, y supervivencia del ARN. Así mismo, de gran importancia fue observar la participación de la autofagia en la regulación a nivel de todo el ciclo de vida de este parásito, y la presencia de perfiles diferenciales entre todos los estadios relacionados con ARNs codificantes para proteínas ribosomales, y la activación de procesos relacionados con la meiosis y la recombinación homóloga con expresión de genes específicos como SPO11 y RAD51. La continuación a este estudio debe ser enfocada no solamente en corroborar que los genes descritos se están transcribiendo, sino que además están siendo traducidos a proteína.

Por último, los resultados acá obtenidos abren una ventana de conocimiento hacia la comprensión de la plasticidad genómica, a así mismo, las vías de señalización reguladas en el estadio infectivo de *T. cruzi* como consecuencia de la exposición a diferentes microambientes, y tipos de estrés durante su ciclo de vida, lo que a su vez brinda una oportunidad para el trabajo en el control de la transmisión de este parásito y al entendimiento de la historia natural de la enfermedad de Chagas.

9. PERSPECTIVAS

- Realizar dos genomas de referencia a partir de clones obtenidos de cepas colombianas con características genómicas diferenciales, lo anterior mediante una metodología híbrida que incluya lecturas cortas y largas seguidas por mapeo por ligamiento, esto con el fin de facilitar los análisis donde se emplean cepas de *Trypanosoma cruzi* colombianas.
- Evaluar las diferencias en la arquitectura genómica entre todos los estadios del ciclo de vida de un clon de *T. cruzi*, teniendo como finalidad identificar los cambios estructurales que puede llegar a tener este parásito dadas las condiciones de estrés a las que se somete y que son fundamentales como estimulo para el inicio de diferenciación morfológica.
- Hasta el momento varios estudios a nivel genómico, multilocus sequence typing (MLST) y marcadores moleculares individuales han inferido la presencia de recombinación sexual *en T. cruzi*, a pesar de que observamos la presencia de genes involucrados en la vía de la meiosis y la recombinación homóloga, con estos resultados solo podemos inferir la expresión de estos genes en este parásito, sin embargo, la función que cumplen no es clara y su participación en procesos de diferenciación o estrés se desconoce. Como se mencionó previamente, estudios posteriores deben enfocarse en corroborar estos resultados a un nivel proteico, incluyendo estrategias de ingeniería genética y un análisis a nivel *in vivo*.
- Análisis donde se pueda evaluar a una mayor escala, que incluya una estrategia de secuenciación hibrida, los re-arreglos de las familias mutagénicas, principales regiones repetitivas, y su relación con las aneuploidías totales y segmentales y los procesos de LOH observados en este estudio.
- Determinar la respuesta a nivel genómico y transcripcional de los diferentes clones de *T. cruzi* al exponer el parásito a radicación. Lo anterior, teniendo en cuenta que previos estudios han demostrado la capacidad de cepas hibridas de responder de manera favorable a este tipo de estrés gracias al aumento de la expresión de genes como el RAD51.
- Determinar a nivel *in vivo* si los procesos altamente estresantes, como la metaciclogénesis, pueden estar generando ruptura de la doble hélice de ADN, que desencadene procesos de recombinación homologa en algunas poblaciones de *T. cruzi*, o las vías que este parásito puede estar siguiendo para aumentar su diversidad genómica.
- Evaluar la remodelación en la expresión genética durante el transcurso del ciclo de vida de *T. cruzi* en el mamífero y su relación con los diferentes tejidos por los que exhibe un alto tropismo y que son fundamentales en la historia natural de la enfermedad de Chagas. Estos estudios no se enfocarán únicamente en la respuesta transcriptómica del parásito sino en la respuesta por parte del hospedero durante la progresión de la infección. Pretendemos realizar estos análisis a un nivel *in vivo* (en modelo murino) e *in vitro*.
- Dada la presencia de la expresión de algunos genes a lo largo del ciclo de vida de *T. cruzi*

como los relacionados con las proteínas ribosomales, autofagia y meiosis y recombinación homologa se debe ver su influencia en la progresión del ciclo de vida mediante análisis de silenciamiento de genes en cada estadio, y su influencia en la diferenciación del parásito.

- Evaluar a otros niveles del dogma central de la biología molecular el proceso de infección de *T. cruzi* en tejidos y hospederos en general, para dicho fin, realizaremos análisis de proteómica y metabolómica, donde se incluyan diferentes tejidos y análisis *in vitro* en ratones y vectores de este parasito.
- Analizar del secretoma a partir de diferentes clones de *T. cruzi* pretende evaluar el transcriptoma y proteoma asociado a estar vesículas y su influencia en la progresión de manera exitosa del ciclo de vida de este parásito.
- Realizar un análisis de metabolómica en pacientes (después de una exhausta revisión y aprobación por parte de un comité de ética) que presenten diferentes características de la enfermedad de Chagas Crónica, esto incluiría pacientes asintomáticos, con Cardiopatía Chagásica Crónica, y con megasíndromes. Lo anterior con el fin de realizar un acercamiento a la interacción huésped – patógeno en los diferentes escenarios que se observan en los pacientes infectados con este parásito.
- Se deben extrapolar los análisis y métodos realizados en esta tesis hacia otras DTUs y genotipos, como TcBat, en orden de aumentar el conocimiento sobre su genoma, la regulación génica en su ciclo de vida, y en el caso puntual de TcBat intentar entender en que se basa la capacidad infectiva disminuida que se le es atribuida en hospederos.
- Un análisis de tropismo de cepas asociadas al domicilio, resistentes a los medicamentos y asociadas a las infecciones orales pretende ser realizado a partir de cepas transfectadas con luciferasas y un posterior análisis mediante bioluminiscencia de ratones infectados, que permita realizar un seguimiento en tiempo real de la evolución de la infección y la asociación de los parásitos a diferentes órganos.
- Caracterizar la resistencia al Benzidazol y Nifurtimox de las cepas de *T. cruzi* circulantes en Colombia, al igual que los genes o vías de señalización involucradas en estos procesos. Lo anterior en búsqueda de entender los escenarios de la enfermedad de Chagas presentes en Colombia.

10. PRODUCTOS DE LA TESIS

Los artículos se encuentran a lo largo del documento, los anexos correspondientes a la información suplementaria se encuentran en la carpeta de anexos de artículos divididos en carpetas por artículo. Todos los productos que se mencionarán a continuación se encuentran en la carpeta de anexos de productos de la tesis divididos según los numerales a continuación:

10.1 ARTÍCULOS CIENTIFICOS

- **Artículo 1: Cruz-Saavedra L**., Schwabl P., Munoz M., Patino L., Vallejo GA, Llewellyn M., Ramírez, J. D. Evidence of genomic plasticity in *Trypanosoma cruzi* I driven by aneuploidy and loss of heterozygosity. (**SOMETIDO)**

- **Artículo 2: Cruz-Saavedra L**, Muñoz M, Patiño LH, Vallejo GA, Guhl F, Ramírez JD. Slight temperature changes cause rapid transcriptomic responses in *Trypanosoma cruzi* metacyclic trypomastigotes. Parasit Vectors. 2020 May 14;13(1):255. doi: 10.1186/s13071-020-04125-y. PMID: 32410662; PMCID: PMC7226949

- **Artículo 3: Cruz-Saavedra L**, Muñoz M, León C, Patarroyo MA, Arevalo G, Pavia P, Vallejo G, Carranza JC, Ramírez JD. Purification of *Trypanosoma cruzi* metacyclic trypomastigotes by ion exchange chromatography in sepharose-DEAE, a novel methodology for host-pathogen interaction studies. J Microbiol Methods. 2017 Nov;142:27-32. doi: 10.1016/j.mimet.2017.08.021. Epub 2017 Sep 1. PMID: 28865682.

- **Artículo 4: Cruz-Saavedra L**, Vallejo GA, Guhl F, Messenger LA, Ramírez JD. Transcriptional remodeling during metacyclogenesis in *Trypanosoma cruzi* I. Virulence. 2020 Dec;11(1):969-980. doi: 10.1080/21505594.2020.1797274. PMID: 32715914; PMCID: PMC7549971.

- **Artículo 5: Cruz-Saavedra L**, Vallejo GA, Guhl F, Ramírez JD. Transcriptomic changes across the life cycle of *Trypanosoma cruzi* II. PeerJ. 2020 May 14;8:e8947. doi: 10.7717/peerj.8947. PMID: 32461822; PMCID: PMC7231504.

10.2 CAPITULOS DE LIBROS

- **Cruz-Saavedra L**, Paniz-Mondolfi A, Ramírez JD. Benaim G, Sordillo E. The role of tryptophan in Chagas disease and other trypanosomatid infections. BIOPHOTONICS, TRYPTOPHAN AND DISEASE. Academic Press-El sevier. 2021; Chapter 5. PP. 55-66 https://elsev.spi-global.com/books/EComp/SORDILLO978-0-12-822790-9/1/OTc4LTAtMTIt/index.php?Type=E

10.3 PRESENTACIÓN EN EVENTOS

Septiembre/2020 **Virtual**	**XXI MOLECULAR PARASITOLOGY MEETING** Tipo de evento: Congreso Ámbito: Internacional **Nombre del producto: Segmental changes in chromosomal allele frequency and loss of heterozygocity in *Trypanosoma cruzi*.** Tipo de producto: Poster
Diciembre/2019 **Cali, Colombia**	**XVII CONGRESO COLOMBIANO DE PARASITOLOGÍA Y MEDICINA TROPICAL** Tipo de evento: Congreso Ámbito: Nacional Nombre del producto: Remodelación transcripcional durante la metaciclogénesis de *Trypanosoma cruzi*. Tipo de producto: Poster
Noviembre/2019 **Ciudad de Panamá, Panamá**	**XXV CONGRESO DE LA FEDERACIÓN LATINOAMERICANA DE PARASITOLOGÍA FLAP** Tipo de evento: Congreso Ámbito: Internacional Nombre del producto: Evaluación de Arquitectura Genómica Comparativa de *Trypanosoma cruzi*. **Reconocimiento: 1° lugar modalidad cartel** Tipo de producto: Poster
Agosto/2018 **Gyeongsang, South Korea**	**14TH INTERNATIONAL CONGRESS OF PARASITOLOGY (ICOPA)** Tipo de evento: Congreso Ámbito: Internacional Nombre del producto: Purification of *Trypanosoma cruzi* metacyclic trypomastigotes from LIT culture by ion exchange chromatography in sepharose-DEAE. Tipo de producto: Poster
Abril/2017 **Bogotá, Colombia**	**SEGUNDA REUNION COLOMBIANA LEISHMANIASIS Y ENFERMEDAD DE CHAGAS** Tipo de evento: Congreso Ámbito: Nacional Nombre del producto: Purificación de tripomastigotes metacíclicos de *Trypanosoma cruzi* por cromatografía de intercambio iónico en sefarosa-DEAE. Tipo de producto: Ponencia

10.4 CURSOS Y SIMPOSIOS

Virtual/2021	**“Welcome Genome Campus - Advanced Course: NGS Bioinformatics”** **Tipo de evento: Curso** **Ámbito: Internacional**

Milán – Italia/2019	**"Genome assembly and annotation Workshop - Elixir"** Tipo de evento: curso Ámbito: Internacional
Querétaro – México/2018	**Análisis Bioinformático de Transcriptomas (RNA-Seq)** Tipo de evento: Simposio
University of Georgia – United States/2017	**2017 EuPathDB Workshop** Tipo de evento: curso Ámbito: Internacional

10.5 PASANTÍAS

Glasgow, Escocia/ Reino Unido. 2019.	**"Comparative genomics of *Trypanosoma cruzi* I"** **Pasantía doctoral** Institute of Biodiversity Animal Health and Comparative Medicine. Glasgow University Duración: 6 meses

10.6 BECAS Y RECONOCIMIENTOS

Diciembre/2019 Ciudad de Panamá/ Panamá	**Primer lugar de trabajos científicos de investigación en la modalidad cartel.** Título: Genómica comparativa de *Trypanosoma cruzi* I. Federación Latinoamericana de Parasitología FLAP
Mayo/2019 Bogotá/Colombia	**Beca Pasantía estudiantes doctorales** Universidad del Rosario
Julio/2017 Bogotá/Colombia	**Beca asistente graduado/estudiante de doctorado** Facultad de Ciencias Naturales y Matemáticas Universidad el Rosario

11. BIBLIOGRAFÍA

1. NCBI. Taxonomy Browser. 2018.

2. WHO | What is Chagas disease? WHO. 2016.

3. Cucunubá ZM, Okuwoga O, Basáñez MG, Nouvellet P. Increased mortality attributed to Chagas disease: a systematic review and meta-analysis. Parasit Vectors. 2016;27;9:42. doi: 10.1186/s13071-016-1315-x. PMID: 26813568; PMCID: PMC4728795.

4. Guhl F, Ramírez JD. Retrospective molecular integrated epidemiology of Chagas disease in Colombia. Infect Genet Evol. 2013;20:148-54.

5. Zingales B, Miles MA, Campbell DA, Tibayrenc M, Macedo AM, Teixeira MM, et al. The revised *Trypanosoma cruzi* subspecific nomenclature: rationale, epidemiological relevance and research applications. Infect Genet Evol. 2012;12(2):240-53.

6. Zingales B, Andrade SG, Briones MR, Campbell DA, Chiari E, Fernandes O, et al. A new consensus for *Trypanosoma cruzi* intraspecific nomenclature: second revision meeting recommends TcI to TcVI. Mem Inst Oswaldo Cruz. 2009;104(7):1051-4.

7. Zingales B. *Trypanosoma cruzi* genetic diversity: Something new for something known about Chagas disease manifestations, serodiagnosis and drug sensitivity. Acta Trop. 2018;184:38-52.

8. Velasquez N, Herrera G, Hernández C, Muñoz M, Ramírez JD. Discrete Typing Units (DTUs) of *Trypanosoma cruzi*: Geographical and biological distribution in the Americas. Sci Data. 2021;Sometido.

9. Cura CI, Mejía-Jaramillo AM, Duffy T, Burgos JM, Rodriguero M, Cardinal MV, et al. *Trypanosoma cruzi* I genotypes in different geographical regions and transmission cycles based on a microsatellite motif of the intergenic spacer of spliced-leader genes. Int J Parasitol. 2010;40(14):1599-607.

10. Herrera C, Bargues MD, Fajardo A, Montilla M, Triana O, Vallejo GA, et al. Identifying four *Trypanosoma cruzi* I isolate haplotypes from different geographic regions in Colombia. Infection, Genetics and Evolution. 2007;7(4):535-9.

11. Herrera C, Guhl F, Falla A, Fajardo A, Montilla M, Adolfo Vallejo G, et al. Genetic variability and phylogenetic relationships within *Trypanosoma cruzi* I isolated in Colombia based on miniexon gene sequences. Journal of parasitology research. 2009;2009.

12. Ramírez JD, Guhl F, Messenger LA, Lewis MD, Montilla M, Cucunuba Z, et al. Contemporary cryptic sexuality in *Trypanosoma cruzi*. Mol Ecol. 2012;21(17):4216-26.

13. Llewellyn MS, Miles MA, Carrasco HJ, Lewis MD, Yeo M, Vargas J, et al. Genome-scale multilocus microsatellite typing of *Trypanosoma cruzi* discrete typing unit I reveals phylogeographic structure and specific genotypes linked to human infection. PLoS pathogens. 2009;5(5):e1000410.

14. Ramírez JD, Guhl F, Rendón LM, Rosas F, Marin-Neto JA, Morillo CA. Chagas cardiomyopathy manifestations and *Trypanosoma cruzi* genotypes circulating in chronic Chagasic patients. PLoS Negl Trop Dis. 2010;4(11):e899.

15. Ramírez JD, Montilla M, Cucunubá ZM, Floréz AC, Zambrano P, Guhl F. Molecular epidemiology of human oral Chagas disease outbreaks in Colombia. PLoS Negl Trop Dis. 2013;7(2):e2041. doi: 10.1371/journal.pntd.0002041. Epub 201321. PMID: 23437405; PMCID: PMC3578743.

16. Zumaya-Estrada FA, Messenger LA, Lopez-Ordonez T, Lewis MD, Flores-Lopez CA, Martínez-Ibarra AJ, et al. North American import? Charting the origins of an enigmatic *Trypanosoma cruzi* domestic genotype. Parasit Vectors. 2012;5:226.

17. Hernández C, Cucunubá Z, Flórez C, Olivera M, Valencia C, Zambrano P, et al. Molecular diagnosis of Chagas disease in Colombia: parasitic loads and discrete typing units in patients from acute and chronic phases. PLoS neglected tropical diseases. 2016;10(9):e0004997.

18. Cruz L, Vivas A, Montilla M, Hernández C, Flórez C, Parra E, et al. Comparative study of the biological properties of *Trypanosoma cruzi* I genotypes in a murine experimental model. Infect Genet Evol. 2015;29:110-7.

19. Costales JA, Kotton CN, Zurita-Leal AC, Garcia-Perez J, Llewellyn MS, Messenger LA, et al. Chagas disease reactivation in a heart transplant patient infected by domestic *Trypanosoma cruzi* discrete typing unit I (TcI DOM). Parasites & vectors. 2015;8(1):435.

20. Rassi A, de Rezende JM. American trypanosomiasis (Chagas disease). Infectious Disease Clinics. 2012;26(2):275-91.

21. Teixeira DE, Benchimol M, Crepaldi PH, de Souza W. Interactive multimedia to teach the life cycle of *Trypanosoma cruzi*, the causative agent of Chagas disease. PLoS Negl Trop Dis. 2012;6(8):e1749. doi: 10.1371/journal.pntd.0001749. Epub 2012 Aug 28. PMID: 22970330; PMCID: PMC3429381.

22. Maeda FY, Cortez C, Yoshida N. Cell signaling during *Trypanosoma cruzi* invasion. Front Immunol. 2012;28;3:361. doi: 10.3389/fimmu.2012.00361. PMID: 23230440; PMCID: PMC3515895.

23. de Souza, W., & Attias, M. New advances in scanning microscopy and its application to study parasitic protozoa. *Exp Parasitol,* 2018:190, 10-33. doi:10.1016/j.exppara.2018.04.018

24. Avila AR, Dallagiovanna B, Yamada-Ogatta SF, Monteiro-Góes V, Fragoso SP, Krieger MA, et al. Stage-specific gene expression during *Trypanosoma cruzi* metacyclogenesis. Genet Mol Res. 2003;2(1):159-68.

25. Garcia ES, Genta FA, de Azambuja P, Schaub GA. Interactions between intestinal compounds of triatomines and *Trypanosoma cruzi*. Trends Parasitol. 2010;26(10):499-505.

26. Contreras VT, Morel CM, Goldenberg S. Stage specific gene expression precedes morphological changes during *Trypanosoma cruzi* metacyclogenesis. Mol Biochem Parasitol. 1985;14(1):83-96. doi: 10.1016/0166-6851(85)90108-2. PMID: 3885031.

27. Gonçalves CS, Ávila AR, de Souza W, Motta MCM, Cavalcanti DP. Revisiting the *Trypanosoma cruzi* metacyclogenesis: morphological and ultrastructural analyses during cell differentiation. Parasit Vectors. 2018;6;11(1):83. doi: 10.1186/s13071-018-2664-4. PMID: Amorim 29409544; PMCID: PMC5801705.

28. Amorim JC, Batista M, da Cunha ES, Lucena ACR, Lima CVP, Sousa K, Krieger MA, Marchini FK. Quantitative proteome and phosphoproteome analyses highlight the adherent population during

Trypanosoma cruzi metacyclogenesis. Sci Rep. 2017;29;7(1):9899. doi: 10.1038/s41598-017-10292-3. PMID: 28852088; PMCID: PMC5574995.

29. Bayer-Santos E, Cunha-e-Silva NL, Yoshida N, Franco da Silveira J. Expression and cellular trafficking of GP82 and GP90 glycoproteins during *Trypanosoma cruzi* metacyclogenesis. Parasit Vectors. 2013;1;6:127. doi: 10.1186/1756-3305-6-127. PMID: 23634710; PMCID: PMC3652755.

30. Ennes-Vidal V, Pitaluga AN, Britto CFPC, Branquinha MH, Santos ALSD, Menna-Barreto RFS, d'Avila-Levy CM. Expression and cellular localisation of *Trypanosoma cruzi* calpains. Mem Inst Oswaldo Cruz. 2020;12;115:e200142. doi: 10.1590/0074-02760200142. PMID: 33053076; PMCID: PMC7552305.

31. Barisón MJ, Rapado LN, Merino EF, Furusho Pral EM, Mantilla BS, Marchese L, Nowicki C, Silber AM, Cassera MB. Metabolomic profiling reveals a finely tuned, starvation-induced metabolic switch in *Trypanosoma cruzi* epimastigotes. J Biol Chem. 2017;26;292(21):8964-8977. doi: 10.1074/jbc.M117.778522. Epub 2017 Mar 29. PMID: 28356355; PMCID: PMC5448128.

32. Hamedi A, Botelho L, Britto C, Fragoso SP, Umaki AC, Goldenberg S, Bottu G, Salmon D. In vitro metacyclogenesis of *Trypanosoma cruzi* induced by starvation correlates with a transient adenylyl cyclase stimulation as well as with a constitutive upregulation of adenylyl cyclase expression. Mol Biochem Parasitol. 2015;200(1-2):9-18. doi: 10.1016/j.molbiopara.2015.04.002. Epub 2015 Apr 23. PMID: 25912925.

33. Vanrell MC, Losinno AD, Cueto JA, Balcazar D, Fraccaroli LV, Carrillo C, Romano PS. The regulation of autophagy differentially affects *Trypanosoma cruzi* metacyclogenesis. PLoS Negl Trop Dis. 2017;1;11(11):e0006049. doi: 10.1371/journal.pntd.0006049. PMID: 29091711; PMCID: PMC5683653.

34. Özdemir V. OMICS 2.0: An Accelerator for Global Science, Systems Medicine and Responsible Innovation. OMICS. 2015;19(10):579-80. doi: 10.1089/omi.2015.0133. PMID: 26484977; PMCID: PMC4615774.

35. Boeke JD, Church G, Hessel A, Kelley NJ, Arkin A, Cai Y, et al. GENOME ENGINEERING. The Genome Project-Write. Science. 2016;353(6295):126-7.

36. Green ED, Watson JD, Collins FS. Human Genome Project: Twenty-five years of big biology. Nature. 2015;526(7571):29-31.

37. El-Sayed NM, Myler PJ, Bartholomeu DC, Nilsson D, Aggarwal G, Tran AN, et al. The genome sequence of *Trypanosoma cruzi*, etiologic agent of Chagas disease. Science. 2005;309(5733):409-15.

38. El-Sayed NM, Myler PJ, Blandin G, Berriman M, Crabtree J, Aggarwal G, et al. Comparative genomics of trypanosomatid parasitic protozoa. Science. 2005;309(5733):404-9.

39. Franzén O, Ochaya S, Sherwood E, Lewis MD, Llewellyn MS, Miles MA, et al. Shotgun sequencing analysis of *Trypanosoma cruzi* I Sylvio X10/1 and comparison with T. cruzi VI CL Brener. PLoS Negl Trop Dis. 2011;5(3):e984.

40. Franzén O, Talavera-López C, Ochaya S, Butler CE, Messenger LA, Lewis MD, et al. Comparative genomic analysis of human infective *Trypanosoma cruzi* lineages with the bat-restricted subspecies T. cruzi marinkellei. BMC Genomics. 2012;13:531.

41. Grisard EC, Teixeira SM, de Almeida LG, Stoco PH, Gerber AL, Talavera-López C, et al. *Trypanosoma cruzi* Clone Dm28c Draft Genome Sequence. Genome Announc. 2014;2(1).

42. Berná L, Rodriguez M, Chiribao ML, Parodi-Talice A, Pita S, Rijo G, et al. Expanding an expanded genome: long-read sequencing of *Trypanosoma cruzi*. Microb Genom. 2018

43. Callejas-Hernández F, Rastrojo A, Poveda C, Gironès N, Fresno M. Genomic assemblies of newly sequenced *Trypanosoma cruzi* strains reveal new genomic expansion and greater complexity. Sci Rep. 2018;8(1):14631.

44. Schwabl P, Imamura H, Van den Broeck F, Costales JA, Maiguashca J, Miles MA, et al. Parallel sexual and parasexual population genomic structure in *Trypanosoma cruzi*. bioRxiv. 2018:338277.

45. Wang W, Peng D, Baptista RP, Li Y, Kissinger JC, Tarleton RL. Strain-specific genome evolution in *Trypanosoma cruzi*, the agent of Chagas disease. PLoS Pathog. 2021;28;17(1):e1009254. doi: 10.1371/journal.ppat.1009254. PMID: 33508020; PMCID: PMC7872254.

46. Udoko AN, Johnson CA, Dykan A, Rachakonda G, Villalta F, Mandape SN, et al. Early Regulation of Profibrotic Genes in Primary Human Cardiac Myocytes by *Trypanosoma cruzi*. PLoS Negl Trop Dis. 2016;10(1):e0003747.

47. Li Y, Shah-Simpson S, Okrah K, Belew AT, Choi J, Caradonna KL, et al. Transcriptome remodeling in *Trypanosoma cruzi* and human cells during intracellular infection. PLoS pathogens. 2016;12(4):e1005511.

48. Houston-Ludlam GA, Belew AT, El-Sayed NM. Comparative Transcriptome Profiling of Human Foreskin Fibroblasts Infected with the Sylvio and Y Strains of *Trypanosoma cruzi*. PLoS One. 2016;11(8):e0159197.

49. Belew AT, Junqueira C, Rodrigues-Luiz GF, Valente BM, Oliveira AER, Polidoro RB, et al. Comparative transcriptome profiling of virulent and non-virulent *Trypanosoma cruzi* underlines the role of surface proteins during infection. PLoS pathogens. 2017;13(12):e1006767.

50. Berná L, Chiribao ML, Greif G, Rodriguez M, Alvarez-Valin F, Robello C. Transcriptomic analysis reveals metabolic switches and surface remodeling as key processes for stage transition in. PeerJ. 2017;5:e3017.

51. Patino LH, Ramírez JD. RNA-seq in kinetoplastids: A powerful tool for the understanding of the biology and host-pathogen interactions. Infect Genet Evol. 2017 Apr;49:273-282. doi: 10.1016/j.meegid.2017.02.003. Epub 2017 Feb 4. PMID: 28179142.